5-2019

PLATISCITY OF C. ELEGANS GERMLINE STEM CELLS UNDER NUTRITIONAL AND METABOLIC STRESS

Kenneth Trimmer

PLASTICITY OF *C. ELEGANS* GERMLINE STEM CELLS UNDER NUTRITIONAL AND METABOLIC STRESS

By

Kenneth Andrew Trimmer, B.S.

APPROVED:

_____
Swathi Arur, Ph.D.
Advisory Professor

_____
Richard Behringer, Ph.D.

_____
Jichao Chen, Ph.D.

_____
Francesca Cole, Ph.D.

_____
Zheng Zhou, Ph.D.

APPROVED:

_____
Dean, The University of Texas
MD Anderson Cancer Center UTHealth Graduate School of Biomedical Sciences

PLATISCITY OF *C. ELEGANS* GERMLINE STEM CELLS UNDER NUTRITIONAL AND METABOLIC STRESS

A

Dissertation

Presented to the faculty of

The University of Texas

MD Anderson Cancer Center UTHealth

Graduate School of Biomedical Sciences

In Partial Fulfillment

For the Degree of

DOCTOR OF PHILOSOPHY

By

Kenneth Andrew Trimmer, B.S.

Houston, Texas

May, 2019

DEDICATION

I would like to dedicate this thesis to my family.

ACKNOWLEDGEMENTS

First and foremost, I would like to thank my mentor Dr. Swathi Arur for her guidance and support. She has provided me not only with a foundation upon which to grow as a scientist, but also valuable insight into how to think like one. I would also like to thank her for being a valued friend. I would like to thank the members of my current advisory committee, Dr. Richard Behringer, Dr. Jichao Chen, Dr. Francesca Cole, and Dr. Zheng Zhou as well as the past members, Dr. Michael Galko and Dr. Jill Schumacher. Each one of them has offered me suggestions and presented questions which have furthered my studies greatly. I would like to thank the present and past members of the lab for fruitful discussions, for keeping me on my toes at lab meeting and for being my drinking buddies.

I would also like to thank the Genes and Development program as well as the GSBS for providing me a framework within which to undertake my studies. I am also appreciative of the past and present directors of the Genetics Microscopy Core, Henry Adams and Dr. Adrianna Paulucci, who have taught me much about microscopy and the art of taking an image. I would especially like to thank my parents who have always supported me. I am also grateful for all the friendships I have made, whether it be my lab mates or my fellow graduate students. In particular, I am thankful for Dr. Alejandro Villar-Prados who has always been a close friend. Last but not least, I could not have performed this research without external support from an NIH supplement, and the Caenorhabditis Genetics Center which provided many strains.

PLATISCITY OF *C. ELEGANS* GERMLINE STEM CELLS UNDER NUTRITIONAL AND METABOLIC STRESS

Kenneth Andrew Trimmer, B.S.

Advisory Professor: Swathi Arur, Ph.D.

Stem cells are integral for tissue maintenance and fertility. Therefore, understanding how stem cells are regulated under stress is imperative. When confronted with acute starvation, stem cells must conserve energy and metabolites to cope with the lack of an external source. *Caenorhabditis elegans* germline stem cells (GSCs) are an excellent model for studying stem cell properties and regulation as they can divide throughout the life of the organism. While GSCs are an adult stem cell population, their cell cycle structure more closely mimics mouse and human embryonic stem cells with short G1 and long S phases. In this thesis, I report that adult GSCs regulate both the G1 and G2 phases to maintain their unique cell cycle structure. I find that the short G1 is promoted by the metabolic regulator *gsk-3*. Loss of *gsk-3* inhibits S phase entry and progression through transcriptional down-regulation of *cdk-2*. Since metabolic signaling regulates *gsk-3*, I propose that controlling G1 progression may allow the cells to buffer metabolic stress. These observations also made me wonder how stem cells would respond to the extreme conditions of acute starvation.

Adult GSCs are known to undergo a cell cycle arrest during acute starvation, so I investigated the mechanisms and cellular behaviors underlying this arrest. I find that acute starvation causes a reversible G2 arrest which is independent of the canonical DNA damage signaling arrest. Instead, this reversible G2 arrest is regulated by the Insulin signaling and TOR signaling pathways. Detailed investigation of the TOR signaling axis revealed that the G2 arrest is partially dependent on stress kinase

signaling, and is mediated by *cdk-1*regulation. I find that *cdk-1* is both translationally and post-translationally regulated to impose the strong starvation-induced G2 arrest. Together, these data reveal novel paradigms through which adult GSCs maintain tissue homeostasis and regenerate tissues to respond to either chronic metabolic stress or acute nutritional deprivation. Given the cell cycle structure conservation between *C. elegans* GSCs and mammalian embryonic stem cells, I propose that gap phase regulation may also drive stem cell homeostasis in mouse and human embryonic stem cells in response to environmental and metabolic perturbation.

TABLE OF CONTENTS

LIST OF FIGURES

LIST OF TABLES

ABBREVIATIONS

ADI – Adjusted division index

AKT – thymomoa viral proto-oncogene

AMPK – AMP-activated protein kinase

Atg14 – Autophagy related 14

Atm – Ataxia-telangiectasia mutated

Atr – Ataxia telangiectasia and Rad3 related

ASC – Adult stem cell

Bmp – Bone morphogenic protein

BrdU – 5-bromo-2’-deoxyuridine

C. elegans – *Caenorhabditis elegans*

CAK – Cdk activating kinase

Cdc6 – Cell division cycle 6

Cdc25 – Cell division cycle 25

CDK – Cyclin dependent kinase

Cdt1 - Chromosome licensing and DNA replication factor 1

Chk1 – Checkpoint kinase 1

Chk2 – Checkpoint kinase 2

CKI – Cdk inhibitor

CRS – Cytoplasmic retention sequence

D. melanogaster – *Drosophila melanogaster*

DAPI - 4',6-diamidine-2-phenylindole dihydrochloride

DTC – Distal tip cell

EdU – 5-ethynyl-2’-deoxyuridine

Eif4e – Eukaryotic translation initiation factor 4E

Eif4ebp – Eukaryotic translation initiation factor 4E binding protein

Eif4g – Eukaryotic translation initiation factor 4G

FISH – Fluorescent in-situ hybridization

FOXO – Forkhead box O

FRB – Fkbp12-Rapamycin binding domain

GPCR – G-protein coupled receptor

GSC – Germline stem cell

Gsk3β – glycogen synthase kinase 3 beta

Hif1a – hypoxia inducible factor 1, alpha subunit

IR – Ionizing radiation

IRS – Insulin receptor substrate

MAPK – mitogen associated protein kinase

Mapkap1 – Mitogen-activated protein kinase associated protein 1

Mcm2-7 – mini-chromosome maintenance subunits 2-7

Mdm2 - transformed mouse 3T3 cell double minute 2

mESC – mouse Embryonic Stem Cell

Mlst8 – MTOR associated protein LST8 homolog (*S. cervisiae*)

Mtor – mechanistic target of rapamycin

Myt1 – Myelin transcription factor 1

ORC – Origin recognition complex

Orc1-6 – Origin recognition complex subunits 1-6

p70s6k – ribosomal protein S6 kinase, polypeptide 1

PGC – Primordial germ cell

PI3K – Phosphoinositide 3 kinase

PIP_2 – Phosphatidylinositol 4,5-diphosphate

PIP_3 – Phosphatidylinositol 3,4,5-triphosphate

Plk1 – Polo like kinase 1

PP2A – Protein phosphatase 2

pRB – Retinoblastoma protein

PRC – pre-replication complex

Prr5 – Proline rich 5 (renal)

Prr5l – Proline rich 5 like

Pten – Phosphatase and tensin homolog

qRT-PCR – Quantitative real time polymerase chain reaction

Rag – recombination activating

Rheb – Ras homolog enriched in brain

Rictor – RPTOR independent companion of MTOR, complex 2

Rpa1 – Replication protein A1

Rptor – Regulatory associated protein of MTOR, complex 1

RTK – Receptor tyrosine kinase

ssDNA – Single stranded DNA

TOR – target of rapamycin

TORC1 – Target of rapamycin complex 1

TORC2 – Target of rapamycin complex 2

TSC – Tuberous sclerosis complex

Tsc1 – Tuberous sclerosis 1

Tsc2 – Tuberous sclerosis 2

UV – Ultraviolet radiation

Wnt – Wingless/Integrated

CHAPTER 1: INTRODUCTION

1.1 Stem Cells

Stem cells are vital for establishing tissues during development, as well as maintaining those tissues once formed during both development and in adulthood in the context of tissue repair or regeneration. These tissues are made up of a variety of different cell types, with each cell type driving distinct functions. These functions have evolved to work in concert, keeping the organism healthy to successfully reproduce. Despite this extensive complexity, an organism develops from a single fertilized oocyte. Therefore, all stem cells, including a fertilized oocyte, must have two central properties: self-renewal and differentiation. Self-renewal is the ability of a stem cell to divide and retain its identity as a stem cell, in other words, to maintain its fate while expanding the stem cell population. However, a stem cell may change its fate and differentiate into a different cell type. Over the course of development, stem cells self-renew and differentiate in response to regulation by both internal and external factors. Through progressive waves of differentiation, a lineage is formed which provides a link between the fertilized oocyte and the differentiated cell types in each tissue. The combination of multiple lineages gives rise to a fate map (Figure 1). Each branching point in the fate map is the result of a differentiation event of a stem cell. Since differentiation typically occurs in a single direction *in vivo*, a useful way to group stem cells is by their potency.

1.1.1: Stem cell potency

The potency of a stem cell is defined by the number of cell types into which that cell can differentiate. As stem cells differentiate, they lose potency and gain specific functions. The cell types which are derived from a particular stem cell result in a cell lineage. To that end, stem cells with a longer lineage will have higher potency. The

potency of stem cells can be divided into four main types: totipotent, pluripotent, multipotent, and unipotent.

Totipotency: Totipotent stem cells are able to produce all the cell types of a complete organism as well as extraembryonic tissues (Hima Bindu and Srilatha 2011). In mouse embryos, the fertilized oocyte and the cells resulting from its divisions until the 8 cell stage are totipotent stem cells, after which asymmetric divisions will occur (Johnson and Ziomek 1981). By the late blastocyst stage, cells which form the trophectoderm and primitive endoderm are differentiated and epiblast cells will no longer form extraembryonic tissues, losing potency (Gardner and Johnson 1973; Gardner and Rossant 1979; Papaioannou et al. 1975; Gardner 1983) (Figure 1).

Pluripotency: Pluripotent stem cells are able to produce all embryonic cell types (Hima Bindu and Srilatha 2011). Pluripotent stem cells such as the mouse embryonic stem cells or human embryonic stem cells can be isolated from the inner cell mass of a blastocyst-stage embryo (Evans and Kaufman 1981; Thomson et al. 1998; Martin 1981). Unlike totipotent stem cells, these cells do not give rise to all extra-embryonic tissues but can give rise to all cell types of an adult organism. However, as these cells differentiate and separate by germ layer, they lose the ability to produce all cell types (Figure 1).

Multipotency: Multipotent stem cells can give rise to cells of multiple lineages, but cannot give rise to all the cells that make up an organism (Hima Bindu and Srilatha 2011). Multipotent stem cells give rise to a family of related cell types. For example, during embryogenesis, the early lung bud forms from the foregut endoderm progenitors. These lung epithelial progenitor cells will give rise to the bronchial airway as well as alveolar sacs, each with very different functions and cell types (Rawlins et al. 2009). Even after development, populations of multipotent stem cells are maintained

throughout the life of an organism to assist in regenerating tissue upon damage such as adult hematopoietic stem cells in mammals which give rise to the blood tissue and its various cell types (Spangrude, Heimfeld, and Weissman 1988; Wu et al. 1968) (Figure 1).

Unipotency: Unipotent stem cells give rise to only a single type of cell (Hima Bindu and Srilatha 2011). In gonochoristic species, this includes the germline stem cells (GSCs) which produce only male or female gametes essential for reproduction (Figure 1).

During embryogenesis, different levels of potency give rise to a hierarchy of stem cells as shown in the fate map (Figure 1). Totipotent stem cells can differentiate to produce pluripotent stem cells and extraembryonic cells. Pluripotent stem cells, in turn, can differentiate to produce various lineages of multipotent stem cells. Through waves of differentiation, cell types are refined until they reach their final fate as a terminally differentiated cell in adults. However, just producing all the adult cell types is not sufficient to form a functional adult organism. Self-renewal and differentiation must be regulated in order to form functional tissues.

1.1.2: Stem cell fate regulation

In order to develop a functional organism consisting of complex systems of tissues and cells from a single fertilized oocyte, many cell behaviors such as proliferation, differentiation and migration must be coordinated. Therefore, stem cell fate changes are tightly regulated throughout embryogenesis. Internal factors such, as asymmetric segregation of proteins and maternal transcripts in the early *Caenorhabditis elegans (C. elegans)* embryo, cell-autonomously drive fate decisions by setting up polarity within the cell (Reviewed in Betschinger and Knoblich 2004; Cheeks et al. 2004; Evans

et al. 1994; Guedes and Priess 1997; Schubert et al. 2000; Seydoux and Fire 1994; Tenenhaus, Schubert, and Seydoux 1998). External factors from developmental signaling determine fate in response to the signaling environment, like Wnt (Wingless/Integrated) signaling which induces a lung progenitor fate in endoderm progenitors (Goss et al. 2009), or Notch signaling which is required for nephron progenitors to differentiate (Chung et al. 2016). In contrast to fate regulation by internal factors, signaling allows for fate control of populations of cells. This is especially useful for maintaining populations of stem cells in adult animals.

1.1.3: Adult stem cells

After development is complete, adult stem cell (ASC) populations are maintained in many tissues. Though there are other methods of repairing damaged tissues, such as dedifferentiation in the case of facultative stem cells, ASC populations are retained to maintain tissue function by replenishing exhausted cells or repairing tissue damage. Many ASC populations are normally “quiescent”, which is characterized by a lack of proliferation, such that the cells remain in a dormant state in their host tissues (Reviewed in Rumman, Dhawan, and Kassem 2015). Upon damage to the host tissues, these ASC populations proliferate briefly, generate progenitor cells, then re-enter quiescence; the newly generated progenitor cells will then replace any cells lost or damaged during tissue damage. This behavior can be found in a variety of ASC populations, such as bulge stem cells in the hair follicle, or satellite cells in the muscle (Cotsarelis, Sun, and Lavker 1990; Schultz, Gibson, and Champion 1978; Snow 1977). Populations of ASCs such as hematopoietic stem cells are likewise maintained in quiescence, though they assist in the maintenance of their tissue rather than responding to damage alone (Bradford et al. 1997; Van Zant 1984). Aberrant exit from

quiescence can lead to depletion of these ASC populations (Shea et al. 2010; Viatour et al. 2008). For long-term ASC maintenance, stem cell niches provide active pools of signaling to promote both quiescence and a stem cell fate (Reviewed in Ferraro, Celso, and Scadden 2010). However, while most populations of ASCs replenish or repair damage of tissues, adult populations of germline stem cells continuously provide gametes for reproduction.

1.1.4: Germline stem cells

Since GSCs will produce gametes which are central to the perpetuation of species, it is necessary that they be as free from deleterious mutations as possible. Anytime a cell divides, it must replicate its DNA, a process which has the potential to introduce new mutations due to replication fidelity or DNA damage (Reviewed in Kunkel 2004; Reviewed in Liu et al. 2016). Therefore, to prevent large changes to the DNA which will be transferred to the next generation, the germline lineages are protected from somatic lineages early in development in the form of primordial germ cells (PGCs).

Like other stem cells, PGC fate can be specified by either internal or external factors. In mammals, PGCs are induced during embryogenesis from a portion of the proximal epiblast by Bmp (Bone morphogenic protein) and Wnt signaling (Ohinata et al. 2009; Lawson et al. 1999). These PGCs then migrate along the hindgut to the genital ridge where they will eventually incorporate into either the testes or ovaries (Molyneaux et al. 2001; Tam and Snow 1981). In *Drosophila melanogaster (D. melanogaster)* and *C. elegans*, PGCs are specified very early by inheriting germplasm (Illmensee and Mahowald 1974, 1976; Wolf, Priess, and Hirsh 1983). As embryogenesis continues, the PGCs lie dormant. However, during larval development, the PGCs divide to form

germline stem cells which are incorporated into gonadal niches to enable the cells to maintain their germ cell fate and produce gametes as GSCs.

While male GSC populations are typically maintained throughout the life of an organism, female GSC populations are depleted in the adults of mammals and some insect species (Spradling et al. 2011). In these species, GSCs are depleted by the time embryogenesis has completed, preventing the formation of new gametes. Due to the difficulty of studying this population in mammals, the model systems of *D. melanogaster*, *C. elegans*, and *Danio rerio*, which maintain an oogenic population of germline stem cells throughout adulthood, are often used.

Regulation of GSC fate in each organism appears to be quite different, and one factor for this difference in regulation appears to be the structure of the niche which maintains the GSCs. For example, the female oogenic stem cell niche in *D. melanogaster* is oriented in such a manner that only the cells adjacent to the niche maintain the GSC fate (Lopez-Onieva, Fernandez-Minan, and Gonzalez-Reyes 2008; Wang, Li, and Cai 2008). As the GSCs divide, one daughter cell divides away from the niche and is thus oriented away from the stem cell hub, resulting in a very clear asymmetric division. No longer in contact with the niche, this daughter cell begins to divide and differentiate into an oocyte with its accompanying nurse cells. However, in the *C. elegans* GSC niche, the distal tip cell (DTC) extends processes which touch a variety GSCs and provide a fate maintenance signal. In this system, as cells leave the niche, they gradually differentiate and cease to divide.

1.1.5: *C. elegans* germline stem cells and their niche

C. elegans GSCs originate from two PGCs which are set aside early in embryonic development, later dividing to form the GSCs and their differentiated progeny (Figure

2). Towards the end of embryogenesis, they reside medial and ventral in the animal. The PGCs remain arrested until the larva hatches. After hatching, *C. elegans* undergoes four larval stages designated L1 – L4. At mid L1, in the presence of nutrition, the PGCs start to divide and form the GSC compartment. As the GSCs divide and the population expands, the somatic gonad surrounding them grows laterally, with the DTCs leading the migration of the distal end. Towards the end of L3, the DTCs migrate dorsally then medially to form two U-shaped gonads in the adult. Throughout gonad development, the GSCs self-renew to fill the growing gonad. Around late-L3, the proximal GSCs begin to differentiate and enter meiosis.

In the hermaphroditic *C. elegans* germline, the GSCs are multipotent, able to differentiate into both spermatozoa and oocytes. Spermatozoa are formed during L4, after which the immature germ cells undergo a fate switch to oocyte production. The GSC population is maintained so that it can continuously produce oocytes during adulthood. As such, the GSCs are regulated not only in terms of terminal differentiated fate, but the decision to self-renew or differentiate is regulated as well due to signaling from the GSC niche.

The GSCs are maintained in a niche called the progenitor region which is defined by the DTC (Figure 3). The DTC displays mesenchymal characteristics and extends processes termed cytonemes. These cytonemes contain a membrane-bound Delta homolog, *lag-2*, which activates Notch signaling through one of the two *C. elegans* Notch receptors, *glp-1* (Henderson et al. 1994; Lambie and Kimble 1991). Both the DTC and Notch signaling are required for GSC self-renewal as removal of the DTC as well as mutants in *lag-2* or *glp-1* result in loss of the GSC population (Austin and Kimble 1987; Kimble and White 1981; Lambie and Kimble 1991). Activation of Notch signaling drives a transcriptional program through its cofactor *lag-1* which represses

gld-1, *gld-2*, *gld-3,* and *nos-3*, the main drivers of entry into meiosis (Eckmann et al. 2004; Hansen, Hubbard, and Schedl 2004; Hansen et al. 2004; Kadyk and Kimble 1998). *gld-1* and *nos-3*, and *gld-2* and *gld-3* work in pairs to either repress translation of mitotic mRNAs (*gld-1*, *nos-3*) or enhance translation of meiotic mRNAs (*gld-2*, *gld-3*) (Eckmann et al. 2004; Hansen, Hubbard, and Schedl 2004; Jan et al. 1999; Marin and Evans 2003; Ryder et al. 2004). Along these lines, *gld-1* represses *glp-1* mRNA translation in a feedback loop (Marin and Evans 2003). As cells leave the region of *glp-1* activity, they transition into meiosis which can be visualized either by a nuclear morphology reminiscent of a crescent shape, or by the accumulation of meiotic proteins such as the synaptonemal complex proteins *him-3* and *syp-1* on the chromatin.

In healthy, wildtype animals, the DTC maintains a stereotypical progenitor region length of 20 cell diameters (Figure 3A). Changes in Notch (*glp-1*) signaling which affect the decision between self-renewal and differentiation can alter this length. Partial loss of *glp-1* function results in a smaller gonad with a shorter progenitor region (Dorsett, Westlund, and Schedl 2009; Kodoyianni, Maine, and Kimble 1992; Qiao et al. 1995). Conversely, temperature-sensitive gain of function mutations in *glp-1* result in a longer progenitor region even when *glp-1* is activated for short periods of time. Constitutive activation of *glp-1* results in a complete germline tumor where germ cells never enter meiosis (Berry, Westlund, and Schedl 1997; Pepper, Killian, and Hubbard 2003). Downstream, *gld-1;gld-2* double mutants, which inactivate two major meiosis promoting components, result in uncontrolled proliferation and produces a germline tumor (Kadyk and Kimble 1998). Therefore, the length of the progenitor region can be used as an indicator of the state of the self-renewal vs. differentiation balance.

Perhaps due to the nature of this structure, there is no evidence of asymmetric divisions as occurs in other stem cell populations. Asymmetric divisions are inherently

regulated, often occurring in the same direction with the differentiating daughter cell leaving a niche. Over the course of my investigations, I attempted to observe whether divisions in the progenitor region were regulated directionally. I tracked divisions throughout the progenitor region and found that orientation appeared random with regards to either the distal-proximal axis (Figure 4), or to the distal tip cell cytonemes (Figure 5). Other groups have assayed the GSCs for evidence of asymmetric divisions as well. Gerhold et al used live imaging of mitoses to look for differences in the duration of cell division (Gerhold et al. 2015). Rosu and Cohen-Fix labeled populations of cells and followed their progeny (Rosu and Cohen-Fix 2017). Neither study found any evidence for asymmetric divisions. (Gerhold et al. 2015; Rosu and Cohen-Fix 2017). However, while GSCs do not divide asymmetrically, their cell cycle is heavily regulated as will be discussed in the next section.

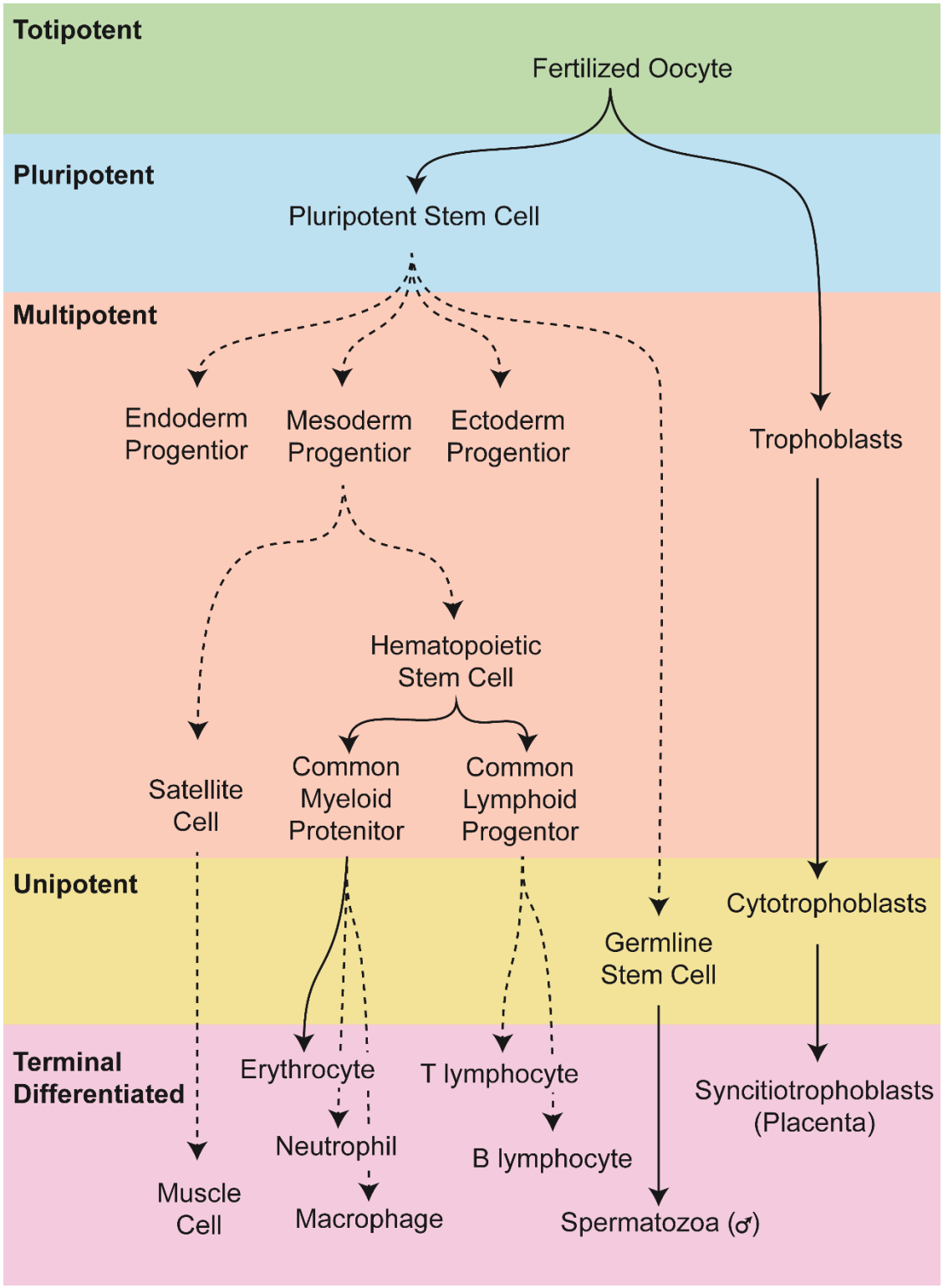

Figure 1: Stem cell fate map

Fate map of select lineages during mammalian development. Solid line depicts a direct differentiation event. Dashed line depicts multiple differentiation events.

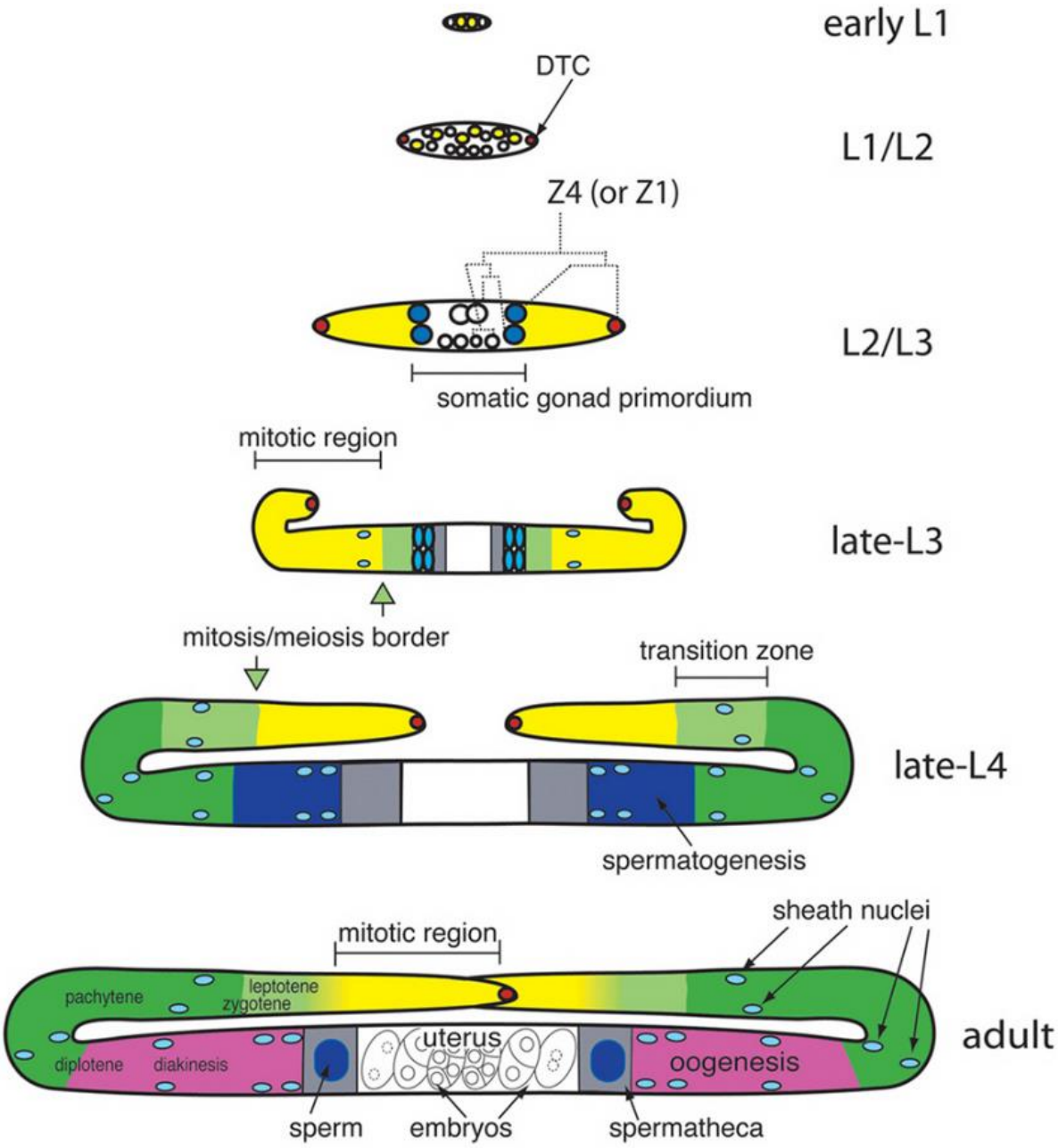
early L1
DTC
L1/L2
Z4 (or Z1)
L2/L3
somatic gonad primordium
mitotic region
late-L3
mitosis/meiosis border
transition zone
late-L4
spermatogenesis
sheath nuclei
mitotic region
pachytene
leptotene
zygotene
uterus
diplotene
diakinesis
oogenesis
adult
sperm
embryos
spermatheca

Figure 2: *C. elegans* larval gonad development

Adapted from Wormbook chapter “Introduction to the germline”. ”Cartoon representation of gonadogenesis” by E. Jane Albert Hubbard and David Greenstein which is licensed under CC BY 2.5 (http://creativecommons.org/licenses/by/2.5/). Shown is panel B from the original image. Cartoon representation of larval hermaphrodite gonad development. GSCs in yellow, distal tip cell in red, meiosis in green, sperm in dark blue, oocytes in purple, and somatic gonad in light blue.

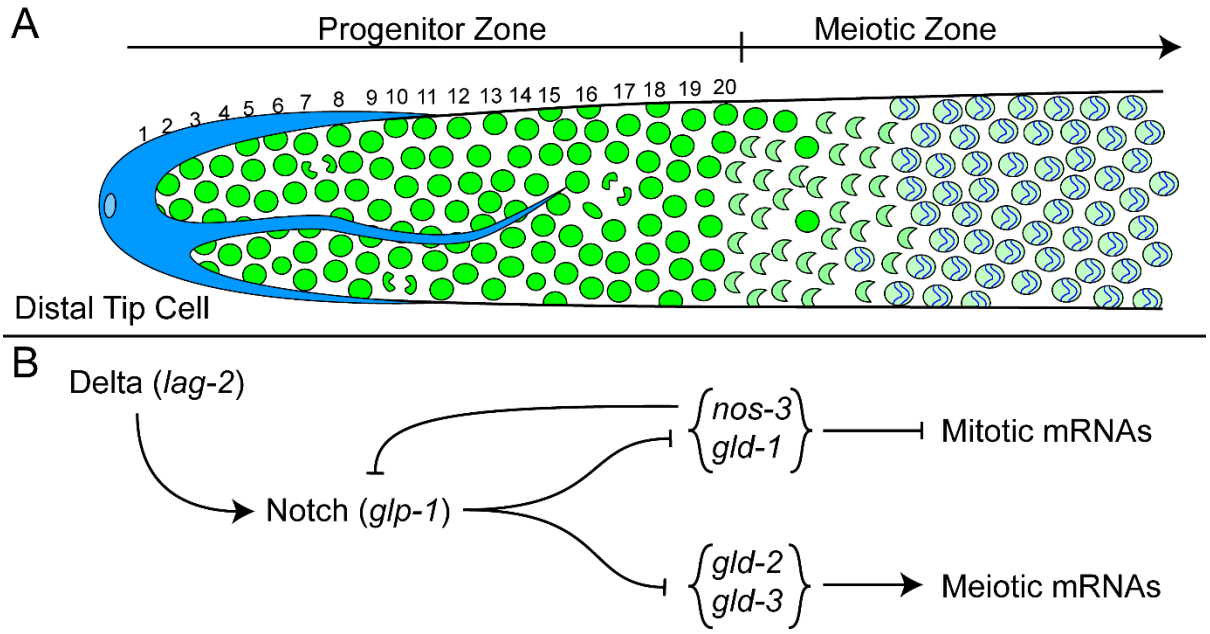

Figure 3: The *C. elegans* GSC niche

(A) Schematic representation of the GSC niche (progenitor zone) in *C. elegans* oriented with the distal tip cell to the left. DTC is in blue with a cytoneme extending into the progenitor region, germ cells are in green with GSCs (solid green), meiotic cells (crescent shaped and green circles with blue lines). Numbers mark each cell row with a typical 20 cell diameters from the distal tip cell to the end of the progenitor region. (B) Genetic network of mitosis/meiosis decision. Delta ligand is provided by the distal tip cell. *C. elegans* gene names are in parentheses.

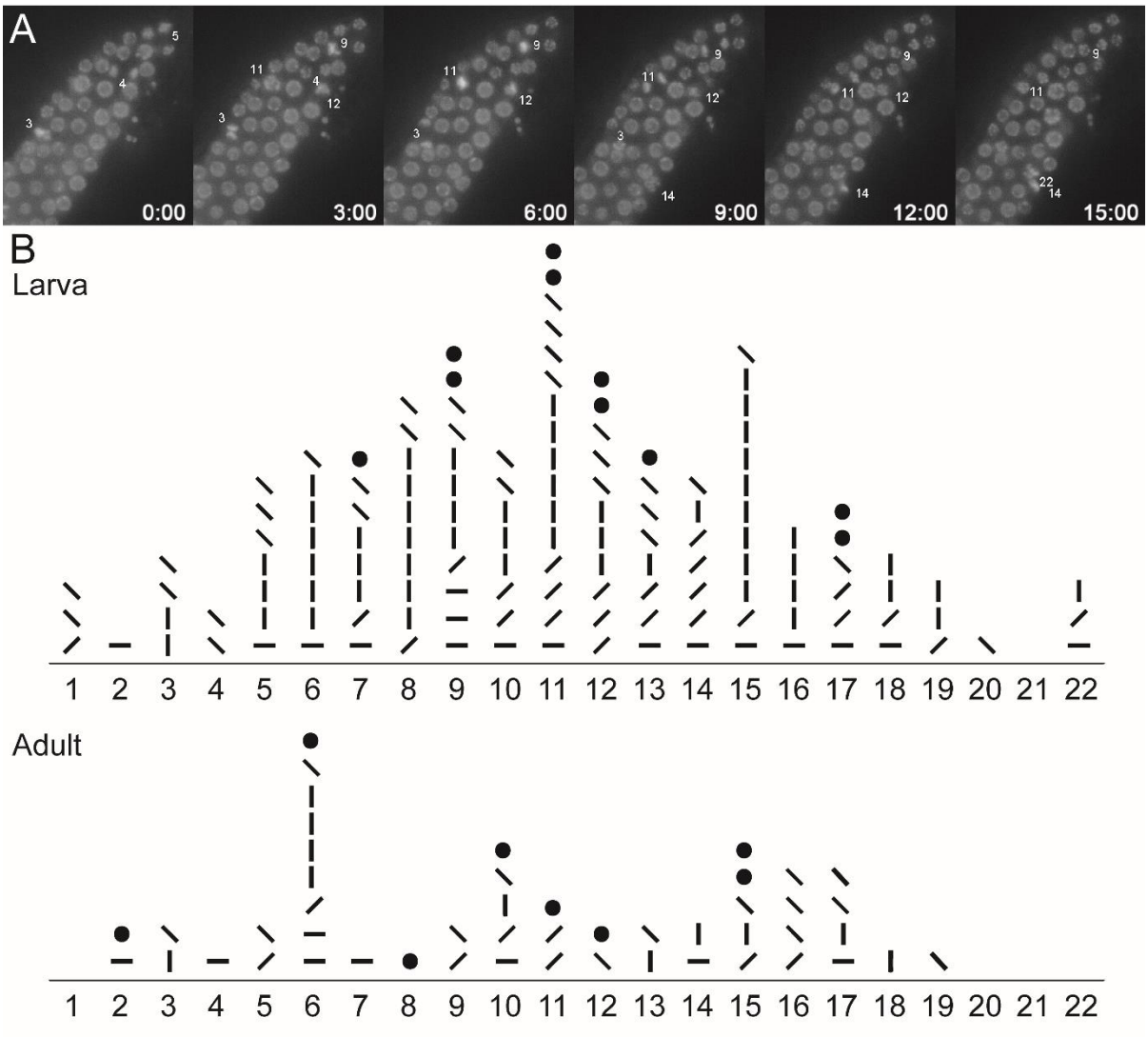

Figure 4: GSC divisions are random with respect to the distal-proximal axis

(A) Time course of dividing cells in the progenitor region. Dividing cells are numbered. Time from the start of acquisition is shown in the bottom right of each frame. An mCherry::HIS-51 transgene (white) labels nuclei. (B) Orientation of divisions in larva (early L4) and adults (24 hours past L4). Graph is aligned along the axis of the germline from distal (left) to proximal (right). Numbering along the x-axis indicates the cell row where a division initiated. Lines depict the orientation of the metaphase plate with respect to the distal-proximal axis. Circles depict a metaphase plate which was oriented parallel with the plane of acquisition.

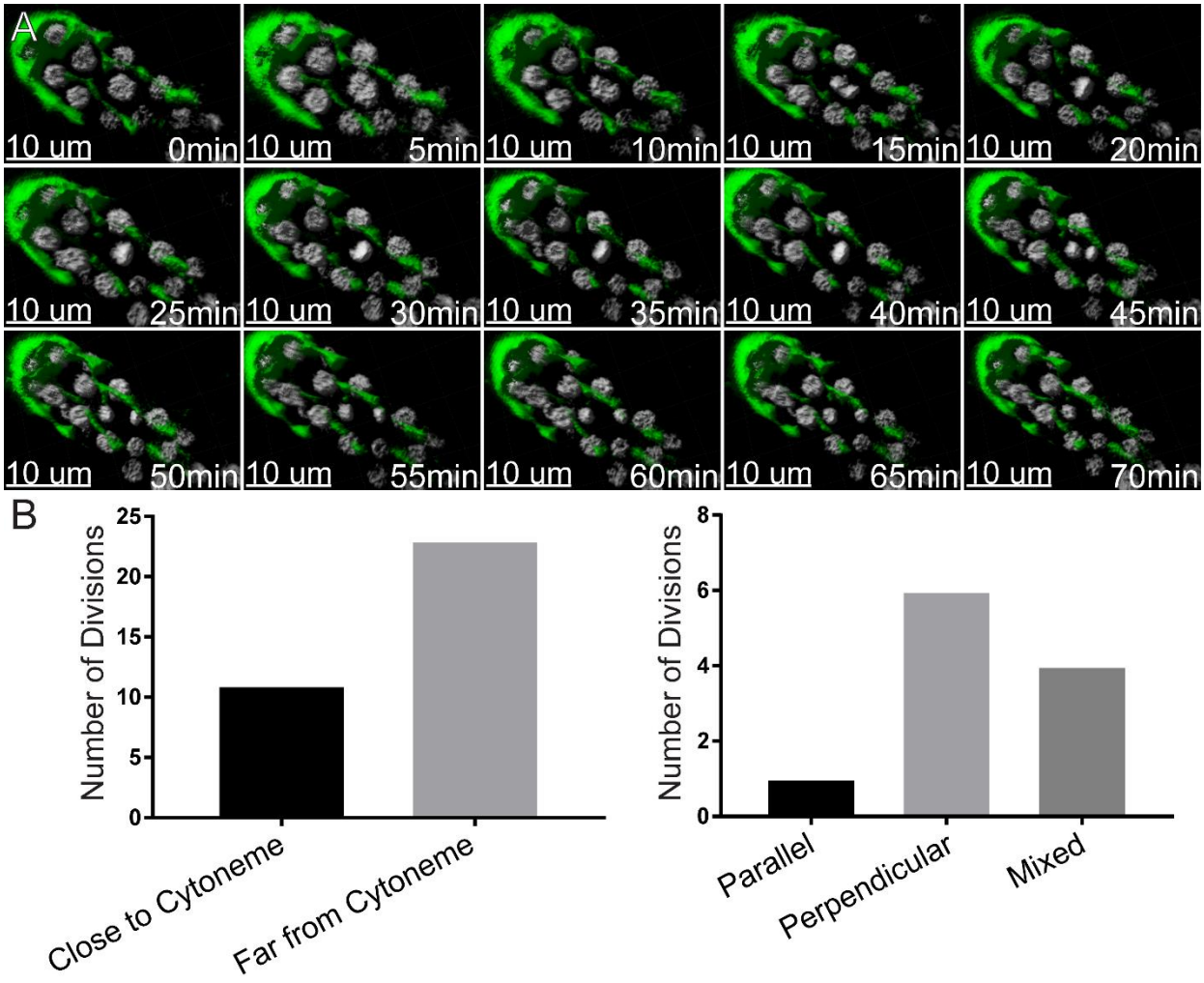

Figure 5: GSC divisions are random with respect to the DTC cytonemes

Analysis of the orientation of mitotic divisions in the progenitor region. (A) Time slices of a representative division. *lag-2::gfp* (green) labels the DTC and cytonemes, an mCherry::HIS-51 transgene (white) labels nuclei. Images were taken as z-stacks and assembled in Imaris. Dividing cell is oriented in the middle of the frame. Clipping planes were used to remove overlapping nuclei and out of focus fluorescence from the DTC. Time from the start of acquisition is shown in the bottom right of each frame. Scale bar: 10µm. (B) Analysis of whether or not divisions occurred adjacent to a cytoneme is shown on the left. Analysis of whether adjacent divisions occurred parallel, perpendicular, or at some angle in between, compared to the closest cytoneme.

1.2 The Cell Cycle

In order for stem cells to self-renew, they must first divide. There are many steps to prepare a cell for division. In order to divide, a cell must contain enough components for two daughter cells such as cytoplasm, organelles, DNA, nutrients, and energy. Therefore, once a cell enters the cell cycle, cell growth occurs during interphase (G1, S, and G2 phases) which is followed by cell division during M phase. Each of these phases and the transitions between them are regulated by cyclin dependent kinases (CDKs) (Figure 6).

1.2.1 Cyclin dependent kinases

CDKs are a class of proteins which phosphorylate targets to drive cell cycle progression. (Reviewed in Morgan 1995; Reviewed in Vermeulen, Van Bockstaele, and Berneman 2003). In mammalian somatic cell culture, five distinct CDKs function to drive cell cycle progression at each phase: Cdk2, Cdk4, and Cdk6 regulate at G1, Cdk2 regulates S, Cdk1 regulates G2, and Cdk7 activates Cdk1 and Cdk2 in all phases (Figure 6). As each of these phases governs different steps in cell growth, CDKs phosphorylate different substrates at each phase to drive the different cell cycle transitions. Therefore, in order to regulate cell cycle growth and progression, each CDK is regulated by a variety of methods: cofactor binding, inhibitor binding, localization, and phosphorylation.

Cofactor Binding: CDKs require cofactors called cyclins to function. Cyclins activate their partner CDK as well as determine their substrate specificity (Reviewed in Arellano and Moreno 1997) (Figure 6). For example, while both Cdk2-Cyclin E and Cdk2-Cyclin A complexes are required for S phase progression, each drives different activities during DNA replication by differential phosphorylation of their targets

(Coverley, Laman, and Laskey 2002). Cyclins are regulated by transcription throughout the cell cycle and, except for Cyclin D, are expressed cyclically allowing CDKs to activate at specific times, (Figure 6) (Evans et al. 1983; Pines 1991). Cyclin D isoforms are expressed in response to growth factors and bind to Cdk4/6 to drive cell cycle entry and G1 progression (Reviewed in Sherr 1994). Cyclin E is expressed during G1 and binds to Cdk2 to drive S phase entry (Figure 6) (Ohtsubo et al. 1995). During S phase, the expression of Cyclin A gradually increases and binds to Cdk2 to promote DNA replication (Figure 6) (Girard et al. 1991; Walker and Maller 1991). Cyclin B expression gradually increases during G2 and both Cyclin A and Cyclin B bind to Cdk1 to drive entry into M phase (Figure 6) (Arellano and Moreno 1997; Fung, Ma, and Poon 2007; King, Jackson, and Kirschner 1994). Coordinated regulation of cyclins through transcriptional programs thus regulates timing of the cell cycle. For precise regulation, the CDKs also need to be turned off when not needed, and CDK inhibitor proteins bind to CDKs and block cell cycle progression.

Inhibitor Binding: CDK inhibitors (CKIs) bind to either CDKs or CDK complexes and prevent their activity (Reviewed in Besson, Dowdy, and Roberts 2008). CKIs are divided into two major classes, the INK4 family and the Cip/Kip family. The INK4 family of CKIs (p15, p16, p18, and p19) form stable complexes with Cdk4/6, preventing Cyclin D binding and G1 progression (Chan et al. 1995; Guan et al. 1994; Hannon and Beach 1994; Hirai et al. 1995; Serrano, Hannon, and Beach 1993). The Cip/Kip family of CKIs (p21, p27, and p57) inhibit CDK activity by binding to the CDK-Cyclin pair, allowing them to regulate all cell cycle phases (Gu, Rosenblatt, and Morgan 1992; Harper et al. 1993; Polyak, Kato, et al. 1994; Polyak, Lee, et al. 1994; Toyoshima and Hunter 1994; Xiong et al. 1993; Lee, Reynisdottir, and Massague 1995; Matsuoka et al. 1995).

Localization: CDKs mediate cell cycle progression by phosphorylating substrates in the nucleus. Therefore, re-localization of CDKs or CDK-cyclin complexes restricts their activity. A clear example of this type of regulation is the nuclear exclusion of Cyclin B via its cytoplasmic retention sequence (CRS). The Cyclin B CRS natively binds to cofactors which actively export Cdk1-Cyclin B complexes from the nucleus (Pines and Hunter 1994; Yang et al. 1998). Phosphorylation of the CRS of Cyclin B by Cdk1 and Plk1 (Polo like kinase 1) allows Cdk1-Cyclin B to remain in the nucleus which is necessary for entry into mitosis (Borgne et al. 1999; Hagting et al. 1999; Toyoshima-Morimoto et al. 2001).

Phosphorylation: In addition to all of the mechanisms of regulation listed above, CDKs can be also activated or inhibited by phosphorylation. Phosphorylation of CDKs on the T loop (Cdk1 on T161, Cdk2 on T160, and Cdk4 on T172) by the Cdk activating kinase (CAK) increases their activity and cyclin binding (Fisher and Morgan 1994; Gould et al. 1991; Gu, Rosenblatt, and Morgan 1992; Kato et al. 1994; Morgan 1995). However, phosphorylation in the ATP binding domain of Cdk1 (T14Y15), by Wee1 and Myt1 (Myelin transcription factor 1) kinases, and Cdk2 result in their inhibition (Gu, Rosenblatt, and Morgan 1992; Morgan 1995). These inhibitory phosphorylations must be removed by the Cdc25 (Cell division cycle 25) phosphatases to activate the CDKs (Reviewed in Kiyokawa and Ray 2008). Together, the activation and inhibitory phosphorylation events are powerful mechanisms for regulating CDK function and can be used to track the activity status of CDKs.

1.2.2 G1 phase regulation (Figure 7)

Once the previous mitosis is complete, the cell reaches a point where a decision is taken to either remain in the cell cycle or exit the cell cycle. In mammalian cultured

cells, removal of serum or growth factors results in an exit of the cell from the cell cycle into a G0 phase; the G0 phase is also known as a state of quiescence which is discussed later in this Chapter (1.2.6). In response to growth factors, quiescent cells express Cyclin D, promoting reentry of the cell cycle into G1 phase (Matsushime et al. 1991). As Cyclin D transcription increases, it is thought to out-compete the INK4 CKIs for CDK binding resulting in active Cdk4/6-Cyclin D complexes (Sherr and Roberts 1999). Progression through G1 occurs through inhibition of pRb (Retinoblastoma protein) which is phosphorylated and inhibited by the Cdk4/6-Cyclin D complex (Norbury, Blow, and Nurse 1991; Buchkovich, Duffy, and Harlow 1989; Kato et al. 1993).

pRb binds to the E2F-Dp1 heterodimer transcription factors and recruits histone deacetylases which inhibit nearby transcription through epigenetic modification (Brehm et al. 1998; Rubin et al. 2005). E2F/Dp1 complexes bind to promoters of genes that mediate cell cycle progression such as Cyclin D, Cyclin E and Cdk1 (Bracken et al. 2004). Once pRb is phosphorylated by the Cdk4/6-Cyclin D complex, it does not bind to E2F allowing for active E2F-Dp1 complex to form (Weintraub, Prater, and Dean 1992), which results in an increase in the transcription of both Cyclin D and Cyclin E, allowing for more Cdk4/6-Cyclin D and Cdk2-Cyclin E complexes to form. Active Cdk4/6-Cyclin D and Cdk2-Cyclin E complexes, in turn, phosphorylate pRb resulting in a feed-forward loop which leads to hyper-phosphorylation of pRb. After a certain level of CDK activation has been achieved, the cell no longer responds to mitogen signaling as it passes the ‘restriction point’, committing the cell to pass through the cell cycle (Pardee 1974). In addition to G1/S phase progression, this positive feedback loop promotes transcription of proteins involved in DNA licensing, a required process of G1 (Polager et al. 2002).

Licensing of DNA provides a starting point for DNA replication and its regulation helps prevent re-replication (Reviewed in Li and Jin 2010). Loss of DNA licensing factors leads to chromosomal fragmentation, genomic instability, incomplete replication, and can induce several types of cancer (Bagley et al. 2012; Shima et al. 2007). In order to license the DNA, the Origin Recognition Complex (ORC), a complex of Orc proteins (Orc1-6), identifies licensing sites and recruits Cdc6 (Cell division cycle 6) and Cdt1 (Chromosome licensing and DNA replication factor 1), forming the Pre-replication Complex (PRC). The PRC then loads hetero-hexamers of Mcm2-7 (Mini-chromosome maintenance) proteins, which form part of a helicase during DNA replication. The process of licensing also appears to promote the expression of Cyclin D expression and plays a role in activating Cdk2 complexes (Nevis, Cordeiro-Stone, and Cook 2009; Liu et al. 2009). Since active Cdk2-Cyclin E complexes are necessary for DNA replication, this demonstrates that both DNA licensing and pRb inhibition are necessary for progression into S phase.

1.2.3 S phase regulation (Figure 8)

S phase of the cell cycle, or synthesis phase, is the phase in which the cell synthesizes a new copy of its DNA. While much of the regulation during this phase pertains to repairing DNA damage and is discussed below, the process of replication is also regulated. At the start of S phase, DNA replication machinery is assembled at licensed replication origins by active Cdk2-Cyclin E (Coverley, Laman, and Laskey 2002; Zou and Stillman 2000). As Cyclin A expression increased during S phase, active Cdk2-Cyclin A complexes which sanction the origins to fire, causing the replication machinery to begin replicating the DNA, while simultaneously inhibiting the assembly of replication machinery at potential replication origins (Coverley, Laman, and Laskey

2002; Copeland et al. 2010). The interplay between Cdk2-Cyclin E and Cdk2-Cyclin A activity provides a small window in which replication machinery can be assembled while preventing re-licensing of DNA that has already been replicated. After activation by Cdk2-Cyclin A, replication occurs outward bi-directionally from the origin as two replication forks. Since not all forks fire at the same time, forks can be divided into early- and late-replicating forks. Recent reports suggest that early forks may fire in coordination with transcriptional machinery such that replication machinery and transcriptional machinery travel in the same direction (Chen et al. 2019). This would avoid head-on collisions between the two competing complexes which could lead to DNA damage (Hamperl et al. 2017). In this model, later forks would fire only if an early fork had stalled. However, regulation of firing early vs. late forks is still relatively unknown (Reviewed in Masai et al. 2010).

Just as there is regulation for initiating and maintaining DNA replication, there is regulation to ensure complete DNA replication. The Atr (Ataxia telangiectasia and Rad3 related) kinase, part of the DNA damage signaling pathway described below, prevents cell division until DNA replication has completed (Nishijima et al. 2003). However, caffeine in high concentrations will uncouple this regulation through inhibition of Atr, allowing for cell division to proceed even when the DNA is not completed replicated (Schlegel and Pardee 1986; Nishijima et al. 2003).

1.2.4 G2 phase regulation (Figure 9)

Once DNA replication has completed, the cell prepares to divide. During this period, Cyclin B expression increases resulting in the formation of active Cdk1-Cyclin B complexes. However, before binding to Cyclin B, Cdk1 is inactivated by phosphorylation in the endoplasmic reticulum by Myt1 on threonine 14 (T14) (Liu et al.

1997). After binding to Cyclin B, activation of the Cdk1-Cyclin B complex requires removal of inhibitory phosphorylations by the Cdc25 phosphatases, as well as activation by CAK (Figure 9) (Timofeev et al. 2009; Fisher and Morgan 1994). While removal of the inhibitory phosphorylations can occur either in the cytoplasm or nucleus, active Cdk1-Cyclin B is required in the nucleus to drive cell division (Franckhauser et al. 2010).

Nuclear localization of the Cdk1-Cyclin B complex is regulated by the CRS located on Cyclin B which drives the export of Cdk1-Cyclin B complexes from the nucleus (Pines and Hunter 1994; Hagting et al. 1999). Once the Cdk1-Cyclin B complex is active, this export sequence is phosphorylated by Plk1 and Cdk1, inhibiting the CRS and allowing active Cdk1-Cyclin B to enter the nucleus (Borgne et al. 1999; Toyoshima-Morimoto et al. 2001). However, the activity of nuclear-localized Cdk1-Cyclin B complexes is inhibited by phosphorylation on tyrosine 15 (Y15) of Cdk1 by Wee1 kinases specifically to prevent cell division from occurring aberrantly (McGowan and Russell 1995; Russell and Nurse 1987; Den Haese et al. 1995). Therefore, both Wee1 inhibition and Cdc25 activation are necessary for mitotic progression.

1.2.5 DNA damage signaling (Figure 10)

Damage to the DNA is extremely deleterious to cellular life, and in particular, it can severely affect progression through the S and M phases of the cell cycle. To prevent the cell cycle from continuing while DNA is damaged, there are mechanisms in place to arrest the damaged cell during interphase. This allows time for the cell to repair the DNA, though if the damage is too prevalent, it can lead to cell death through apoptosis. DNA damage is caused by multiple factors and the resulting cellular responses flow through two different kinase cascades. Double strand breaks, formed by sources

including ionizing radiation (IR), are largely sensed by Atm (Ataxia-telangiectasia mutated), a serine-threonine kinase (Shiloh 2003). Atr, however, responds to inter-strand crosslinks, formed by sources including ultraviolet radiation (UV), and single strand breaks in addition to double strand breaks (Reviewed in Shiloh 2003). When either kinase is recruited to the site of DNA damage, it is activated by auto-phosphorylation (Liu et al. 2011; So, Davis, and Chen 2009). This results in phosphorylation of various downstream substrates, including Chk1 (Checkpoint kinase 1) and Chk2 (Checkpoint kinase 2) which phosphorylate yet more substrates (Reviewed in Shiloh 2003). This both initiates DNA repair as well as activates the DNA damage checkpoints at G1/S, S, and G2/M.

G1/S Checkpoint: In response to DNA damage, Chk1 and Chk2 effector kinases phosphorylate Cdc25a, leading to its degradation (Mailand et al. 2000). Cdc25a is required to remove inhibitory phosphorylations from Cdk2 complexes, so its destruction leads to inhibition of Cdk2 activity, inhibiting the G1/S transition (Falck et al. 2001; Lee, Bielawska, and Obeid 2000). However, the p53 transcription factor appears to be a major driver of long-term maintenance of the DNA damage checkpoint at G1/S (Reviewed in Levine 1997). Normally, p53 is degraded by Mdm2 (Transformed mouse 3T3 cell double minute 2), but stabilization of p53 occurs due to phosphorylation from Atm and Atr and their downstream effector kinases Chk1 and Chk2 (Liu et al. 2011; So, Davis, and Chen 2009; Shieh et al. 1997; Banin et al. 1998; Shieh et al. 2000; Haupt et al. 1997; Levine 1997; Tibbetts et al. 1999). p53 then increases transcription of the p21 CKI which inhibits the activity of Cdk4, Cdk6 and Cdk2 complexes leading to cell cycle arrest at G1/S (Harper et al. 1995).

Intra-S Checkpoint: If DNA damage occurs during S phase, the cell will extend S phase in order to attempt to repair the damage. The replication fork formed during DNA

replication is sensitive not only to many sources of DNA damage such as inter-strand crosslinks, double strand breaks, and pyrimidine dimers, but also to nucleotide depletion. Together these constitute sources of replication stress which will activate the Atm and Atr kinases triggering the intra-S checkpoint (Reviewed in Berti and Vindigni 2016). Replication stress causes stalling of the replication fork, where the DNA polymerase can no longer progress, leading to the production of single stranded DNA (ssDNA) (Byun et al. 2005; Pages and Fuchs 2003). ssDNA recruits the ssDNA binding protein Rpa1 (Replication protein A1) (Reviewed in Wold 1997). While Rpa1 is involved in unwinding the DNA during replication, it transiently binds to ssDNA from the lagging strand as well (Fairman and Stillman 1988; Wobbe et al. 1987; Wold and Kelly 1988; Audry et al. 2015; Reviewed in MacNeill 2001). Long term Rpa1 binding, like that found at a stalled replication fork, will trigger the intra-S checkpoint by activating Atr (Zou and Elledge 2003). Activation by phosphorylation of Atr, or its effector Chk1, will lead to Cdc25a inhibition and degradation which can no longer remove the inhibitory phosphorylations from Cdk2 complexes (Goto et al. 2019; Shen et al. 2018). Due to this, Cdk2 complexes may be inhibited as a potential mechanism for arresting the cell.

G2/M Checkpoint: DNA damage during G2 will stabilize p53 leading to increased transcription of p21, which also inhibits the activity of Cdk1 complexes (Harper et al. 1995). In addition to p21, p53 also promotes transcription of 14-3-3 σ, an adapter protein which can bind to and exclude Cyclin B from the nucleus (Hermeking et al. 1997). However, the major driver of the G2/M checkpoint appears to be inhibition of Cdk1 itself. Activation of Cdk1 requires the removal of the T14 and Y15 inhibitory phosphorylations (Jin, Gu, and Morgan 1996). Cdc25c phosphatase normally removes these, but if it is phosphorylated by the Chk1 and Chk2 kinases not only is its activity inhibited, but it is actively exported from the nucleus by 14-3-3 proteins (Falck et al.

2001; Sanchez et al. 1997; Peng et al. 1997; Lopez-Girona et al. 1999; Zeng et al. 1998). This prevents the removal of inhibitory phosphorylations (T14Y15) on nuclear populations of Cdk1; keeping it in an inhibited state and preventing the G2/M transition.

1.2.6 Quiescence

Many adult stem cell populations are maintained in a state of quiescence at the G0 phase of the cell cycle (Reviewed in Rumman, Dhawan, and Kassem 2015). This is a state akin to hibernation, where the cell does not proliferate, but is paused until it receives signals to re-enter the cell cycle at G1, progress through the cell cycle, and divide. Mechanistically, entry into quiescence is thought to be driven by low Cyclin D expression during G2 and low CDK activity at the end of M phase of the previous cell cycle (Spencer et al. 2013; Sa et al. 2002). Once in G0, quiescence is maintained by expression of CKIs and pRb (Viatour et al. 2008; Cheng et al. 2000; Matsumoto et al. 2011; Zou et al. 2011; Hosoyama et al. 2011; Sankaran, Orkin, and Walkley 2008). Re-entry into the cell cycle is thought to be driven by the expression of Cyclin D, which activates Cdk4/6 (Ladha et al. 1998). Therefore, at a cell cycle level, regulation of quiescence appears to utilize G1 regulators.

1.2.7 Alternate cell cycle regulation

The cell cycle regulation described above results in well-defined gap phases which last for significant portions of the cell cycle. However, early embryonic cells from *C. elegans*, *D. melanogaster* and *Xenopus laevis* require rapid expansion, and thus abbreviate the gap (G1 and G2) phases, which when coupled with rapid DNA replication, results in an exceedingly fast cell cycle to generate the requisite number of cells for the onset of early gastrulation events (Edgar and McGhee 1988; Kermi, Lo

Furno, and Maiorano 2017; Graham 1966b, 1966a; Takada and Cha 2011). Mouse embryonic stem cells (mESCs) also display rapid expansion in culture. While they maintain a G2 phase and S phase length similar to that of differentiated mouse somatic cells, the G1 phase is abbreviated (Stead et al. 2002). Their abbreviated G1 phase appears to be due to a constant expression of Cyclin E, Cyclin A, and Cdk2, allowing these cells to rapidly enter S phase (White and Dalton 2005; Stead et al. 2002) (Figure 11). Accordingly, they do not appear to engage the G1/S checkpoint in response to DNA damage, only the G2/M checkpoint (Chuykin et al. 2008; Hirao et al. 2000). While p53 is expressed in these cells, it isn't stabilized in response to DNA damage (Chuykin et al. 2008). Thus, some cells may not utilize all aspects of the regulation above.

1.2.8 Cell cycle structure of the *C. elegans* GSCs

In adult *C. elegans* GSCs, the cell cycle structure and its regulation are reminiscent of mESCs. The GSCs cycle continuously and asynchronously. In addition, from BrdU (5-bromo-2'-deoxyuridine) and EdU (5-ethynyl-2'-deoxyuridine) labeling studies, there is no evidence of quiescence in this population (Crittenden et al. 2006; Fox et al. 2011). The cell cycle structure and regulation of GSCs appear to be similar throughout the progenitor zone. With the total cell cycle length ranging from 8 – 12 hours depending on the study, a majority of the cells are in S phase (~60-70%) with a very low percentage in either M or G1 phase (~5% each) (Crittenden et al. 2006; Fox et al. 2011). Analysis of cell cycle regulators has shown that there is constant expression of Cyclin E (*cye-1*) and Cdk2 (*cdk-2*), and CDK-2 appears to be active in all cells (Fox et al. 2011; Brodigan et al. 2003). Active CDK-2 is required for cell cycle progression since RNAi of *cye-1* and *cdk-2* lead to a cell cycle arrest (Fay and Han 2000; Fox et al. 2011; Furuta et al. 2018). However, the sole Cdk4/6 homolog, *cdk-4*, is not required for

cell cycle progression in the germline (Fox et al. 2011). Therefore, it is likely that constant CDK-2 activity promotes the short G1 and that the normal G1 regulators are unnecessary. Depletion of the Cdk1 homolog (*cdk-1*) also results in cell cycle arrest, so it is likely required for the G2/M transition in addition to the G1/S transition (Boxem, Srinivasan, and van den Heuvel 1999).

Along those lines, DNA damage signaling is functional in GSCs as well. IR and UV damage each lead to cell cycle arrest in GSCs (Gartner et al. 2000; Stergiou et al. 2007). IR and UV treatments result in an increase in apoptosis in the germline during meiosis, though to date there is no evidence of cell death within the GSC population. Moreover, similar to the mammalian context, deletion of the Atm homolog (*atm-1*) appears to abrogate the IR arrest, whereas deletion of the Atr homolog (*atl-1*) will abrogate both the IR and UV induced cell cycle arrest (Garcia-Muse and Boulton 2005; Lee et al. 2010). However, the IR-induced arrest is not abrogated by deletion of the p53 homolog (*cep-1*) supporting the lack of an active G1/S checkpoint in these cells (Schumacher et al. 2001). While it is important to regulate the cell cycle in response to DNA damage, raw materials in the form of nutrients are required for any cell growth to occur. Therefore, eukaryotic cells have developed additional signaling pathways to detect internal and external nutrient and metabolite availability.

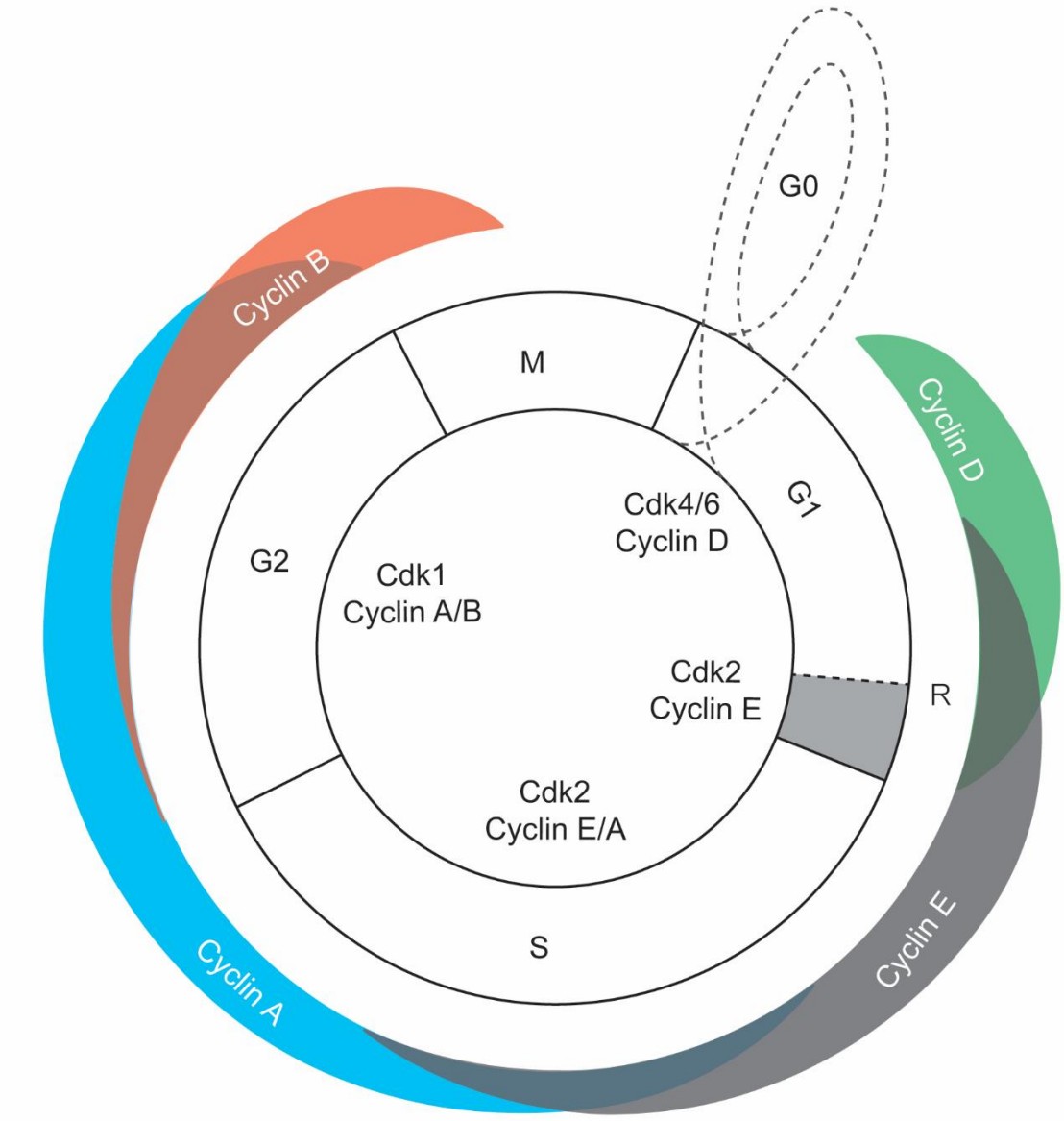

Figure 6: Cyclin and CDK regulation of the mammalian cell cycle

Overview of the mammalian cell cycle. Cells which do not receive mitogens will exit into a G0 (quiescent) state. Cyclins are expressed temporally to activate their partner CDK. Towards the end of G1, as cells pass the restriction point (R) they are committed to the cell cycle and no longer require mitogens.

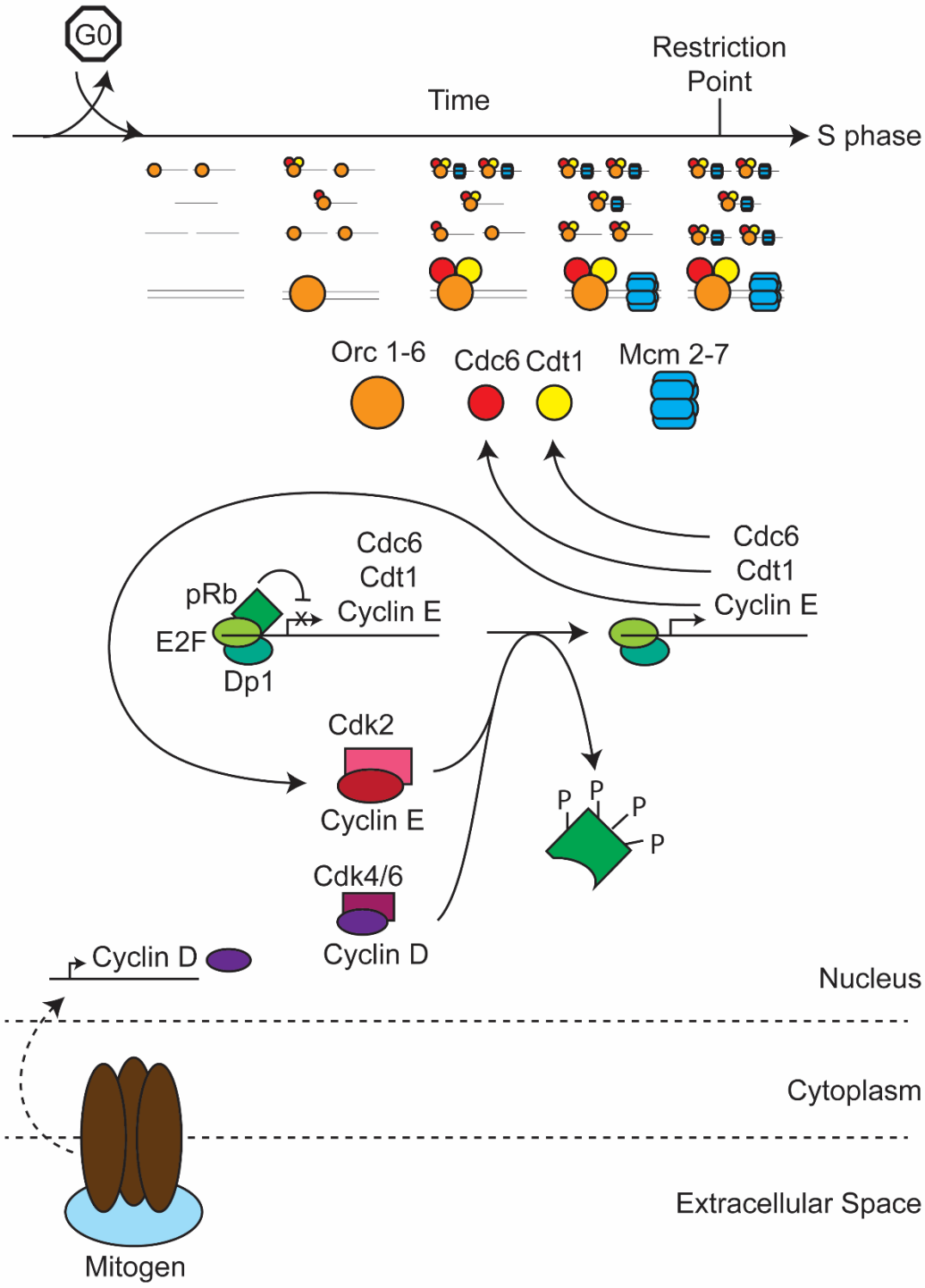

Figure 7: Mammalian G1 regulation

Overview of G1 regulation in mammalian cells. In response to mitogens, Cyclin D levels rise and pRb is inhibited, promoting cell cycle regulator transcription in a positive feedback loop leading to increased pRb inhibition. Cells license the DNA for replication.

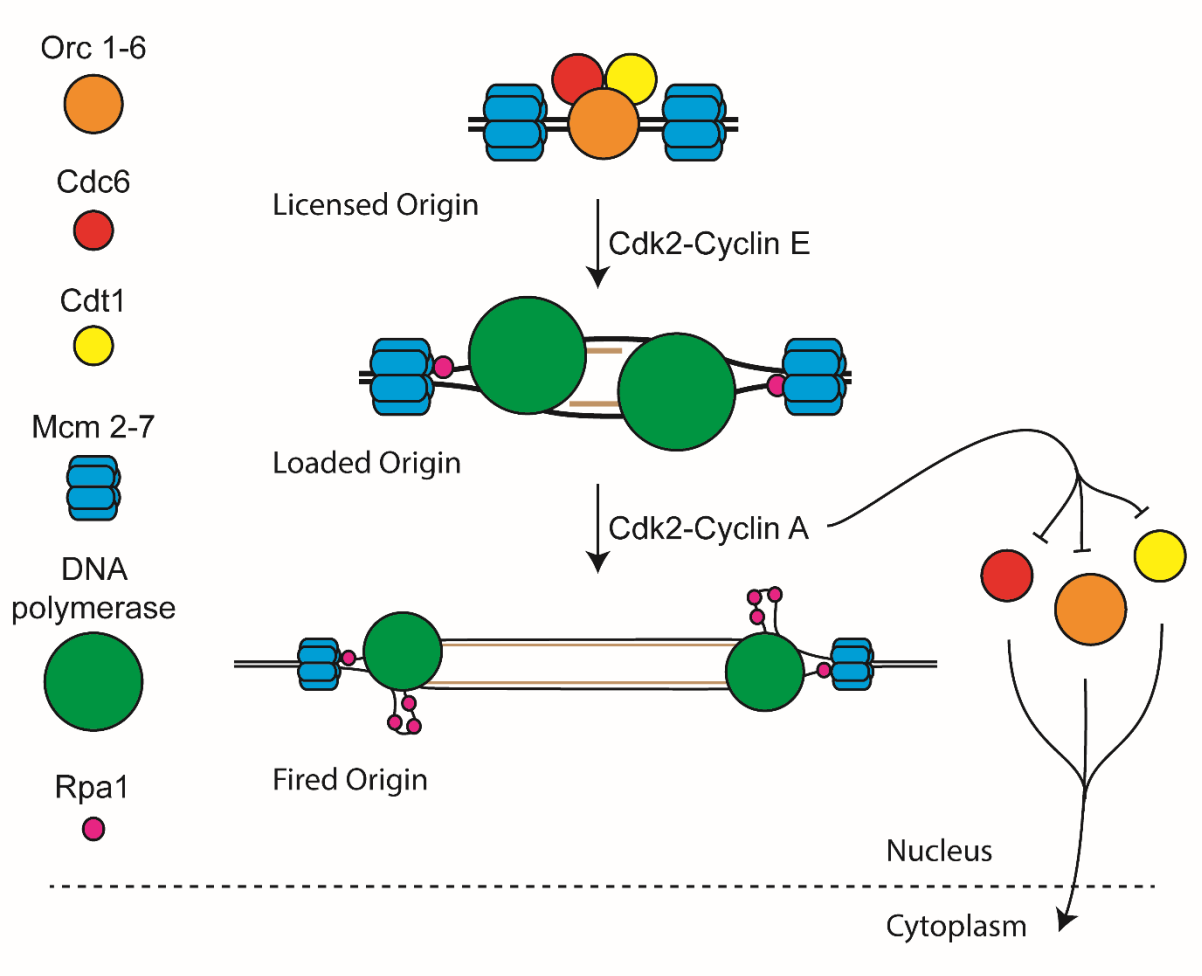

Figure 8: The role of Cdk2 in regulating DNA replication

Cdk2-Cyclin E activity promotes loading of the DNA polymerase and other replication factors. Cdk2-Cyclin A activity promotes elongation of the nascent DNA strands while inhibiting re-licensing by export of DNA licensing factors.

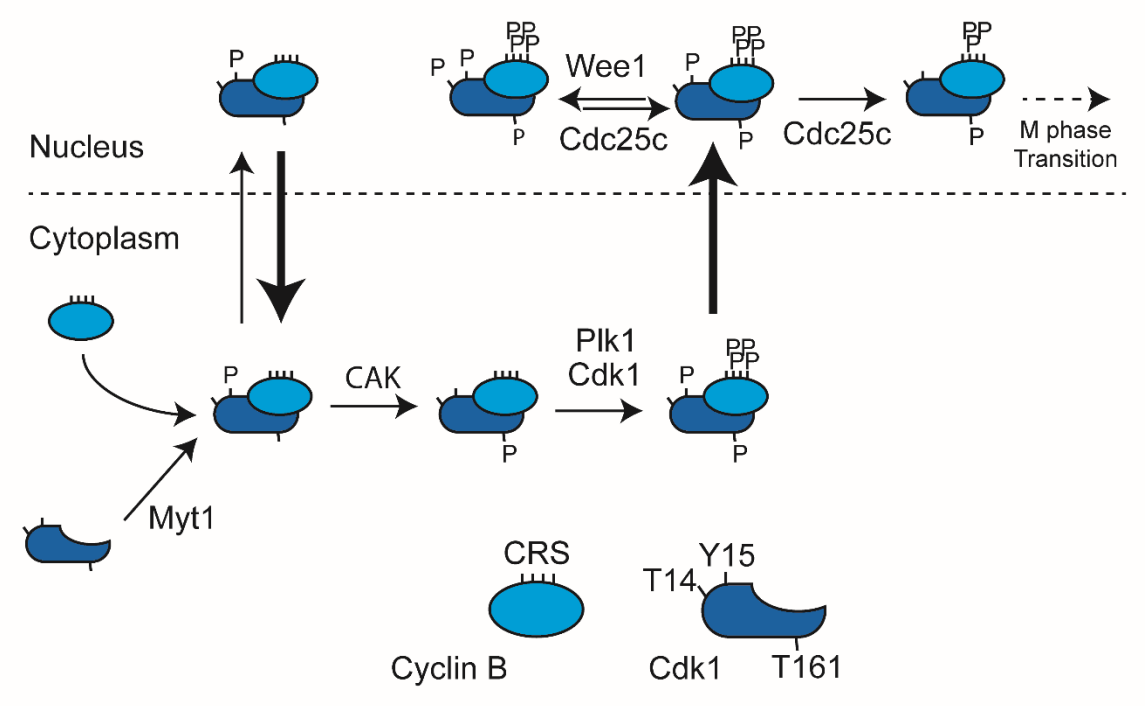

Figure 9: Cdk1 Regulation at the G2/M boundary

Cdk1-Cyclin B activity and nuclear localization is regulated by a number of phosphorylation and de-phosphorylation events. Phosphorylation on T14 and/or Y15 of Cdk1 are inhibitory. Phosphorylation on T161 of Cdk1 results in its activation. Phosphorylation on the CRS of Cyclin B is required for nuclear localization of the Cdk1-Cyclin B complex.

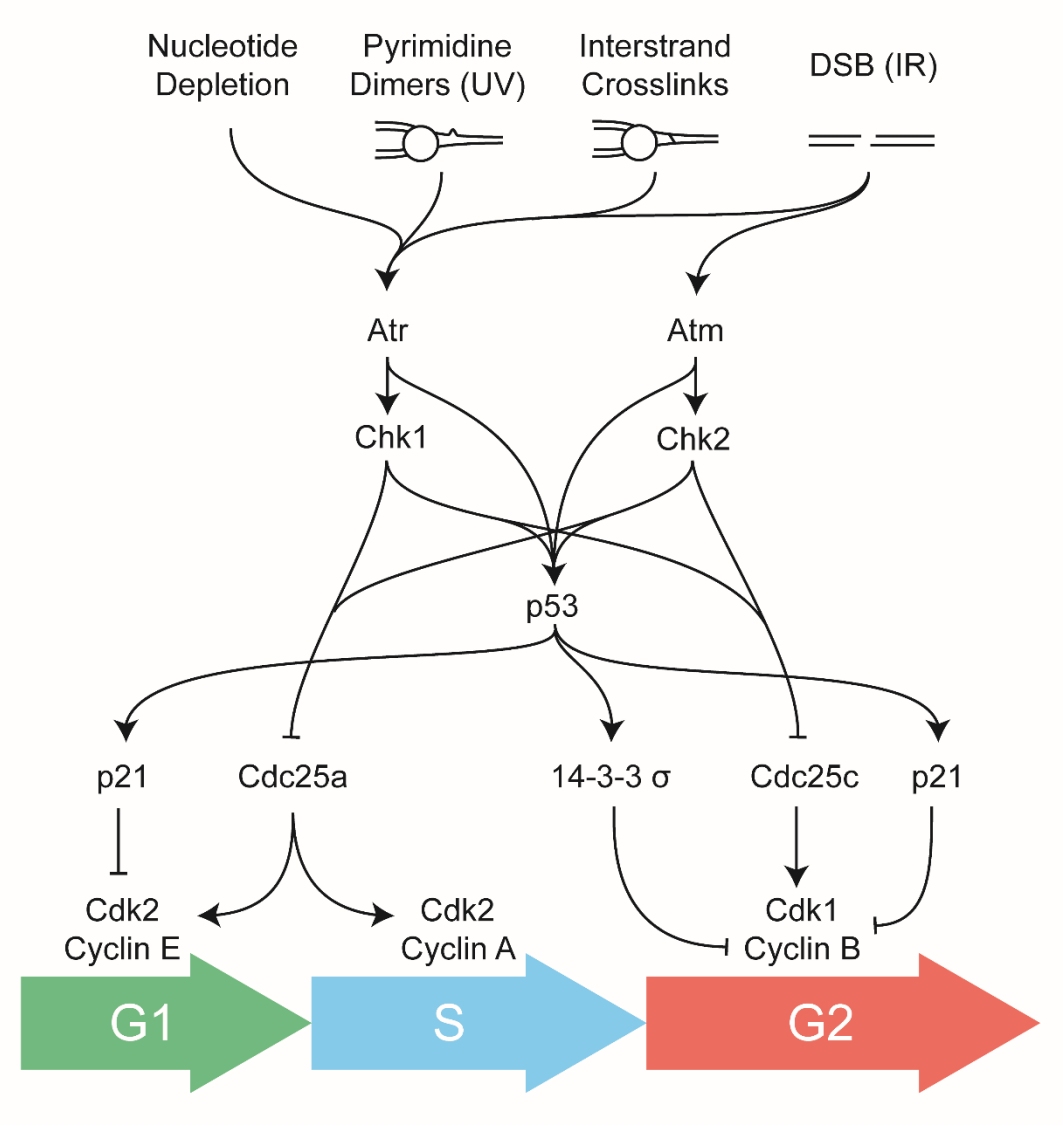

Figure 10: Cell cycle control by DNA damage signaling

Overview of cell cycle control in response to DNA damage at different cell cycle stages.

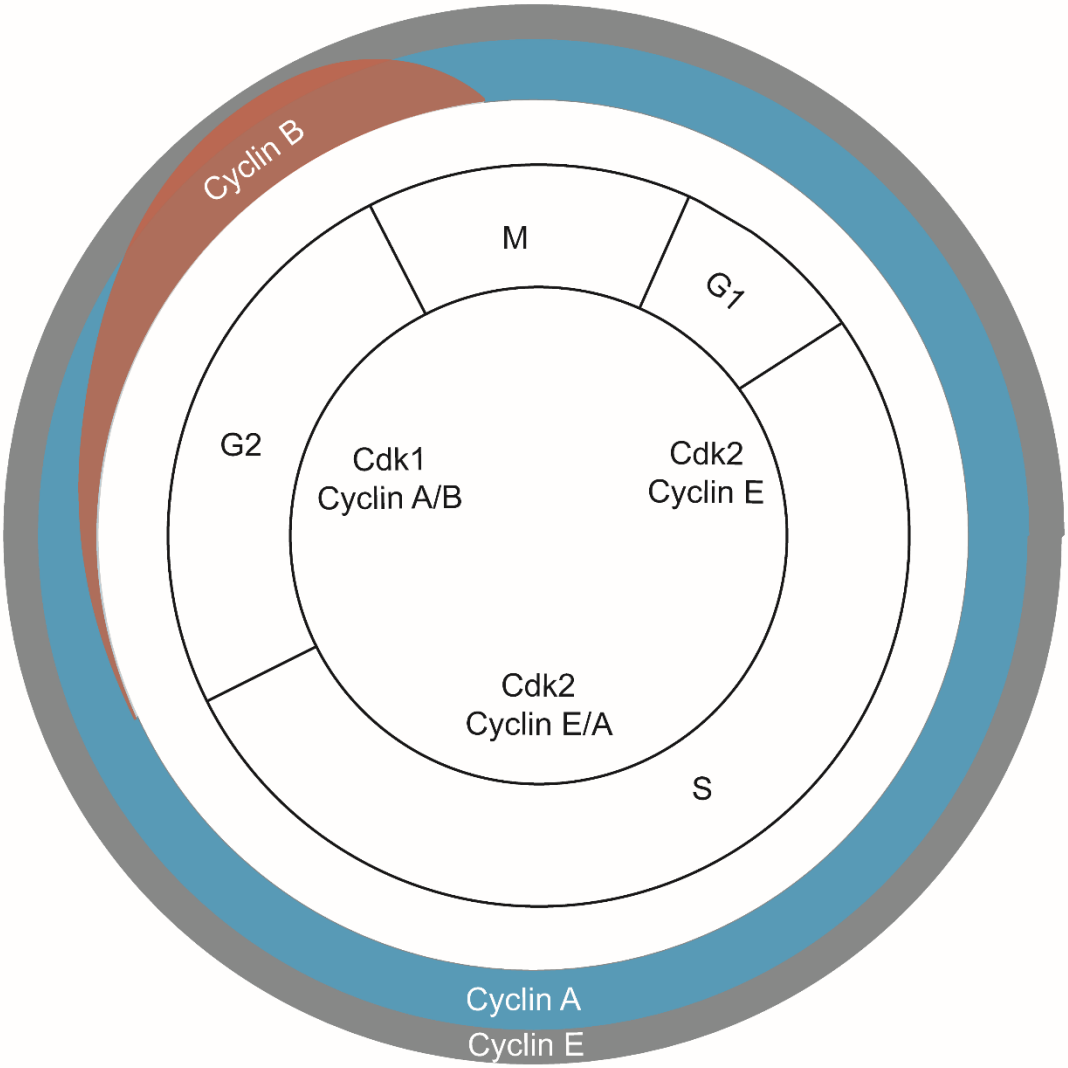

Figure 11: Altered cell cycle regulation in mESCs

Overview of cell cycle phase proportions and cyclin expression in mESCs.

1.3 Metabolic and Nutritional Regulation

For organisms to survive, it is necessary to receive a constant influx of nutrients. These nutrients are necessary to sustain tissues and cells in a working state. If this need is not met, it can result in harm to the organism's tissues and cells. Therefore, it is important for an organism to be able to sense its environment and determine whether those nutrients are available. In response to such signals, cells and tissues modulate their cellular behavior to adapt to the environment and nutritional availability. One organism which has evolved a number of methods of adjusting to a lack of external nutrients is *C. elegans*. For example, during early larval development, lack of nutrients or overcrowding drives the animal into an alternate developmental state termed "dauer". In this state, the animals are metabolically repressed and can sustain long periods of starvation. Return to normal nutritional conditions results in reentry of the dauer stage animals into L4 and normal development ensues. GSCs, like the somatic cells, have also developed methods to adapt to nutrient availability. Under replete conditions, the *C. elegans* GSCs are constantly dividing. The GSCs adjust to changes in nutrient availability in a rapid manner, making it a good model system to study the effects of starvation on continuously dividing populations of cells. In *C. elegans* GSCs, most nutritional signaling appears to pass through either an insulin – PI3K (Phosphoinositide 3 Kinase) – AKT (Thymoma viral proto-oncogene) signaling axis or TOR (Target of rapamycin) signaling (Figure 12). Therefore, I will focus on those two pathways for this chapter.

1.3.1: Insulin Signaling

Insulins and insulin-like peptides are a class of metabolic signaling peptides which promote the uptake and storage of systemic glucose as glycogen (Fukumoto et al.

1989; Suzuki and Kono 1980). Binding of insulin to the insulin receptor activates a number of signaling pathways involved in metabolism, cell growth and proliferation (Reviewed in De Meyts 2000; Reviewed in Taniguchi, Emanuelli, and Kahn 2006). The insulin receptor is a receptor tyrosine kinase (RTK) which functions as an α2β2 tetramer (Olson, Bamberger, and Lane 1988; Schenker and Kohanski 1991). The insulin receptor gene encodes both subunits, with the α-subunit responsible for ligand binding, and the β-subunit responsible for kinase activity (Deutsch et al. 1983; Kasuga, Hedo, et al. 1982; Pilch and Czech 1979; Shia and Pilch 1983; Yip, Moule, and Yeung 1982). Upon insulin binding, it auto-phosphorylates on intracellular tyrosine residues leading to its activation (Kasuga, Zick, Blith, et al. 1982; Kasuga, Zick, Blithe, et al. 1982; Rosen et al. 1983; Van Obberghen et al. 1983). In mammals, this leads to phosphorylation of the insulin-receptor substrate (IRS) proteins which become adapters and activate downstream signaling complexes. Activation of these adapters recruits and activates downstream signaling modules including the PI3K-AKT signaling axis.

1.3.2: The PI3K-AKT signaling axis

Phosphoinositide 3 kinases (PI3Ks) are activated in response to a variety of G-protein coupled receptors (GPCRs) and RTKs (Reviewed in Vanhaesebroeck et al. 2010). PI3Ks are heterodimers that are made up of a regulatory and a catalytic subunit. They are activated by protein-protein interactions through recruitment to an activated signaling adapter (Klippel et al. 1996). In response to activation, PI3Ks phosphorylate PIP_2 (Phosphatidylinositol 4,5-diphosphate) to produce PIP_3 (Phosphatidylinositol 3,4,5-triphosphate) (Reviewed in Vanhaesebroeck et al. 2010). Pten (Phosphatase and tensin homolog) negatively regulates this activity by dephosphorylating PIP_3 to PIP_2. PIP_3 functions as a second messenger and activates a number of proteins with PIP_3-

recognition domains including AKT (Franke et al. 1995). AKTs are serine-threonine kinases which are recruited to the membrane through their PIP_3 binding domains and are subsequently activated by phosphoinositide-dependent kinase 1 (Alessi et al. 1997). Upon activation, AKTs will phosphorylate and inactivate multiple downstream effectors such as the FOXO (Forkhead box O) transcription factors, Gsk3β (Glycogen synthase kinase 3 beta), and Tsc2 (Tuberous sclerosis 2), which forms a complex with Tsc1 (Tuberous sclerosis 1), hereafter referred to as the TSC. The FOXO transcription factors are involved in regulating a number of cellular processes such as cell cycle control, stress response, and apoptosis (Reviewed in Tran et al. 2003). Gsk3β and the TSC both regulate TOR signaling in mammals.

1.3.3: TOR Signaling

Mtor (Mechanistic target of rapamycin) is a serine-threonine kinase which mediates TOR signaling in its response to energy, nutrient, and metabolite cues by regulating cell growth, proliferation, survival and metabolism (Reviewed in Saxton and Sabatini 2017). Mtor functions in two separate complexes designated TORC1 (Mtor, Rptor (Regulatory associated protein of MTOR, complex 1), and Mlst8 (MTOR associated protein LST8 homolog (*S. cerevisiae*))) and TORC2 (Mtor, Rictor (RPTOR independent companion of MTOR, complex 2), mLST8, Mapkap1 (Mitogen-activated protein kinase associated protein 1), and either Prr5 (Proline rich 5 (renal)) or Prr5l (Proline rich 5 like)).

The TORC2 complex recognizes PIP_3 through its Mapkap1 cofactor, leading to activation and regulation of cell survival and proliferation (Jacinto et al. 2006). Many of its functions are executed through phosphorylation of AKT (Sarbassov et al. 2005). However, this activating phosphorylation appears important only for certain substrates of AKT. For example, phosphorylation of AKT downstream to TORC2 is required for

phosphorylation and inactivation of the FOXO transcription factors, but does not affect Tsc2 phosphorylation (Guertin et al. 2006; Jacinto et al. 2006). Thus, TORC2 activation of AKT does not affect TORC1.

The TORC1 complex utilizes the Rheb (Ras homolog enriched in brain) GTPase to activate and regulate autophagy, metabolism, and protein synthesis. In mammals, a large pool of Rheb protein is thought to be bound to the lysosome, and so recruitment of TORC1 to the lysosome plays a large role in its activation (Inoki et al. 2003; Tee et al. 2003). From work in mammals, Rag (recombination activating) GTPase activity recruits TORC1 to the lysosomal surface in response to amino acid sensing proteins. Activation of TORC1 leads to phosphorylation of its downstream effectors some of which include p70s6k (ribosomal protein S6 kinase, polypeptide 1), Eif4ebp (Eukaryotic translation initiation factor 4E binding protein), Atg14 (Autophagy related 14), and Hif1a (Hypoxia inducible factor 1, alpha subunit)).

However, activation of TORC1 requires more than amino acid sensing. Other upstream signals from energy status (by sensing ATP) and growth factor signaling are required for full TORC1 activation. Low energy status, as well as hypoxia and DNA damage, is sensed by AMPK (AMP-activated protein kinase) and can either directly regulate TORC1 by phosphorylation and inhibition of Rptor, or by phosphorylation and activation of Tsc2 (Gwinn et al. 2008; Inoki, Zhu, and Guan 2003; Feng et al. 2007; Brugarolas et al. 2004). Tsc2, which is downstream to the Insulin-PI3K-AKT signaling axis, inhibits Rheb through the TSC which subsequently inhibits TORC1 activation (Inoki et al. 2003; Menon et al. 2014; Tee et al. 2003). Phosphorylation of Tsc2 dissociates it from Tsc1 and the lysosomal surface, allowing Rheb to activate TORC1 (Menon et al. 2014). Other regulators of the TSC include the Ras-MAPK (Mitogen associated protein kinase) pathway and Gsk3β.

1.3.4: Gsk3β

Gsk3β functions in several signaling pathways, such as the insulin, TOR and Wnt pathways, to regulate proliferation, differentiation, and apoptosis (Bouskila et al. 2008; Campbell et al. 2012; McManus et al. 2005; Parisi et al. 2011), in addition to its original role of inhibiting glycogen synthase (Larner et al. 1968; Rylatt et al. 1980). This poises Gsk3β as an integrator of various signaling pathways. Gsk3β is a serine-threonine kinase which is constitutively active when first translated. Phosphorylation events thus inactivate Gsk3β unlike most other kinases, where phosphorylations are necessary for their activity (Jope and Johnson 2004). Specifically, phosphorylation on Ser-9 on the N-terminus by various kinases, such as AKT and p70s6k, will inhibit the kinase. Since Gsk3β phosphorylates its substrates on serines or threonines which are 3-5 amino acids away from a phosphorylation, phosphorylated Ser-9 functions as bait, blocking the kinase binding pocket and preventing other substrates from binding.

1.3.5: Nutritional Signaling in cell cycle regulation in yeast, flies and vertebrate systems

Downstream from the insulin receptor, the Ras-MAPK pathway is well known for activating Cyclin D transcription resulting in G1 progression as previously discussed (Chapter 1.2.2). Additionally, the PI3K-AKT module appears to promote G1 progression as well by increase Cyclin D and Cyclin E expression in response to insulin-like growth factors (Mairet-Coello, Tury, and DiCicco-Bloom 2009). Similarly, TOR signaling regulates the G1 phase of the cell cycle as well.

From studies in yeast and mammalian cell culture, downregulation of, or mutations in, Mtor and its downstream effectors result in a G1 arrest (Abraham and Wiederrecht 1996; Fingar et al. 2004; Rohde, Heitman, and Cardenas 2001). However, in

embryonic stem cells, removal of the downstream effector p70s6k only affects proliferation rate mildly suggesting a different regulation (Kawasome et al. 1998). Additionally, there is evidence for the involvement of nutritional signaling in G2 regulation as well.

In *Drosophila* germ cells, there is evidence that Insulin signaling and TOR signaling independently regulate G2 (Hsu, LaFever, and Drummond-Barbosa 2008; LaFever et al. 2010). In fission yeast, the Mtor homolog for the TORC1 complex, Tor1, signals through stress kinases to regulate Cdc25 (Lopez-Aviles et al. 2008; Lopez-Aviles et al. 2005). In budding yeast, Tor1 signals through PP2A (Protein phosphatase 2) which is required for polo-like kinase translocation into the nucleus, driving mitotic progression (Nakashima et al. 2008). This provides a link between TOR signaling and cell cycle regulators.

1.3.6: Nutritional Signaling in *C. elegans*

C. elegans is a free-living nematode that is often found on rotting fruits and is uniquely sensitive to nutritional availability in its surroundings. It has evolved a number of adaptations to deal with a lack of nutrients, including cell cycle arrest of the PGCs (Fukuyama, Rougvie, and Rothman 2006), and an alternate developmental stage named dauer (Golden and Riddle 1984). Upon hatching, if no nutrients are available, the PGCs maintain a G2 arrest until food is available. If nutrition becomes unavailable during L2 stage of development, the worm enters the alternate developmental pathway-dauer. As a dauer, *C. elegans* can survive for months without food, and when replete conditions are available, it will molt into an L4 and continue its development (Golden and Riddle 1984). Thus, nutritional signaling plays important roles for the survival of this organism.

Most of the nutritional signaling components described above are conserved in *C. elegans* (Table 1) with a few exceptions. While the *C. elegans* insulin receptor homolog (*daf-2*) appears to have a similar gene structure for encoding the receptor, DAF-2 has a C-terminal extension which may function as a signaling adapter similar to the IRS proteins (Kimura et al. 1997). Although there are functional IRS homologs in *C. elegans* (*ist-1*, *aap-1*), these are not necessary for dauer formation, suggesting that *daf-2* itself may be able to function as the signaling adapter for the PI3K homolog *age-1* (Munoz and Riddle 2003). In addition, *C. elegans* does not generate insulin. Instead, 40 different insulin-like peptides are secreted from the sensory neurons to regulate the insulin receptor and mediate its effects (Li, Kennedy, and Ruvkun 2003; Kawano et al. 2000; Duret et al. 1998; Pierce et al. 2001).

Links between Insulin signaling and TOR signaling are few. To date, no Tsc1 or Tsc2 homologs have been identified in *C. elegans*. Since the TSC forms a major link between Insulin signaling and TORC1 in mammals, this suggests that the Insulin signaling and TOR signaling may not crosstalk in *C. elegans*. Similarly, there is little evidence that TORC2 functions through AKT. Mutations in the Rictor homolog *rict-1* produce a number of phenotypes such as increased fat storage, and small animal size (Jones et al. 2009; Soukas et al. 2009). However, while the increased fat storage phenotype is observed in the AKT homolog, *akt-1* or *akt-2*, mutants, the phenotype is enhanced in double mutants with *rict-1*, suggesting that the two pathways function in parallel (Jones et al. 2009; Soukas et al. 2009). One link that does exist, however, is that the FOXO homolog *daf-16* negatively regulates the expression of the Raptor homolog *daf-15* (Jia, Chen, and Riddle 2004). Together, these observations suggest that Insulin signaling and TOR signaling may function relatively separately in *C.elegans* compared to mammals.

1.3.7: Nutritional Signaling in the *C. elegans* germline

In the *C. elegans* germline, nutritional signaling has been shown to regulate both developing oocytes as well as GSCs. In developing oocytes, the insulin receptor *daf-2* provides the signal to activate *let-60-mpk-1* (Ras-Mapk1) signaling to control oocyte production (Lopez et al. 2013b). In larval GSCs, mutation of the *daf-2* receptor results in decreased proliferation in a *daf-16* dependent manner (Michaelson et al. 2010). In a study on the TOR signaling downstream effector *rsks-1* (p70s6k), it was found that *daf-2rsks-1* double mutants enhanced the *rsks-1* single mutant phenotype for low GSC proliferation in larval stage L4 animals which suggests that Insulin signaling and TOR signaling drive proliferation in parallel pathways. (Korta, Tuck, and Hubbard 2012). Together, these studies raise the possibility that nutritional signaling may control the cell cycle in *C. elegans* GSCs. The mechanisms that mediate this remain unknown.

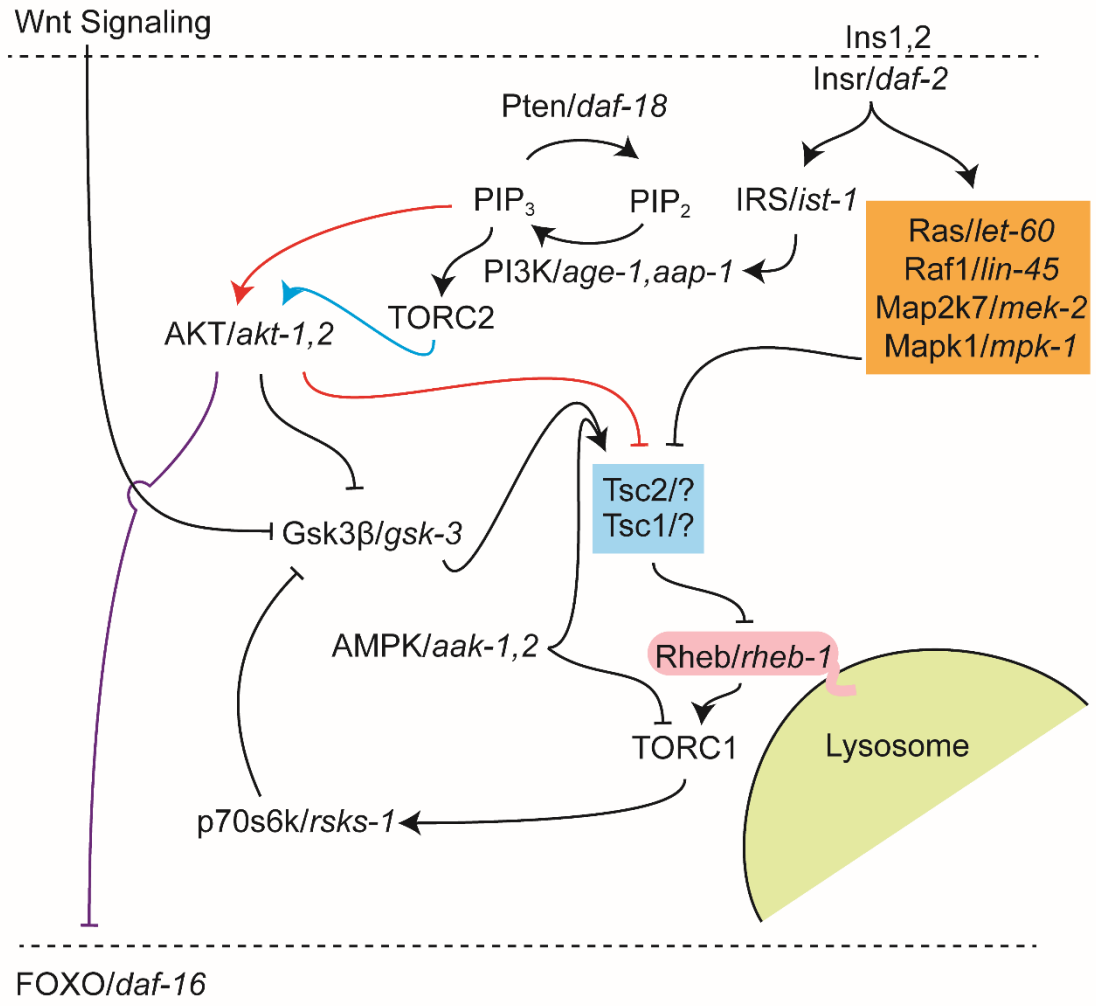

Figure 12: The Insulin and TOR nutritional signaling network

Overview of common nutritional signaling network components and their connectivity. Red and blue arrows depict different inputs into AKT, which produce different responses. The blue input produces only the purple response, while the red input produces both red and purple responses.

Mouse	*C. elegans*
Ins1, Ins2	*ins-3,4,6,9,19,32, daf-28*
Insr	*daf-2*
Irs1, Irs2, Irs3, Irs4	*ist-1, aap-1*
PI3K regulatory Pik3r1, Pik3r2, Pik3r3, Pik3r4, Pik3r5, Pik3r6	*aap-1*
PI3K catalytic Pik3ca, Pik3cb, Pik3cd, Pik3cg	*age-1*
Akt1, Akt2, Akt3	*akt-1,akt-2*
Pten	*daf-18*
Foxo1, Foxo3, Foxo4, Foxo6	*daf-16*
Tsc1	?
Tsc2	?
AMPK - Prkaa1, Prkaa2	*aak-1, aak-2*
Gsk3β	*gsk-3*
Mtor	*let-363*
Rictor	*rict-1*
Rptor	*daf-15*
Mlst8	*mlst-8*
p70s6k	*rsks-1*
Eif4ebp	?

Table 1: Nutritional signaling homologs in *C. elegans*

Table listing the mouse nutritional signaling components on the left, and their *C. elegans* homologs on the right. Question marks denote that there is no known homolog in *C. elegans*.

CHAPTER 2: MATERIALS AND METHODS

Chapter 2: Materials and Methods

Some of the contents of this chapter are reproduced/adapted with permission from "Furuta et al. 2018" with permission from Development (http://www.biologists.com/development).

Full citation:

Furuta, T., H. J. Joo, K. A. Trimmer, S. Y. Chen, and S. Arur. 2018. 'GSK-3 promotes S-phase entry and progression in *C. elegans* germline stem cells to maintain tissue output', Development, 145, doi: 10.1242/dev.161042

2.1: Materials

2.1.1: Chemicals and Buffers

Chemicals	Information
Hydroxyurea	(Sigma-Aldrich, cat. no. H8627)
16% Paraformaldehyde	(Electron Microscopy Sciences, cat. no. 15710)
3% Paraformaldehyde	20% (v/v) 16% Paraformaldehyde in (0.1M) Potassium Phosphate buffer at pH 7.2
Methanol	(Electron Microscopy Sciences, cat. no. 18510)
30% Normal Goat Serum	
DAPI	(Sigma-Aldrich, cat. no. D9542
K_2HPO_4 (pH 7.2)	(SIGMA-ALDRICH, cat. no. P3786)
1x PBS	(SIGMA Life Science, cat. no. P2194)
Tween 20	(Fischer Scientific, cat. no. BP337-500)
M9 buffer	(Stiernagle 2006) (3 g KH_2PO_4, 6 g Na_2HPO_4, 5 g NaCl, 1 ml 1 M $MgSO_4$, H_2O to 1 liter. Sterilize by autoclaving.)
Sterile M9T	M9 Buffer with 0.1% Tween sterilized using a 0.22µm filter

Click-iT® Plus EdU Alexa Fluor® 594 Imaging Kit	(ThermoFisher Scientific, cat# C10639)
Alexa Fluor 647 picolyl azide	(ThermoFisher Scientific, cat# A10277)

Cupric Sulfate	(Sigma-Aldrich, cat. no. C-7631)
Proteinase K	(10 mg/mL) (Roche, cat. no. 3115879001)
Worm lysis buffer	5% (v/v)10mg/mL Proteinase K in 1X PCR buffer
Apex Hot Start Taq BLUE Master Mix, 2X	(Genesee Scientifitc, cat. no. 42-143)
Agarose	(Sigma-Aldrich, cat. no. A6877
Ethidium Bromide	(Sigma-Aldrich, cat. no. 46067)
L-Lysine-monoHCL	(Sigma-Aldrich, cat. no. L-9037)
Sodium Periodate ($NaIO_4$)	(Sigma-Aldrich, cat. no. S1878)
Vectashield Anti-fade	(Vector Labs, cat. no. H-1000)

2.1.2: *C. elegans* Strains and Culture

Strains were made and handled using standard methods (Brenner 1974).

Strains used in this study:

Strain	Genotype
N2	Wildtype
AUM1239	naSi2[mex-5p>mCherry::his51::nos-2 3'UTR>GFP::his-51::nos-2 3'UTR] II; (? - unc-119 [ed3]) III.
AUM1246	naSi2 [pmex-5>mCh::his-51::nos-2 3' UTR>GFP::his-51::nos-2 3'UTR] (II); qIs56 (plag-2::GFP::lag-2 3'UTR) (V)
EG4322	*ttTi5605 II*; *unc-119(ed3) III*
EG8082	*unc-119(ed3) III*; *oxTi365 V*
AUM1012	*gsk-3(nr2047)/hT2[bli-4(e937)let-?(q782) qIs48] I; unc-119(ed3)III/ hT2 [bli-4(e937)let-?(q782) qIs48] (I; III)*
AUM1054	*gsk-3(tm2223) I/ hT2 [bli-4(e937)let-?(q782) qIs48] (I; III)*
BS121	*glp-1(bn18ts) III*
BS3148	*glp-1(ar202ts) III*
AUM1081	*gsk-3(tm2223) I/ hT2[bli-4(e937)let-?(q782)qIs48] (I;III)*. Line 1
AUM1082	*gsk-3(tm2223) I/ hT2[bli-4(e937)let-?(q782)qIs48] (I;III)*. Line 2
AUM1260	*gsk-3(nr2047)/oxTi398 I*
AUM1262	*gsk-3(nr2047)/oxTi398 I; gtIs64[mcm-3::GFP]; odIs57[Ppie-1::mCherry::H2B].* Line 1
AUM1266	*gsk-3(nr2047)/oxTi398 I; gtIs64[mcm-3::GFP]; odIs57[Ppie-1::mCherry::H2B].* Line 2
AUM1279	*gsk-3(nr2047)/ oxTi398 I*; *ddIs30[Ppie-1::YFP::CDK-2]*
AUM2026	*gsk-3(nr2047)I;unc-119(ed3) III*; *vizIs26[Ppie-1::GFP::GSK-3*(WT)::*pie-1* 3'UTR *unc-119(+)]*

AUM2027	*gsk-3(nr2047)I;unc-119(ed3) III*; *vizIs27[Ppie-1::GFP::GSK-3*(WT)::*pie-1* 3'UTR *unc-119(+)]*
AUM2028	*gsk-3(nr2047)I;unc-119(ed3) III*; *vizIs28[Ppie-1::GFP::GSK-3*(WT)::*pie-1* 3'UTR *unc-119(+)]*
AUM2029	*gsk-3(nr2047)I;unc-119(ed3) III*; *visIs29[Ppie-1::GFP::GSK-3*(WT)::*pie-1* 3'UTR *unc-119(+)]*
AUM2083	*vizSi44 [Pmex-5::GFP::GSK-3*(WT)::*tbb-2 3'UTR unc-119(+)] *ttTi5605 II; unc-119(ed3) III*
AUM2059	*vizSi20[Pmex-5::GFP::GSK-3* [K65A,E77A,D180A,D161A]::*gsk-3* 3'UTR*] *ttTi5605 II; unc-119(ed3)III*
AUM1295	*gsk-3(nr2047)/ hT2 [bli-4(e937)let-?(q782) qIs48] I; vizSi20[Pmex-5::GFP::GSK-3* [K65A,E77A,D180A,D161A]::*gsk-3* 3'UTR*] *ttTi5605 II; unc-119(ed3)/hT2 [bli-4(e937)let-?(q782) qIs48]III*
TG1753	*unc-119(ed3) III; gtIs64 [pie-1p::GFP(lap)::mcm-3 + unc-119(+)] ltIs37 [pie-1p::mCherry::his-58 + unc-119(+)]*
TH98	*unc-119(ed3) III; ddIs30 [Ppie-1::YFP::CDK-2 (K03e5.3a) unc-119(+)] II*
WM69	*gsk-3(nr2047) I/ hT2 [bli-4(e937)let-?(q782) qIs48)] (I; III)*
AUM1294	*gsk-3(nr2047) I/ hT2 [bli-4(e937)let-?(q782) qIs48)] (I; III);glp-1(ar202ts)III/hT2 [bli-4(e937)let-?(q782) qIs48)] (I; III)*
AUM1293	*gsk-3(nr2047) I/ hT2*[*bli-4(e937)let-?(q782) qIs48)*] *(I; III); glp-1(bn18ts) III/ hT2 [bli-4(e937)let-?(q782) qIs48)] (I; III);*
EG7843	*ttTi398 [Peft-3::tdTomato::H2B::unc-54* 3'UTR *Cbr-unc-119(+)]*
EG7844	*ttTi413 [Peft-3::tdTomato::H2B::unc-54* 3'UTR *Cbr-unc-119(+)]*
AUM2073	*vizSi34 [cdk-2[Promoter]::NLS::GFP::tbb-2* 3' UTR] **ttTi5605 II*; *unc-119(ed3) III*
AUM2071	*unc-119(ed3)*;*vizSi32[cdk-2[Intron1]::NLS::GFP::tbb-2* 3'UTR*] *oxTi365 V*
AUM1339	*gsk-3(nr2047) I / ht2 [bli-4(e937)let-?(q782) qIs48)] (I; III);vizSi32 [cdk-2[Intron1] ::NLS::GFP::tbb-2* 3'UTR*] *oxTi365 V*
JJ2213	*zuIs252[Pnmy-21::PGL-1::mRFP; unc119(+)] unc119(ed3)III*
AUM1076	*gsk-3(nr2047) I / ht2 [bli-4(e937)let-?(q782) qIs48)] (I; III); zuIs252[Pnmy-21::PGL-1::mRFP; unc119(+)] unc119(ed3)III*
AUM1079	*gsk-3(tm2223) I / ht2 [bli-4(e937)let-?(q782) qIs48)] (I; III); zuIs252[Pnmy-21::PGL-1::mRFP; unc119(+)] unc119(ed3)III*
VC381	*atm-1(gk186) I*
DW101	*atl-1(tm853) V/nT1 [unc-?(n754) let-? qIs50] (IV;V)*
AUM1449	*atm-1(gk186) (I); naSi2 (II); atl-1(tm853)/tmC12(V)*
CB1370	*daf-2(e1370) III*
AUM1018	*rsks-1(ok1255)/hT2 GFP [bli-4(e937)let-?(q782) qIs48) I; III*
AUM1291	*daf-2(e1370)rsks-1(ok1255) III*
AUM1479	*let-363(viz27[del2196-2287ins5xG])*
EU1062	*sur-6(or550) I*
AUM2082	*vizSi43[Pmex-5::GFP::cdk-1(cDNA)::cdk-1 3'UTR, unc119(+)]*ttTi5605II; unc-119(ed3)III*

KB3	*kgb-1(um3) IV*

2.1.3: Antibodies

The following primary antibodies were used: rabbit anti-HIM-3 (5347.00.02, Sdix) (1:1000); rabbit anti-REC-8 (29470002, Novus); mouse anti-phospho-Histone H3 (Ser10) (05-806, Millipore) (1:500); rabbit anti-GFP (ab6556, Abcam) (1:400); rabbit anti-CYE-1 and anti-CDT-1 were gifts from Dr. Edward T. Kipreos (University of Georgia); guinea pig anti-Lamin was a gift from Dr. Kelly Liu (Cornell University) (1:800); Anti-alpha Tubulin (T9026, Sigma) (1:1000); rabbit anti-CDK-1, a gift from Dr. Jill Schumacher (MD Anderson Cancer Center), was received as serum and IgG purified (1:50); rabbit anti-(pT14pY15) Cdk1 (44686G, Biosource) (1:200); rabbit anti-(pS345) Chk1 (2341, Cell Signaling) (1:400).

The following secondary antibodies were used at (1:1000): donkey anti-mouse Alexa 594 (A21203, ThermoFisher Scientific), goat anti-mouse Alexa Cy5 (A10524, ThermoFisher Scientific), goat anti-mouse Alexa 488 (A21202, ThermoFisher Scientific), goat anti-rabbit Alexa 488 (A11008, ThermoFisher Scientific), donkey anti-rabbit Alexa 594 (A21207, ThermoFisher Scientific), goat anti-guinea pig Alexa 594 (A11026, ThermoFisher Scientific), anti-rabbit HRP (1858415, Pierce Biotechnology), and anti-mouse HRP (1858413, Pierce Biotechnology) secondary antibodies.

2.1.4: Transgenic construction of GFP::GSK-3

To generate a GFP::GSK-3 construct, the *gsk-3* coding region from the start codon to the translation stop was amplified as one PCR product of 5.5 Kb with KOD polymerase (Novagen, Madison, WI), using the following primers:

attb1 GSK-3 ggggacaagtttgtacaaaaaagcaggcttgATGAATAAGCAGTTACTATCGT

attb2 GSK-3 ggggaccactttgtacaagaaagctgggtTTAAGCCGATGGGCCAGCCACA

After amplification from N2 cDNA, the fragment was cloned into the pDONR221 vector of the gateway system using BP reaction. The pDONR plasmid was then sequenced to confirm integrity and recombined into the pID3.02 *pie-1* GFP plasmid (pENTR) containing the *unc-119* transformation marker using the gateway LR reaction to generate pSYC003[P*pie-1::GFP::GSK-3::pie-1* 3'UTR]. Microparticle biolistic transformation was used to create low-copy integrated transgenic lines in *unc-119(ed3)* animals as described (Praitis 2006). Wildtype animals were individually cloned and assayed for integration of the transgene. Six integrated lines were obtained and named *vizIs26, vizIs27, vizIs28, vizIs29, vizIs30* and *vizIs31.*

To generate *mex-5* driven GSK-3 transgenes, the full-length coding region of *gsk-3* was amplified from N2 cDNA and cloned via the Gateway system into pDONR221. The clones were verified for sequence integrity, and combined with P*mex-5::GFP* (pJA245) and the *tbb-23* 3'UTR (pCM1.36). The final clone, *Pmex-5::GFP::GSK-3::tbb-2* 3'UTR, was cloned into the destination vector pCFJ150 via LR clonase reaction. The pSYC001 plasmid, obtained from the LR reaction, was sequence verified for integrity.

Kinase dead GSK-3 was generated by modifying pSYC001 with a series of site-directed mutagenesis using the following primers:

GSK-3_K65A_FP: AAATGAAATGGTTGCAATCgctAAAGTTCTTCA,

GSK3_K65A_RP: GTTTGTCCTGAAGAACTTTagcGATTGCAACCA,

GSK3_E77A_FP: CAAACGATTCAAGAATCGTgctCTACAGATTAT

GSK3_E77A_RP: ATTTTCGCATAATCTGTAGagcACGATTCTTGA

GSK3_D161A_FP: CATTGGAATCTGTCACCGTgctATTAAGCCTCA

GSK3_D161A_RP: GCAAATTCTGAGGCTTAATagcACGGTGACAGA

GSK3_D180A_FP: CGGAGTGCTTAAGCTCTGTgctTTTGGATCTGC

GSK3_D180A_RP: AATATTTGGCAGATCCAAAagcACAGAGCTTAA.

The final GSK-3(KD) pENTR clone pSYC099 was sequenced to verify all the modifications.

To generate *mex-5* driven GSK-3 transgenes, pSYC001(GSK-3(wt)), or pSYC099(GSK-3(KD K65A, E77A, D161A, D180A)) was combined with Pmex-5::GFP (pJA245), *tbb-2* 3'UTR (pCM1.36), and inserted into the pCFJ150 destination vector using the multi fragment gateway system. The final expression constructs pHJJ002(*Pmex-5::GFP::GSK-3(wt)::tbb-2 3'UTR*) or pSYC100 (*Pmex-5::GFP::GSK-3(KD)::tbb-2 3'UTR*) were sequenced for the junctions.

These constructs were injected into EG4322 worms for Chromosome II integration, and selected as described previously (Drake et al. 2014; Zeiser et al. 2011).

2.1.5: CDK-2 transcriptional reporter construction

A 2kb region directly upstream of *cdk-2* exon 1 (Wormbase Ver 258) was amplified for the "promoter" construct using the following primers:

GGGGACAACTTTGTATAGAAAAGTTGATcgcgggaagataagtggagagggag

GGGGACTGCTTTTTTGTACAAACTTGTttttccacttttaaccagcattttt.

1880bp (Wormbase Ver 258) of Intron 1 was amplified using the following primers:

GGGGGACAACTTTGTATAGAAAAGTTGATgtgttacaagttctttgtgcaa

GGGGACTGCTTTTTTGTACAAACTTGTctggaagataattaagattttc.

The amplified fragments were cloned into pDONR P4P1R vector using BP reaction to make pENTR clones, pSYC122, and pSYC111. SV40NLS::GFP with synthetic introns was amplified from pPD95.67 using the following primers:

GgggacaagtttgtacaaaaaagcaggcttgATGACTGCTCCAAAGAAGAAGCG,

ggggaccactttgtacaagaaagctgggtCTATTTGTATAGTTCATCCATGCC

and cloned into the pDONR221 vector. The plasmids were assembled with the *tbb-2* 3'UTR, pCM1.36 and pCFJ150 for MosSCI recombination site using Gateway LR reaction. Final expression plasmids were pSYC112 (Intron *cdk-2*::SV40NLS::GFP::tbb-2 3'UTR MosSCIsite ttTi5605) and pSYC123 (promoter *cdk-2*::SV40NLS::GFP::tbb-2 3'UTR MosSCIsite ttTi5605), sequenced for integrity.

2.1.6: *let-363(viz27[del2196-2287ins5xG])* allele construction

A loss of function allele for *let-363*, was made by removal of the fkbp12-rapamycin binding (FRB) domain using CRISPR. A coCRISPR strategy was based on (Paix, Folkmann, and Seydoux 2017). Two potential CRISPR cut sites flanking the FRB were identified and the corresponding crRNAs ordered from Dharmacon:

TTGTTCGTTGCGCAATTCTG

ACTTGCCACTTTGAACTCGT

The repair template was designed to remove a 381bp segment of genomic DNA corresponding to Trp2196 - Thr2287 of *let-363* and substituting a 5xG linker and introducing a restriction site for StuI. This resulted in an ssODN as shown below with the 5xG linker in red and the silent mutations to introduce the StuI site in lowercase:

GTGACAGAAGAGCTTGTTCGTTGCGCAATTCTGGGAGGAGGTGGaGGccTGAACT

CGTTGGATCTTGTCTACGTATCACCTAATTTGG

The CRISPR injection mixture was injected into N2, and roller F1s were screened for the mutation by PCR using the following primers:

AGTTGAAGTGCGCATATGTAGAA

ACTATTGGAGCTGATGGATCGT

These primers produce a wildtype band of 675bp, a band at 290 if both crRNAs cut without repair, and a band at 309bp for both cuts with repair. 6 lines were isolated with the correct bands, and genomic DNA was sent for sequencing using the primers above. 5 lines returned with the expected sequence.

2.2: Methods

2.2.1: Germline dissection and staining

All animals were dissected as adults at 24 hours past the L4 stage of development, unless otherwise mentioned. Germlines were dissected as described previously (Arur et al. 2011; Arur et al. 2009; Drake et al. 2014; Suen et al. 2013). For antibody staining, dissected germlines were fixed with 3% paraformaldehyde with 100mM K_2HPO_4 (pH 7.2) for 10 min, and post-fixed with 100% methanol at -20°C for at least 30 min. Fixed germlines were blocked with 30% normal goat serum (NGS) at room temperature for 1 hour, and incubated with primary antibodies diluted in 30% NGS at 4°C overnight. After three washes, the germlines were treated with secondary antibodies diluted in 30% NGS at room temperature for 2 hrs. Antibody-treated germlines were then stained with 2µg/ml DAPI (4',6-diamidine-2-phenylindole dihydrochloride) in PBST buffer (8mM Na2HPO4, 150mM NaCl, 2mM KH_2PO_4, 3mM KCl, 0.05% Tween® 20, pH 7.4) for 20 min, washed and finally suspended in 10µl of Vectashield (anti fade agent).

2.2.2: Analysis of germ cell numbers

Cell numbers were counted using ImageJ and a custom macro I wrote. This macro assists the user in counting nuclei with a z-stack when nuclei are present in more than

one slice. Briefly, the user uses the point selection tool to mark nuclei. The macro then counts the cell and puts markers on the surrounding slices at the same (x, y)-coordinates (Fig 13A). This allows the user to view which nuclei have already been marked on a different slice.

2.2.3: EdU Labeling (Feeding)

EdU feeding experiments were performed as described previously (Fox et al. 2011). Briefly MG1693 was grown with 20uM EdU and seeded onto NGM plates. Hermaphrodites were transferred to EdU plates and incubated for either 30 minutes or the amount of time specified. Animals were then dissected and processed for antibody staining.

2.2.4: Development of the EdU Labeling by Soaking

To determine whether soaking adult hermaphroditic worms with the EdU analog allowed for efficient incorporation and detection, I soaked worms for 10 minutes with a series of EdU concentrations (50, 100, 200, 500 µM final concentrations) in M9 buffer with 0.1% Tween (M9T). I found that the concentration of EdU did not affect EdU signal intensity or background (Figure 14), so I proceeded with a concentration of 500 µM in the work described here.

To compare EdU incorporation rate via soaking to the previous feeding EdU method, I performed the 30 minute EdU feeding assay and the 10 minute soaking assay in parallel and compared the percent of EdU labeled cells out of the total proliferative cells, or S phase index. The S phase index measured in germline stem cells was similar between EdU incorporation *via* feeding or soaking (67%±13% and 55%±7% respectively) (mean±SD) (Fig. 13 B, C). The 10-minute soak seems to be a

more accurate representation of the S phase index, since it labeled only those cells that were replicating in a time window of 10 minutes. Overall, these data suggest that soaking the worms for 10 minutes in a solution of EdU is as effective as previous methods at identifying cells in S phase, and provides a rapid and efficient method of EdU incorporation.

2.2.5: Final method used for EdU incorporation by soaking

N2 worms were grown on nematode growth medium (NGM) plates with *E. coli* OP50 bacteria to 24 hours past mid-L4, then washed off plates into 1.5 mL eppendorf tubes using M9T (M9 buffer, 0.1% Tween), washed 2 times with M9T, liquid was removed to 100 µL, and worms were transferred to a well of a flat-bottom 48 well plate. 50 uL of liquid was removed and 50 µL of a 1mM solution of EdU in M9T was added (500µM final) and incubated at room temperature in the dark for 10 or 15 minutes. Following incubation, worms were transferred to 1.5 mL eppendorf tubes and washed once with PBST, followed by either starvation, feeding, or dissection and processing as required.

2.2.6: EdU Processing

After animals were dissected and fixed, germlines were processed using the Click-iT® Plus EdU Alexa Fluor® 594 Imaging Kit (ThermoFisher Scientific, cat# C10639) per the manufacturer's recommendations, with a minor modification. Instead of the copper protectant provided with the kit (Component E), 2 mM $CuSO_4$ was used. To visualize EdU incorporation at 647nm, Alexa Fluor 594 picolyl azide (Component B) was substituted with Alexa Fluor 647 Azide (ThermoFisher Scientific, cat# A10277) at 5µM final concentration.

2.2.7: Measuring progenitor zone length, M phase and S phase indices

Progenitor zone length was measured by counting the number of rows from the distal tip until either the onset of the first HIM-3 positive nucleus or the first crescent shaped nucleus. Each nucleus was visualized by DAPI. M phase index was calculated as percent of number of pH3 positive cells in the progenitor zone over the total number of cells in the progenitor zone. S phase index was calculated as a percent of EdU positive cells in the progenitor zone over the total number of cells in the progenitor zone. The criterion used for distinguishing the progenitors from meiotic cells was the absence of HIM-3.

2.2.8: Measuring the adjusted division index

Progenitor zone length was measured by counting the number of rows from the distal tip until either the onset of the first HIM-3 positive nucleus or the first crescent shaped nucleus. Each nucleus was visualized by DAPI. Germlines were stained with pH3 to detect dividing cells The adjusted division index (ADI) was calculated as the number of pH3 positive cells in the progenitor zone divided by the progenitor zone length in cell diameters (# of pH3 / Cell Rows).

2.2.9: Larval germ cell counts

Larval germ cell counts were performed using whole mount visualization of *zuIs252*[PGL-1::mRFP] and DAPI. Counts were performed at L1, early L2, early L3 and early L4 in both wildtype and two *gsk-3* alleles (tm2223 and nr2047).

2.2.10: Allelic detection PCR

Single worms were picked into 5µL of worm lysis buffer in a 200µL PCR tube. The sample was frozen at -80°C for at least 1 hour. A PCR machine was used to first lyse the worm by heating the tube to 65°C for 60 minutes, followed by inactivation of proteinase K at 95°C for 15 minutes, followed by a hold at 4°C. PCR was performed by adding 9 uL of “master mix” to each tube: 6uL of 2X Apex PCR mix, 1uL of each primer (10µM), and water for any remaining volume. PCR reaction was run for 35-40 cycles. PCR bands were then resolved by running the reaction on a 1-2% agarose gel in TBE with 2.5uL per 50mL of 10% (v/v) Ethidium Bromide. Gels were imaged on a Biorad GelDoc™ XR+. The following primers were used for detecting specific alleles:

***oxTi398* detection**

TF001 GGTGGTTCGACAGTCAAGGT

TF003 ggaatagcgctgagacacag

TF004 ggactccgaatggattcatc

Detects 471bp PCR product in WT and 298bp in *oxTi398*

***ddIs30*[YFP::CDK-2] detection**

TF010 aaaatgttcactgataagcacac

GFP676F GATGGAAGCGTTCAACTAGCAGAC

Detects 275bp PCR product in *ddIs30*

***gsk-3(nr2047)* detection**

gSeq Mid B1 GAACGGAGAAGCTGATACATG

nr2047 MuF CTACATGGCTGATAGCTTGG

nr2047 MuB CCGGGAAATGGCTTGATCTA

Detects 350bp PCR product in WT and 530bp in *nr2047*.

***atm-1(gk186)* detection**

atm-1(gk186) F CAAAAAATTATCACATAATACG

atm-1(gk186) R GGAAGCGTTCTTTTCGTCATCA

atm-1(gk186) Rint CTTCCAGTTGGCTGATGCATAC

Detects 450bp PCR product in WT and 200bp in delFRB

***atl-1(tm853)* detection**

atl-1(tm853) F TCGAGTTGGCTCAAAATGGGA

atl-1(tm853) R ACTGGAAAGCAACGACCAGT

atl-1(tm853) Rint CAGTTCCCAGACACGACTGA

Detects 675bp PCR product in WT and 310bp in delFRB

***rsks-1(ok1255)* detection**

rsks-1(ok1255) F GGAGATGCGGAAGCTATGCTC

rsks-1(ok1255) R CACCAGCTCTCGACATAGACG

rsks-1(ok1255) Rint CCATATCCTCCCTTGCCAAGAAC

Detects 200bp PCR product in WT and 420bp in ok1255

***let-363(viz27[del2196-2287ins5xG])* detection**

let-363(delFRB) F AGTTGAAGTGCGCATATGTAGAA

let-363(delFRB) R ACTATTGGAGCTGATGGATCGT

Detects 675bp PCR product in WT and 310bp in delFRB

2.2.11: PLP mounting for GFP visualization

To assay the *vizSi32*[*Intron cdk-2::NLS::GFP::tbb-2 3'UTR*] reporter in the *wt* and *gsk-3(nr2047)* backgrounds, the animals were dissected in the same dish 24hrs past L4 in PBST and fixed for 3 min using 4% PLP (Hixson et al. 1981) with 4µg/ml DAPI. After washing the fixed germlines three times with 1x PBST, germlines were mounted on a 2% agarose pad and observed immediately. The pictures were taken on the same slide with identical exposure and gain for the GFP channel.

2.2.12: Image acquisition and processing

For full germlines, each gonad was captured as a montage. The focal plane was maintained throughout the experiment, and each image was captured with overlapping cell boundaries at 40x or 63x objectives (Arur et al. 2009). For analysis of distal regions, a z-stack was acquired through the entire distal region using sections 0.6 µm thick. While analysis is performed on all sections, only the top planes were used for figures. All epifluorescence images were taken on a Zeiss Axio Imager upright microscope by using AxioVs40 V4.8.2.0 SP1 micro-imaging software and a Zeiss Axio MRm camera. All confocal images were taken on a Zeiss LSM800 laser point scanning confocal using Zen 2.5 (blue edition). The montages and images were then assembled in Adobe Photoshop CS5.1 and processed identically.

2.2.13: Quantitative real-time PCR (qRT-PCR)

Total RNA was isolated from at least 100 dissected germlines using the miRNeasy Mini Kit (Qiagen). cDNA was synthesized from 500 ng of total RNA using the iScript cDNA Synthesis Kit (Bio-Rad Laboratories). cDNA was amplified for qRT-PCR using

iTaq Universal SYBR Green Supermix (Bio-Rad Laboratories) according to the manufacturer's instructions. Amplified cDNA was monitored after each cycle and the ΔCt was measured using the CFX96 Real time system (Bio-Rad Laboratories). The relative expression rate was determined using the ΔCt method as described in the manufacturer's instructions (Bio-Rad Laboratories). Average expression of the reference gene *act-1* was used to control for template levels.

2.2.14: RNA interference (RNAi) analysis

RNAi was performed by feeding as described previously (Arur et al. 2009).The *let-363* RNAi clone was generated by amplification of an N-terminal fragment of *let-363* cDNA (203bp-1149bp) from an in house N2 cDNA library with the following primers:

let-363_FP_Not1 ATGCGCGGCCGCaggctgctcgagaactcagcagatatgt

let-363_RP_Pst1 ATGCCTGCAGtattatctgacgaacacaatcgagtatcttc

Each primer contained a restriction enzyme cutting site for either Not1 or Pst1. The amplicon was digested by Not1 and Pst1 to insert into the pPD129.36 vector RNAi expression vector. *dpl-1*, *efl-1*, *lin-3*5, *pmk-1*, *pmk-2*, *kgb-1*, *jnk-1, wee-1.3*, *ifg-1* RNAi clones were sequence verified from either the Vidal ORFeome Library, or Ahringer RNAi library. RNAi clones were grown overnight on solid LB agar plates containing 100μg/ml of Ampicillin and 50μg/ml of Tetracyclin at 37°C. Single colonies were then inoculated into LB liquid cultures containing 100μg/ml of Ampicillin and 50μg/ml of Tetracyclin and grown to necessary densities as described previously (Arur et al. 2009). The cultures were then seeded onto the standard NGM agar plates supplemented with 1 mM isopropyl β-D-1-thiogalactopyranoside (IPTG) and containing 100μg/ml of Ampicillin and 50μg/ml of Tetracyclin. Fresh plates were incubated at room temperature for at least 3 days to allow for bacterial lawn growth. For P0 RNAi, L4

stage animals of the genotype listed were transferred to RNAi plates, and dissected for analysis at the listed time point. For P0 hatch RNAi, L4 stages animals from the listed genotype were allowed to lay progeny on the RNAi plates for 24 hours. Mothers were then destroyed and the progeny was allowed to grow. L4s were then transferred to new RNAi plates of the same type and incubated for the listed time. For F1 RNAi, L4 stages of wildtype or *gsk-3* heterozygous animals were allowed to lay progeny on the RNAi plates for 24 hours, and transferred to a fresh RNAi plate every 24-hours for an additional three days. Progeny which were laid after the first day were used. Wildtype and *gsk-3* homozygous F1 progeny from these plates were then synchronized at mid-L4 stage and dissected for analysis at 48 hours past mid-L4.

2.2.15: Western Blot analysis

Wildtype (N2), and *vizIs27* L4 hermaphrodites were hand-picked (250 for each lane), grown for 24 hours and then harvested for western analysis as previously described (Arur et al. 2011; Arur et al. 2009). The extracts were resolved on 10% SDS-PAGE, transferred to PVDF membrane, and probed with antibodies to GFP (made in house, used at 1:500, (Lopez et al. 2013a)) and alpha tubulin (1:1000). Western blots were developed using SuperSignal West Pico Chemiluminescent Substrate (Pierce, Rockford, IL), on Kodak BioMax MS films.

2.2.16: Hairpin Chain Reaction based fluorescence in situ hybridization (FISH)

cdk-1 mRNA, *cdk-2* mRNA, and *pgl-1* mRNA FISH were performed using hairpin chain reaction as described (Gao et al. 2017; Choi et al. 2016; Xuan and Hsing 2014) except that the analysis in the present study was conducted on dissected germlines that were fixed in 3% Paraformaldehyde, 0.25% glutaraldehyde solution at room

temperature for 2 hours. The probes were obtained from Molecular Instruments. Inc (Berkley, CA) and manufacturer's instructions followed.

2.2.17: Starvation assays

Worms were grown on NGM plates with *E. coli* OP50 bacteria to 24 hours past mid-L4, then washed 4 times with sterile M9T and transferred to unseeded plates. All starvation was performed on 100mm agarose plates (2% agarose, 0.3% NaCl, 0.5% cholesterol, 1mM $CaCl_2$, 1mM $MgSO_4$, 25mM KH_2PO_4 pH6) for the indicated times. If re-feeding was required, worms were washed off NGM plates using M9T, and plated onto seeded NGM plates.

2.2.18: Hydroxyurea treatment

300µL of 850M Hydroxyurea was spread onto a 10cm NGM plate seeded with OP50 for a final concentration of 25mM. Plates were incubated overnight. Animals were picked onto the hydroxyurea plate and incubated for 12 hours.

2.2.19: TEM microscopy

Samples were fixed with a solution containing 3% glutaraldehyde plus 2% paraformaldehyde in 0.1 M cacodylate buffer, pH 7.3, then washed in 0.1 M sodium cacodylate buffer and treated with 0.1% Millipore-filtered cacodylate buffered tannic acid, postfixed with 1% buffered osmium, and stained en bloc with 1% Millipore-filtered uranyl acetate. The samples were dehydrated in increasing concentrations of ethanol, infiltrated, and embedded in LX-112 medium. The samples were polymerized in a 60 C oven for approximately 3 days. Ultrathin sections were cut in a Leica Ultracut microtome (Leica, Deerfield, IL), stained with uranyl acetate and lead citrate in a Leica

EM Stainer, and examined in a JEM 1010 transmission electron microscope (JEOL, USA, Inc., Peabody, MA) at an accelerating voltage of 80 kV. Digital images were obtained using AMT Imaging System (Advanced Microscopy Techniques Corp, Danvers, MA).

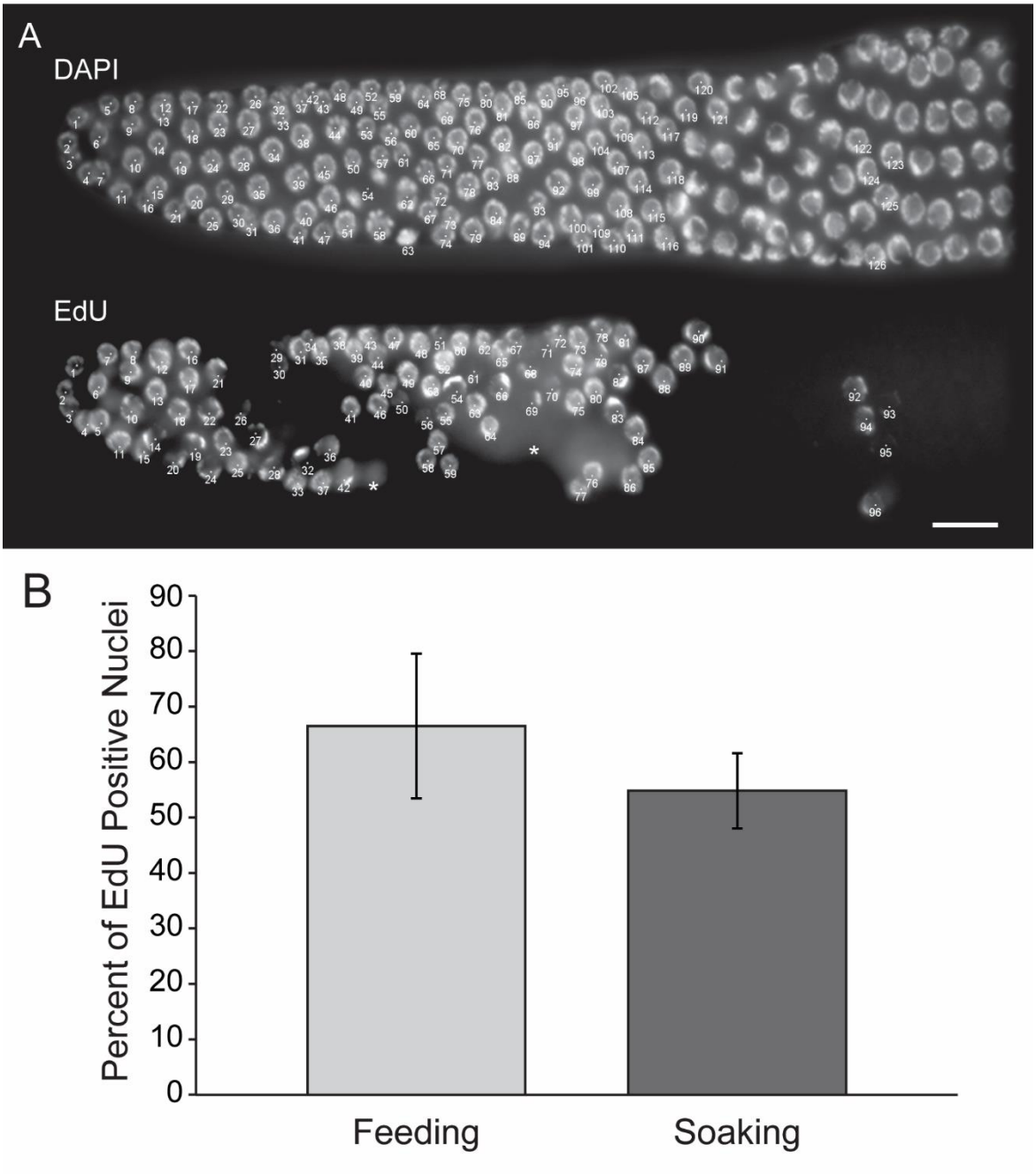

Figure 13: Comparison of feeding and soaking EdU methods

Analysis of S phase index. (A) Dissected germline oriented with distal tip to the left. Animal was soaked in EdU for 10min followed by dissection and staining for DAPI (top) and EdU (bottom). Cells are numbered and labeled using the ImageJ macro. Scale bar: 20µm. (B) S phase index measured in a 30 minute feeding EdU pulse vs. in a 10 minute soaking EdU pulse.

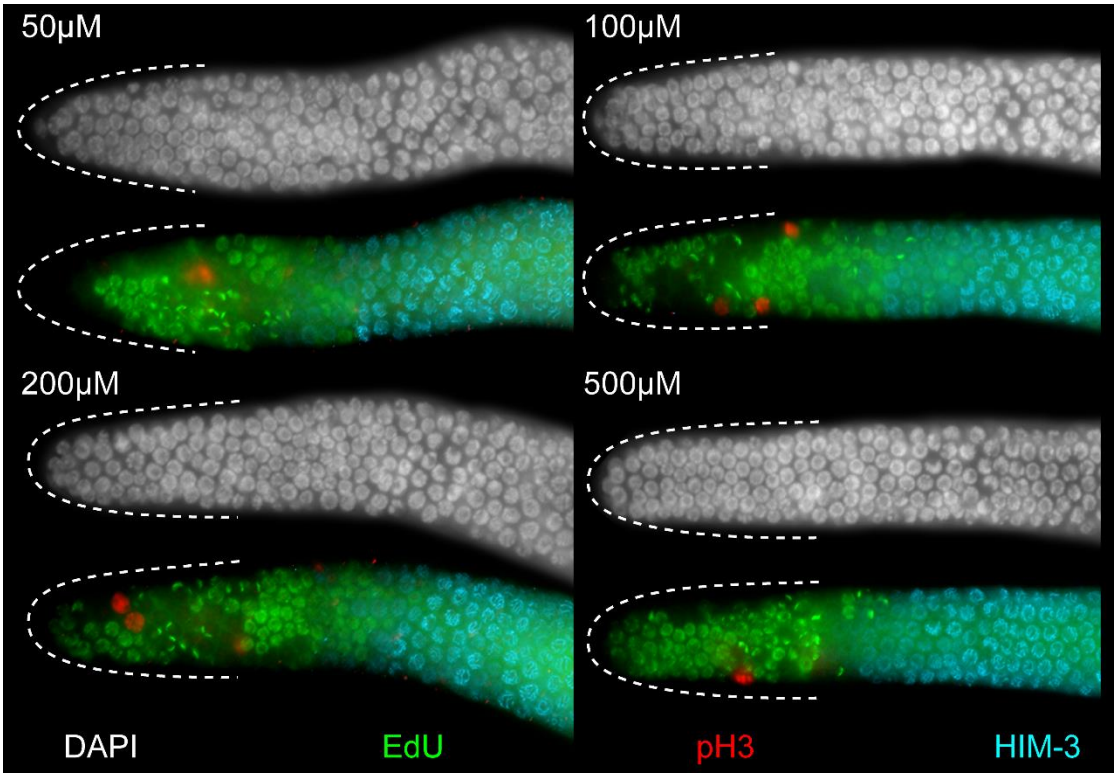

Figure 14: Soaking in higher concentrations of EdU does not affect background

Dissected germlines from wildtype animals after exposure to EdU by soaking. Concentration of EdU is displayed for each panel. Distal tip is outlined with a dashed line and oriented to the left. Stained with DAPI (white), EdU (green), pH3 (red), and HIM-3 (blue).

CHAPTER 3: *gsk-3* TRANSCRIPTIONALLY REGULATES *cdk-2* TO PROMOTE G1 AND S PHASE PROGRESSION TO PROMOTE GSC PROLIFERATION

Chapter 3: *gsk-3* transcriptionally regulates *cdk-2* to promote G1-S phase of the cell cycle and GSC proliferation

Some of the contents of this chapter are reproduced/adapted with permission from "Furuta et al. 2018". Permission is from Development (http://www.biologists.com/development).

Full citation:

* Furuta, T., * H. J. Joo, * K. A. Trimmer, S. Y. Chen, and S. Arur. 2018. 'GSK-3 promotes S-phase entry and progression in *C. elegans* germline stem cells to maintain tissue output', Development, 145, doi: 10.1242/dev.161042

* Equal contribution, alphabetically ordered

3.1: Introduction

Cells proliferate and regulate tissue development or turnover in response to environmental and metabolic fluxes. Several key metabolic or environmental factors and pathways have been identified (Chapter 1.3) that regulate proliferation. In this chapter, I will focus on the role of *gsk-3* in regulating cell proliferation of the germline stem cells to maintain a pool of proliferating stem cells.

Gsk3β plays many roles in response to both environmental and cell-cell cues as discussed previously (Chapter 1.3.4). Because Gsk3β is a kinase, it both regulates downstream substrates for its function and is often regulated by environmental and physiological inputs. In collaboration with two other members of the lab, we uncovered a role for *gsk-3* in regulating plasticity of the *C. elegans* GSCs in response to nutritional and metabolite changes.

GSK-3 was identified as a substrate of MPK-1 signaling during germline development (Arur et al., 2009). To understand its function in germline development, we acquired two deletion alleles (*nr2047* and *tm2223*). The *nr2047* allele carries a deletion with breakpoints located in introns 2 and 3, completely removing the 3rd exon; *tm2223* allele carries a deletion removing a portion of exon 3. Exon 3 houses the kinase domain, thus both of these alleles remove a similar portion of the kinase domain and result in frameshifts leading to truncated proteins (Figure 15). Because the two deletion alleles remove a significant portion of the kinase domain, we hypothesize that these are strong loss of function alleles.

Each of the two *gsk-3* alleles results in viable adult animals when segregated from a heterozygous parent. The adult homozygous animals are sterile, and the few embryos laid born die early due to polarity defects (Schlesinger et al. 1999). While assaying the function of *gsk-3* in relation to the *let-60/mpk-1* signaling pathway we noticed a dramatic phenotype in the adult germlines from homozygous *gsk-3* alleles: the pool of GSCs in the adult germline was dramatically reduced. Thus, we set out to determine the role of *gsk-3* in regulating GSC function.

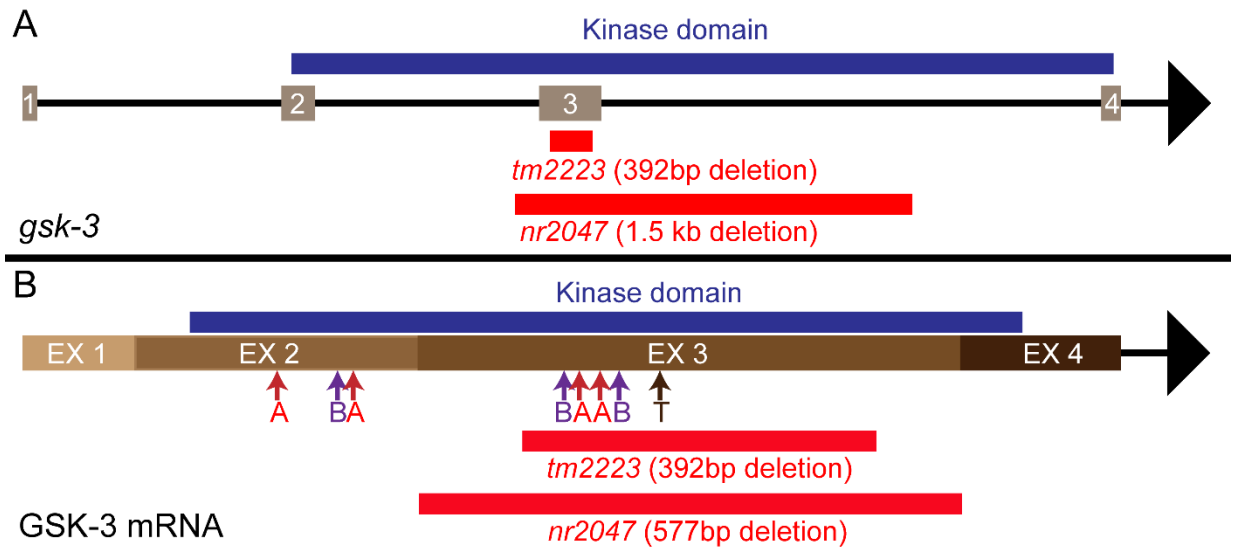

Figure 15: *gsk-3* mutant allele structure

(A) Stick diagram of the *gsk-3* gene with the exons and kinase domain labeled. Deletion break points for the nr2047 and tm2223 alleles are displayed. (B) Stick diagram of the *gsk-3* mRNA with exons and kinase domain labeled. Arrows with "A" label the active site residues which transfer a phosphate to the substrate (K65, E77, D161, and D180). Arrows with "B" label residues which bind to primed substrates (R76, R160, K185). The arrow with "T" labels the phosphorylation site on the t-loop which opens up the catalytic site.

3.2: *gsk-3* Regulates GSC Proliferation in a Germline Autonomous and Kinase-dependent Manner during Larval and Adult Development

The adult wildtype *C. elegans* germline harbors a population of ~200-250 GSCs maintained by Notch signaling in the progenitor zone (Berry, Westlund, and Schedl 1997; Fox and Schedl 2015; Fox et al. 2011) (Figure 3). As the GSCs move away from the distal tip cell (DTC) (Figure 3) they differentiate and enter meiosis at ~20-22 cell diameters, in both larval (specifically the last stage of larval development, the larval stage 4 or L4) and adult germlines. However, in the *gsk-3* mutant alleles (both *nr2047* and *tm2333*) the progenitor region contained only ~90 GSCs, which is significantly fewer than the ~200-250 found in wildtype ($p<0.001$) (Figure 16A, 16B). To determine whether the lower number of GSCs in the adult germline was due to a defect in the early expansion of the GSC population, or lack of maintenance of an established adult GSC population, we analyzed larval developing germlines. The number of GSCs in *gsk-3* mutants was significantly reduced as early as L3, with 14 germ cells compared to the wildtype ~34 germ cells (Table T2). These data suggest that the defect in *gsk-3* mutant GSCs may occur at the stage of stem cell expansion, which occurs during larval development. By L4 stage and into adulthood, the *gsk-3* mutant reached and maintained a population of ~90 GSCs throughout adulthood (Figure 16D). Together, these data suggest that the GSCs fail to expand in number in the *gsk-3* mutants during early larval stages, and the number established during larval development is then maintained into adulthood.

During larval development, several environmental and pheromone pathways regulate germline development, whose signals are relayed to the germ cells regulated through the sensory neurons (Reviewed in Korta and Hubbard 2010). To test whether the GSC defect was due to a germline autonomous function of *gsk-3*, we generated

germline-specific GFP::GSK-3 transgenes driven by either a *pie-1* or a *mex-5* germline specific promoter (Merritt et al. 2008) and regulated by a *tbb-1* 3' UTR for even expression. The transgenes were each integrated at a single site in the *C. elegans* genome, and both constructs drive wildtype GSK-3 in the germline (Figure 17A). Expression of a germline driven GFP::GSK-3 at a single copy knock-in localizes to nuclear and cytoplasmic compartments in the progenitor zone (Figure 17B). This transgene is expressed only in germ cells and so did not rescue any of the somatic defects of the *gsk-3* mutants, such as small size and uncoordinated movements, as would be expected from the restricted promoter activity (Gleason, Szyleyko, and Eisenmann 2006; Maduro et al. 2001). Expression of the transgene completely rescued the GSC defect in *gsk-3* mutants (Figure 17C-E), suggesting that *gsk-3* functions autonomously in the germline to regulate the expansion of the GSC population.

To determine whether the role of *gsk-3* in regulating GSC expansion was dependent on its kinase activity, we mutated the kinase core residues (K65, E77, D161 and D180) to alanine to generate a kinase dead GSK-3 transgene (Doble and Woodgett 2003). The resulting transgene, GFP::GSK-3 (K65A, E77A, D161A and D180A) which we refer to as GFP::GSK-3 kinase-dead (GFP::GSK-3 KD), is driven by the same germline specific promoter used to express the wildtype GFP::GSK-3 above. While GFP::GSK-3 and GFP::GSK-3 KD are expressed at similar levels and in similar cellular compartments in the GSCs (Figure 17B, 18A), GSK-3 KD did not rescue the GSC defects (Figure 18B). These data together demonstrate that *gsk-3* functions germline-autonomously in a kinase-dependent manner to regulate GSC expansion.

To determine whether the defects in GSCs were indeed due to lack of stem cell expansion vs increased differentiation of GSC population which would artificially mimic a GSC expansion defect, we tested whether *gsk-3* mutant GSCs have increased

differentiation or loss of self-renewal. The length of the progenitor zone can be used to determine the balance of self-renewal with differentiation as discussed previously (Chapter 1.1.5). If the length is 20-22 cell diameters, there is likely no change in the rate of differentiation, however, if the length is increased, it would suggest increased self-renewal at the expense of differentiation. The length of the progenitor zone was maintained at 20-22 cell diameters from the DTC in both wildtype and *gsk-3* mutants, suggesting that the defect in GSC population in *gsk-3* mutants is not due to altered differentiation (Figure 16C, 16E, 17C, 17E).

We next investigated whether the *gsk-3* mutant GSCs remained responsive to Notch signaling for self-renewal. To determine this, we assayed GSCs in conditions with decreased or increased Notch receptor (*glp-1*) activity by utilizing the *glp-1* temperature-sensitive alleles *bn18ts* (reduction of function) and *ar202gf* (gain of function). Both of these alleles behave similarly to wildtype at the permissive temperature of 15°C, but at the restrictive temperature of 25°C, GSCs will exclusively differentiate (*bn18ts*) or self-renew (*ar202gf*) (Figure 19) (Dorsett, Westlund, and Schedl 2009; Kodoyianni, Maine, and Kimble 1992; Pepper, Killian, and Hubbard 2003; Berry, Westlund, and Schedl 1997). The animals were shifted to the restrictive temperature as embryos to assay their respective phenotypes. The wildtype or *gsk-3(nr2047)* mutants do not display any temperature-sensitive behavior and at all temperatures the GSCs are maintained at numbers similar to those found previously (Figure 19A, B). When *glp-1(bn18ts)* and *gsk-3(nr2047);glp-1(bn18ts)* mutants are assayed at the permissive temperature, germlines produce both GSCs and meiotic cells (Figure 19C). At the restrictive temperature, however, both the *glp-1(bn18ts)* and the *gsk-3(nr2047);glp-1(bn18ts)* double mutant results in loss of the GSC population

with only sperm produced in 100% of adult germlines (Figure 19D). These data suggest that the *gsk*-3 mutant GSCs require *glp-1* activity to self-renew.

Next, to determine whether the *gsk-3* mutant GSCs self-renew in response to increased Notch signaling, we investigated the *glp-1(ar202gf)* gain of function allele. At the permissive temperature of 15ºC, *glp-1(ar202gf)* mutant and the *gsk-3*(*nr2047);glp-1(ar202gf)* mutants maintain GSCs and meiotic cells in adults(Figure 19E). In contrast, shifting *glp-1(ar202gf)* or *gsk-3*(*nr2047);glp-1*(*ar202gf)* mutants (again as embryos) to the restrictive temperature of 25°C results in tumorous germlines as the GSCs self-renew at the expense of differentiation (Figure 19F). The *gsk-3(nr2047);glp-1(ar202gf)* mutant tumors, however, appear “skinnier” relative to *glp-1(ar202gf)* single mutant tumor (Figure 19E, 19F). This indicates that *glp-1* activity is sufficient to drive self-renewal at the expense of differentiation in *gsk*-3 mutants. Together, these data demonstrate that responsiveness to *glp-1* signaling was not affected in *gsk-3* mutant GSCs.

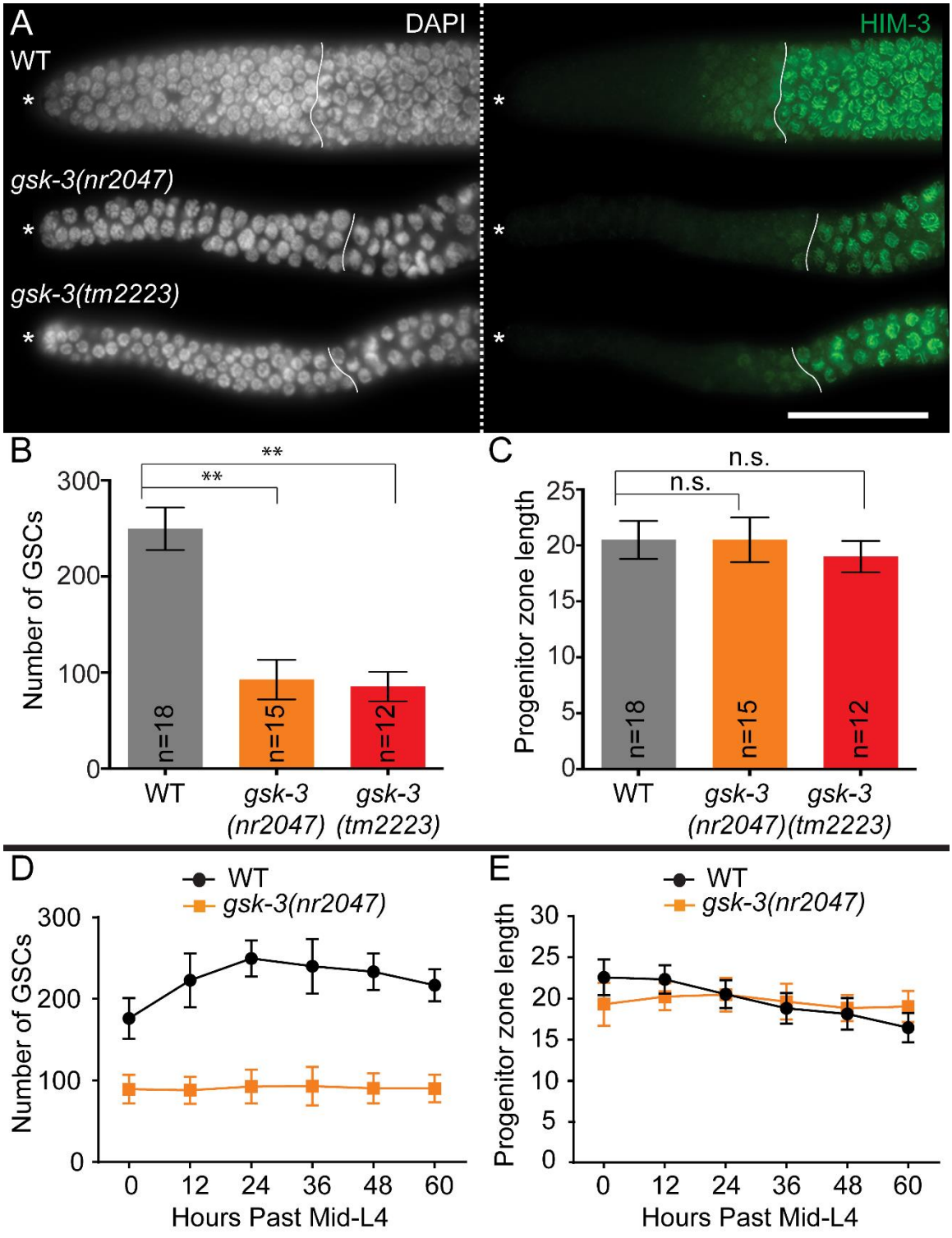
A
DAPI
HIM-3
WT
gsk-3(nr2047)
gsk-3(tm2223)
B
Number of GSCs
300
200
100
0
**
**
n=18
n=15
n=12
WT
gsk-3 (nr2047)
gsk-3 (tm2223)
C
Progenitor zone length
25
20
15
10
5
0
n.s.
n.s.
n=18
n=15
n=12
WT
gsk-3 (nr2047)
gsk-3 (tm2223)
D
WT
gsk-3(nr2047)
Number of GSCs
300
200
100
0
0
12
24
36
48
60
Hours Past Mid-L4
E
WT
gsk-3(nr2047)
Progenitor zone length
30
25
20
15
10
5
0
0
12
24
36
48
60
Hours Past Mid-L4

Figure 16: *gsk-3* mutants maintain fewer GSCs

(A) Dissected germlines from adult (24 hours past L4) wildtype (top) and *gsk-3(tm2223)* (middle), and *gsk-3(nr2047)* labeled with REC-8 (green, GSCs) and DAPI (white, DNA). (B) Graph displaying the number of GSCs in wildtype, *gsk-3(tm2223)*, and *gsk-3(nr2047)* at 24 hours past L4. (C) Graph displaying the number of cell diameters between the distal tip cell and the transition zone in wildtype, *gsk-3(tm2223)*, and *gsk-3(nr2047)* at 24 hours past L4. (D) Graph displaying the total number of GSCs in wildtype and *gsk-3(nr2047)* mutant animals on a time course from mid-L4 until 60 hours after mid-L4. (E) Graph displaying the number of cell diameters between the distal tip cell and the transition zone in wildtype and *gsk-3(nr2047)* mutant animals on a time course from mid-L4 until 60 hours after mid-L4. In B and C, error bars indicate mean ± SD. **P<0.001, and n.s., not significant.

Developmental Stage	PGL-1::mCherry positive cells		
	WT	*gsk-3(nr2047)*	*gsk-3(tm2223)*
L1	2	2	2
Early L2	12	10±2	9±2
Early L3	34±1	14±2	13±2
Early L4	80±2	60±2	53±2

N=30 animals for each stage

Table 2: *gsk-3* promotes developmental germ cell expansion

Whole mount germ cell counts at larval stages in wildtype and two *gsk-3* mutant alleles (*nr2047* and *tm2223*) utilizing a PGL-1::mCherry transgene to identify germ cells. *gsk-3* mutants (*nr2047* and *tm2223*) contain fewer germ cells than wildtype throughout development. Counts are presented as mean ± SD.

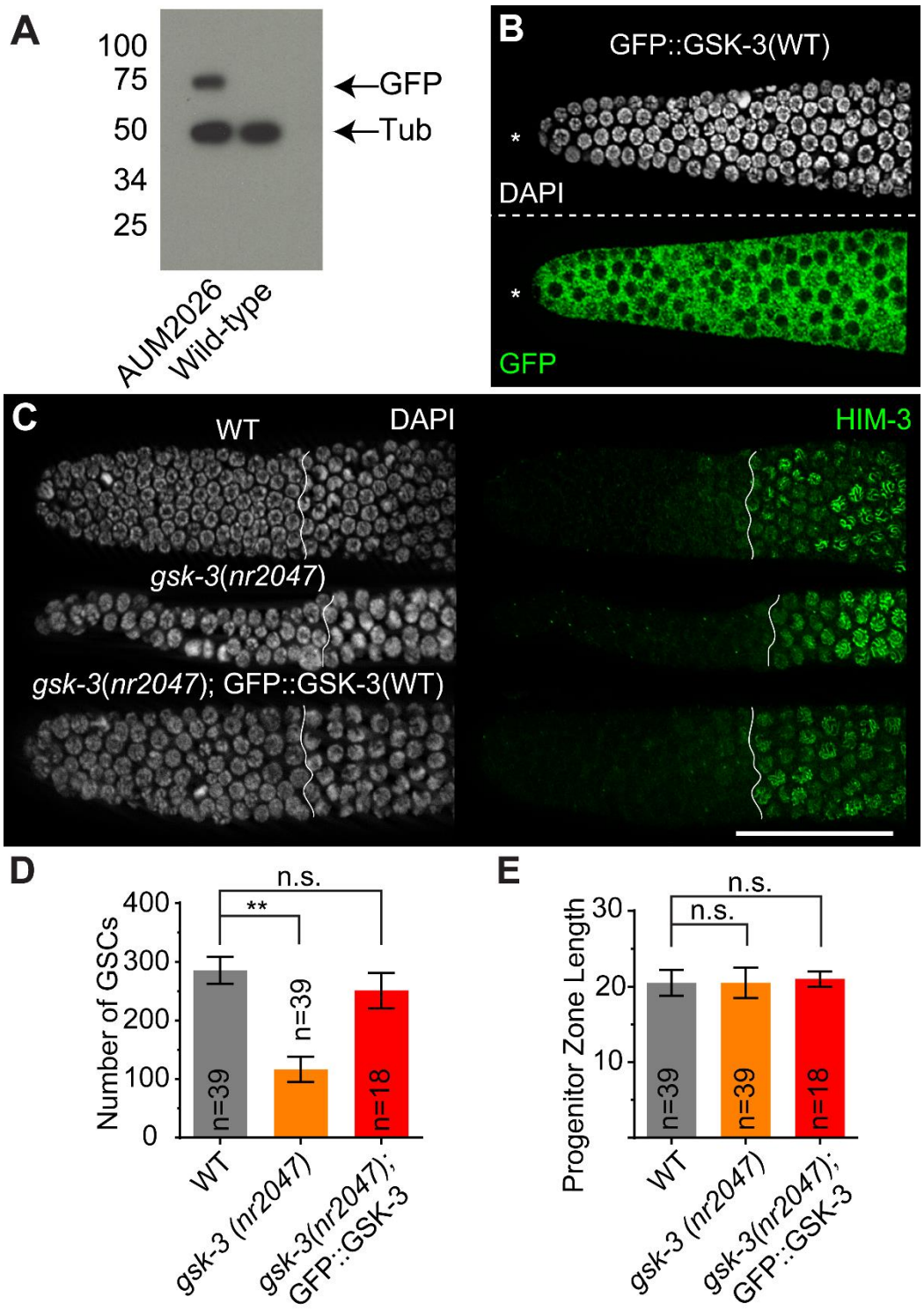
A
100
75
50
34
25
GFP
Tub
AUM2026
Wild-type
B
GFP::GSK-3(WT)
*
DAPI
*
GFP
C
WT
DAPI
HIM-3
gsk-3(nr2047)
gsk-3(nr2047); GFP::GSK-3(WT)
D
Number of GSCs
400
300
200
100
0
n.s.
**
n=39
n=39
n=18
WT
gsk-3 (nr2047)
gsk-3(nr2047); GFP::GSK-3
E
Progenitor Zone Length
30
20
10
n.s.
n.s.
n=39
n=39
n=18
WT
gsk-3 (nr2047)
gsk-3(nr2047); GFP::GSK-3

Figure 17: The *gsk-3* mutant GSC defect is germline autonomous

(A, B) Transgenic expression of a germline driven GFP::GSK-3(WT) AUM2026 (*vizIs27[Ppie-1::GFP::GSK-3]*) is detected by western blot (A) and immunofluorescence (B). (A) Western blot analysis was performed using an anti-GFP antibody on WT and *gsk-3 (nr2047);vizIs27[Ppie-1::GFP::GSK-3(WT)]* whole worm extracts. A 75kDa band corresponding to GFP::GSK-3 was detected in the *gsk-3(nr2047);[Ppie-1::GFP::GSK-3(WT)]* worms, but not in wildtype (N2). anti-Tubulin was used as an internal control. (B) Dissected germline from adult (24 hours past L4) GFP::GSK-3(WT) AUM2026 (*vizIs27[Ppie-1::GFP::GSK-3]*) labeled for GFP (Shah et al.). (C) Dissected germlines from adult (24 hours past L4) wildtype (top), *gsk-3(nr2047)* (middle), and *gsk-3(nr2047);vizIs27[Ppie-1::GFP::GSK-3(WT)]* (bottom) labeled with HIM-3 (green, GSCs) and DAPI (white, DNA). (D) Graph displaying the number of GSCs in wildtype, *gsk-3(nr2047)*, and *gsk-3(nr2047);vizIs27[Ppie-1::GFP::GSK-3(WT)]*. (E) Graph displaying the length of the progenitor zone in wildtype, *gsk-3(nr2047)*, and *gsk-3(nr2047);vizIs27[Ppie-1::GFP::GSK-3(WT)]*. All images are oriented with distal tip (asterisk) to the left and the end of the progenitor zone marked by a solid line. Scale bar: 40µm.

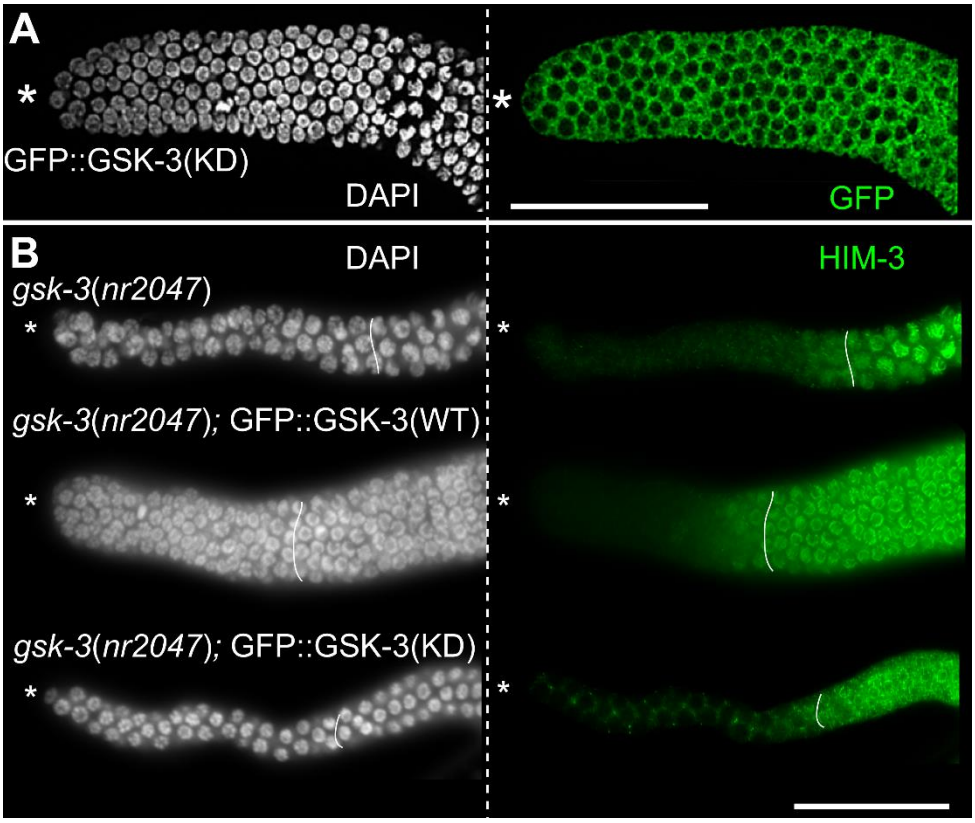

Figure 18: The *gsk-3* mutant GSC defect is kinase dependent

(A) Expression of a germline driven kinase dead GFP::GSK-3 transgene (*vizSi20[Pmex-5::GFP::GSK-3(KD)]*) at a single copy knock-in localizes to nuclear and cytoplasmic compartments in the progenitor zone. DAPI (white) labels the DNA, while GFP (green) labels transgene expression. (B) Wildtype GFP::GSK-3 (*vizSi44*) rescues the GSC number (B, middle) while the kinase dead GSP::GSK-3 does not (B, bottom). DAPI (white) labels the DNA, while HIM-3 (green) labels meiotic cells. Images are oriented with distal tip (asterisk) to the left and the end of the progenitor zone marked by a solid line. Scale bars: 40µm.

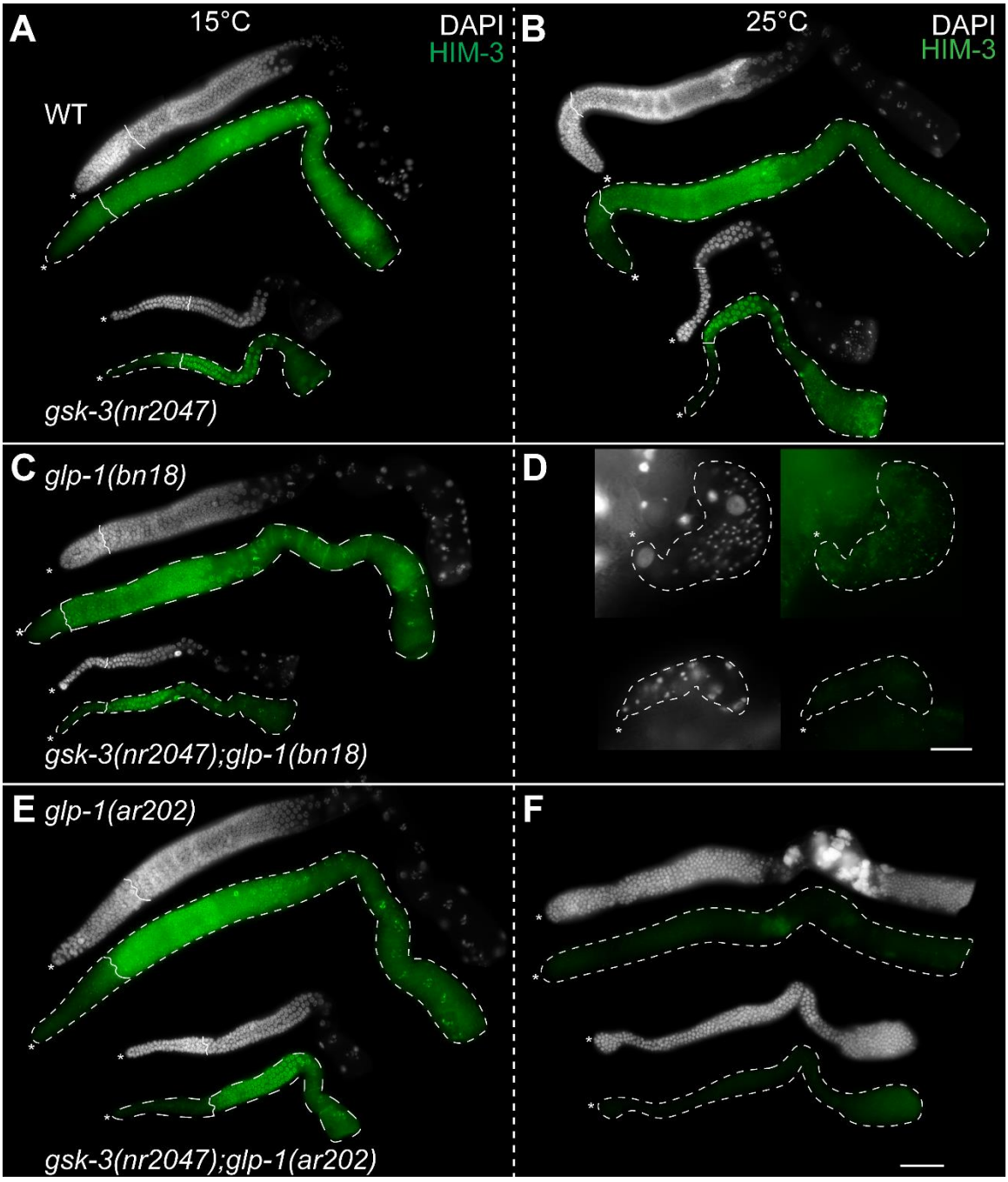
A
15°C
DAPI
HIM-3
WT
gsk-3(nr2047)
B
25°C
DAPI
HIM-3
C
glp-1(bn18)
gsk-3(nr2047);glp-1(bn18)
D
E
glp-1(ar202)
gsk-3(nr2047);glp-1(ar202)
F

Figure 19: Self-renewal through Notch Signaling is unaffected in *gsk-3* mutants

Dissected germlines from adult (24 hours past L4) animals of indicated genotypes labeled with DAPI (white, DNA) and HIM-3 (green, meiotic cells) are oriented from left (progenitor zone) to right (oocytes). The left panel shows micrographs of germlines from animals maintained at permissive temperature of 15°C (A, C, E); the right panel displays adult germlines from animals shifted to the restrictive temperature of 25°C as embryos (B, D, F). (A, B) N2s and *gsk-3(nr2047)* mutants are displayed. (C, D) *glp-1*(*bn18ts*) and *gsk-3(nr2047);glp-1(bn18ts)* mutants are displayed. (E, F) *glp-1(ar202gf)* and *gsk-3*(*nr2047);glp-1(ar202gf) mutants are displayed.* Each experiment was performed three times, and each time an N of 30 germlines was assayed. HIM-3 staining is outlined with a dashed line. All images are oriented with distal tip (asterisk) to the left and the end of the progenitor zone marked by a solid line. Scale bars: 20µm (D), and 50µm (A-C,E,F).

3.3: *gsk-3* Mutant GSCs Enter and Progress through S Phase Inefficiently

We had identified the defect in early larval development in *gsk-3* mutants as a failure of GSCs to expand. During early larval development, the GSCs are undergoing a rapid cell cycle to expand into the niche. As neither differentiation nor self-renewal was affected in *gsk-3* mutant GSCs, we investigated the cell cycle parameters of *gsk-3* GSCs. Cell cycle parameters were investigated via immunofluorescence analysis on dissected germlines using phospho-histone H3 (pH3) labeling to mark M phase and EdU incorporation to mark S phase. The *gsk-3* mutant GSCs labeled with pH3, indicating that they entered a productive M phase (Figure 20A, B). Mitotic index, which is the number of pH3 positive cells over the total number of cells, is used to measure the frequency of germ cell divisions. There was no significant difference in mitotic index found between wildtype and *gsk-3* mutant GSCs (Figure 20C). In contrast, S phase was markedly altered in *gsk-3* mutant GSCs. In wildtype animals, 100% of the germlines incorporated EdU with an S phase index (assayed by number of GSCs that are EdU positive divided by the total number of GSCs) of ~ 55% in adults, and ~67% in L4's (Figure 20A, 20B, 20D) on a 15-minute EdU pulse. In *gsk-3* mutants however, ~90% of *gsk-3* mutant germlines failed to incorporate detectable EdU both as adults (Figure 20A) and L4s (Figure 20B), and of those germlines that did, the S phase index was only ~6% (Figure 20D). These data suggest that cell cycle progression is affected in GSCs with a defect in S phase.

These results could potentially be due to the fact that the *gsk-3* mutant GSCs has a longer S phase of the cell cycle, or were more synchronous relative to wildtype. To determine whether the lack of EdU incorporation was due to increased length of each cell cycle phase we fed the worms the EdU bacteria for longer times of 1, 3, and 5 hours. Wildtype GSCs incorporate EdU label robustly after 1 hour of feeding with EdU

bacteria (Figure 21). By 5 hours of continuous labeling, ~90% of the cells in the progenitor zone are labeled with EdU (Figure 21). Loss of *gsk-3*, however, results in extremely poor EdU incorporation even after 1, 3, or 5 hours of continuous feeding, suggesting a severe defect in S phase entry or replication rate (Figure 21). It is also likely, however, that the lack of EdU incorporation could be a reflection of low EdU accessibility itself due to low EdU bacteria uptake, which occurs when mutants cannot feed well, or decreased bacterial digestion.

To test whether the lack of EdU incorporation was a reflection of S phase defects or defects in feeding we assayed mutants that have a low pharyngeal pumping rate and thus feed at a lower rate, *eat-2* mutants. The rate of pharyngeal pumping, used as a measure of feeding, in wildtype animals is ~280 pumps per minute while *eat-2* mutants eat at a rate of ~80 pumps per minute (Figure 22A). Feeding EdU bacteria to *eat-2* mutants for 30 minutes resulted in an EdU intensity similar to wildtype (Figure 22B). In contrast, *gsk-3* mutants, which eat at an intermediate rate of ~200 pumps per minute, had weak EdU intensity (Figure 22). Since the pumping rate of *eat-2* mutants was lower than *gsk-3* mutants or wildtype, and they incorporated EdU efficiently, low bacterial intake was likely not the cause of the EdU incorporation defect.

We next investigated whether the lack of EdU incorporation in *gsk-3* mutant GSCs was due to a decreased rate of bacterial digestion in *gsk-3* mutants resulting in rapid degradation of the EdU label. To test this, I developed a method to incorporate EdU without using bacteria. Instead of indirect EdU exposure, I soaked the worms in a 200µM solution of EdU for 10 minutes and dissected immediately after EdU incubation. Upon 10 minutes of EdU soaking, wildtype GSCs incorporated EdU efficiently and 100% of the germlines were labeled at ~67% S phase index (Figure 23). However, EdU incorporation was still very low in the *gsk-3* mutant GSCs (Figure 23). This data

demonstrates that direct EdU exposure is insufficient to recover EdU incorporation, suggesting that the EdU incorporation defect is not due to the feeding method of EdU incorporation. As a majority of *gsk-3* mutant germlines failed to incorporate detectable EdU, it is likely that GSCs in *gsk-3* mutants incorporate fewer molecules of EdU per GSC compared to wildtype GSCs, suggesting a defect in S phase progression. In addition, the lower S phase index in those *gsk-3* mutants with visible incorporation hints at an S phase entry defect. Therefore, we next tested whether there were any changes to S phase entry in *gsk-3* mutants.

To test whether the GSCs in *gsk-3* mutant animals lengthened G1 due to inefficient S phase entry, we assayed for subcellular GFP::MCM-3 (*gtIs64*) localization (Sonneville et al. 2012). Mcm3 is a component of the DNA licensing complex that accumulates in the nucleus in early-mid G1 in vertebrate cultured cells, and is phosphorylated by Cdk2 and re-localized to the cytoplasm in late G1 or early S to prevent re-replication (Li et al. 2011); thus, nuclear localization of Mcm3 indicates nuclei in G1 (Blow 1993; Chong and Blow 1996). To test whether GFP::MCM-3 had cellular localization dynamics in *C. elegans* GSCs similar to vertebrate cultured cells, we depleted *cdk-2* in GFP::MCM-3 animals and determined its localization. As previously described (Fox et al. 2011), depletion of *cdk-2* results in a G1 cell cycle arrest wherein all cells are negative for EdU (S phase) and pH3 (M phase) (Figure 24A). GFP::MCM-3 localizes to GSC nuclei upon depletion of *cdk-2* (Figure 24B) indicating that GFP::MCM-3 changed cellular localization in GSCs in response to the loss of *cdk-2*, and by extension G1 arrest, as would be predicted from the vertebrate systems. Additionally, GFP::MCM-3 was excluded from meiotic germ cell nuclei in animals treated with *cdk-2* RNAi (Figure 24B), indicating that the reporter changed localization based on the type of cell cycle. Wildtype germlines displayed cytoplasmic

GFP::MCM-3 in both GSCs and meiotic cells (Figure 24B) which is consistent with previous reports that the GSCs have a very short (seemingly absent) G1. In contrast, GFP::MCM-3 was nuclear in *gsk-3* mutant GSCs (Figure 24B) in 56% ± 3% of the cells and was cytoplasmic when the cells entered meiosis (Figure 24B). Taken together, these data suggest that *gsk-3* mutant GSCs are in G1 for a longer period of time relative to wildtype GSCs due to inefficient entry into S phase in addition to the inefficient S phase progression found earlier. Furthermore, increased nuclear GFP::MCM-3 also suggests that CDK-2 activity may be affected in *gsk-3* mutants, which could result in both of these observed defects.

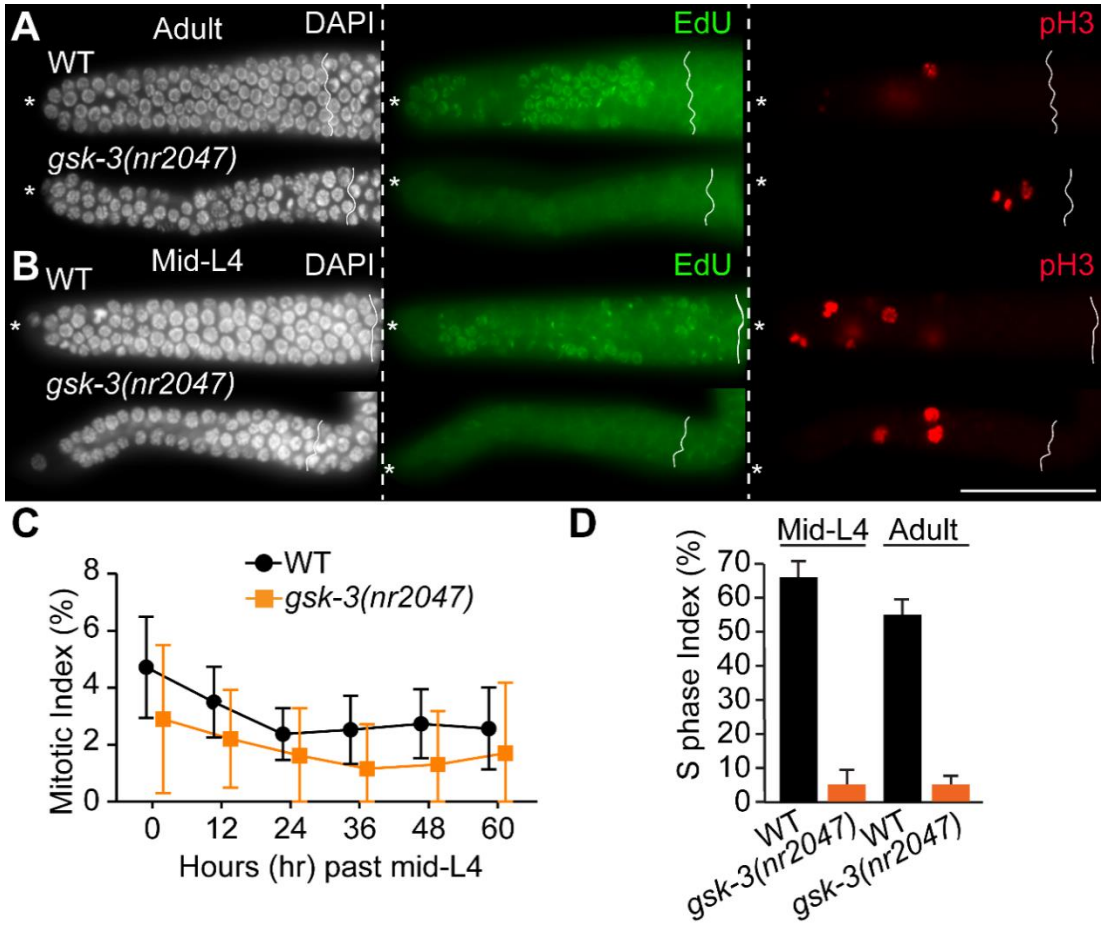

Figure 20: *gsk-3* mutant GSCs cycle but do not incorporate EdU

Dissected germlines from wildtype and *gsk-3* mutants at from adult (24 hours past mid-L4) (A) and mid-L4 (B). The progenitor region is oriented with the DTC (*) on the left and are labeled for Nuclei (DAPI, white) pH3 (red) and EdU (green). Pictures were taken at the same gain and exposure, and processed in the same tube to compare the level of EdU incorporation. (C) Mitotic index of wildtype and *gsk-3* mutant GSCs over a time course from mid-L4 to 60 hours past mid-L4 (B) S phase index of those germlines in which EdU labeling was detected from wildtype and *gsk-3* mutant GSCs. Each experiment in (A, B) was performed eight times, and 30-40 germlines were assayed each time. Error bars represent the standard deviation obtained from at least 30 germlines each from three independent experiments. End of each progenitor zone is labeled with a solid line. Scale bar: 40µm.

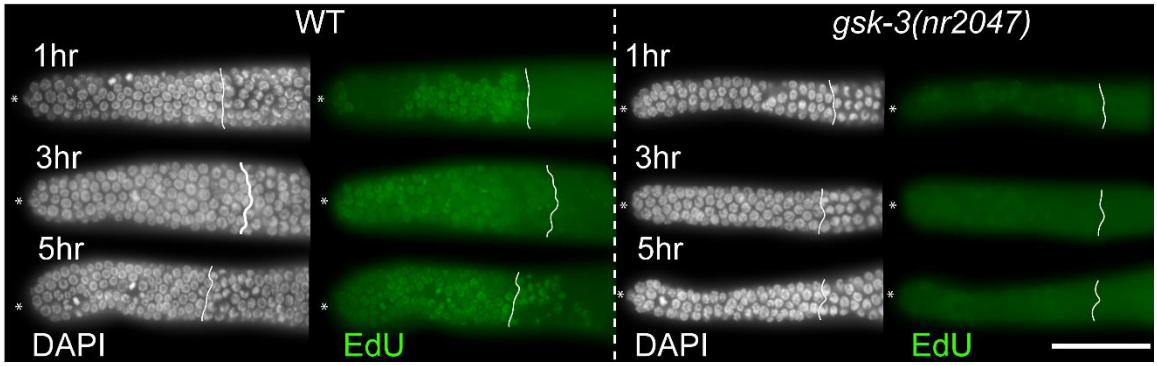

Figure 21: *gsk-3* mutant GSCs do not incorporate EdU after long pulses

Wildtype and *gsk-3*(*nr2047*) mutant worms were fed with EdU bacteria for 1 hour, 3 hours or 5 hours, and processed for detection of EdU incorporation. DAPI (white) labels DNA, and EdU (green) labels actively replicating S phase cells. Distal tip of each germline is labeled with an asterisk. Proximal end of each progenitor zone is labeled with a solid line. Scale bar: 40μm.

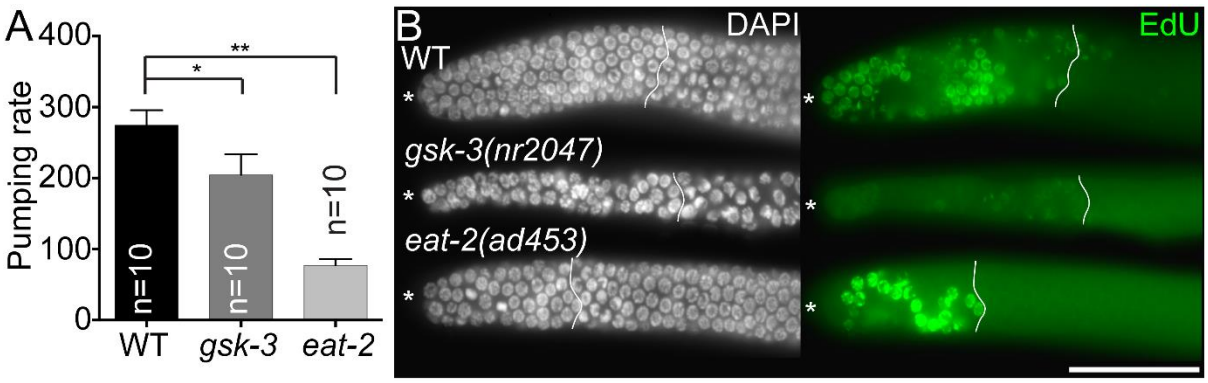

Figure 22: EdU incorporation is not dependent on the rate of bacterial eating

All microscopy images in this figure represent the progenitor region of a dissected hermaphroditic adult germline with distal tip on the left of the photograph. DAPI marks DNA, and EdU labels actively replicating S phase cells. (A) *eat-2* mutants are defective in pharyngeal pumping, and thus a model for dietary restriction. *gsk-3* mutants display pharyngeal pumping rate less than wildtype animals, but significantly higher than *eat-2* mutant. Values indicate the mean ± S.D. *P<0.05, **P<0.001. n= number of animals counted. (B) Dissected germlines from the genotypes listed. DAPI (white) labels DNA, and EdU (green) labels actively replicating S phase cells. Distal tip of each germline is labeled with an asterisk. Proximal end of each progenitor zone is labeled with a solid line. Scale bar: 40 μm.

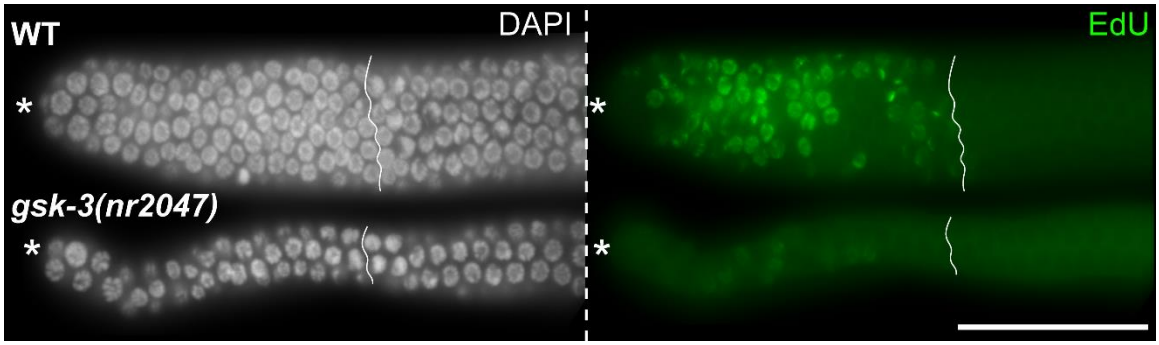

Figure 23: EdU soaking does not rescue EdU incorporation in *gsk-3* mutants

Dissected germlines from wildtype and *gsk-3* mutants after soaking in 200μM EdU for 15 minutes. DAPI (white) labels DNA, and EdU (green) labels actively replicating S phase cells. Distal tip of each germline is labeled with an asterisk. Proximal end of each progenitor zone is labeled with a solid line. Scale bar: 40μm.

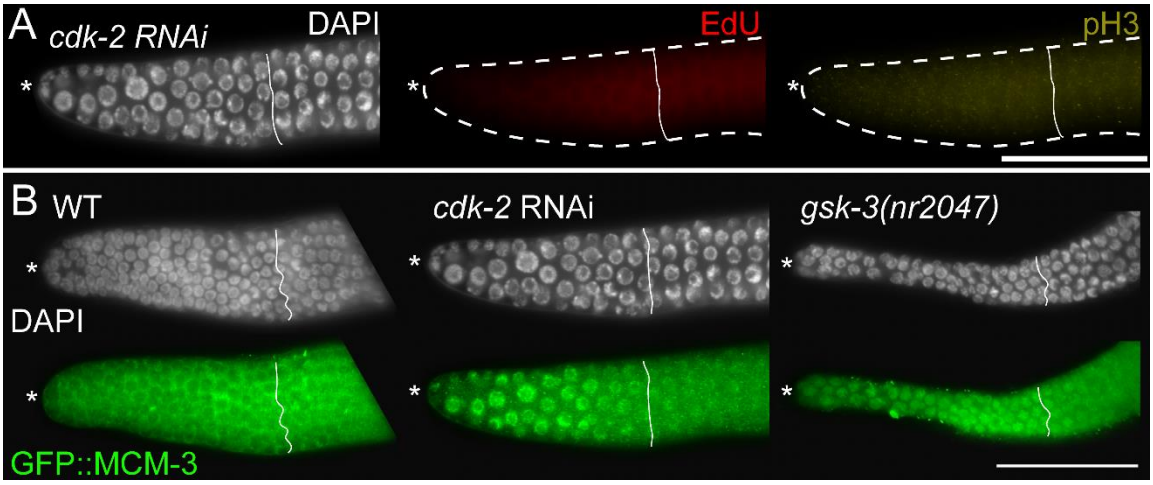

Figure 24: *gsk-3* mutant GSCs retain nuclear MCM-3

(A) Dissected germline from a *cdk-2* (RNAi) animal with distal end (asterisk) pointing left. DNA in white (DAPI), EdU in red (S phase), and pH3 in yellow (M phase). EdU and pH3 labeled channels are outlined with a dashed line. (B) Dissected germline from wildtype, *cdk-2* (RNAi), and a *gsk-3(nr2047)* mutant with distal end (asterisk) pointing left. DNA in white (DAPI) and MCM-3 (GFP) in green. The end of the progenitor zone is labeled with a white line. Scale bar: 40µm.

3.4: *gsk-3* Promotes *cdk-2* Transcription to Regulate a Rapid G1/S Transition

To assess whether there were any changes in CDK-2 activity, we assayed processes and proteins which can inhibit its activity such as DNA licensing and CDK inhibitor proteins. DNA licensing is required for DNA replication as it provides starting points for the DNA polymerases. The act of DNA licensing activates Cdk2 in mammalian cell culture, preventing progress from G1 to S phase in its absence (Nevis, Cordeiro-Stone, and Cook 2009). Therefore, if *C. elegans* GSCs are regulated similarly, loss of a DNA licensing factor may result in difficulty with entry and progression through the S phase. To test this hypothesis, we reduced the expression of five DNA licensing factors (Table 3) by RNAi in both wildtype and *gsk-3* mutant germlines and assayed for evidence of an arrest by cellular “fried egg” morphology (DAPI), characteristic of cell cycle arrest in GSCs. While GSCs in wildtype animals with control RNAi (GFP) appeared normal and displayed no signs of cell cycle arrest, GSCs in wildtype animals upon RNAi of components which recognize DNA licensing sites presented with DNA fragmentation and re-replication defects (Figure 25A). Surprisingly, however, GSCs from *gsk-3* mutants upon RNAi of the licensing complex components did not result in fragmentation or re-replication defects. If *gsk-3* was down-regulating one of these factors, RNAi of that factor should appear similar to *gsk-3* mutants. However, since the *gsk-3* mutants did not show a similar phenotype, and were able to rescue the DNA fragmentation and re-replication phenotypes of DNA licensing factor reduction, it is unlikely that *gsk-3* mutants reduce DNA licensing factors.

To next determine whether CDK inhibitors and negative regulators were responsible for the *gsk-3* mutant GSC phenotypes, we investigated two negative regulators of *cdk-2*, pRb (*lin-35*) and p57 (*cki-2*). *lin-35* is a negative regulator of mid-G1 phase of the somatic cell cycles in *C. elegans* (Boxem and van den Heuvel 2001)

and negatively regulates transcription of Cdk2 through inhibition of E2Fs in mammalian cell culture (DeGregori et al. 1997). *cki-2* is thought to negatively regulate late G1 phase in proliferative cells of the soma (Buck, Chiu, and Saito 2009; Kalchhauser et al. 2011) and negatively regulates Cdk2-Cyclin E activity in mammalian cell culture (Lee, Reynisdottir, and Massague 1995). If GSCs are regulated similarly to mammals and *C. elegans* somatic cells, increased expression of either inhibitor should decrease *cdk-2* activity. To test the hypothesis that *lin-35* or *cki-2* affects the progression of G1 into S phase, we depleted *lin-35 via* RNAi and analyzed *gsk-3;cki-2* double mutant germlines. Neither loss of *lin-35* nor loss of *cki-2* rescued the *gsk-3* mutant GSC phenotype, although there was a slight decrease in the progenitor region length of wildtype germline upon of loss of *cki-2* (Figure 26). This suggests that the *gsk-3* mutant GSC phenotype is not due to increased expression of *lin-35* or *cki-2*.

Since we did not observe any altered expression of *cdk-2* regulators that may affect *gsk-3* GSCs, we assayed expression of the *cdk-2* and *cye-1* themselves. *cdk-2* and *cye-1* are expressed in all wildtype GSCs and their loss results in a cell cycle arrest in all of the GSCs suggesting that CDK-2 and CYE-1 are active in all of the GSCs, irrespective of the phase of the cell cycle (Fox et al. 2011) (Figure 27, 28). Thus, to determine whether CDK-2 function was reduced in *gsk-3* mutant germlines and thus responsible for the GSC defects, we assayed for CYE-1 and CDK-2 expression.

We observed that CYE-1 was still expressed in *gsk-3* mutant germlines albeit at a slightly lower in *gsk-3* mutant germlines (Figure 27). This suggested that CYE-1 may not be regulated by *gsk-3*, or responsible for the *gsk*-3 GSC phenotype. Since no CDK-2 antibody exists, we obtained a transgenic YFP::CDK-2 (Cowan and Hyman 2006) driven by the germline-specific *pie-1* promoter and expressed it in the *gsk-3* mutant background to assess its localization. Surprisingly, the transgenic expression of

YFP::CDK-2 in *gsk-3* mutant background rescued the *gsk-3* GSC numbers (Figure 28A-E) and S phase onset and progression (Figure 28A-D, 28F). Additionally, CDK-2 is expressed throughout the GSCs in both wildtype and *gsk-3* mutant cells in this context (Figure 28G, 28H). Because *pie-1* driven YFP::CDK-2 rescued the *gsk-3* mutant GSC defects and localized to the *gsk-3* mutant GSCs in a manner similar to wildtype, it suggested that the defects in *gsk-3* mutants are driven by decreased CDK-2 function and that the relevant regulation of CDK-2 *via* GSK-3 was not through post-translational mechanisms, such as regulating CDK-2 protein degradation or activity through phosphorylation. Together, these data demonstrate that *gsk-3* mutant GSCs enter and progress through S phase slowly due to lower CDK-2 accumulation, likely at the transcriptional level.

To determine whether GSK-3 regulates CDK-2 levels transcriptionally in the GSCs, we assayed for CDK-2 mRNA in dissected germlines from *gsk-3* and wildtype animals, using qRT-PCR. CDK-2 mRNA levels were lower by 10-fold in *gsk-3* mutant germlines compared to wildtype (Figure 29A), and were restored in *gsk-3* mutant animals carrying the transgenic YFP::CDK-2 (Figure 29A). To determine whether the lower transcript level of CDK-2 in *gsk-3* mutant germlines was specific to the GSC population, we performed single molecule hairpin chain reaction FISH (Shah et al. 2016) with CDK-2 mRNA probes in wildtype and *gsk-3* mutant germlines. CDK-2 mRNA accumulates throughout the progenitor zone, predominantly in the cytoplasm, and is specific to *cdk-2* (Figure 29B, 29D). However, in *gsk-3* mutant germlines *cdk-2* mRNA levels are much lower relative to wildtype germlines (Figure 29A, 29C). These data demonstrate that GSK-3 promotes *cdk-2* mRNA transcription in wildtype GSCs and reduction of CDK-2 expression in *gsk-3* mutants leads to defects in S phase entry and progression.

To directly assess whether *gsk-3* regulates the transcription of *cdk-2*, we designed a transcriptional reporter for *cdk-2*. However, a perusal of the *cdk-2* gene structure on Wormbase (ver WS258), revealed that intron 1, rather than the promoter annotated by Wormbase (ver WS258), contained multiple transcription factor and RNA polymerase II binding sites as well as SL1 and SL2 splice sites (Wormbase WS258) (Figure 30). These observations suggested that intron 1, rather than the promoter, may drive *cdk-2* expression. Thus, we generated two distinct transgenes: one with the Wormbase predicted 2Kb promoter driving GFP (*cdk-2[Pr]::GFP*), and one containing the intron 1 driving GFP (*cdk-2[In1]::GFP*) (Figure 31A, 31B). As hypothesized, we observed that *cdk-2[Pr]::GFP* did not express in the germline, suggesting that the predicted promoter does not drive *cdk-2* expression (*vizSi34*, data not shown, Wormbase WS258). Instead, *cdk-2[In1]::GFP* was expressed throughout the germline (Figure 31C), suggesting that intron 1 drives *cdk-2* expression in the germline. In comparison to wildtype, expression of *cdk-2[In1]::GFP* in *gsk-3* mutants resulted in lower GFP accumulation of the reporter in the progenitor zone, but not in oocytes (Figure 13C). Taken together, these data demonstrate that *gsk-3* regulates *cdk-2* transcription in the GSCs.

Human Licensing Factors	*C. elegans* homologs	
	Gene name	Sequence
ORC1	*orc-1*	Y39A1A.12
ORC2	*orc-2*	F59E10.1
ORC3	*orc-3*	Y119D3B.11
ORC4	*orc-4*	Y39A1A.13
ORC5	*orc-5*	ZC168.3
CDC6	*cdc-6*	C43E11.10
CDT1	*cdt-1*	Y54E10A.15
MCM2	*mcm-2*	Y17G7B.5
MCM3	*mcm-3*	C25D7.6
MCM4	*mcm-4*	Y39G10AR.14
MCM5	*mcm-5*	R10E4.4
MCM6	*mcm-6*	ZK632.1
MCM7	*mcm-7*	F32D1.10

Table T3: DNA licensing factor homologs in *C. elegans*

Human DNA licensing factors are listed along with their *C. elegans* homologs and a sequence identifier. Highlighted sequences were tested by RNAi.

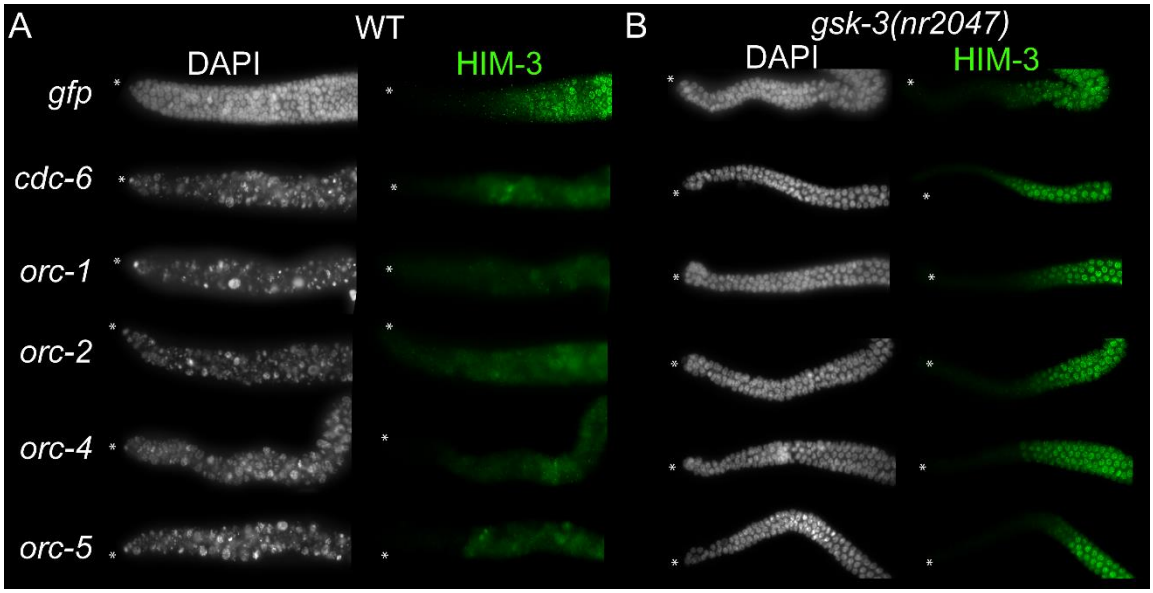

Figure 25: DNA licensing factors do not contribute to *gsk-3* mutant GSC defects

All microscopy images in this figure display the progenitor region of a dissected germline after control RNAi (gfp) or RNAi of 5 members of the origin recognition and licensing complex in wildtype (A) and *gsk-3* mutants (B). Distal tip of the germline (asterisk) is on the left of the photograph. DAPI (white) enables the visualization of DNA, while HIM-3 (Shah et al.) enables visualization of meiotic cells.

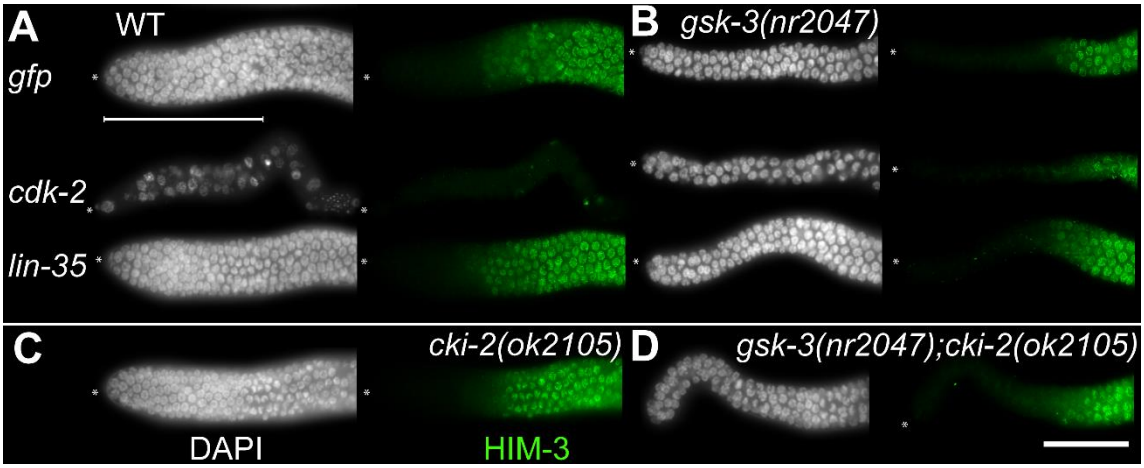

Figure 26: *cdk-2* inhibitors do not contribute to the *gsk-3* mutant GSC defects

(A, B) Progenitor regions of a dissected germline after control RNAi and RNAi of *cdk-2* and *lin-35* in wildtype (A) and *gsk-3* mutants (B). (C, D) Progenitor regions of a dissected germline from *cki-2(ok2105)* single and *gsk-3(nr2047);cki-2(ok2105)* double mutants. Distal tip of the germline (asterisk) is on the left of the photograph. DAPI (white) enables the visualization of DNA, while HIM-3 (Shah et al.) enables visualization of meiotic cells. Scale bar: 40µm

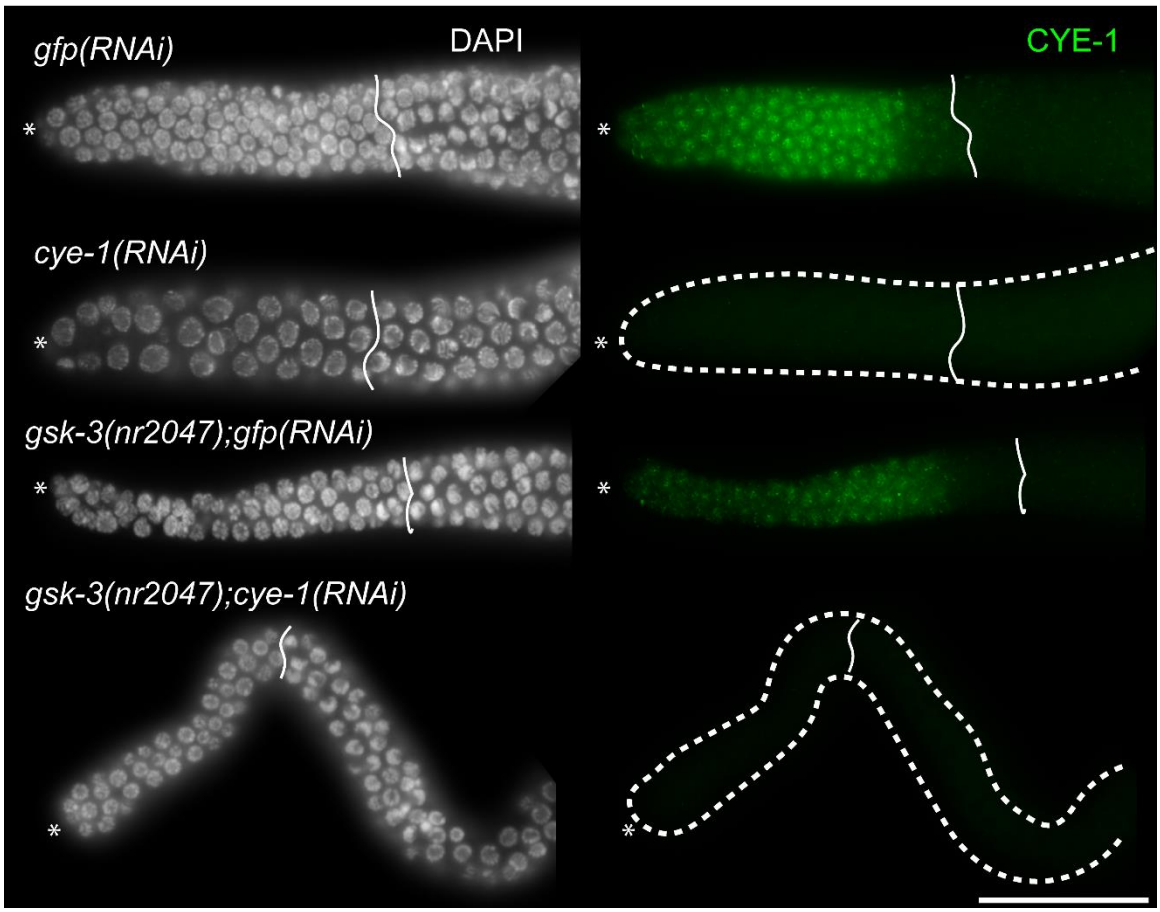

Figure 27: CYE-1 protein is expressed in *gsk-3* mutant GSCs

Dissected germlines from wildtype and *gsk-3(nr2047)* mutant animals, oriented with distal end (*) to the left. Anti-*cye-1* antibody labels Cyclin E in all the GSCs evenly in both wildtype and *gsk-3* mutant germlines, and is specific to *cye-1* RNAi. End of progenitor zone is labeled with a white line. Scale bar: 40µm.

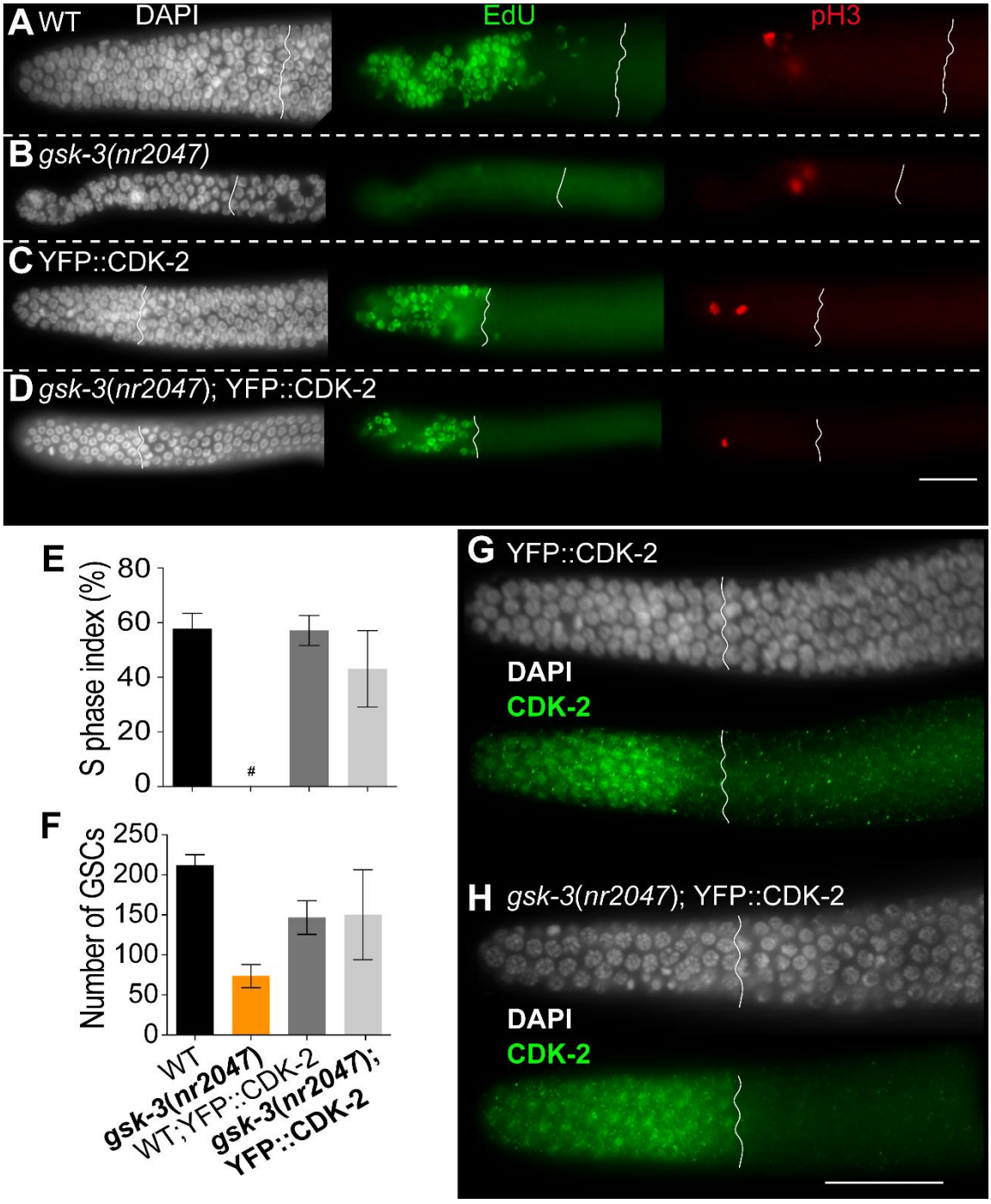
A WT
DAPI
EdU
pH3
B gsk-3(nr2047)
C YFP::CDK-2
D gsk-3(nr2047); YFP::CDK-2
E
S phase index (%)
80
60
40
20
0
#
F
Number of GSCs
250
200
150
100
50
0
WT
gsk-3(nr2047)
WT;YFP::CDK-2
gsk-3(nr2047); YFP::CDK-2
G YFP::CDK-2
DAPI
CDK-2
H gsk-3(nr2047); YFP::CDK-2
DAPI
CDK-2

Figure 28: CDK-2 overexpression rescues the *gsk-3* mutant GSC defect

Dissected germlines displaying the progenitor zone oriented with the DTC to the left in all photographs in this figure. (A-D) Transgenic expression of YFP::CDK-2 (*ddIs30*, via Ppie-1 promoter) in *gsk-3* mutant germlines results in EdU incorporation upon a 10 minute EdU pulse (D), *gsk-3* single mutants incorporate very low or no EdU with the same treatment (B). (E-F) *pie-1* driven YFP::CDK-2 rescues the S phase index (E) and the total number of GSCs of *gsk-3* mutant germlines (F). (G-H) YFP::CDK-2 is expressed uniformly in all of the GSCs in wildtype and *gsk*-3 mutants. (A-H) the experiments were performed four times, each time 30-35 germlines analyzed. End of each progenitor zone is labeled with a solid line. Scale bar: 40µm.

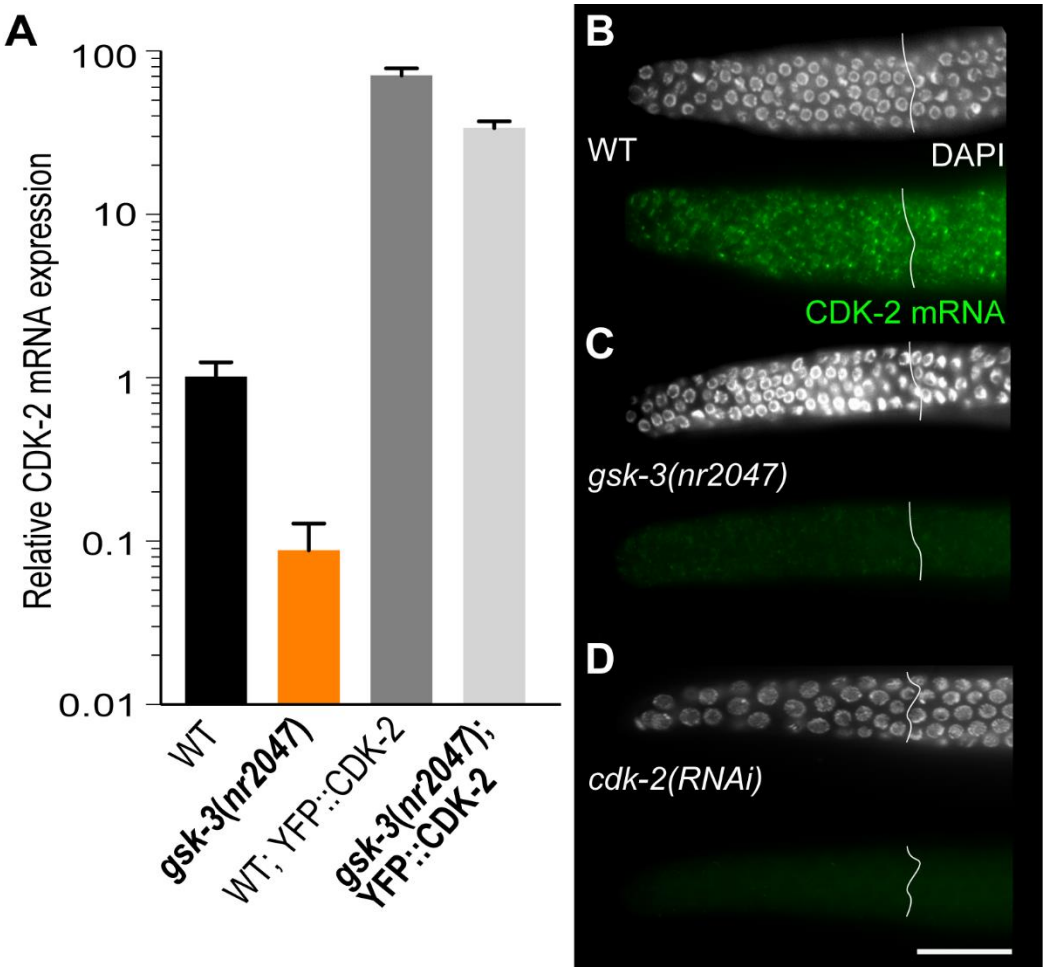

Figure 29: *cdk-2* mRNA is downregulated in *gsk-3* mutant GSCs

(**A**) qRT-PCR demonstrates significantly lower levels of *cdk-2* mRNA in *gsk-3* mutant germlines relative to wildtype. YFP::CDK-2 has higher *cdk-2* mRNA compared to wildtype, revealing over-expression of CDK-2 in the transgene. (**B-D**) *cdk-2* FISH analysis on dissected germlines shows cytoplasmic expression of *cdk-2* in wildtype (B) that is absent in *cdk-2* depleted germlines (D) and low in *gsk-3* mutant germlines (C). Panel A the experiment was performed three times and each time 100 germlines were dissected and assayed by qRT-PCR. (B-D) the experiment was performed three times, each time 12-15 germlines were assayed. All experiments were performed on adult animals, at 24 hours past L4 stage of development. End of each progenitor zone is labeled with a solid line. Scale bar: 40µm.

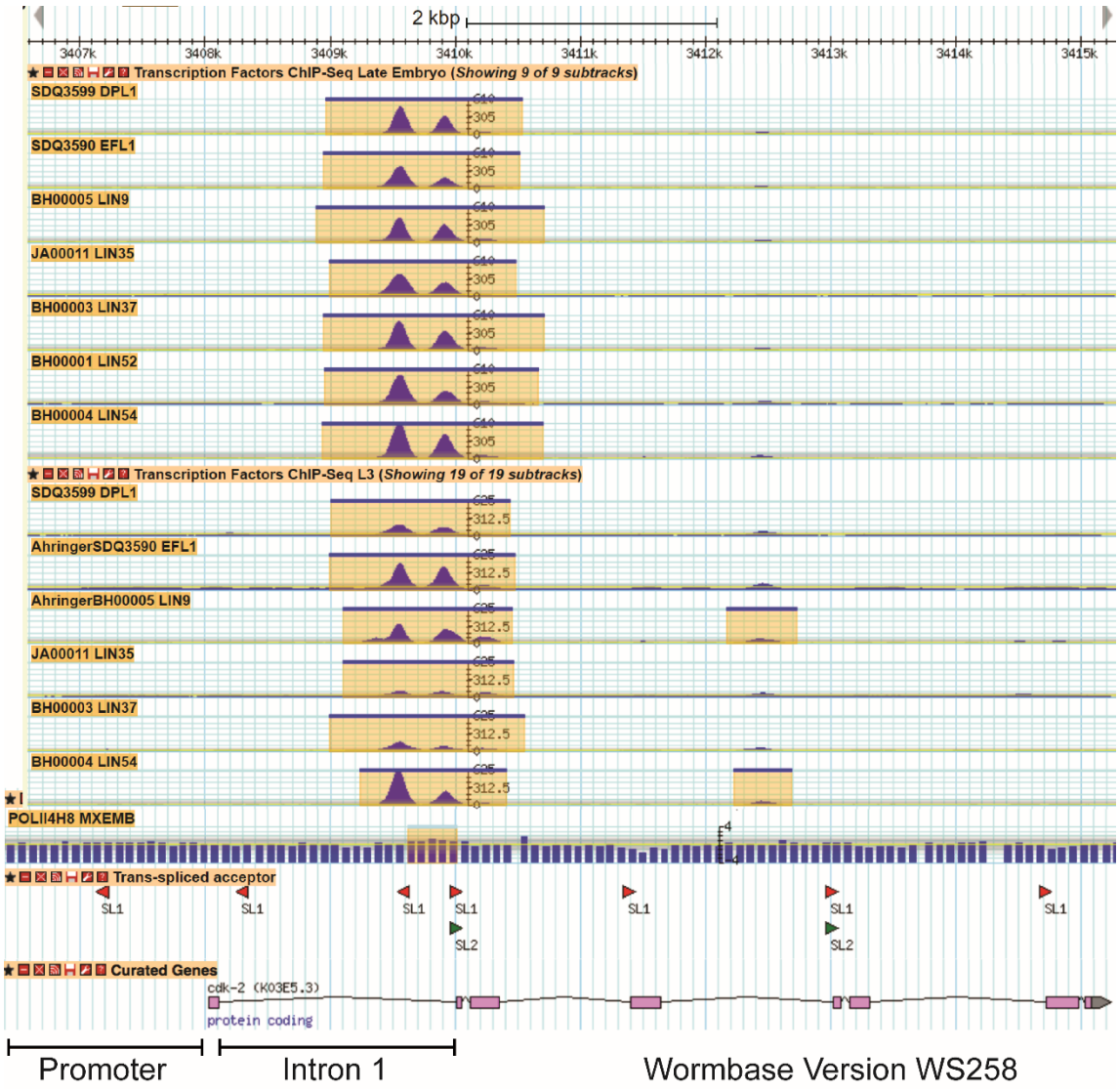

Figure 30: Intron 1 of *cdk-2* is the promoter (WS258)

Screen shot of Wormbase Ver. WS258 depicting the binding of various transcription factors as well as DNA polymerase II via Chip analysis to the “intron 1” of *cdk-2* along with predicted SL1 and SL2 trans-splicing sites. Regions highlighted in yellow are predicted binding sites. Transcription factors which did not bind to either the promoter or the intron were removed from the figure. CHIPs which did not show binding of DNA polymerase II to either the promoter or the intron were removed from the figure.

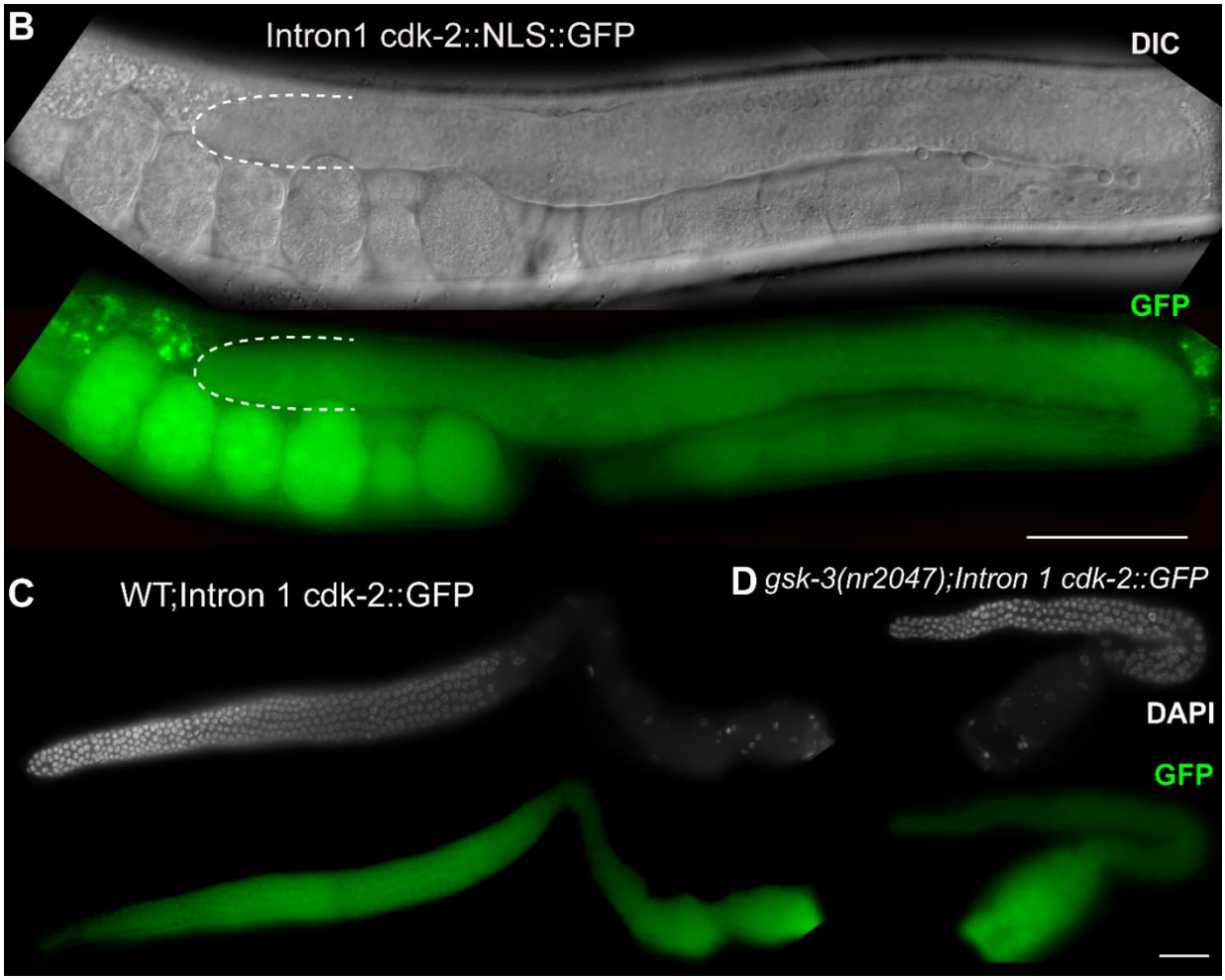

Figure 31: *gsk-3* promotes *cdk-2* transcription which is driven by intron 1

(A) Gene structure of *cdk-2* on Wormbase Ver WS258. (B) Differential interference contrast (DIC) and GFP live image depicting the expression of the transcriptional reporter driven by Intron 1 of *cdk-2* in the germline and embryos. Dashed line marks outline of distal germline. (C-D) Dissected germlines for adult (24 hours past L4) wildtype and *gsk-3* mutants carrying the *cdk-2* transcriptional reporter driven by Intron 1 reporter, mounted in PLP media on the same slide, reveal expression of the *cdk-2* transcriptional reporter in the progenitor zone (C) of wildtype but not *gsk-3* mutant (D). End of each progenitor zone is labeled with a solid line. Scale bars: 50µm.

3.5: DPL-1 Mediates GSK-3-dependent Regulation of CDK-2 Transcription and S Phase Progression

To determine the factors that regulate *cdk-2* transcription downstream to GSK-3, we perused the ChIP data for the *cdk-2* intron 1 using Wormbase, and identified several transcription factors that bind to it, most notably, *efl-1* and *dpl-1*, homologs of the E2F transcription factor family and the Dp1 transcription factor (Chapter 1.2.2, Figure 32), which promote S phase entry in vertebrate systems (Almasan et al. 1995; Muller et al. 1997). Because loss of *efl-1* or *dpl-1* individually does not inhibit S phase in *C. elegans* (Ceol and Horvitz 2001; Chi and Reinke 2006, 2009), suggesting that they do not promote S phase in *C. elegans*, we wondered whether they repress rather than promote S phase in the context of *gsk-3* mutants. To determine whether these factors regulate S phase entry and progression downstream to *gsk-3*, we assayed them via RNAi-mediated depletion in the *gsk-3* background. Depletion of *dpl-1* in L4 animals from wildtype or *gsk-3* heterozygous animals resulted in strong embryonic lethality in F1 progeny, as did the double mutants between *dpl-1* and *gsk-3* (not shown). Thus, we depleted *dpl-1* starting at L4 in wildtype and *gsk-3* mutant animals for 48 hours and assayed for EdU incorporation in the germlines (Figure 33). Wildtype GSCs from control (luciferase) RNAi and *dpl-1* RNAi exhibited normal EdU incorporation with S phase indices of ~55% and ~67% respectively (Figure 33A, 33C, 33F), as well as endomitotic oocytes in the proximal germlines, as described previously (Chi and Reinke 2006, 2009). *dpl-1* RNAi in *gsk-3* mutant animals restored EdU incorporation in GSCs in all the germlines with an S phase index of ~35% (Figure 33B, 33D, 33F), partially rescuing the S phase progression defect. These data suggest that *gsk-3* normally inhibits *dpl-1* in the GSCs to promote S phase progression.

To determine whether *dpl-1* regulated *cdk-2* mRNA levels, we performed FISH analysis on *gsk-3(nr2047);dpl-1(RNAi)* dissected germlines. We found that the *cdk-2* mRNA was restored in the *gsk-3(nr2047);dpl-1(RNAi)* double mutant germlines and was equivalent to *dpl-1* RNAi alone (Figure 34). In summary, these data demonstrate that *gsk-3* inhibits *dpl-1* to maintain persistent high levels (and thus activity) of CDK-2 mRNA expression in wildtype GSCs, resulting in rapid S phase entry and progression.

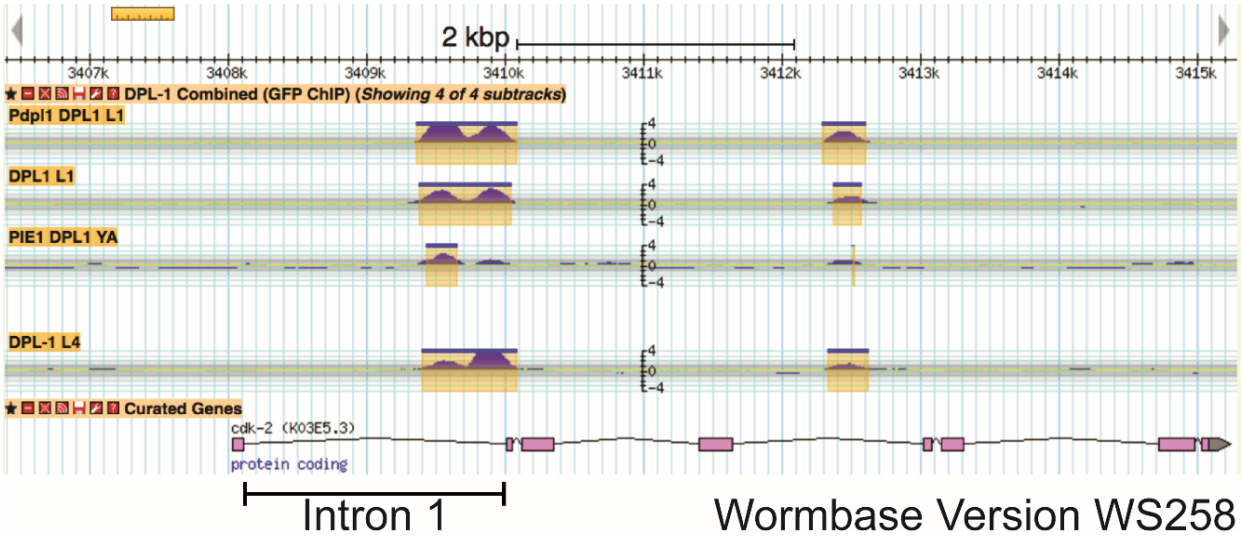

Figure 32: DPL-1 binds to the *cdk-2* intron1

Screen shot of Wormbase Ver. WS258 depicting the binding of DPL-1 via ChIP analysis to the “intron 1” of *cdk-2*.

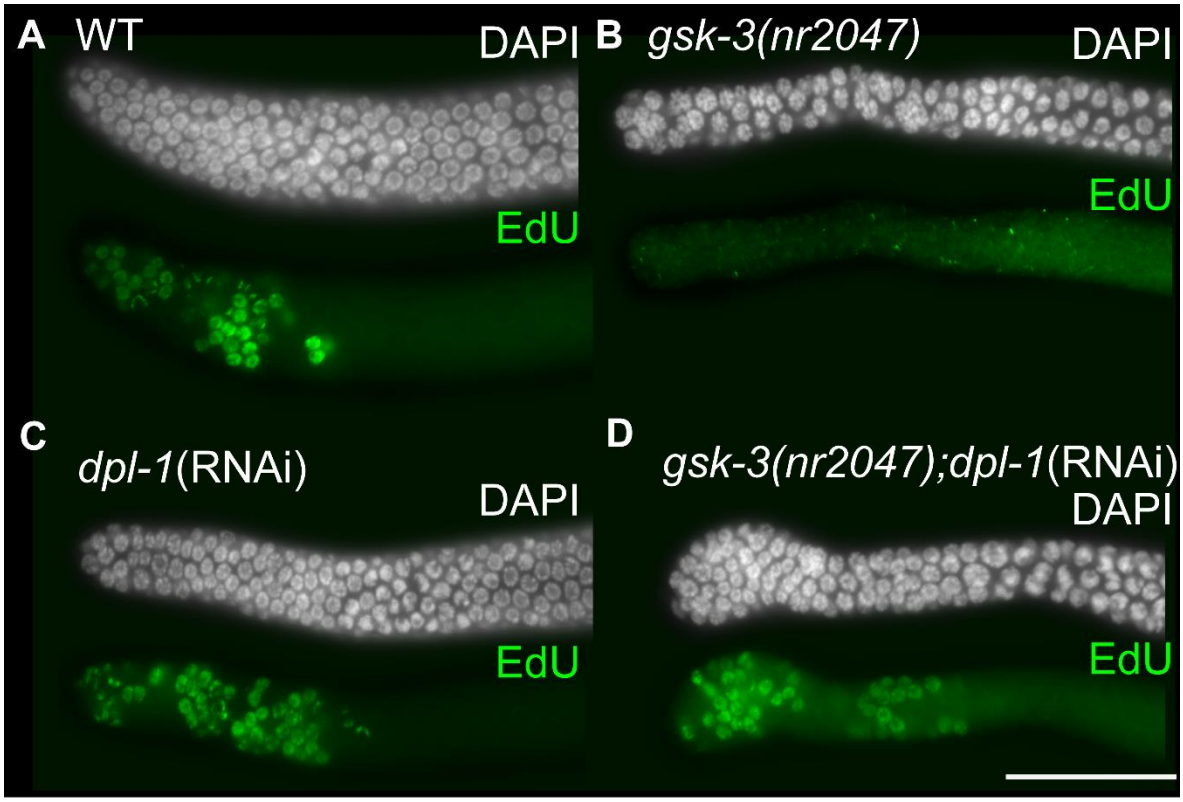
A WT
DAPI
EdU
B gsk-3(nr2047)
DAPI
EdU
C dpl-1(RNAi)
DAPI
EdU
D gsk-3(nr2047);dpl-1(RNAi)
DAPI
EdU

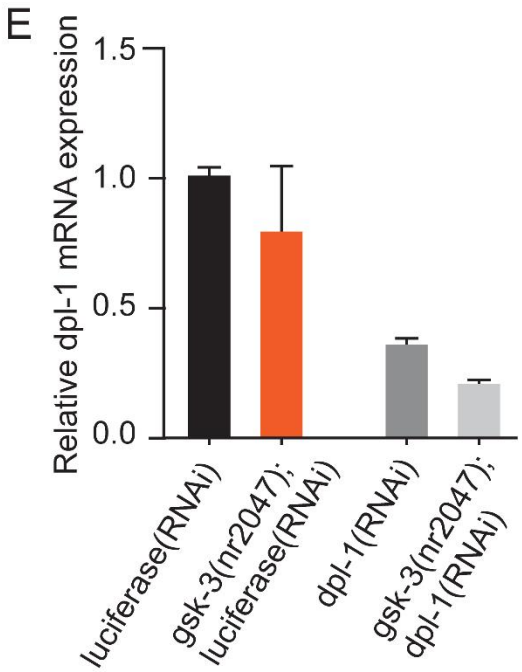
E
Relative dpl-1 mRNA expression
1.5
1.0
0.5
0.0
luciferase(RNAi)
gsk-3(nr2047); luciferase(RNAi)
dpl-1(RNAi)
gsk-3(nr2047); dpl-1(RNAi)

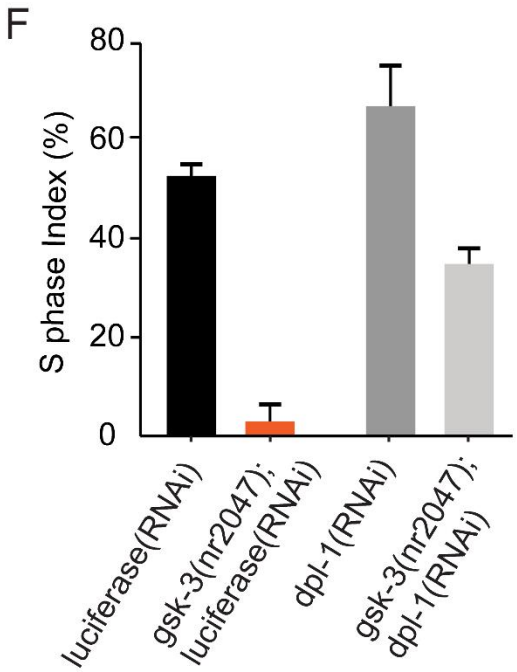
F
S phase Index (%)
80
60
40
20
0
luciferase(RNAi)
gsk-3(nr2047); luciferase(RNAi)
dpl-1(RNAi)
gsk-3(nr2047); dpl-1(RNAi)

Figure 33: *dpl-1* RNAi rescues the *gsk-3* mutant GSC proliferation defect

Dissected adult (24 hours past L4) germlines displaying the progenitor zone oriented with the DTC to the left in all photographs in this figure. (**A-D**) RNAi-mediated depletion of *dpl-1* in *gsk-3* mutant animals results in restoration of EdU incorporation, assayed by a 10-minute EdU pulse (D), *gsk-3* single mutant germlines incorporate very low EdU (B). (B) RNAi mediated depletion of *dpl-1* in wildtype and *gsk-3* mutant germlines results in a strong reduction of *dpl-1* mRNA abundance. (C) RNAi mediated depletion rescues the EdU incorporation and restores the S phase index to ~35% in *gsk-3* mutant GSCs. The RNAi experiments were performed five times, and for A-D 20-22 germlines were imaged each time. Scale bar: 40µm.

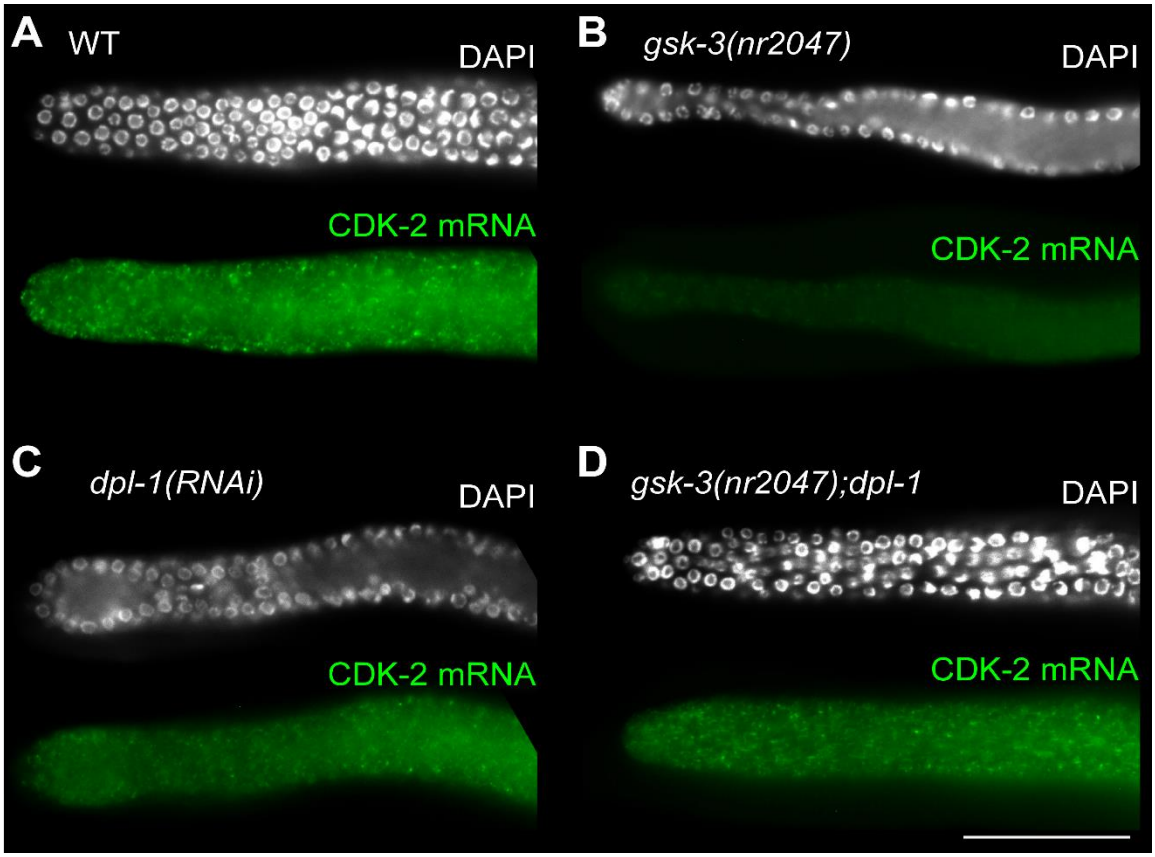

Figure 34: *dpl-1* RNAi rescues *cdk-2* transcription in *gsk-3* mutants

(A-D) RNAi-mediated depletion of *dpl-1* in *gsk-3* mutant animals results in accumulation of *cdk-2* mRNA (D), *gsk-3* single mutant germlines exhibit very low accumulation of *cdk-2* mRNA (B). The photographs for *cdk-2* FISH were captured at 220ms each. A-D, 10-12 germlines were imaged each time. Scale bar: 40µm.

3.6 Conclusion and Model

We report on a novel mechanism through which *C. elegans* germline stem cells maintain their unique cell cycle structure with an abbreviated G1 phase (Figure 35). We find that *gsk-3* promotes S phase entry and progression in a metabolically rich environment to mediate rapid expansion during the larval stages. GSK-3 function does not impact the balance between differentiation and self-renewal of the stem cells, revealing a specific function of this physiological regulator in maintaining the pool of GSC. The observed lack of EdU incorporation in *gsk-3* mutants is likely not due to EdU accessibility to the germline, but rather points to difficulty of S phase entry and progression. We find that it is not due to aberrant DNA licensing or CDK-2 inhibition, but rather due to low expression of CDK-2 itself. We next find that CDK-2 is inhibited transcriptionally in *gsk-3* mutants, which is rescued by RNAi of the cell cycle regulator *dpl-1*. This results in a situation where *cdk-2* mRNA expression is regulated by *gsk-3* to maintain a continuously high expression in the GSCs, resulting in high CDK-2 protein levels, so that when the cells reach the end of mitotic M phase they can transition into S phase with minimal time spent in G1. This results in an abbreviated G1 phase of the cell cycle thus allowing GSCs to proliferate rapidly to meet the tissue demands imposed by continuous production of embryos. Additionally, since *gsk-3* is a metabolic regulator, GSCs may respond to chronic metabolic stress to control cell cycle progression through *gsk-3*.

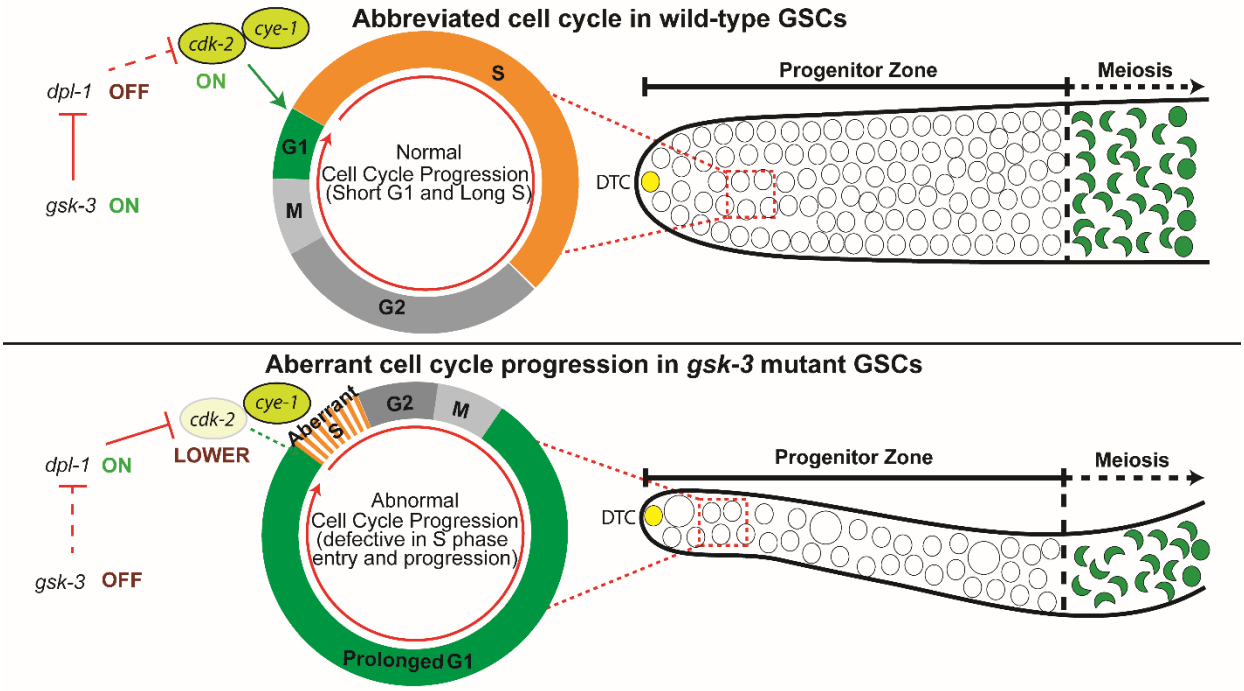

Figure 35: *gsk-3* Model

GSK-3 beta inhibits DP1 transcriptional repressor to maintain persistent high levels of CDK-2 and mediate a short G1 coupled with rapid S phase entry and progression in *C. elegans* germline stem cells.

CHAPTER 4: ACUTE NUTRITIONAL DEPRIVATION AND GERMLINE STEM CELL PLASTICITY

Chapter 4: Acute Nutritional Deprivation and Germline Stem Cell Plasticity

4.1: Introduction

Cell cycle control is integral to the plasticity of a constantly dividing population of stem cells such as the *C. elegans* GSCs. In conditions such as acute starvation or lack of nutrients, the inability to halt the cell cycle would result in an exhaustion of energy and nutrients. *C. elegans* PGCs and GSCs also arrest in conditions of acute starvation, likely to cope with the hostile environment. PGCs arrest at G2 when the larva hatches in the absence of food. This arrest is abrogated by loss of PTEN (*daf-18)* and PI3K (*age-1)* or AKT (*akt-1*) (Fukuyama, Rougvie, and Rothman 2006). Thus, signaling through the PI3K-AKT axis regulates the PGC arrest in hostile environmental conditions.

GSC arrest appears in response to acute starvation in both L4 and adult animals as well. Acute starvation of L4 worms results in shrinkage of the germline and gamete production halts (Angelo and Van Gilst 2009). Return of the animal to replete nutrition results in regeneration of the germline and gamete production resumes. These data suggested that GSCs display plasticity an ability to adapt to environmental conditions. Seidel and Kimble 2015, discovered that the GSCs undergo cell cycle arrest during this time, though the nature and regulation of the arrest remain unknown (Seidel and Kimble 2015). In this chapter, I investigated the nature of the GSC arrest and uncovered its regulation through nutritional signaling.

4.2: The Adult *C. elegans* GSCs Reversibly Arrest at G2 during Starvation

Acute starvation of adult *C. elegans* causes all the GSCs to stop cell divisions and enter cell cycle arrest. This arrest is completely in place as early as 4 hours of starvation (Figure 36A, B) (Seidel and Kimble 2015). To determine the cause of this arrest, I characterized the cell cycle state of GSCs and assayed for M and S phase using pH3 and EdU labeling respectively. Current methods in the field for EdU incorporation use feeding of the EdU analog through thymidine deficient bacteria grown in the presence of the EdU analog (Fox et al. 2011). Since feeding is incompatible with acute starvation, I devised a method to incorporate EdU by soaking the animal in an EdU solution for 10 minutes (described in detail in Materials and Methods). In this chapter, all EdU incorporation and S phase indices in GSCs from starved or fed control animals were labeled with the soaking EdU method. GSCs from fed animals demonstrated an average of ~4 dividing cells with ~ 60% S phase index (Figure 36B, 36C). However, GSCs from animals without food for more than 4 hours displayed a distinct lack of pH3 labeled cells. These data suggest that the GSCs may be blocked from entering the M phase. To determine whether the S phase would alter with longer starvation times, I assayed GSC starvation for 4, 8, 12, and 18 hours, and observed that the S phase index does not change significantly upon extended starvation times (Figure 36C). Even in GSCs from animals without food for 18 hours, which is ~3 times longer than normal S phase length, I observed that the percentage of cells in S phase had not altered significantly. Since the GSCs are not actively entering M phase (as they do not display any pH3 positive nuclei), they are not transitioning into G1. Therefore, there are no new cells to enter S phase during starvation. With no new input into S phase, and no apparent output from S phase, these data suggest that the cells which were in S phase at the beginning of starvation remain in S phase for at least 3 times

longer than expected, leading to the model that starvation causes an extended S phase in the GSCs along with a cell cycle arrest. This cell cycle arrest is reversible since refeeding the animals after twelve hours of starvation causes pH3 positive cells to reappear (Figure 36A).

Together, these data reveal that the *C. elegans* GSCs undergo a reversible cell cycle arrest with an extended S phase. The finding that a cell cycle arrest is imposed in GSCs in *C. elegans* was also demonstrated by the Kimble lab during the course of this work (Seidel and Kimble 2015). What remains unknown is the nature of the arrest and the underlying mechanism.

I hypothesized that the arrest was most likely in the G2 phase of the cell cycle, which until now the field has only assayed using nuclear size as an assay. However, if cell cycle arrest is induced via cdk-1 or cdk-2 depletion, the GSC nuclei expand into a “fried egg” morphology. Therefore, nuclear size is an imprecise measure of cell cycle phase during cell cycle arrest. Therefore, to determine whether the GSCs arrested at G2, I performed an EdU pulse-chase experiment and assayed the various stages of the cell cycle upon starvation and refeeding (Figure 37).

Since starved germlines incorporate EdU, cells in S phase can be labeled at any point during starvation. Therefore, I reasoned that if starved germlines are pulsed with EdU and released from starvation the S phase labeled cells would also label with pH3 when the cells divide after re-entering the cell cycle (Figure 37). Such cells would be double positive – S phase and M phase labeled. However, if there are cells which arrest in the G2 phase of the cell cycle, then they would not incorporate the EdU label. Once these cells divide upon release of the arrest, they would only be labeled for pH3 and be single label positive. Since G2 is after S phase, any EdU negative cells observed dividing before EdU positive cells would have been from G2 (Figure 37).

To determine the stage at which the cells were arrested during starvation I pulsed the animals with EdU after a 12 hour starvation, then refed them for 1 hour, 2 hours and 4 hours. As expected the control starved germlines displayed no pH3 positive cells. Upon 1 hour of refeeding, a majority of the germlines displayed no pH3 staining in the GSC population suggesting that the cells were in an arrested state, likely because the nutritional trigger had not been detected (Figure 38B). However, ~30% of the animals displayed pH3 positive cells suggesting that in these animals, the nutritional cues had triggered re-entry into the cell cycle (Figure 38A, 38B). A majority of these pH3 positive cells were EdU negative (Figure 38B) suggesting that the first set of cells to renter the cell cycle upon refeeding had arrested at the G2 stage. By 4 hours of refeeding, a significant proportion of the GSCs were both pH3 and EdU positive. The spike of divisions observed in some animals at 1 hour of refeeding is consistent with a cell cycle arrest and a piling up of germ cells at that point of the cell cycle. Upon the release of that arrest, this synchronized portion of cells enter mitosis together, and with most of them being EdU negative, these cells were most likely released from a G2 arrest.

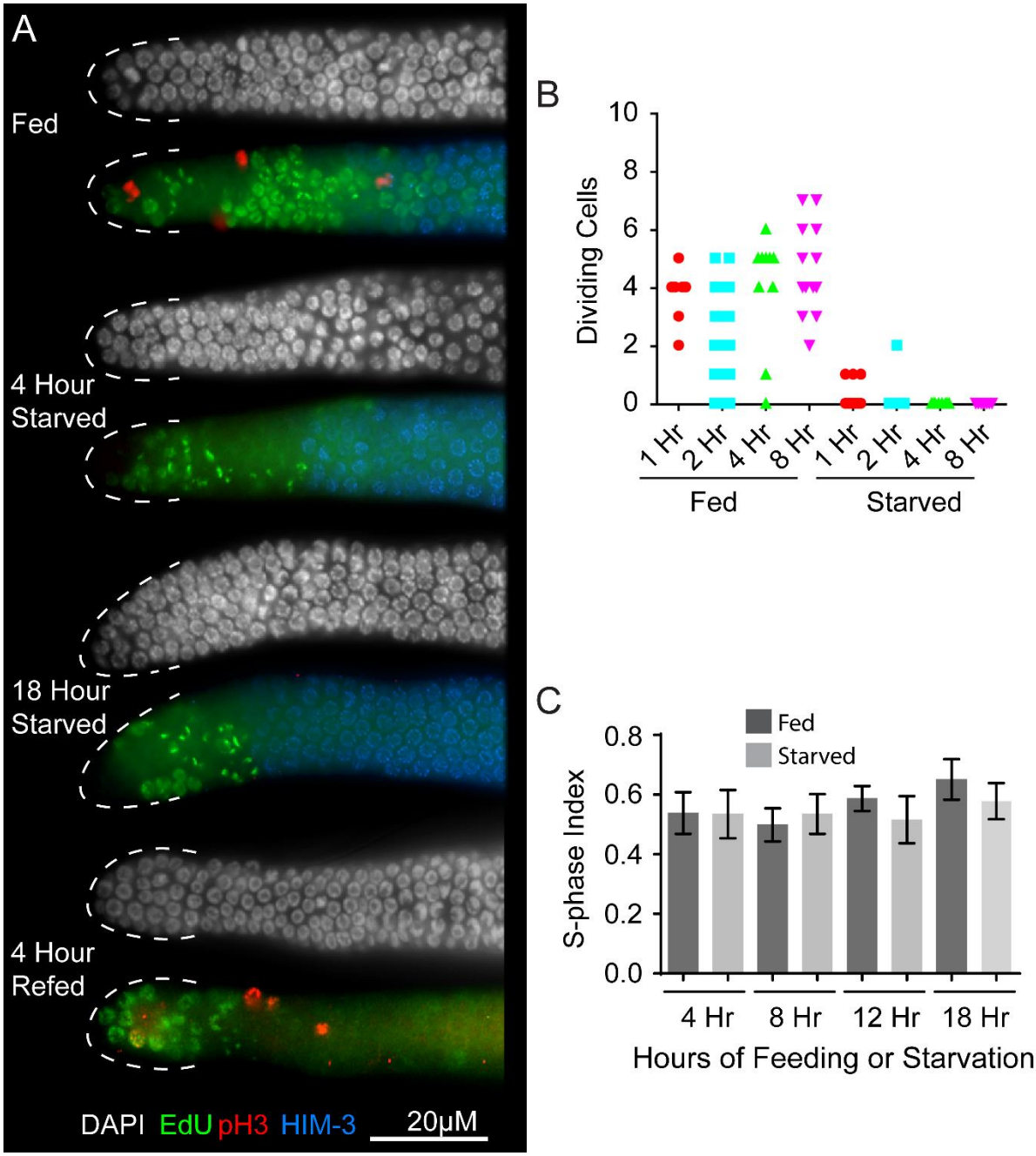
A
Fed
4 Hour
Starved
18 Hour
Starved
4 Hour
Refed
DAPI EdU pH3 HIM-3
20μM
B
Dividing Cells
10
8
6
4
2
0
1 Hr
2 Hr
4 Hr
8 Hr
1 Hr
2 Hr
4 Hr
8 Hr
Fed
Starved
C
Fed
Starved
S-phase Index
0.8
0.6
0.4
0.2
0.0
4 Hr
8 Hr
12 Hr
18 Hr
Hours of Feeding or Starvation

Figure 36: Starvation induces a reversible cell cycle arrest

(A) Dissected germlines with distal tips outlined with a dashed line and oriented to the left. Stained with DAPI (white), EdU (green) pH3 (red), and HIM-3 (blue). Last germline does not have HIM-3. From top to bottom, animals were: (1) Fed for 4 hours after reaching 24 hours past L4; (2) Starved for 4 hours after reaching 24 hours past L4; (3) Starved for 18 hours after reaching 24 hours past L4; (4) Starved for 12 hours after reaching 24 hours past mid L4 followed by recovery to replete conditions (NGM plate with OP50) for 4 hours. (B) Dividing cells were counted in fed and starved germlines. Time point listed is the duration of feeding or starvation after reaching 24 hours past mid L4. (C) S phase index of germlines from fed and starved animals. Time point listed is the duration of feeding or starvation after reaching 24 hours past mid. Scale bar: 20μm.

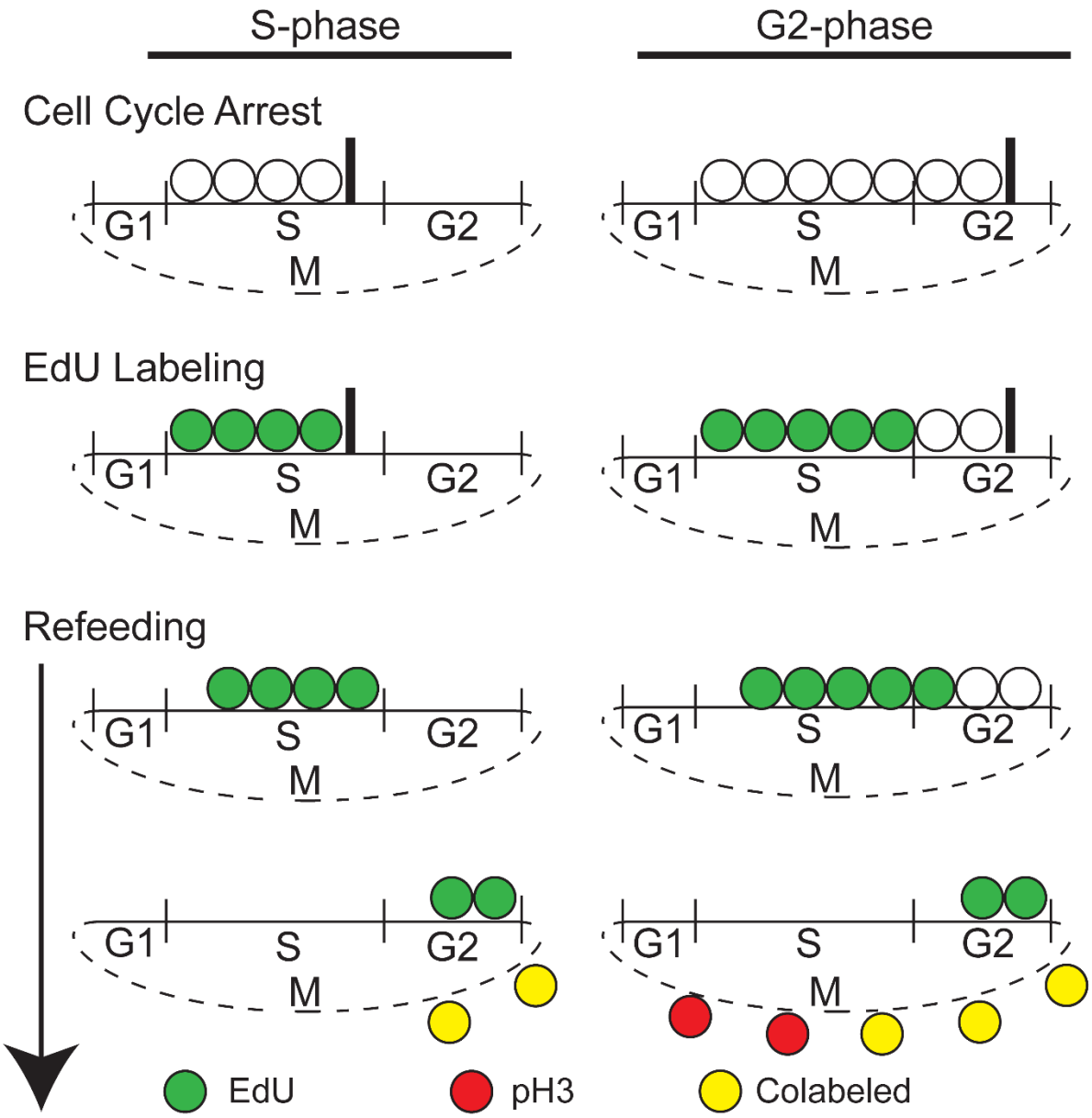

Figure 37: Detecting G2 cells after releasing the reversible arrest

Experimental plan for detecting G2 cells by pulsing EdU and releasing the reversible starvation-induced arrest. Time is on the y-axis. Circles represent cells. Solid line next to circles represents an arrest. Cells can be unlabeled (white) or labeled for EdU (green), pH3 (red), or both (yellow).

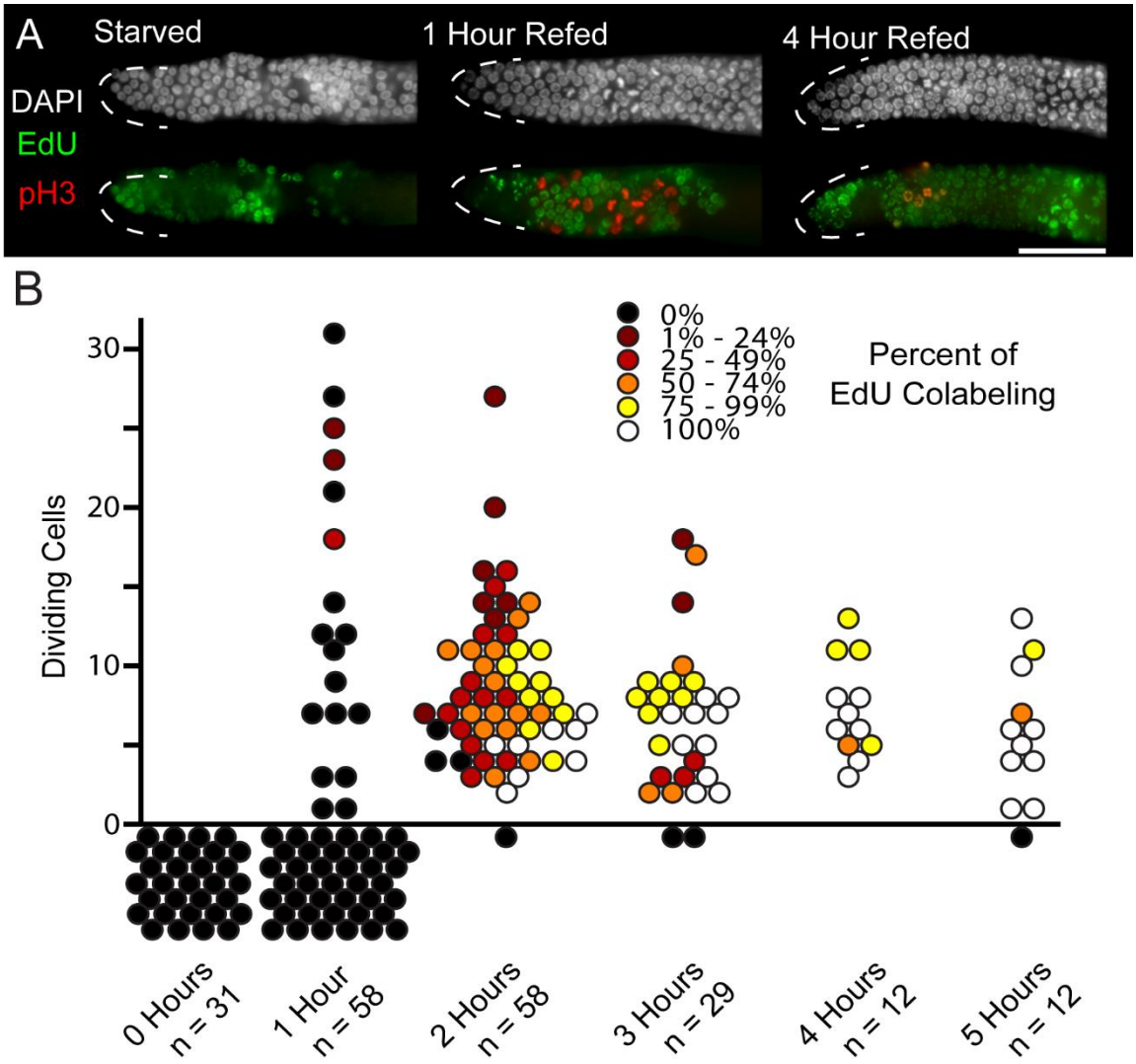

Figure 38: Starvation induces a G2 arrest.

(A) Dissected wildtype germlines after starvation (left) and refeeding (middle and right) with distal tips outlined with a dashed line and oriented to the left. Stained with DAPI (white), EdU (green) pH3 (red). (B) Analysis of EdU colabeling after an EdU pulse-chase experiment. Circles represent individual germlines. Height on the y-axis represents the number of dividing cells in that germline. Color depicts the percent of dividing cells which are co-labeled with EdU. Circles below the X-axis had no dividing cells. Scale bar: 20µm.

4.3: The Starvation-induced G2 Arrest is Independent of DNA Damage Signaling

Since the reversible starvation-induced arrest occurred at the G2 stage, I investigated the role of the DNA damage signaling pathway, which is known to induce a G2 arrest. Starvation has the potential to induce DNA damage through replication stress. If replication continues during starvation, nucleotide depletion is possible due to the lack of an external source of precursors. This replication stress activates Atm and/or Atr kinase which can result in a cell cycle arrest by inhibiting CDK-1 (Zeng et al. 1998). As discussed previously Atm and Atr kinases inhibit Cdk1 through a kinase cascade which leads to a G2 arrest through inhibition of Cdk1-Cyclin B complexes (Chapter 1.2.4). Since *atl-1* has been implicated in regulating cell cycle arrest in GSCs in response to DNA damage, I assayed the activation state of the *chk-1* kinase in GSCs with and without starvation.

In response to Atr activation, Chk1 is phosphorylated at Ser345 and activated. In *C. elegans*, CHK-1 is phosphorylated in response to replication stress from hydroxyurea treatment but not double strand breaks (Lee et al. 2010). I assayed for phospho-CHK-1 status using Hydroxyurea as a positive control. Hydroxyurea treated control GSCs displayed a high level of phospho-CHK-1 staining, suggesting that the *atl-1* pathway activated in response to replication stress in the GSCs (Figure 39). Comparison of GSCs from fed vs starved germlines revealed only a low level of pCHK-1 label, suggesting replication stress may not occur during starvation to induce a cell cycle arrest.

While there was no observable replication stress during starvation, it is possible that other forms of DNA damage were incurred. Therefore, I next investigated whether the DNA damage response played a role in mediating the starvation-induced G2 arrest. *atm-1* and *atl-1* are the major signaling modules through which DNA damage signals in

GSCs. I reasoned that if DNA damage was responsible for the starvation arrest, removal of these kinases would abrogate that arrest. I assayed *atm-1* and *atl-1* single and double mutant GSCs at 24 hours past L4 upon fed and starved treatment for 12 hours. Under fed conditions, wildtype, *atm-1* and *atl-1* GSCs displayed pH3 positive cells, and upon starvation, all genotypes lacked pH3 positive cells, suggesting that the cell cycle arrest was induced (Figure 40). However, while *atm-1* and *atl-1* are thought to be sufficient to mediate the cell cycle arrest due to DNA damage, *atl-1* can compensate for *atm-1* in response to DSBs (Lee et al. 2010). To test whether *atm*-1 and *atl-1* were redundant with each other, I assayed the *atm-1;atl-1* double mutant. As before, fed wildtype and *atm-1;atl-1* double mutant GSCs displayed pH3 positive cells (Figure 41). Upon starvation, wildtype GSCs displayed the G2 arrest and did not label with pH3. However, the *atm-1;atl-1* double mutant germlines displayed pH3 positive GSCs that were seemingly undergoing mitotic catastrophe, with extreme DNA damage (Figure 41, arrowhead). Mitotic catastrophe occurs when a cell attempts to divide with high levels of DNA damage, eventually resulting in cell death. Considering that there is no evidence for programmed cell death or clearance of cell corpses in the progenitor zone of the *C. elegans* GSCs, it is likely that a mitotic catastrophe event perdures for a long time after initiating. Since mitotic catastrophe is a result of extreme DNA damage, their presence in the *atm-1;atl-1* double was not surprising; the mitotic catastrophe likely occurred from lack of *atm-1;atl-1* irrespective of starvation state (as is obvious to a lower extent in GSCs from fed animals). Since I was unable to assess the role of *atm-1* and *atl-1* in regulating the starvation-induced G2 arrest in these experiments, I performed the pulse-chase experiments as described above to assess whether the GSCs arrest in G2 at all in the absence of *atm-1* and *atl-1* upon starvation.

In wildtype GSCs, the EdU pulse-chase experiment revealed an increase in EdU negative pH3 positive cells upon 1 hour of refeeding (Figure 38). I hypothesize that this increase in pH3 positive, EdU negative cells was likely due to a build-up of cells in G2. If a similar build-up were to occur in the absence of the *atm-1* and *atl-1* kinases, there is likely a portion of the G2 arrest which is independent of the DNA damage response. Therefore, I starved *atm-1;atl-1* animals at 12 hours past L4 for 18 hours. I then pulsed the starved animals with EdU for 15 minutes and performed a refeeding time course for 1, 1.5, 2, and 4 hours. As before, the refeeding led to a sharp increase in pH3 positive, EdU negative cells around the 1-1.5 hour mark (Figure 42). At the 4 hour mark, all the germlines contained pH3 cells, although the numbers were lower than those seen at 1-1.5 hours; most of the pH3 positive cells are EdU positive (Figure 42). The similarity in the emergence of EdU negative, pH3 positive cells at 1-1.5 hour of refeeding upon long starvation in wildtype and *atm-1;atl-1* double mutant germlines suggests that starvation induces a G2 arrest even in the absence of the *atm-1* and *atl-1* kinases, and therefore in the absence of DNA damage signaling. These data demonstrate that the starvation-induced G2 arrest is independent of the DNA Damage signaling pathway. I next investigated the mechanism that may regulate the starvation-induced reversible G2 checkpoint.

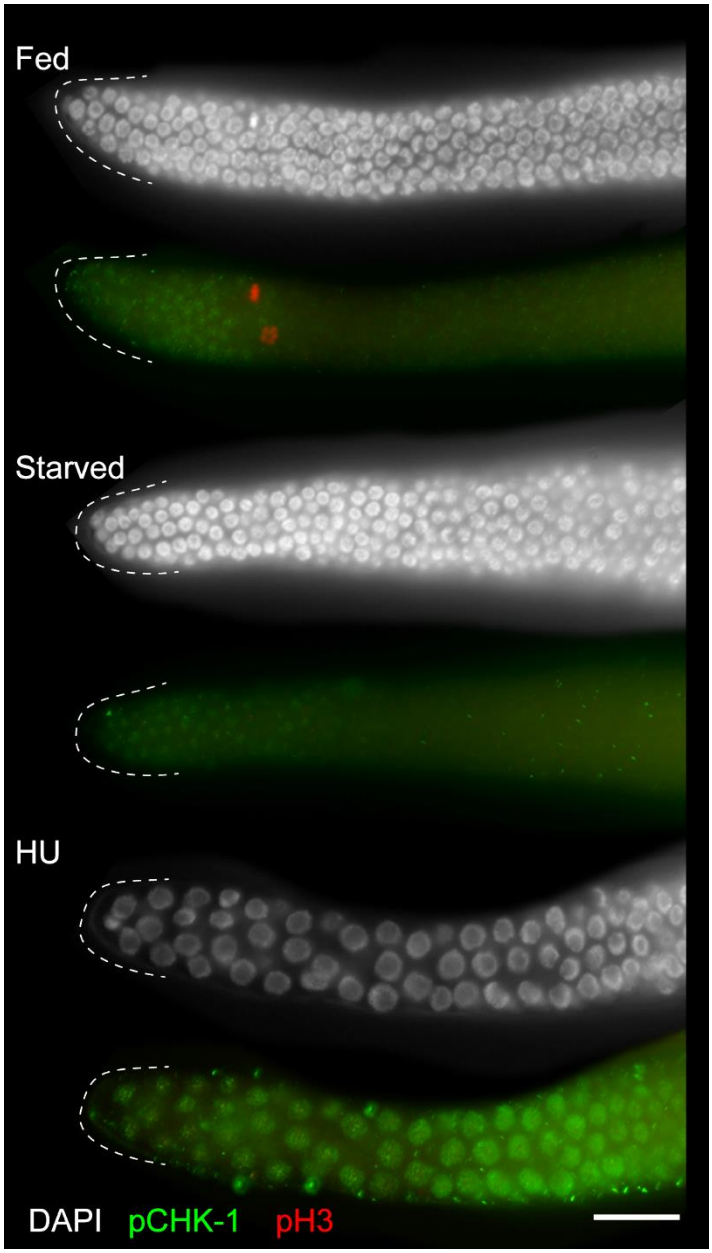

Figure 39: Starvation does not activate CHK-1

Dissected germlines from wildtype animals which were either fed (top), starved (middle), or fed and hydroxyurea treated (bottom). Distal tip is outlined with a dashed line and germlines are oriented with the distal tip to the left. Germlines are stained for DAPI (white), (pSer345)CHK-1 (green) and pH3 (red). Scale bar is 20µm.

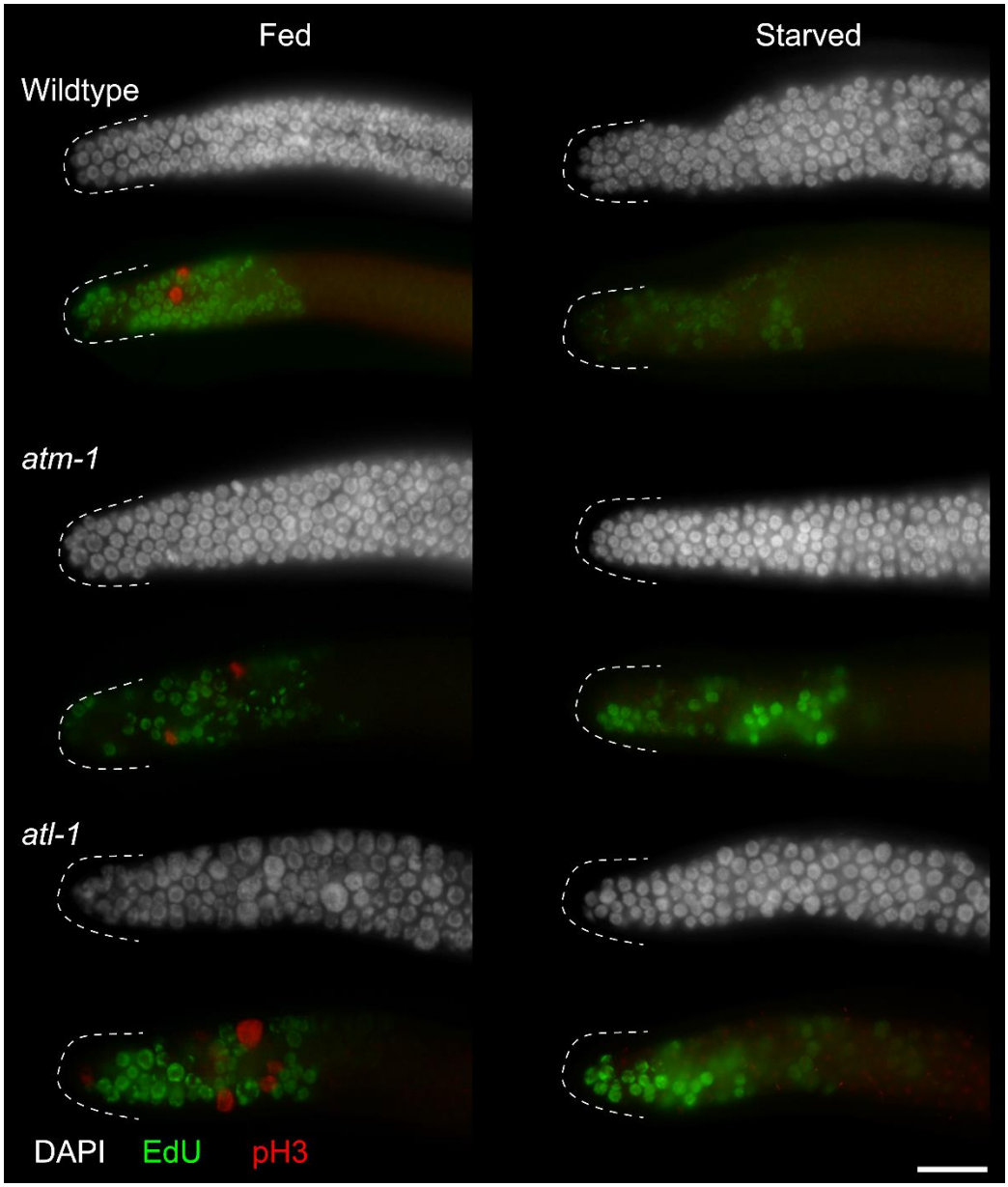

Figure 40: The starvation arrest does not require individual DNA damage kinases

Dissected germlines from *atm-1* and *atl-1* single mutants with wildtype control which were either fed or starved. Distal tip is outlined by a dashed line and is oriented to the left. Germlines are stained with DAPI (white), EdU (green), and pH3 (red). Scale bar: 20µm.

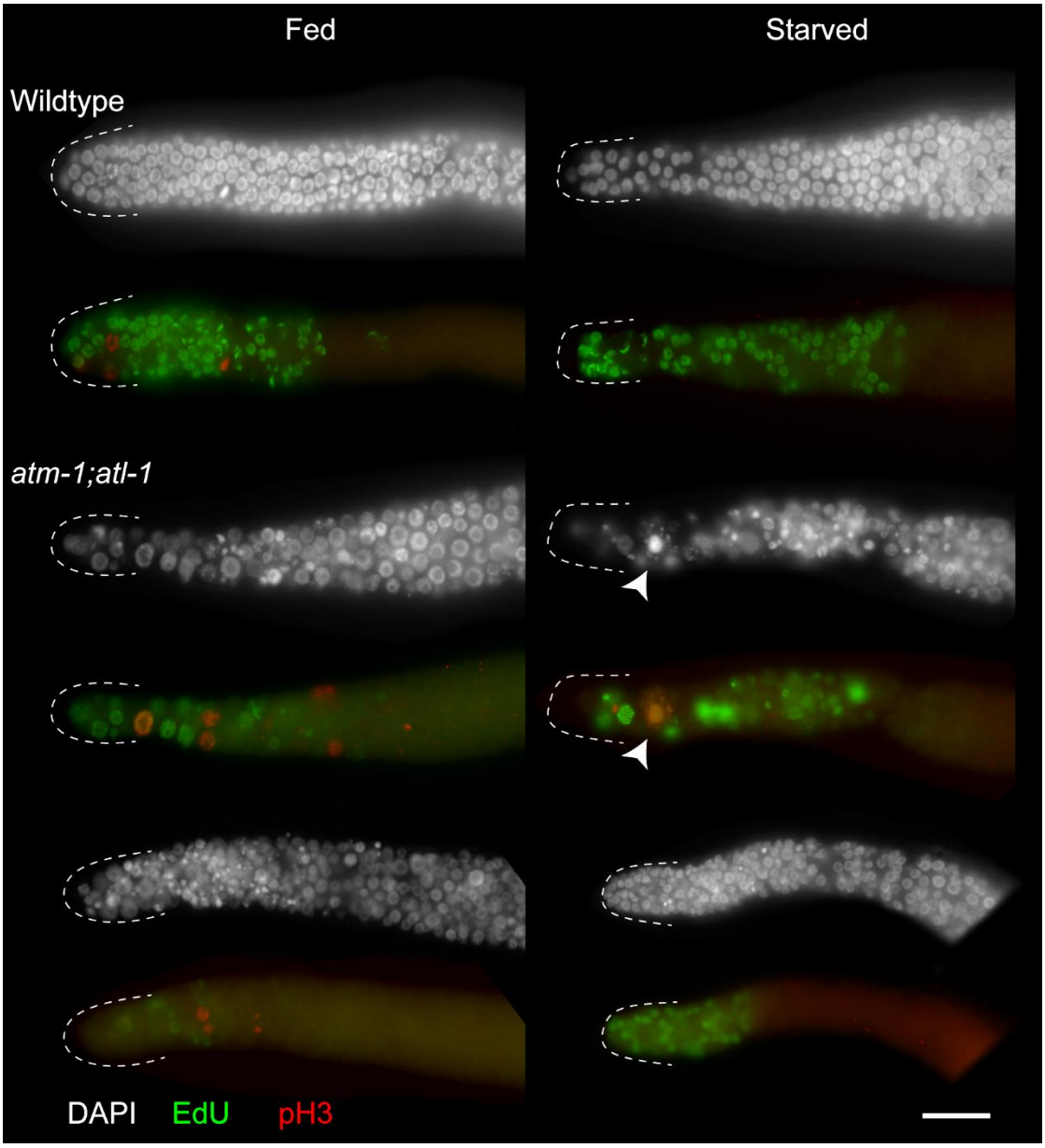

Figure 41: Starvation induces mitotic catastrophe in *atm-1;atl-1* double mutants

Dissected germlines from *atm-1;atl-1* double mutants along with wildtype controls which were either fed or starved. Distal tip is outlined by a dashed line and is oriented to the left. Germlines are stained with DAPI (white), EdU (green), and pH3 (red). Arrowhead depicts a mitotic catastrophe event during starvation which is pH3 positive. Scale bar: 20µm.

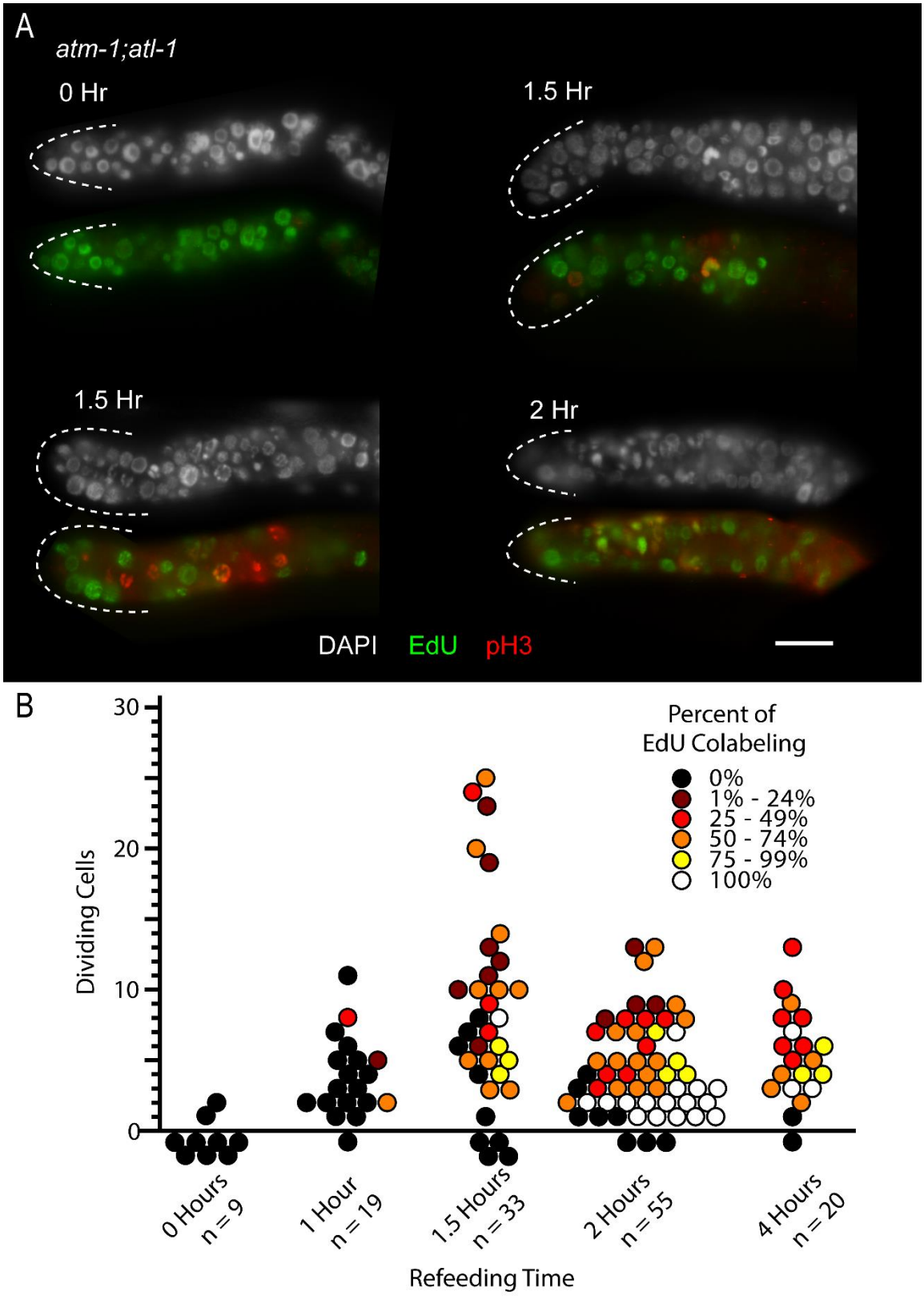
A
atm-1;atl-1
0 Hr
1.5 Hr
1.5 Hr
2 Hr
DAPI
EdU
pH3
B
Dividing Cells
30
20
10
0
Percent of
EdU Colabeling
0%
1% - 24%
25 - 49%
50 - 74%
75 - 99%
100%
0 Hours
n = 9
1 Hour
n = 19
1.5 Hours
n = 33
2 Hours
n = 55
4 Hours
n = 20
Refeeding Time

Figure 42: DNA damage kinases are not necessary for the starvation-induced G2 arrest.

(A) Dissected *atm-1;atl-1* double mutant germlines after starvation (top left) and refeeding (top right, bottom left, bottom right) with distal tips outlined with a dashed line and oriented to the left. Stained with DAPI (white), EdU (green) pH3 (red). Scale bar: 20µm. (B) Analysis of EdU colabeling after an EdU pulse-chase experiment. Circles represent individual germlines. Height on the y-axis represents the number of dividing cells in that germline. Color depicts the percent of dividing cells which are co-labeled with EdU. Circles below the X-axis are germlines with zero dividing cells.

4.4: The Starvation-induced G2 Arrest is Mediated by Nutritional Signaling

The two major nutritional signaling pathways in the *C. elegans* germline are Insulin signaling and TOR signaling (Chapter 1.3.7). Previous studies in the field suggest that both of these pathways play an important role in GSC proliferation in larval animals during the expansion phase (Fukuyama, Rougvie, and Rothman 2006; Michaelson et al. 2010; Korta, Tuck, and Hubbard 2012). To determine whether these two signaling pathways were important for adult GSC arrest I assayed *daf-2(e1370)* mutants to assess the contribution of Insulin signaling and *rsks-1(ok1255)*, a downstream effector of TOR signaling, to assess the contribution of TOR signaling. To rule out any compensation between the two pathways, I also assessed the impact of a loss of both *daf-2* and *rsks-1* with a *daf-2(e1370)rsks-1(ok1255)* double mutant. *daf-2(e1370)* contains a missense mutation in the kinase domain which results in a temperature-sensitive loss of kinase activity at the restrictive temperature of 25°C, while the animal is relatively wildtype at 15°C. Therefore, I used *daf-2(e1370)*, *rsks-1(ok1255)*, and *daf-2(e1370)rsks-1(ok1255)* double mutants at 15°C until 6 hours past mid L4, then shifted for 18 hours to either 25°C or 15°C (Figure 43). In all mutants at either temperature, I observed germlines with dividing cells indicating that a G2 arrest did not occur (Figure 43). However, even a transient arrest or lengthening of G2 would result in a drop in proliferation.

To determine whether there was any evidence of a transient G2 arrest, I counted the pH3 positive cells for each genotype. I reasoned that a lower number of pH3 positive cells would signal either extension of the cell cycle or a transient arrest. However, the length of the progenitor zone can change depending on the degree of differentiation within the germline. Genotypes that result in alteration of the balance between proliferation and differentiation provide less area for GSCs to proliferate, and

thus fewer dividing cells would be observed solely due to a smaller available population. Therefore, I normalized the number of dividing cells by the length of the progenitor region in cell diameters to calculate an adjusted division index (ADI).

I determined the ADI for wildtype at 15°C and 25°C and found that they were similar. In *daf-2* mutants, I observed that at 15°C, the ADI was similar to wildtype, but at the restrictive temperature, the ADI dropped significantly ($p<0.0001$) (Figure 44). However, in *rsks-1* mutants, the ADI was similar to wildtype at either temperature suggesting that *rsks-1* does not contribute to cell cycle progression in adult GSCs (Figure 44). Additionally, in the double mutant, the ADI dropped a similar amount to that in the *daf-2* single mutant at the restrictive temperature, suggesting that *daf-2*, and therefore Insulin signaling, regulates G2/M progression downstream to nutritional input (Figure 44). However, since *rsks-1* is only one of the many downstream effectors of TOR signaling, I chose to investigate TOR itself and assess the contribution of the TOR signaling pathway.

In *C. elegans*, the TOR homolog is *let-363*. Deletions in *let-363* result in a larval arrest at L3, prohibiting investigation into any adult phenotypes (Long et al. 2002). Therefore, to investigate the role of *let-363* in adult GSCs, I depleted *let-363* via RNAi and assayed adult GSCs. Since Mtor kinase is activated in the presence of nutrition, I reasoned that *let-363* RNAi should phenocopy the nutritional arrest. I performed the RNAi at two conditions, a milder condition, where the RNAi was performed in adults for 24 hours followed by assaying the GSCs; and a long term RNAi, where the larvae were subjected to RNAi from hatching with GSCs assayed in the adult (24 hours past L4). The milder 24 hour depletion of *let-363* did not reveal much impact on pH3 positive cells and the RNAi germlines were similar to wildtype germlines (Figure 45). However, with the longer RNAi, I observed that ~30% of germlines were pH3 negative and the

ADI observed was significantly lower than wildtype ($p<0.0001$) (Figure 45). These data suggest that TOR signaling may contribute to G2/M progression in addition to the Insulin signaling. However, due to the inherent variability of RNAi experiments, I generated a loss of function allele in *let-363* and verified these phenotypes.

While LET-363 has not been crystallized, its domain structure is very similar to the human homolog, mTOR, which has been well characterized and crystallized (Yang et al. 2013; Long et al. 2002). I used the homology between the two proteins to design a deletion for *let-363*. The N-terminal portion of LET-363 contains the heat domains to which Rptor (*daf-15*) and Rictor (*rict-1*) bind. The C-terminal portion harbors the Mtor kinase domain which is split in half by the Fkbp12-Rapamycin binding domain (FRB), which protrudes from the kinase domain and partially occludes the substrate cleft (Yang et al. 2013) (Figure 46A, B). The FRB has been found to assist in recruiting p70s6k in mammals. While *rsks-1* does not affect proliferation in adult GSCs, the FRB may recruit other downstream effectors of *let-363*. Therefore, I used CRISPR to remove this domain in an attempt to create a partial loss of function allele.

The FRB bridges exons 26 to 28, so I identified two crRNAs which bordered the domain (Figure 46C). After designing the repair template to contain 5xGly as a flexible linker, I performed the CRISPR injections (Figure 46C). I identified 6 candidates from the injections corresponding to the homology repair using a PCR-based screening method (Figure 46D) (Chapter 2.1.6). Sequencing of the lesion revealed that five of the six candidates contained the desired sequence. The resultant allele, *let-363(viz27)* (Hereafter designated *let-363(ΔFRB))* is viable and does not arrest at L3 as null alleles of *let-363* do. However, *let-363(ΔFRB)* animals are smaller in size than wildtype (data not shown), and while their brood size is the same as wildtype, their rate of egg laying is decreased (Figure 47). To determine whether deletion of the FRB in *let-363* led to an

impact on GSC proliferation, I assayed *let-363(ΔFRB)* germlines. I observed that *let-363(ΔFRB)* germlines appeared skinnier than wildtype (Figure 48A). Additionally, in ~30% of germlines there were no pH3 positive cells (Figure 48B). Upon assaying for ADI, I found that *let-363* had a significantly lower ADI ($p<0.0001$) than wildtype suggesting that loss of TOR signaling leads to a partial cell cycle arrest in adult GSCs (Figure 48C). These data suggest that both Insulin signaling and Tor signaling regulate G2/M progression. Current experiments in the lab are ongoing to assess whether these two pathways function in a redundant manner. More importantly, I wondered how LET-363 may control the cell cycle.

Studies from yeast, also suggest a role for TOR signaling in regulating the cell cycle. I surmised that *let-363* does not function through the canonical TOR signaling pathway and lysosomes since there was anecdotal evidence in the lab and from the field on lack of lysosomes in germ cells. To determine whether germ cells contain lysosomes, I utilized the High Resolution Electron Microscopy Facility at MD Anderson Cancer Center to perform Transmission Electron Microscopy. Lysosomes were identified as circular membrane-bound vesicles approximately 0.5 micron in size (Sigmond et al. 2008). While the gut contains lysosomes, I did not find any in the GSCs (Figure 49). Thus, I assayed for distinct pathways that may mediate the role of TOR signaling in regulating G2/M progression. Since fission yeast does not regulate TOR signaling through lysosomal signaling either, I wondered whether there were parallels in the cell cycle regulation between yeast and *C. elegans* GSCs.

In fission yeast, Tor can regulate p38 stress kinases to regulate Cdc25 (Lopez-Aviles et al. 2008; Lopez-Aviles et al. 2005). Since Cdc25 directly regulates Cdk1, this would provide a link between TOR signaling and cell cycle regulation. To test this, I assayed for the effect of stress kinases in regulating the GSC arrest in *C. elegans*.

There are three p38-like (*pmk-1*, *pmk-2*, *pmk-3*) and four JNK-like (*jnk-1*, *kgb-1*, *kgb-2*, C49C3.10) stress kinases in *C. elegans* which respond to a variety of different stressors from infection to injury (Reviewed in Andrusiak and Jin 2016). To determine whether stress kinases function downstream of *let-363* in GSC response to starvation, I assayed four of these kinases, *pmk-1*, *pmk-2*, *jnk-1*, and *kgb-1*. I did not pursue *pmk-3* because it does not contain the canonical TGY motif through which the p38 family is activated, and so it is likely not activated by an upstream map kinase cascade. I depleted each kinase via an F1 RNAi (the RNA was depleted in the mothers and progeny) and observed changes in the germlines of the F1 progeny. I observed that under fed conditions, all genotypes had ADIs similar to the luciferase control (Figure 50). However, loss of *pmk-2* and *kgb-1* individually displayed an increase in ADI, raising the possibility that they could each partially abrogate the starvation arrest. To investigate their effect on mediating the G2/ M arrest, I assayed for their necessity to induce the arrest. I performed an F1 RNAi of each kinase and starved animals at 24 hours past mid L4. The germlines contained dividing cells which would indicate an incomplete arrest. The luciferase control RNAi, as expected, had zero germlines with pH3 positive cells. Similarly, the germlines from *jnk-1*, *pmk-1*, and *pmk-2* RNAi did not display pH3 positive cells, suggesting that their loss did not abrogate the G2 arrest. However, loss of *kgb-1* by RNAi leads to ~5% of germlines with pH3 positive cells. While this number is small, the data suggests *kgb-1* activity may be necessary for initiating a complete G2 arrest upon starvation. Because RNAi only depletes the RNA and may not affect protein function, which could account for the small effect observed, I obtained a *kgb-1(um3)* mutant allele and performed the analysis. The *um3* allele deletes a large portion of the KGB-1 kinase domain (Smith et al. 2002). Previous studies describe this allele as temperature-sensitive. While it is relatively wildtype at

20°C, the strain is sub-fertile at 15°C. Therefore *kgb-1(um3)* was cultured at 20°C and shifted at mid L4 for 24 hours to 15°C, followed by a 4 hour starvation. As previously shown, wildtype animals underwent complete G2 arrest at 20°C, but at 15°C the G2 arrest in wildtype animals is evident only in 80% of the animals, with the remaining ~20% of germlines displaying pH3 positive cells. These data suggest that temperature enhances the starvation-induced G2 arrest in wildtype. It was interesting however that in the *kgb-1(um3)* mutants at 15°C, ~80% of germlines displayed pH3 positive cells, and at 20°C the *kgb-1(um3)* mutants maintained ~5% of germlines with pH3 positive cells, further suggesting that *kgb-1* assists in the starvation-induced G2 arrest. Since there are reports that active p38 genetically interacts with Cdk1 regulator to inhibit cell cycle progression, I next investigated CDK-1 regulation during starvation.

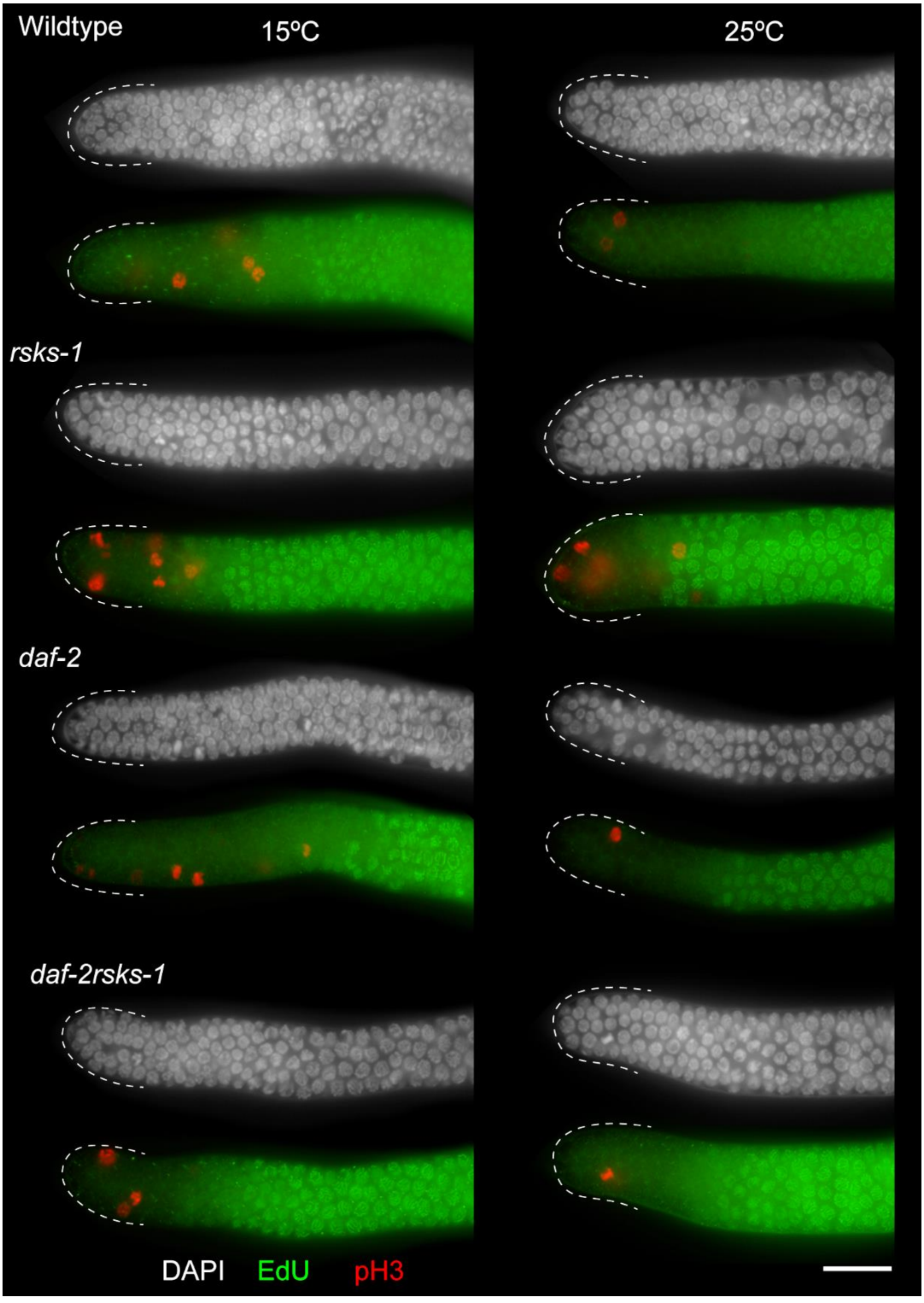
Wildtype
15ºC
25ºC
rsks-1
daf-2
daf-2rsks-1
DAPI
EdU
pH3

Figure 43: *daf-2* and *rsks-1* mutants do not completely arrest

Dissected germlines from the listed genotypes with the distal tip outlined with a dashed line and oriented to the left. Left panel are animals raised at 15°C, Right panel are animals which were shifted to 25°C for 18 hours prior to dissection. All animals were dissected at 24 hours past mid L4. Stained for DAPI (white), EdU (green), and pH3 (red). Scale bar: 20µm.

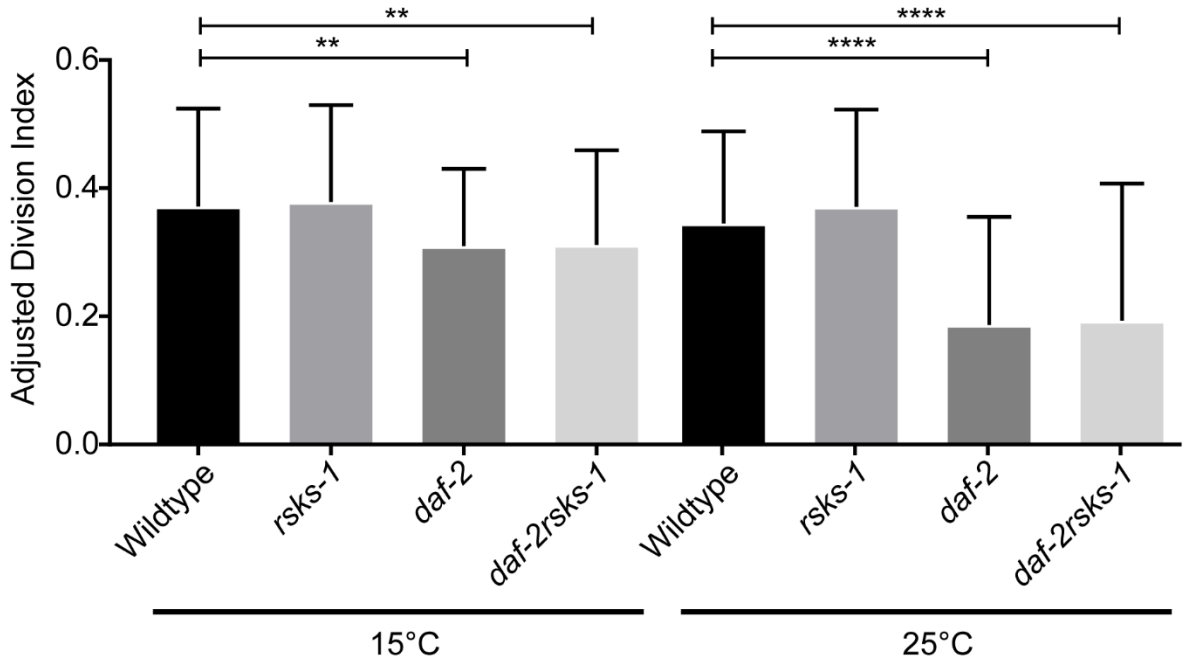

Figure 44: ADI analysis of *daf-2* and *rsks-1* mutants

ADI analysis is measured as the number of pH3 positive cells divided by the number of cell rows in the progenitor region. (**) $p < 0.005$, (****) $P < 0.0001$.

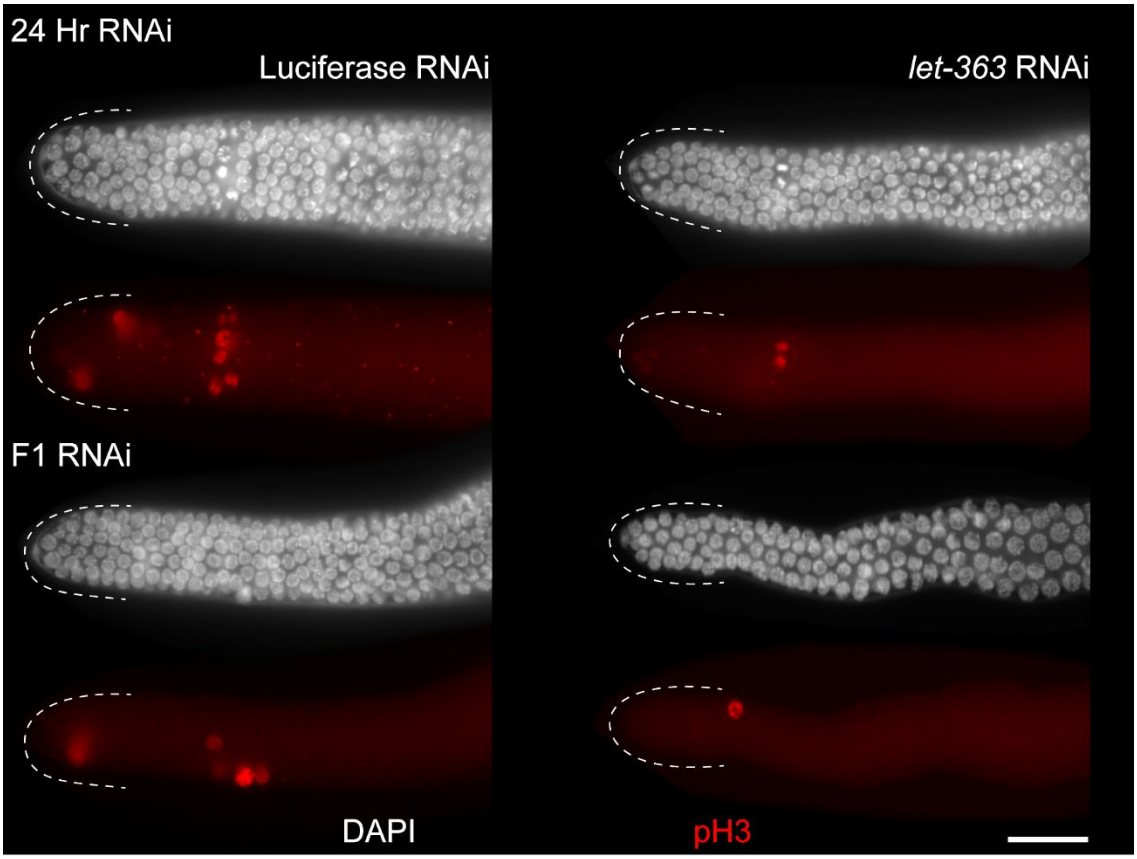
24 Hr RNAi
Luciferase RNAi
let-363 RNAi
F1 RNAi
DAPI
pH3

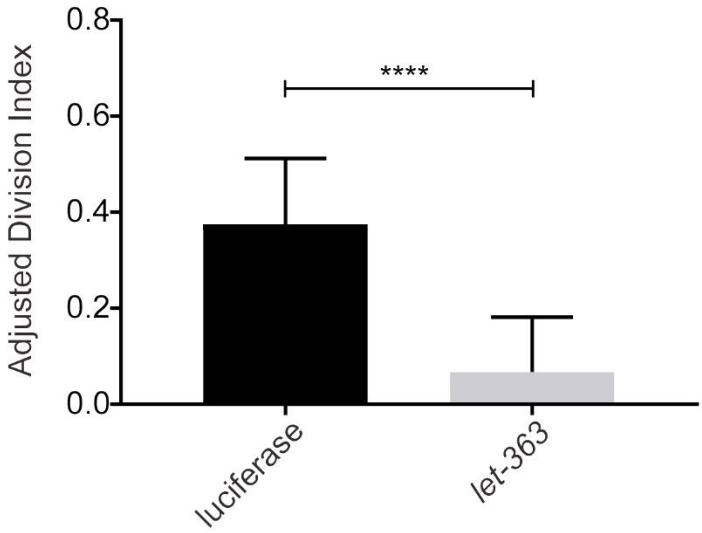
Adjusted Division Index
0.8
0.6
0.4
0.2
0.0
****
luciferase
let-363

Figure 45: RNAi of *let-363* results in decreased proliferation

(A) Dissected germlines form the listed genotypes with the distal tip outlined with a dashed line and oriented to the left. Stained for DAPI (white) and pH3 (red). Scale bar: 20µm. (B) ADI analysis is measured as the number of pH3 positive cells divided by the number of cell rows in the progenitor region. Displayed is the ADI for the long-term (F1) RNAi. (**) $p < 0.005$, (****) $P < 0.0001$.

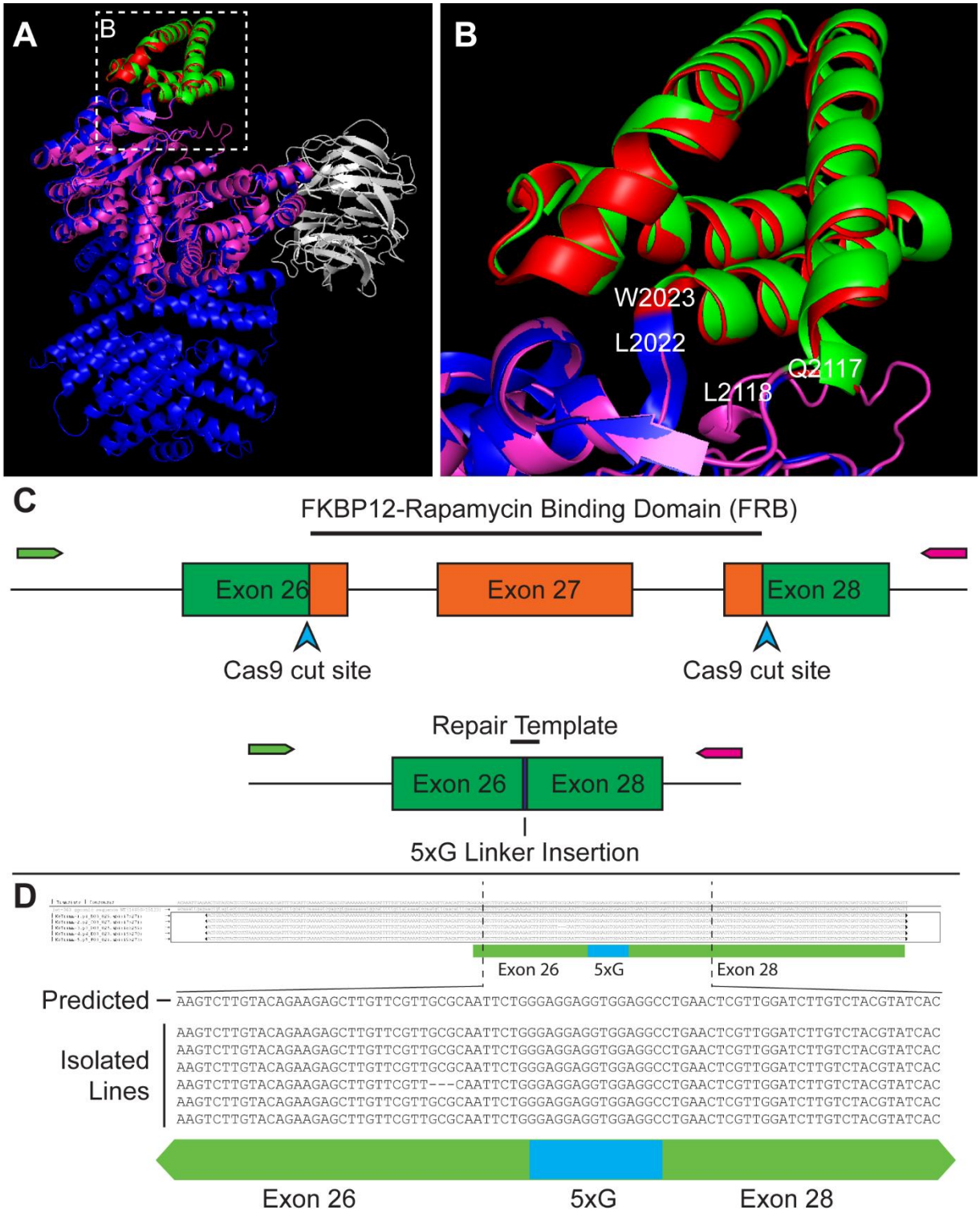
A
B
B
W2023
L2022
Q2117
L2118
C
FKBP12-Rapamycin Binding Domain (FRB)
Exon 26
Exon 27
Exon 28
Cas9 cut site
Cas9 cut site
Repair Template
Exon 26
Exon 28
5xG Linker Insertion
D
Exon 26
5xG
Exon 28
Predicted –
AAGTCTTGTACAGAAGAGCTTGTTCGTTGCGCAATTCTGGGAGGAGGTGGAGGCCTGAACTCGTTGGATCTTGTCTACGTATCAC
Isolated Lines
AAGTCTTGTACAGAAGAGCTTGTTCGTTGCGCAATTCTGGGAGGAGGTGGAGGCCTGAACTCGTTGGATCTTGTCTACGTATCAC
AAGTCTTGTACAGAAGAGCTTGTTCGTTGCGCAATTCTGGGAGGAGGTGGAGGCCTGAACTCGTTGGATCTTGTCTACGTATCAC
AAGTCTTGTACAGAAGAGCTTGTTCGTTGCGCAATTCTGGGAGGAGGTGGAGGCCTGAACTCGTTGGATCTTGTCTACGTATCAC
AAGTCTTGTACAGAAGAGCTTGTTCGTT---CAATTCTGGGAGGAGGTGGAGGCCTGAACTCGTTGGATCTTGTCTACGTATCAC
AAGTCTTGTACAGAAGAGCTTGTTCGTTGCGCAATTCTGGGAGGAGGTGGAGGCCTGAACTCGTTGGATCTTGTCTACGTATCAC
AAGTCTTGTACAGAAGAGCTTGTTCGTTGCGCAATTCTGGGAGGAGGTGGAGGCCTGAACTCGTTGGATCTTGTCTACGTATCAC
Exon 26
5xG
Exon 28

Figure 46: *let-363(ΔFRB)* mutagenesis

(A) 3D model of a c-terminal portion of *let-363* kinase (pink and green) threaded onto the structure of a c-terminal portion of human mTOR (4JSP) (blue and red) using the ITASSER suite. The FRB domain is labeled in green (*let-363*) or red (mTOR). Square denotes the region magnified in (B). (B) Increased magnification of the FRB domain. The amino acids bordering each breakpoint for the FRB allele are labeled. (C) CRISPR design for replacing the FRB domain with a 5xGly flexible linker. Green and pink flags represent PCR primers used for allele detection as well as sequencing (not to scale). (D) Sequencing result from 6 clones generated from CRISPR injections using the above scheme. 5 of the 6 contain the desired edit, while the other one has a 3 base pair deletion (dashes) resulting in a missense mutation.

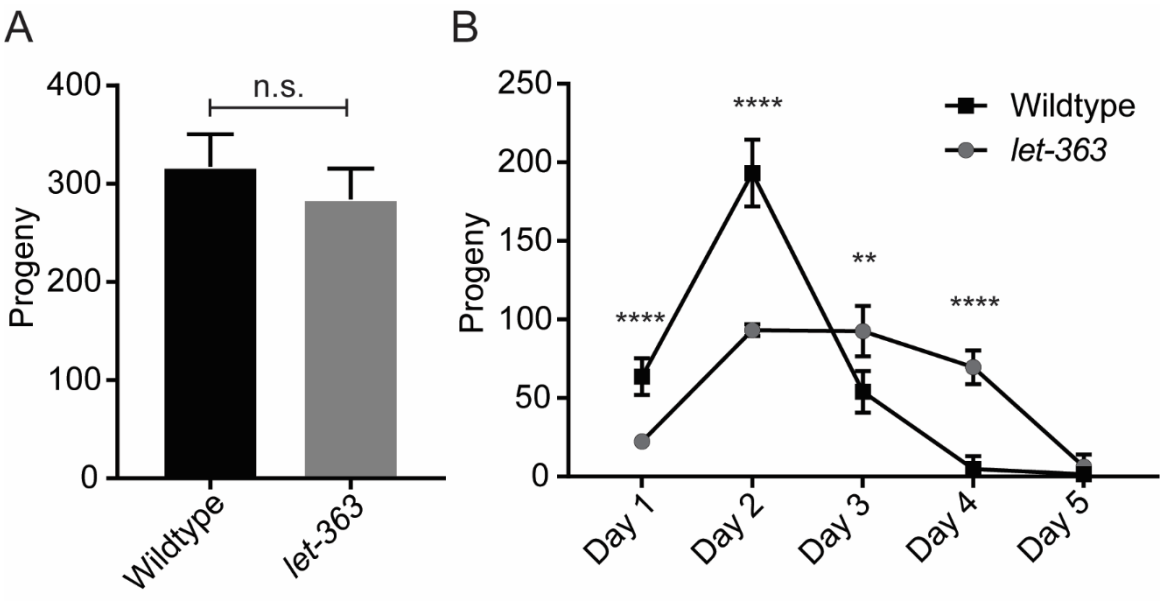

Figure 47: *let-363(ΔFRB)* has a decreased rate of progeny lay

(A) Analysis of the total progeny laid by wildtype and *let-363*(*ΔFRB)*. (B) Break down of the analysis in (A) by day. (**) p < 0.005, (****) P < 0.0001.

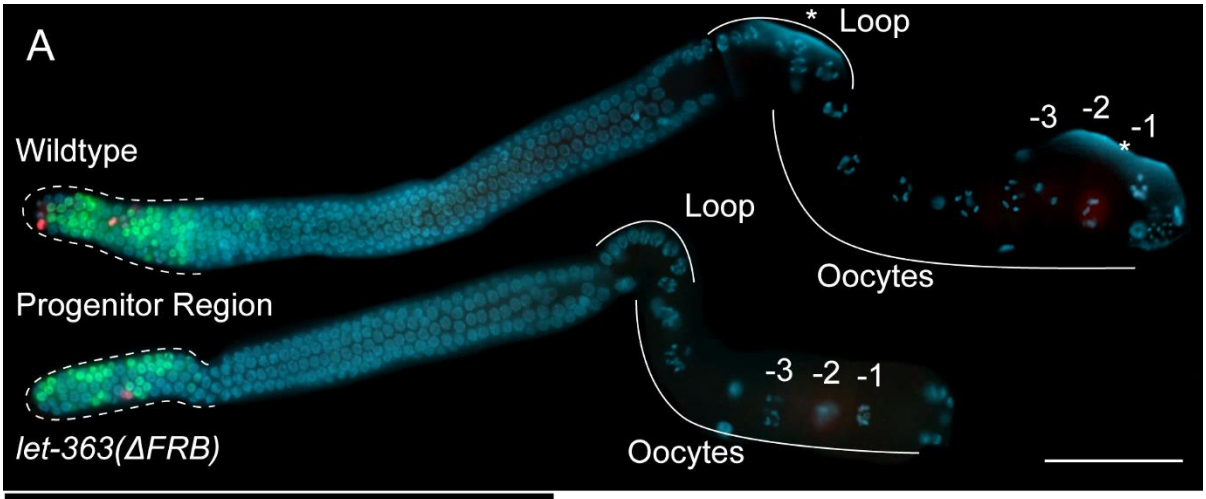
A
Wildtype
Progenitor Region
let-363(ΔFRB)
* Loop
-3 -2 -1
*
Loop
Oocytes
-3 -2 -1
Oocytes

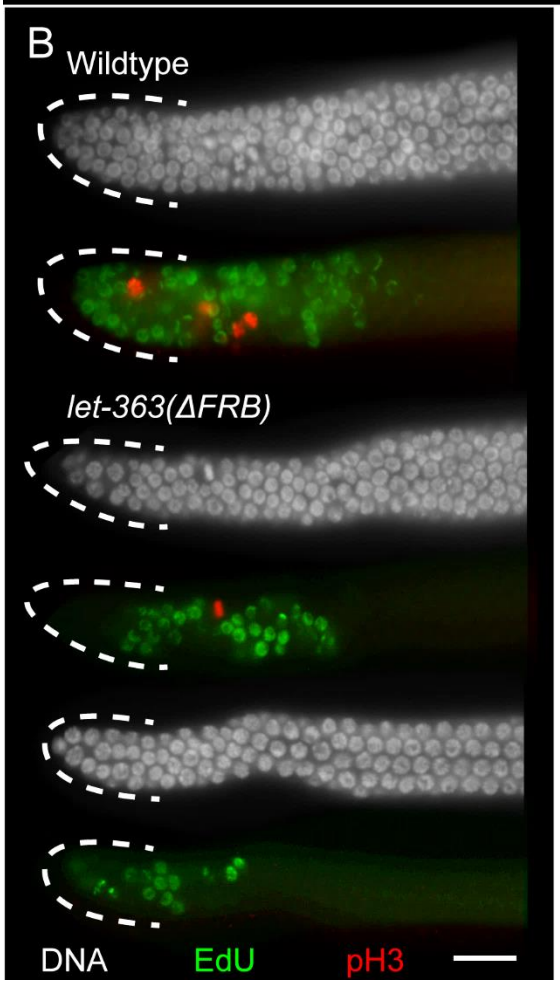
B
Wildtype
let-363(ΔFRB)
DNA
EdU
pH3

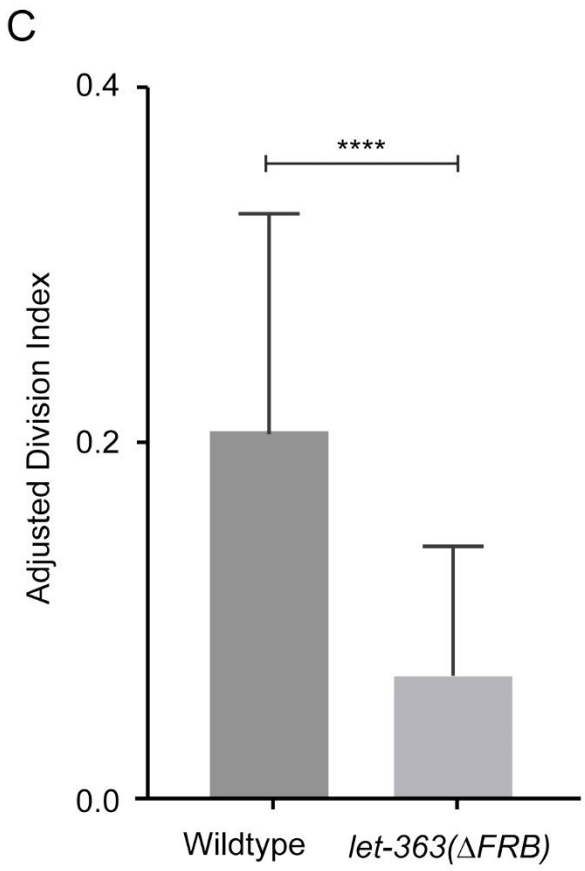
C
0.4
0.2
0.0
****
Adjusted Division Index
Wildtype
let-363(ΔFRB)

Figure 48: *let-363(ΔFRB)* has a proliferation defect

Dissected germlines from wildtype and *let-363(ΔFRB)* oriented with distal tip to the left. (A) Full germlines displayed with the progenitor region outlined. Loop region and the region with developing oocytes are defined by solid lines. Oocytes are labeled up to the -3 oocyte with regards to birth order. Asterisks define regions of increased background due to an adjacent germline. Stained for DAPI (blue), EdU (green), and pH3 (red). Scale bar: 100µm. (B) Progenitor region is displayed with the distal tip outlined with a dashed line and oriented to the left. Stained for DAPI (white), EdU (green), and pH3 (red). (C) ADI analysis is measured as the number of pH3 positive cells divided by the number of cell rows in the progenitor region. (****) $p < 0.0001$. Scale bar: 20µm.

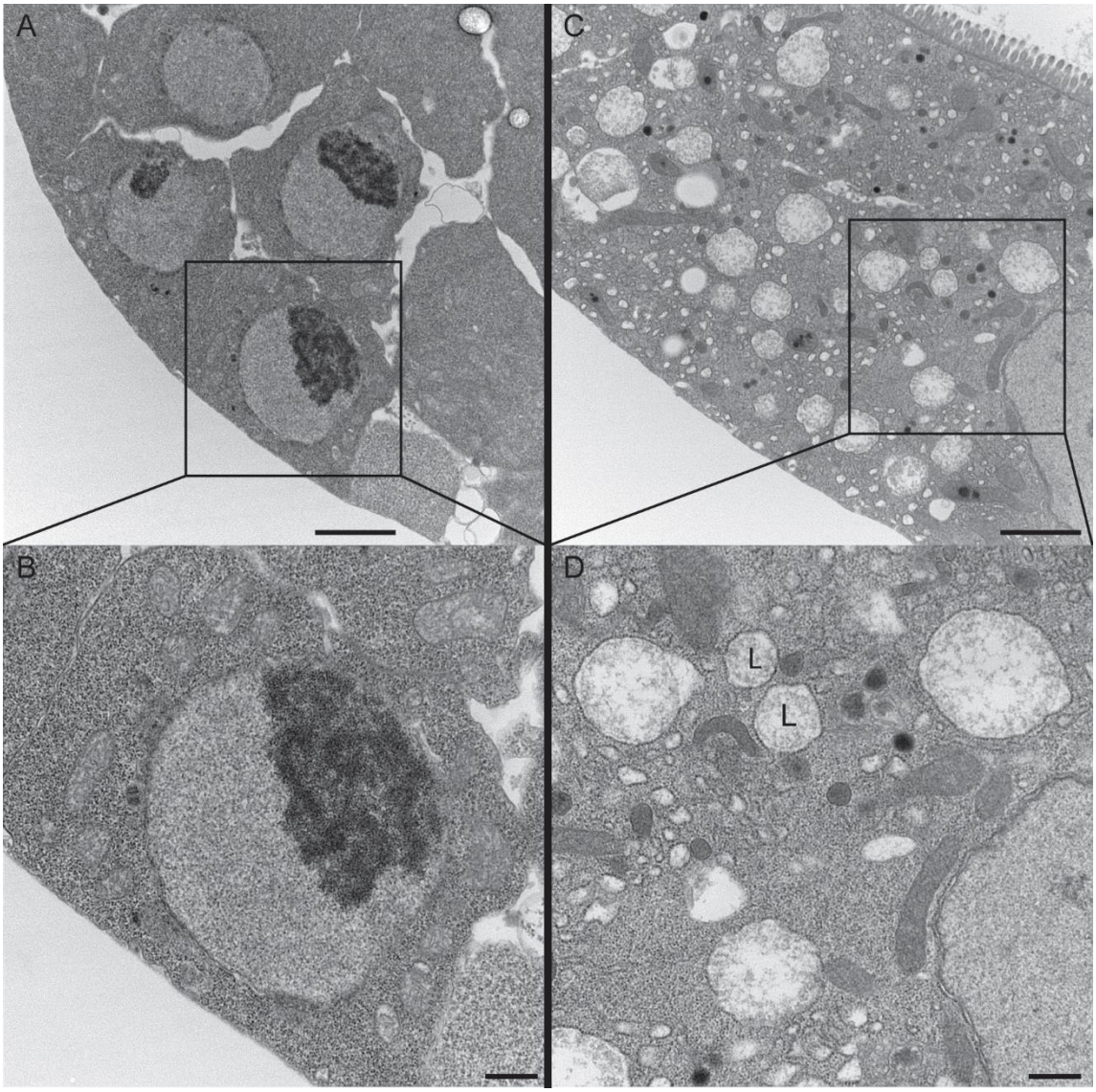

Figure 49: Lysosomes are absent from GSCs

Samples were dissected and fixed in 3% glutaraldehyde plus 2% paraformaldehyde in 0.1 M cacodylate buffer, pH 7.3 prior to submission to the High Resolution Electron Microscopy Facility at MD Anderson Cancer Center where they were prepared by Kenneth Dunner. (A,B) TEM image from the germline. Square denotes magnified region shown in (B). (C,D) TEM image from the gut. Square denotes magnified region shown in (D). Scale bar is: 2 µm(A,C), 0.5 µm(B,D).

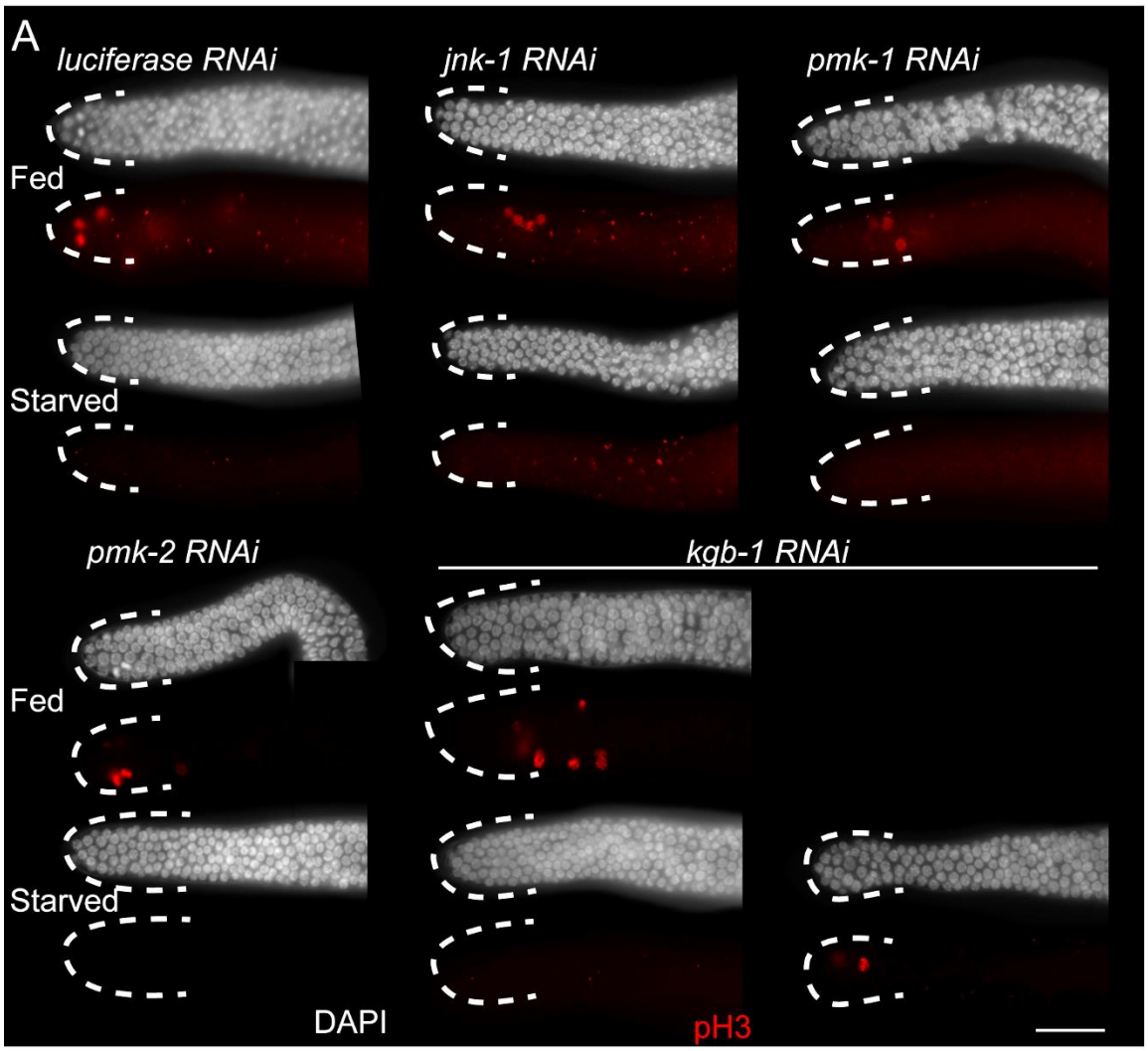
A
luciferase RNAi
jnk-1 RNAi
pmk-1 RNAi
Fed
Starved
pmk-2 RNAi
kgb-1 RNAi
Fed
Starved
DAPI
pH3

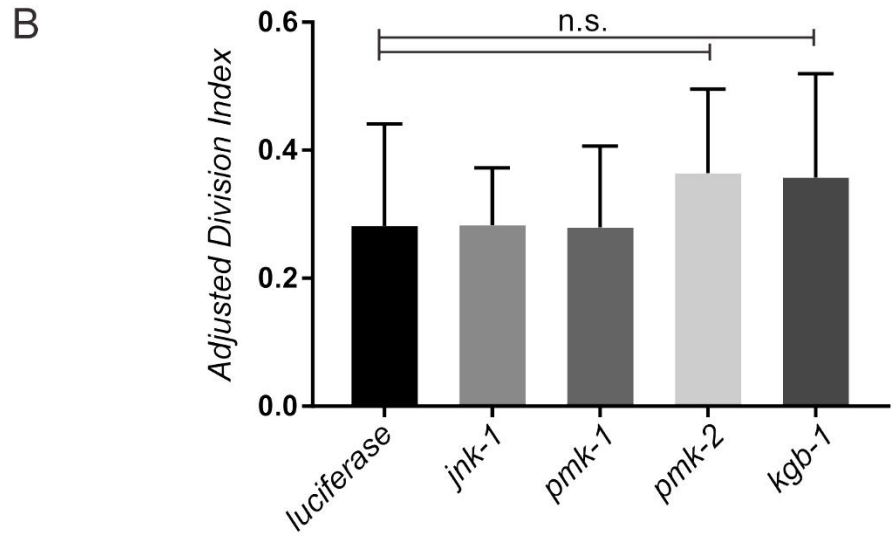
B
n.s.
Adjusted Division Index
0.6
0.4
0.2
0.0
luciferase
jnk-1
pmk-1
pmk-2
kgb-1

Figure 50: Stress kinases may contribute to the starvation-induced G2 arrest

(A) Dissected germlines of animals after RNAi of stress kinases (*jnk-1*, *pmk-1*, *pmk-2*, and *kgb-1*) and a luciferase control with or without starvation. Germlines have the distal tip outlined with a dashed line and are oriented with distal tip to the left. Stained for DAPI (white) and pH3 (red). Scale bar: 20µm. (B) ADI analysis is measured as the number of pH3 positive cells divided by the number of cell rows in the progenitor region. (n.s.) not significant.

4.5: CDK-1 activity is Modulated by Nutritional and MAPK Pathways to Regulate the Reversible Starvation-induced G2 Arrest

Entry into M phase from G2 is controlled by *cdk-1* and *cyb-1* in *C elegans*. *cdk-1* is inhibited by *wee-1*, so to investigate the role of *cdk-1* signaling during starvation, I depleted *wee-1.3* by RNAi. *wee-1.3* is one of the Wee1 homologs in *C. elegans* and is expressed in the germline. After 4 hours of starvation, *wee-1.3* RNAi resulted in ~40% of germlines with pH3 positive cells (Figure 51). This suggested that *wee-1.3* plays a role in either entry or maintenance of the G2 arrest.

To determine whether *wee-1.3* mediated CDK-1 phosphorylation is regulated in response to starvation. I used antibodies to detect (pT14pY15)CDK-1, the inhibitory mark generated by WEE-1 and MYT-1 kinases; and a total CDK-1 antibody to observe overall changes in protein expression. The total CDK-1 antibody was raised by Dr. Andy Golden (NIH/NIDDK) and kindly provided by Jill Schumacher (MD Anderson Cancer Center). Both antibodies are specific to CDK-1 as they are depleted upon *cdk-1* RNAi (Figure 52). Additionally, the (pT14pY15)CDK-1 antibody is responsive to replication stress and DNA damage signaling since it increases in intensity after hydroxyurea treatment (Figure 52). Therefore, using these antibodies, I could assay the inhibitory state of CDK-1 during starvation. I assayed animals at 24 hours past mid L4 in either fed or starved conditions. The starvation was performed for 4 hours. The germlines were then stained with either (pT14pY15)CDK-1 or total CDK-1 as well as pH3. In fed worms, there was noticeable accumulation of both the total CDK-1 as well as the (pT14pY15)CDK-1 in cells that were pH3 negative. This suggested that when the GSCs were not in M phase, CDK-1 was maintained in the nucleus in an inhibited state. In GSCs from starved germlines, the signal for (pT14pY15)CDK-1 was similar to GSCs from fed germlines. However, there was a decrease in total CDK-1 expression

level, and the low-level signal was not nuclear but rather cytoplasmic (Figure 53). To better understand this expression dynamic, the experiment was repeated and analyzed using confocal microscopy. I observed that the fed animals had clear nuclear localization of both total CDK-1 and the inhibitory (pT14pY15)CDK-1 (Figure 53). In starved animals, while the (pT14pY15)CDK-1 signal remained, the nuclear, total CDK-1 signal was not visible (Figure 53). In addition, the overall accumulation of CDK-1 was decreased in starved animals. These data demonstrate two things: 1) total CDK-1 levels are decreased upon starvation and (2) the phosphorylated nuclear signal of CDK-1 does not change upon starvation. At first sight these data seem confusing, however it led me to posit that CDK-1 was regulated at several levels simultaneously during starvation. One process would be responsible for decreasing the overall expression of CDK-1 as was observed. However, for the accumulation of inhibited CDK-1 to remain the same in fed and starved animals, the proportion of inhibited CDK-1 must increase. Therefore, another process would be responsible for this increase in inhibited CDK-1. Combining both processes may cause the strong G2 arrest observed.

I then reasoned that if the proportion of inhibited CDK-1 were high enough in the fed condition, it might be possible to watch the inhibited CDK-1 drop during starvation along with the total CDK-1 signal. To test this, I attempted to saturate the (pT14pY15)CDK-1 signal using hydroxyurea treatment. As seen before, hydroxyurea treatment leads to an increase in the (pT14Y15)CDK-1 signal (Figure 52). If the hydroxyurea treated germlines are then starved and the total CDK-1 levels drop, I would also be able to compare the levels of phospho-CDK-1, and a change in phospho-CDK-1 level should be easily detectable. Therefore, I treated wildtype animals with hydroxyurea for 12 hours and either starved or fed them for 4 hours. After

dissection, the germlines from fed animals were labeled with anti-NOP-1, a nucleolar marker, and combined with the starved samples for each condition. The combined samples were then split into two equal portions and stained with either (pT14pY15)CDK-1 or total CDK-1 antibodies. By staining both fed and starved in the same tube, I was able to rule out any intensity differences due to differences in antibody treatment or exposure. As expected, fed hydroxyurea-treated animals had high (pT14pY15)CDK-1 expression in the GSCs when compared to their control counterparts (Figure 54). However, even with increased signal, there was no change in (pT14pY15)CDK-1 intensity between the fed and starved conditions in hydroxyurea-treated animals (Figure 54). This is in contrast to the drop in total CDK-1 levels, which can be seen in both the hydroxyurea-treated and control animals. In order for the (pT14pY15)CDK-1 intensity to remain the same in control animals, the drop in total CDK-1 levels must be accompanied by an increase in (pT14pY15)CDK-1 levels. Therefore, I posit that the increase in (pT14pY15)CDK-1 may be due to the role of *kgb-1* during starvation. Additionally, I was intrigued by the drop in total CDK-1 levels upon starvation since that seemed like a key mechanism underlying the onset of G2 arrest upon starvation. Thus, I investigated how *cdk*-1 expression was regulated during starvation.

To determine if *cdk-1* was being transcriptionally repressed I assayed for CDK-1 mRNA, using PGL-1 mRNA as an internal control. I fed adult animals (24 hours past L4) and performed FISH using the above probes. I observed that both fed and starved conditions contained comparable fluorescence intensity for CDK-1 mRNA and PGL-1 mRNA. This suggested that *cdk-1* was not being transcriptionally regulated.

Since TOR signaling regulated the G2 arrest, at least in part, it is likely that *cdk-1* expression is translationally regulated. Two downstream effectors of TOR signaling that

regulate translation are *rsks-1* and Eif4ebp1. As observed earlier, *rsks-1* does not play a role in the proliferation of adult GSCs, therefore I investigated the role of Eif4ebp1 in regulating CDK-1 expression. Eif4ebp1 is a negative regulator of 5' cap-dependent mRNA translation which functions by binding Eif4e (Eukaryotic translation initiation factor 4E). Active TORC1 phosphorylates Eif4ebp1, dissociating it from Eif4e. This allows Eif4e to form a complex with Eif4g (Eukaryotic translation initiation factor 4G) to promote translation initiation. In *C. elegans* there is no known homolog of Eif4ebp1. However, while there are multiple genes with homology to regulatory subunit Eif4e, the structural subunit Eif4g has only one homolog (*ifg-1*). Since this complex regulates translation, and some of its components have larval GSC proliferation defects as well as suboptimal fertility, I used RNAi to investigate the function of *ifg-1 (Korta, Tuck, and Hubbard 2012; Long et al. 2002)*. After a 24 hour RNAi treatment, I dissected and analyzed *ifg-1* RNAi germlines. When compared to luciferase RNAi controls, *ifg-1* RNAi germlines displayed significantly lower ADI (Figure 55). This suggests that *ifg-1* depletion, and translational inhibition in general, affects adult GSC proliferation. Therefore, I hypothesize that a decrease in TOR signaling results in lower IFG-1 mediated protein translation which in turn lowers the level of CDK-1, and together with phosphorylation mediated inhibition of CDK-1, the overall lower levels of CDK-1 upon starvation induce the G2 arrest.

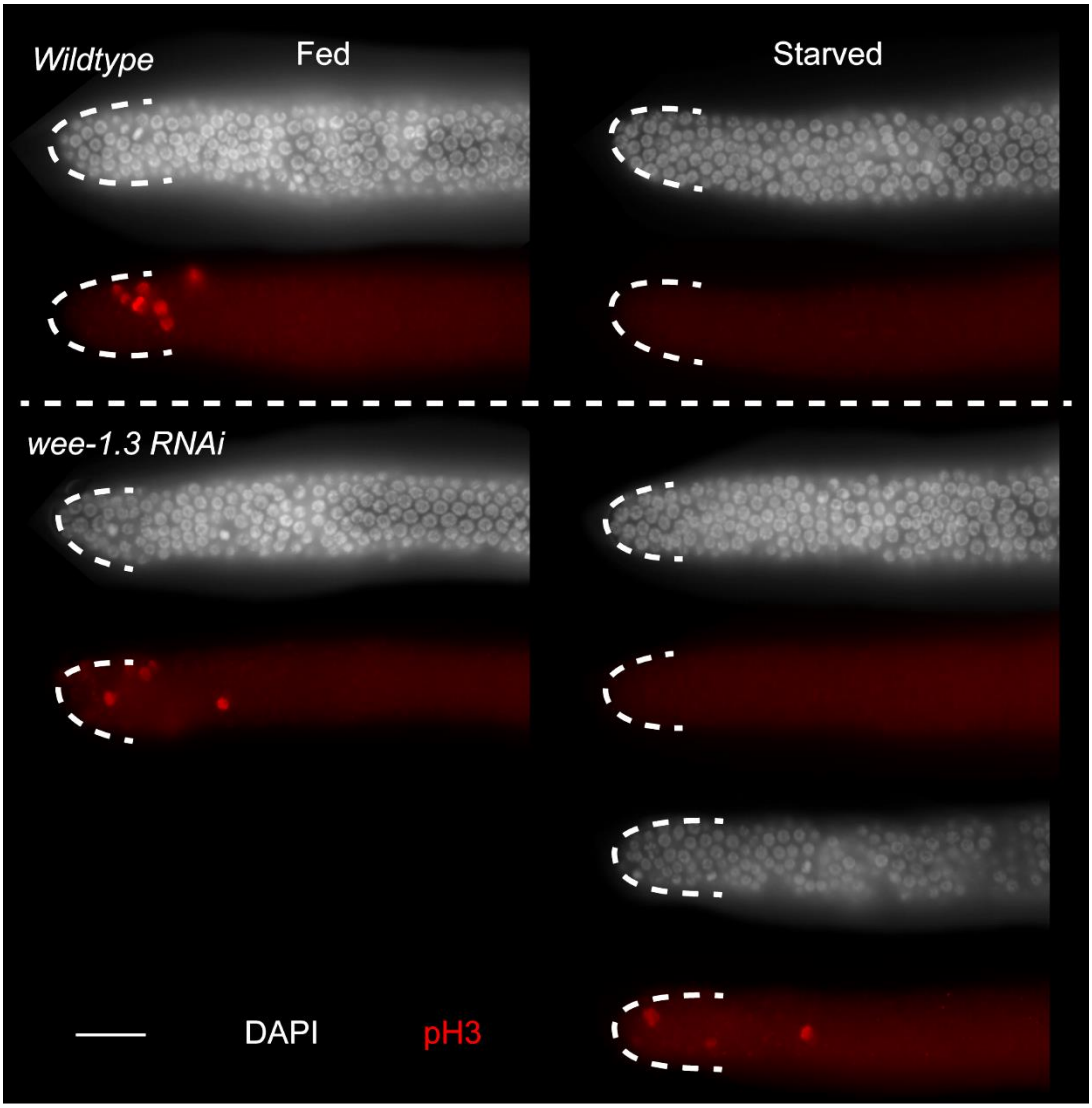

Figure 51: *wee-1.3* regulates the starvation-induced G2 arrest

Dissected germlines of animals after RNAi of *wee-1.3* and a luciferase control with or without starvation. Germlines have the distal tip outlined with a dashed line and are oriented with distal tip to the left. Stained for DAPI (white) and pH3 (red). Scale bar: 20µm.

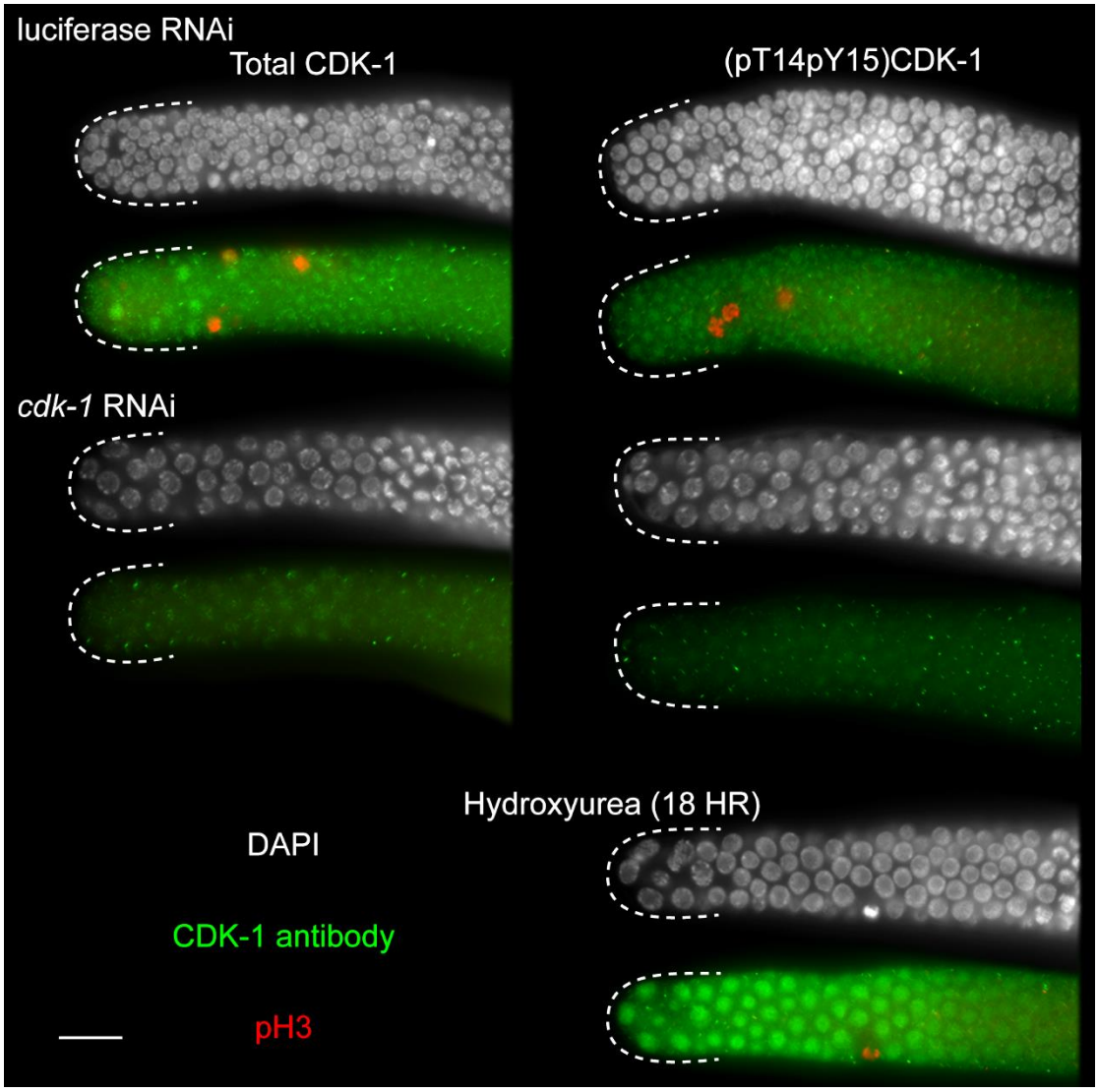

Figure 52: CDK-1 and (pT14pY15)CDK-1 antibodies respond as expected

Dissected wildtype germlines under normal conditions (top), after *cdk-1* depletion (middle), or after Hydroxyurea treatment for 18 hours (bottom). Left panel was stained for total CDK-1, right panel was stained for (pT14pY15)CDK-1. Both panels were stained for DAPI (white) and pH3 (red). Germlines have the distal tip outlined with a dashed line and are oriented with the distal tip to the left. Scale bar: 20µm.

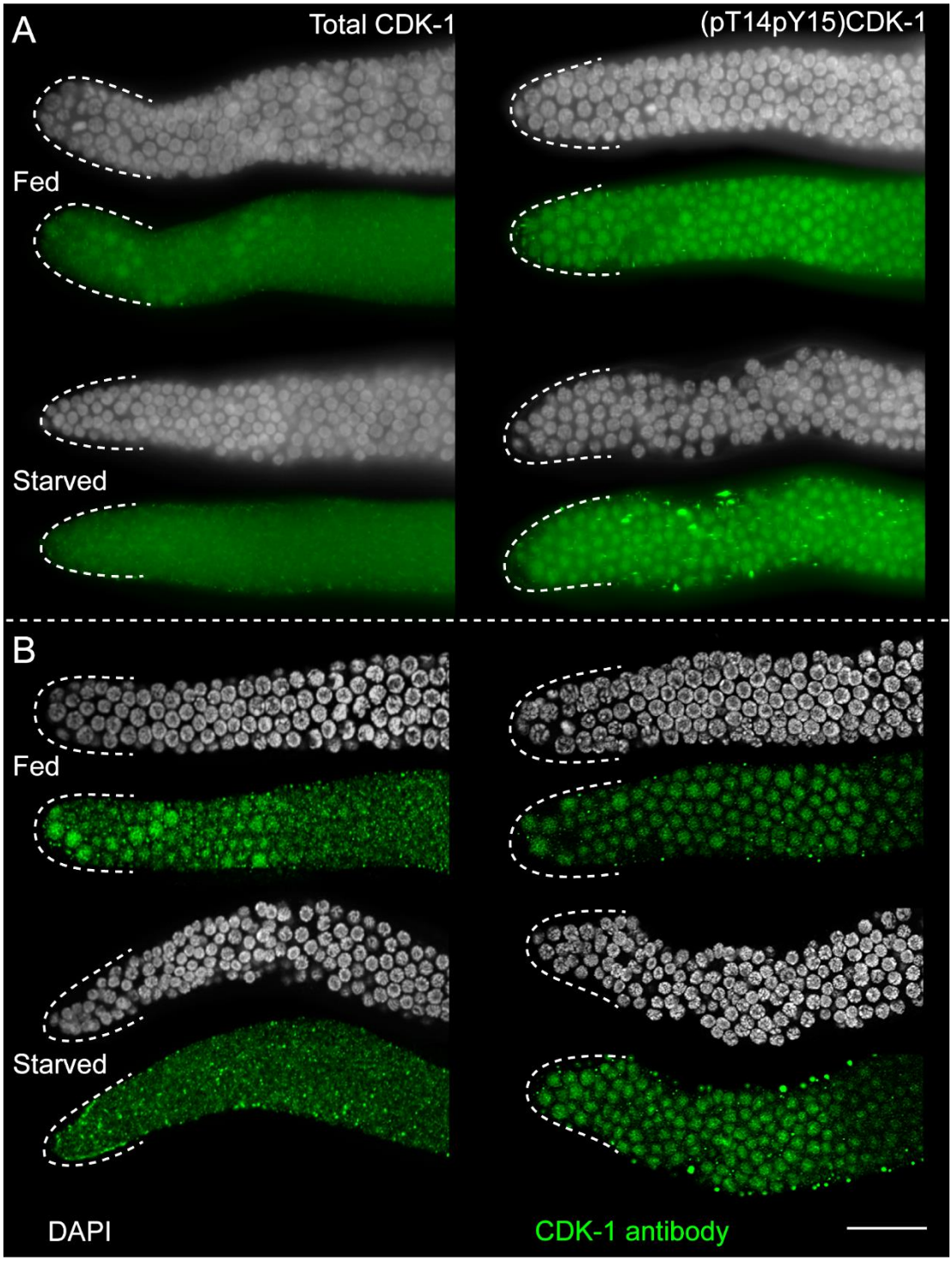
A
Total CDK-1
(pT14pY15)CDK-1
Fed
Starved
B
Fed
Starved
DAPI
CDK-1 antibody

Figure 53: CDK-1 expression decreases as pCDK-1 remains unchanged

Dissected wildtype germlines with or without starvation. Left panel was stained for total CDK-1, right panel was stained for (pT14Y15)CDK-1. Both panels were stained for DAPI (white). Germlines have the distal tip outlined with a dashed line and are oriented with the distal tip to the left. Germlines were either imaged using an epifluorescence (A) or confocal (B) microscope. Scale bar: 20µm.

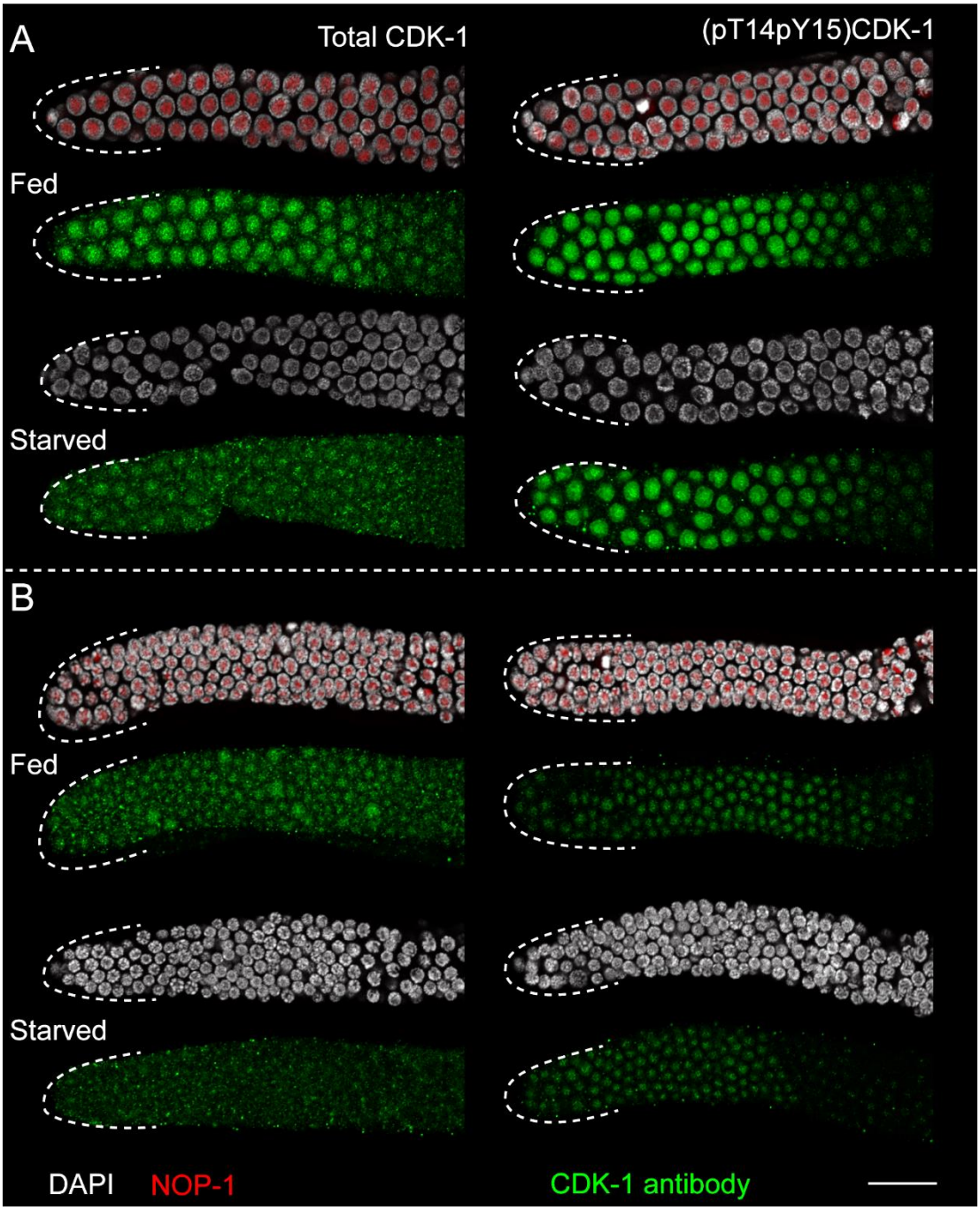
A
Total CDK-1
(pT14pY15)CDK-1
Fed
Starved
B
Fed
Starved
DAPI
NOP-1
CDK-1 antibody

Figure 54: Hydroxyurea exacerbates the regulation of CDK-1 during starvation

Dissected wildtype germlines with or without starvation. Left panel was stained for total CDK-1, right panel was stained for (pT14Y15)CDK-1. After staining fed animals with NOP-1 (red), a nucleolar marker, fed and starved groups were combined and stained in the same tube for DAPI (white) and CDK-1 or (p124Y15)CDK-1 antibody Germlines have the distal tip outlined with a dashed line and are oriented with the distal tip to the left. Animals were either treated with Hydroxyurea (A), or with M9 vehicle control (B). Scale bar: 20µm.

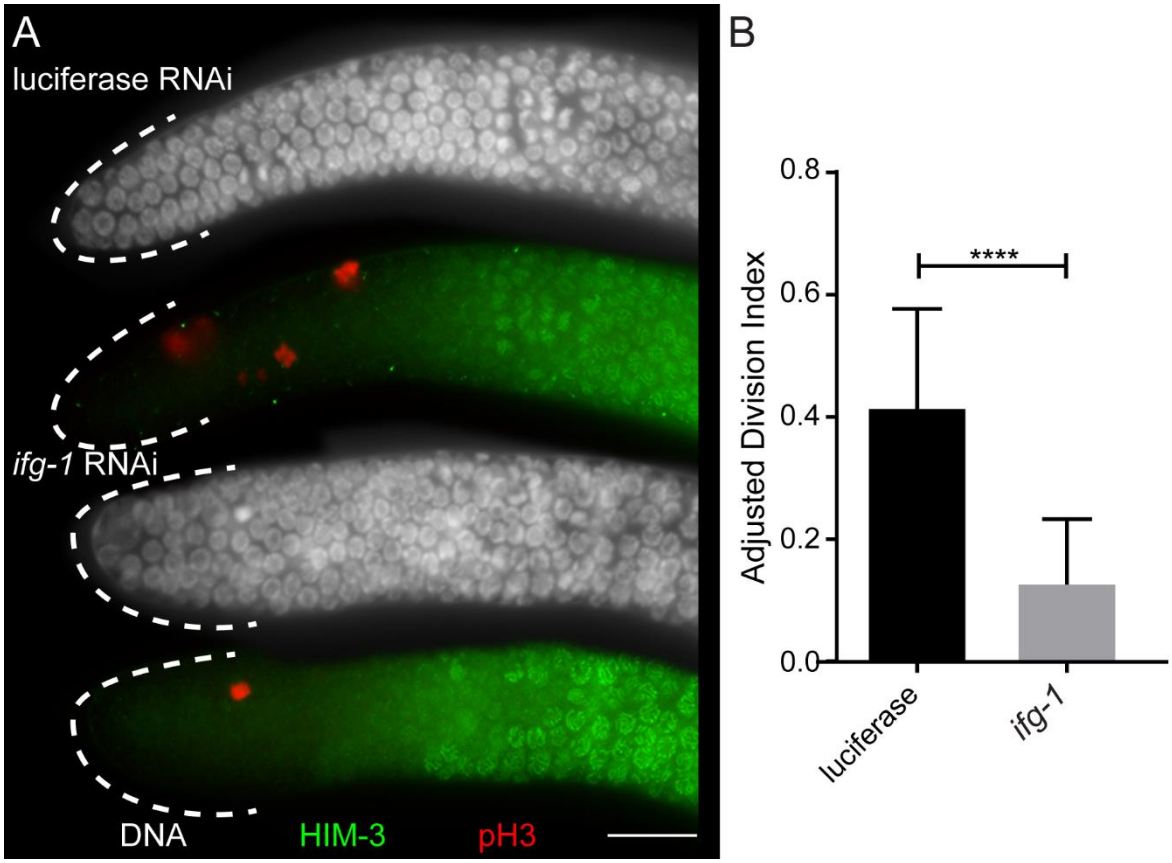

Figure 55: RNAi of the translational regulator *ifg-1* inhibits proliferation

Dissected germlines from animals treated with RNAi for *ifg-1* or luciferase control. Stained for DAPI (white), pH3, and HIM-3. Germlines have the distal tip outlined with a dashed line and are oriented with the distal tip to the left. Germlines were either imaged in an epifluorescence (A) or confocal (B) microscope. Scale bar: 20µm.

4.6: Conclusion and model

Starvation is detrimental to organisms. Therefore, being able to respond to starvation in a way that preserves cellular integrity is important. In this chapter, I uncovered that *C. elegans* GSCs respond to acute starvation with a reversible G2 arrest which is released upon return to replete conditions (Figure 56). I found no evidence of DNA damage due to replication stress during this arrest, and the arrest appears to be independent of DNA damage signaling all together. Instead, this arrest is mediated by nutritional signaling pathways. Loss of Insulin signaling (*daf-2*) or TOR signaling (*let-363*) results in an induction of the G2 arrest, with each contributing partially to the phenotype. Mechanistically, the arrest is partially mediated by stress signaling through *kgb-1* which in turn leads to *cdk-1* inhibition. Consistent with this model, depletion of the negative regulator *wee-1.3* abrogates the G2 arrest, although loss of *wee-1.3* results in a stronger abrogation of the G2 arrest than evidenced in *kgb-1* mutants, suggesting that *cdk-1* is regulated by signals or mechanisms in addition to the one mediated by *kgb-1*. Furthermore, starvation resulted in a reduction of total CDK-1 protein, in addition to the phosphorylation mediated inhibition imposed by *wee-1.3*. The decrease in CDK-1 protein levels was not regulated transcriptionally in response to starvation, but rather may be under translational regulation, as transient depletion of *ifg-1*, which functions downstream of *let-363* to promote translation, causes the onset of G2 arrest. Together, these data put forward the model that Insulin and TOR signaling regulate the G2 arrest in parallel. TOR signaling functions independent of the lysosomes, and via the stress activated kinase *kgb-1* and *ifg-1* to regulate CDK-1 both at the post-translational level and at the translational level to efficiently respond to lack of nutrients in the environment and protect germ cell integrity.

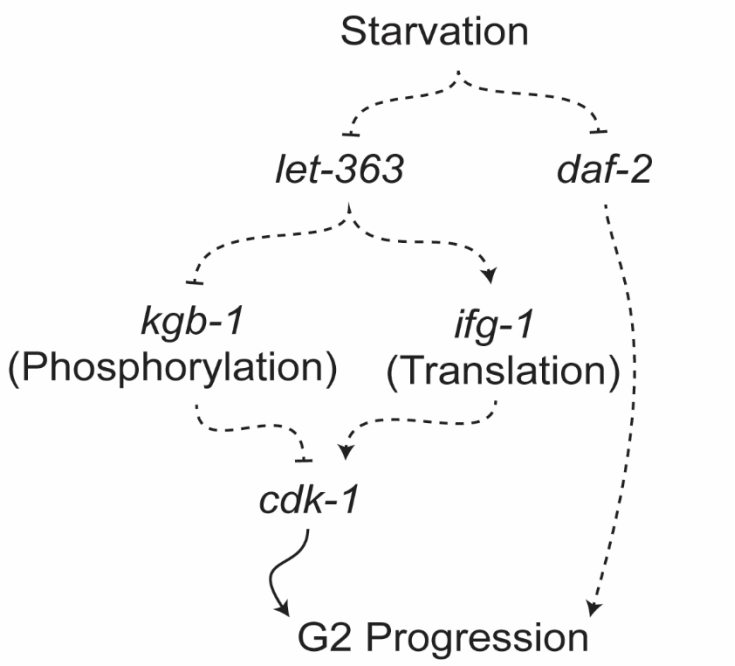

Figure 56: Starvation Model

Starvation inhibits both the *let-363* and *daf-2* signaling pathways to inhibit G2 progression. *let-363* mediates this response by inhibition of *cdk-1* translationally, through *ifg-1*, and post-translationally, by increased inhibitory phosphorylation mediated by *kgb-1*.

CHAPTER 5: DISCUSSION

Chapter 5: Discussion

Full citation:

* Furuta, T., * H. J. Joo, * K. A. Trimmer, S. Y. Chen, and S. Arur. 2018. 'GSK-3 promotes S-phase entry and progression in *C. elegans* germline stem cells to maintain tissue output', Development, 145, doi: 10.1242/dev.161042

* Equal contribution, alphabetically ordered

5.1: Discussion

Stem cells play a critical role in maintaining tissue homeostasis, during tissue repair and regeneration. To faithfully execute these functions stem cells respond to extracellular cues and intrinsic signals to protect the progenitors from environmental or tissue based insult. In this thesis, I identified two cellular mechanisms which regulate the cell cycle in GSCs in response to adverse environmental or metabolic conditions. First: In GSCs, *gsk-3* works to promote proliferation through regulation of the G1 phase of the cell cycle, without affecting the differentiation/self-renewal decision. I find that *gsk-3* promotes EdU incorporation along with promoting a short G1 phase by promoting *cdk-2* transcription. Second: I find that starvation induces a cell cycle arrest at G2 which is independent of the DNA damage G2 arrest. This starvation-induced arrest is mediated by Insulin and TOR signaling. The TOR signaling axis is mediated by the stress kinase *kgb-1* and the translation initiation factor *ifg-1*, culminating in translational

and post-translational regulation of *cdk-1*. Combined, these regulatory components provide plasticity to GSCs in times of adverse environmental or metabolic conditions.

5.1.1: GSCs may lack a DNA licensing checkpoint

In mammalian systems, DNA licensing actively promotes Cdk2 activation, suggesting that the licensing checkpoint is essential for progression into S phase. In fact, depletion of licensing components results in cell cycle arrest in a p53 dependent manner further supporting a DNA licensing checkpoint. During our investigations into the nature of the *gsk-3* mutant GSC phenotype, we found that depletion of the ORC complex members or Cdc6 resulted in DNA fragmentation and re-replication. Since the DNA licensing members were depleted by RNAi, it is likely that they were not completely removed, and so it is possible that some level of DNA licensing occurred, but that the licensing was not extensive enough to cover the entire genome. Surprisingly, in *gsk-3* mutants, this phenotype is rescued. I propose that the extended G1 in *gsk-3* mutants is in part responsible for this rescue. Extension of G1 in *gsk-3* mutants may allow DNA licensing components to complete licensing even if their expression level is reduced. However, that DNA licensing can be incomplete in wildtype supports the idea that there is no obvious DNA licensing checkpoint in *C. elegans* GSCs in addition to the cells displaying a distinct S phase entry regulation as a whole. However, if a p53-dependent DNA licensing checkpoint is in place in C. elegans GSCs, co-depletion of the p53 homolog cep-1 along with DNA licensing factors should appear worse than depletion of DNA licensing factors alone, providing one avenue of determining the presence of this checkpoint.

5.1.2: How does constitutively high expression of CDK-2 regulate G1/S switch?

I find that the *cdk-2* mRNA maintains a constitutively high level of expression in the GSCs, which is necessary for the abbreviated cell cycle structure. The expression of CDK-2 also reflects its activity, as shown previously by phospho-CDC-6 expression, and functional analysis (Fox et al. 2011), and from this study. Using the nuclear to cytoplasmic shuttling of MCM-3 as a dynamic readout of CDK-2 function, we found that MCM-3 is nuclear when CDK-2 function is lower, and cytoplasmic when CDK-2 function (or expression) is high. Interestingly, in *gsk-3* mutant GSCs, MCM-3 is nuclear in about 56% of the cells, the levels of *cdk-2* mRNA are significantly reduced, and the cells incorporate EdU very inefficiently. Further, over-expression of CDK-2 in the *gsk-3* mutants completely rescues the GSC defects. Together, these data suggest that in GSCs, the cell cycle at the G1/S boundary is largely regulated by the accumulation of CDK-2. Consistent with this is the observation that depletion (via RNAi) and reduction of *cdk-2* mRNA result in two distinct phenotypes: cell cycle arrest in the former (Fox et al. 2011) and slow S phase entry and progression in the latter (this study).

That Cdk2 expression levels regulate the G1/S switch may be unique to cells that have a short G1. To put this in the context of canonical mammalian cell cycle progression which is regulated via low Cdk2 activity in G1 to enable pre-replication complexes to assemble at origins (Blow and Hodgson 2002), I propose the following model. Canonically, inactive Cdk2 enables the loading of the pre-replication complex into the nucleus at the end of G1, and active Cdk2 then initiates S phase, both of which are regulated through post-translational mechanisms such as phosphorylation. In the context of GSCs, it is likely that different thresholds of activation form distinct complexes of CDK-2 that mediate its differing roles in G1 and S. For example, it is likely that the pre-replication complex can form at a lower threshold of CDK-2 activity (mimicking an ‘inactive” pool of Cdk2) than a threshold of CDK2 that drives entry and progression

through S phase. Observations from mESCs support this model. In mESCs despite continuous high expression of Cdk2 and Cyclin E, a subset of Cdk2 complexes are in fact “inactivated” at G1, allowing pre-replication complexes to assemble transiently and allow S phase entry (Ohtsuka and Dalton 2008). Additionally, these complexes are thought to be undetectable above the elevated Cdk2 expression (Ohtsuka and Dalton 2008). Therefore, one possible hypothesis is that much like in mESCs, different complexes of CDK-2 exist, and some of these are inactivated at late G1 (despite the high expression of CDK-2) in GSCs coupled with a very transient loading of the pre-replication complex. This notion of a very transient loading of the licensing complex may account for the inability to visualize the nuclear pre-replication complex in wildtype GSCs. Together, this leads to the model that a pool of CDK-2 is inactive, which enables loading of the pre-replication complex, but the high CDK-2/CYE-1 levels throughout GSCs result in the loading being transient thus facilitating an accelerated entry into S phase, effectively coupling the high expression of CDK-2 with the G1/S switch, and abbreviation of G1.

5.1.3: DPL-1 as a transcriptional repressor of CDK-2 to regulate G1 and S phase progression.

Dp1/E2F proteins are canonical G1/S phase regulators across multiple systems, where they promote G1/S phase progression through activation of S phase target genes. However, in *C. elegans* loss of *dpl-1* had not previously revealed any loss of G1/S phase either in the soma (Ceol and Horvitz 2001; Chi and Reinke 2006; Reddien et al. 2007) or the germline (Figure 33, Chapter 3.5). These data suggested that Dp1/E2F may not function canonically to promote S phase in *C. elegans*. Instead, in this study, we made the discovery that DPL-1 represses S phase transcription. EFL-1, the partner of DPL-1,

is closest in homology to E2F4 family of E2F transcription factors (Smith et al. 1996), and in vertebrates E2F4 family members have been implicated in repression of S phase target genes rather than activation (Dominguez-Brauer et al. 2009; Pilkinton, Sandoval, and Colamonici 2007; Popov, Chang, and Serikov 2005). Thus, it is possible, that in *C. elegans*, the DPL-1/EFL-1 complex function more like the Dp1/E2F4 complex in vertebrates and repress G1/S phase target genes. Together, these data reveal a novel mode of cell cycle regulation via transcriptional control of cyclin dependent kinases.

5.1.4: A G2 nutritional checkpoint

Checkpoints are necessary to ensure that the cell cycle completes with fidelity. The well-established DNA damage checkpoint protects against mitotic catastrophe and DNA fragmentation (Vakifahmetoglu, Olsson, and Zhivotovsky 2008). This checkpoint can be triggered in any of G1, S and G2 phases to halt cell cycle progression until the DNA damage has been repaired, and can trigger cell death if the DNA damage is too extensive. The starvation-induced G2 arrest may be reminiscent of a checkpoint as well.

There are reports of nutritional signaling governing the G2/M transition in *D. melanogaster* (Hsu, LaFever, and Drummond-Barbosa 2008). Additionally, I have found that nutritional signaling may be responsible for an arrest at G2. Due to the GSC cell cycle structure, it is likely that a G2 checkpoint would be optimal. Constant expression of *cye-1* and *cdk-2* lead to active CDK-2 in all nuclei. During starvation, it is likely that *cdk-2* remains active, since continuous replication requires active *cdk-2*, as we showed using *gsk-3* mutants. With continuous active CDK-2, it is unlikely that GSCs would enter a quiescent state, which prohibits the known G1 checkpoint. Therefore, the next safest point for the cell to arrest is at G2, when the cell has safely replicated its

DNA and is growing in order to divide. A nutritional checkpoint at the boundary between G2 and mitosis would protect against entry into an energy-intensive process when resources are limited.

5.1.5: Cell cycle plasticity in response to nutrient and metabolic stresses.

The ability to arrest the cell cycle at any phase in the face of metabolic or nutrient stresses gives the *C. elegans* GSCs an ability to adapt to adverse conditions, or plasticity. The regulation of this plasticity described herein may be important for other populations of rapidly dividing cells. Early embryonic populations of stem cells in humans and mice share a similar cell cycle structure with cells in S phase for 50-60% of the cell cycle, leading to relatively short gap phases (White and Dalton 2005). mESCs, in particular, have constitutive Cdk2 activity throughout the cell cycle, resulting in the lack of a restriction point and an inability to enter the canonical quiescence at G0 (Stead et al. 2002). Since G1 is a major arrest point in response to nutritional signaling in many cell types, this altered G1 regulation suggests that mESCs may not retain plasticity to nutrient availability. However, similar to the proliferation defect found due to downregulation of *let-363* found in this study, Mtor is required for proliferation of the inner cell mass from which mESCs are isolated (Gangloff et al. 2004). This appears to mirror the regulation found in *C. elegans* germline stem cells, raising the possibility that mESCs respond to acute starvation with a G2 arrest. Further research into the regulation of the acute starvation-induced arrest of *C. elegans* GSCs, therefore, may provide insights into cell cycle plasticity during early embryonic divisions in mammals, as well as other rapidly dividing populations of cells, including disease states such as cancer.

5.2: Future Directions

5.2.1: *gsk-3* in response to external signaling

As stated previously, the adult *C. elegans* GSCs have a short G1. Here, we provide evidence of a mutant in *gsk-3* which slows S phase entry, effectively lengthening G1. Additionally, this phenotype occurs due to a lack of *gsk-3* kinase activity. However, *gsk-3* can receive signals from multiple pathways. In mammals, *gsk-3* is inactivated in response to Wnt and Insulin signaling. However, if *gsk-3* were to be inactivated similarly in *C. elegans* GSCs, normal fed conditions and/or developmental signaling would result in down-regulation of *cdk-2*, potentially halting the cell cycle. A few possibilities exist to reconcile this. Most inhibitory signals rely on the production of a bait phosphorylation on the N-terminal of *gsk-3 (Jope and Johnson 2004)*. Therefore, one option is that *gsk-3* has lower affinity towards the bait phosphorylation than towards the substrate mediating *cdk-2* expression. A second option would be that *gsk-3* is not regulated by nutritional signaling in *C. elegans*. Regardless, it is still unknown whether and/or how *gsk-3* is regulated in response to nutritional signaling in GSCs.

5.2.2: Insulin signaling in the starvation arrest regulation

Since starvation halts nutritional signaling, it is no surprise that the insulin receptor homolog *daf-2* shows a proliferation defect in adult GSCs. By utilizing a temperature-sensitive *daf-2* mutant, I found that the ADI in GSCs was significantly lower than in wildtype (Figure 43, Chapter 4.4). How the signal is propagated to control the cell cycle is yet to be determined. There is evidence that the FOXO homolog (*daf-16)*, which functions downstream of *daf-2*, can inhibit tumor formation due to increased Notch signaling providing one possibility (Qi et al. 2012; Pinkston-Gosse and Kenyon 2007). Another is that the signal goes through TOR signaling. In mammals Insulin signaling

and TOR signaling are linked by the TSC1/2 complex. To date there is no known homolog for either protein, suggesting that there may be no link between these two pathways in *C. elegans*. However, there is evidence that *daf-16*, in response to TGFβ but not Insulin signaling, can regulate the transcription of the Raptor homolog *daf-15*, providing an alternate link between the pathways (Qi et al. 2017). Whether they are independent in regulating the adult starvation-induced arrest remains to be investigated.

5.2.3: An Extended S phase During Starvation

Sustaining DNA replication for long periods of time can be dangerous. In addition to replication fork stalling and collapse, large swaths of ssDNA can be generated if the replicative helicase uncouples from the DNA polymerase all of which can lead to DNA damage and cell death (Zeman and Cimprich 2014). However, during the GSC starvation arrest, I observe an extended S phase of at least 18 hours, 3 times longer than normal S phase. Therefore, GSCs may be incurring DNA damage and mutations over time.

In addition, there is EdU incorporation at potentially any point during the extended S phase. This is in contrast to hydroxyurea treatment which does not incorporate EdU and suggests that there are nucleotides available during the starvation arrest. In acute starvation, there would be no external source for these nucleotides and the internal source of these nucleotides remains unknown. The apoptotic cells which are in pachytene, more proximal in the germline, could provide these nucleotides. Since there is no sign of re-replication, the GSCs could be undergoing a very slow DNA replication.

BIBLIOGRAPHY

Abraham, R. T., and G. J. Wiederrecht. 1996. 'Immunopharmacology of rapamycin', *Annu Rev Immunol*, 14: 483-510.

Alessi, D. R., S. R. James, C. P. Downes, A. B. Holmes, P. R. Gaffney, C. B. Reese, and P. Cohen. 1997. 'Characterization of a 3-phosphoinositide-dependent protein kinase which phosphorylates and activates protein kinase Balpha', *Curr Biol*, 7: 261-9.

Almasan, A., Y. Yin, R. E. Kelly, E. Y. Lee, A. Bradley, W. Li, J. R. Bertino, and G. M. Wahl. 1995. 'Deficiency of retinoblastoma protein leads to inappropriate S-phase entry, activation of E2F-responsive genes, and apoptosis', *Proc Natl Acad Sci U S A*, 92: 5436-40.

Andrusiak, M. G., and Y. Jin. 2016. 'Context Specificity of Stress-activated Mitogen-activated Protein (MAP) Kinase Signaling: The Story as Told by Caenorhabditis elegans', *J Biol Chem*, 291: 7796-804.

Angelo, G., and M. R. Van Gilst. 2009. 'Starvation protects germline stem cells and extends reproductive longevity in C. elegans', *Science*, 326: 954-8.

Arellano, M., and S. Moreno. 1997. 'Regulation of CDK/cyclin complexes during the cell cycle', *Int J Biochem Cell Biol*, 29: 559-73.

Arur, S., M. Ohmachi, M. Berkseth, S. Nayak, D. Hansen, D. Zarkower, and T. Schedl. 2011. 'MPK-1 ERK controls membrane organization in C. elegans oogenesis via a sex-determination module', *Dev Cell*, 20: 677-88.

Arur, S., M. Ohmachi, S. Nayak, M. Hayes, A. Miranda, A. Hay, A. Golden, and T. Schedl. 2009. 'Multiple ERK substrates execute single biological processes in Caenorhabditis elegans germ-line development', *Proc Natl Acad Sci U S A*, 106: 4776-81.

Audry, J., L. Maestroni, E. Delagoutte, T. Gauthier, T. M. Nakamura, Y. Gachet, C. Saintome, V. Geli, and S. Coulon. 2015. 'RPA prevents G-rich structure formation at lagging-strand telomeres to allow maintenance of chromosome ends', *EMBO J*, 34: 1942-58.

Austin, J., and J. Kimble. 1987. 'glp-1 is required in the germ line for regulation of the decision between mitosis and meiosis in C. elegans', *Cell*, 51: 589-99.

Bagley, B. N., T. M. Keane, V. I. Maklakova, J. G. Marshall, R. A. Lester, M. M. Cancel, A. R. Paulsen, L. E. Bendzick, R. A. Been, S. C. Kogan, R. T. Cormier, C. Kendziorski, D. J. Adams, and L. S. Collier. 2012. 'A dominantly acting murine allele of Mcm4 causes chromosomal abnormalities and promotes tumorigenesis', *PLoS Genet*, 8: e1003034.

Banin, S., L. Moyal, S. Shieh, Y. Taya, C. W. Anderson, L. Chessa, N. I. Smorodinsky, C. Prives, Y. Reiss, Y. Shiloh, and Y. Ziv. 1998. 'Enhanced phosphorylation of p53 by ATM in response to DNA damage', *Science*, 281: 1674-7.

Berry, L. W., B. Westlund, and T. Schedl. 1997. 'Germ-line tumor formation caused by activation of glp-1, a Caenorhabditis elegans member of the Notch family of receptors', *Development*, 124: 925-36.

Berti, M., and A. Vindigni. 2016. 'Replication stress: getting back on track', *Nat Struct Mol Biol*, 23: 103-9.

Besson, A., S. F. Dowdy, and J. M. Roberts. 2008. 'CDK inhibitors: cell cycle regulators and beyond', *Dev Cell*, 14: 159-69.

Betschinger, J., and J. A. Knoblich. 2004. 'Dare to be different: asymmetric cell division in Drosophila, C. elegans and vertebrates', *Curr Biol*, 14: R674-85.

Blow, J. J. 1993. 'Preventing re-replication of DNA in a single cell cycle: evidence for a replication licensing factor', *J Cell Biol*, 122: 993-1002.

Blow, J. J., and B. Hodgson. 2002. 'Replication licensing--defining the proliferative state?', *Trends Cell Biol*, 12: 72-8.

Borgne, A., A. C. Ostvold, S. Flament, and L. Meijer. 1999. 'Intra-M phase-promoting factor phosphorylation of cyclin B at the prophase/metaphase transition', *J Biol Chem*, 274: 11977-86.

Bouskila, M., M. F. Hirshman, J. Jensen, L. J. Goodyear, and K. Sakamoto. 2008. 'Insulin promotes glycogen synthesis in the absence of GSK3 phosphorylation in skeletal muscle', *Am J Physiol Endocrinol Metab*, 294: E28-35.

Boxem, M., D. G. Srinivasan, and S. van den Heuvel. 1999. 'The Caenorhabditis elegans gene ncc-1 encodes a cdc2-related kinase required for M phase in meiotic and mitotic cell divisions, but not for S phase', *Development*, 126: 2227-39.

Boxem, M., and S. van den Heuvel. 2001. 'lin-35 Rb and cki-1 Cip/Kip cooperate in developmental regulation of G1 progression in C. elegans', *Development*, 128: 4349-59.

Bracken, A. P., M. Ciro, A. Cocito, and K. Helin. 2004. 'E2F target genes: unraveling the biology', *Trends Biochem Sci*, 29: 409-17.

Bradford, G. B., B. Williams, R. Rossi, and I. Bertoncello. 1997. 'Quiescence, cycling, and turnover in the primitive hematopoietic stem cell compartment', *Exp Hematol*, 25: 445-53.

Brehm, A., E. A. Miska, D. J. McCance, J. L. Reid, A. J. Bannister, and T. Kouzarides. 1998. 'Retinoblastoma protein recruits histone deacetylase to repress transcription', *Nature*, 391: 597-601.

Brenner, S. 1974. 'The genetics of Caenorhabditis elegans', *Genetics*, 77: 71-94.

Brodigan, T. M., Ji Liu, M. Park, E. T. Kipreos, and M. Krause. 2003. 'Cyclin E expression during development in Caenorhabditis elegans', *Dev Biol*, 254: 102-15.

Brugarolas, J., K. Lei, R. L. Hurley, B. D. Manning, J. H. Reiling, E. Hafen, L. A. Witters, L. W. Ellisen, and W. G. Kaelin, Jr. 2004. 'Regulation of mTOR function in response to hypoxia by REDD1 and the TSC1/TSC2 tumor suppressor complex', *Genes Dev*, 18: 2893-904.

Buchkovich, K., L. A. Duffy, and E. Harlow. 1989. 'The retinoblastoma protein is phosphorylated during specific phases of the cell cycle', *Cell*, 58: 1097-105.

Buck, S. H., D. Chiu, and R. M. Saito. 2009. 'The cyclin-dependent kinase inhibitors, cki-1 and cki-2, act in overlapping but distinct pathways to control cell cycle quiescence during C. elegans development', *Cell Cycle*, 8: 2613-20.

Byun, T. S., M. Pacek, M. C. Yee, J. C. Walter, and K. A. Cimprich. 2005. 'Functional uncoupling of MCM helicase and DNA polymerase activities activates the ATR-dependent checkpoint', *Genes Dev*, 19: 1040-52.

Campbell, J. M., M. B. Nottle, I. Vassiliev, M. Mitchell, and M. Lane. 2012. 'Insulin increases epiblast cell number of in vitro cultured mouse embryos via the PI3K/GSK3/p53 pathway', *Stem Cells Dev*, 21: 2430-41.

Ceol, C. J., and H. R. Horvitz. 2001. 'dpl-1 DP and efl-1 E2F act with lin-35 Rb to antagonize Ras signaling in C. elegans vulval development', *Mol Cell*, 7: 461-73.

Chan, F. K., J. Zhang, L. Cheng, D. N. Shapiro, and A. Winoto. 1995. 'Identification of human and mouse p19, a novel CDK4 and CDK6 inhibitor with homology to p16ink4', *Mol Cell Biol*, 15: 2682-8.

Cheeks, R. J., J. C. Canman, W. N. Gabriel, N. Meyer, S. Strome, and B. Goldstein. 2004. 'C. elegans PAR proteins function by mobilizing and stabilizing asymmetrically localized protein complexes', *Curr Biol*, 14: 851-62.

Chen, Y. H., S. Keegan, M. Kahli, P. Tonzi, D. Fenyo, T. T. Huang, and D. J. Smith. 2019. 'Transcription shapes DNA replication initiation and termination in human cells', *Nat Struct Mol Biol*, 26: 67-77.

Cheng, T., N. Rodrigues, H. Shen, Y. Yang, D. Dombkowski, M. Sykes, and D. T. Scadden. 2000. 'Hematopoietic stem cell quiescence maintained by p21cip1/waf1', *Science*, 287: 1804-8.

Chi, W., and V. Reinke. 2006. 'Promotion of oogenesis and embryogenesis in the C. elegans gonad by EFL-1/DPL-1 (E2F) does not require LIN-35 (pRB)', *Development*, 133: 3147-57.

———. 2009. 'DPL-1 (DP) acts in the germ line to coordinate ovulation and fertilization in C. elegans', *Mech Dev*, 126: 406-16.

Choi, H. M., C. R. Calvert, N. Husain, D. Huss, J. C. Barsi, B. E. Deverman, R. C. Hunter, M. Kato, S. M. Lee, A. C. Abelin, A. Z. Rosenthal, O. S. Akbari, Y. Li, B. A. Hay, P. W. Sternberg, P. H. Patterson, E. H. Davidson, S. K. Mazmanian, D. A. Prober, M. van de Rijn, J. R. Leadbetter, D. K. Newman, C. Readhead, M. E. Bronner, B. Wold, R. Lansford, T. Sauka-Spengler, S. E. Fraser, and N. A. Pierce. 2016. 'Mapping a multiplexed zoo of mRNA expression', *Development*, 143: 3632-37.

Chong, J. P., and J. J. Blow. 1996. 'DNA replication licensing factor', *Prog Cell Cycle Res*, 2: 83-90.

Chung, E., P. Deacon, S. Marable, J. Shin, and J. S. Park. 2016. 'Notch signaling promotes nephrogenesis by downregulating Six2', *Development*, 143: 3907-13.

Chuykin, I. A., M. S. Lianguzova, T. V. Pospelova, and V. A. Pospelov. 2008. 'Activation of DNA damage response signaling in mouse embryonic stem cells', *Cell Cycle*, 7: 2922-8.

Copeland, N. A., H. E. Sercombe, J. F. Ainscough, and D. Coverley. 2010. 'Ciz1 cooperates with cyclin-A-CDK2 to activate mammalian DNA replication in vitro', *J Cell Sci*, 123: 1108-15.

Cotsarelis, G., T. T. Sun, and R. M. Lavker. 1990. 'Label-retaining cells reside in the bulge area of pilosebaceous unit: implications for follicular stem cells, hair cycle, and skin carcinogenesis', *Cell*, 61: 1329-37.

Coverley, D., H. Laman, and R. A. Laskey. 2002. 'Distinct roles for cyclins E and A during DNA replication complex assembly and activation', *Nat Cell Biol*, 4: 523-8.

Cowan, C. R., and A. A. Hyman. 2006. 'Cyclin E-Cdk2 temporally regulates centrosome assembly and establishment of polarity in Caenorhabditis elegans embryos', *Nat Cell Biol*, 8: 1441-7.

Crittenden, S. L., K. A. Leonhard, D. T. Byrd, and J. Kimble. 2006. 'Cellular analyses of the mitotic region in the Caenorhabditis elegans adult germ line', *Mol Biol Cell*, 17: 3051-61.

De Meyts, P. 2000. 'The Insulin Receptor and Its Signal Transduction Network.' in K. R. Feingold, B. Anawalt, A. Boyce, G. Chrousos, K. Dungan, A. Grossman, J. M. Hershman, G. Kaltsas, C. Koch, P. Kopp, M. Korbonits, R. McLachlan, J. E. Morley, M. New, L. Perreault, J. Purnell, R. Rebar, F. Singer, D. L. Trence, A. Vinik and D. P. Wilson (eds.), *Endotext* (South Dartmouth (MA)).

DeGregori, J., G. Leone, A. Miron, L. Jakoi, and J. R. Nevins. 1997. 'Distinct roles for E2F proteins in cell growth control and apoptosis', *Proc Natl Acad Sci U S A*, 94: 7245-50.

Den Haese, G. J., N. Walworth, A. M. Carr, and K. L. Gould. 1995. 'The Wee1 protein kinase regulates T14 phosphorylation of fission yeast Cdc2', *Mol Biol Cell*, 6: 371-85.

Deutsch, P. J., C. F. Wan, O. M. Rosen, and C. S. Rubin. 1983. 'Latent insulin receptors and possible receptor precursors in 3T3-L1 adipocytes', *Proc Natl Acad Sci U S A*, 80: 133-6.

Doble, B. W., and J. R. Woodgett. 2003. 'GSK-3: tricks of the trade for a multi-tasking kinase', *J Cell Sci*, 116: 1175-86.

Dominguez-Brauer, C., Y. J. Chen, P. M. Brauer, J. Pimkina, and P. Raychaudhuri. 2009. 'ARF stimulates XPC to trigger nucleotide excision repair by regulating the repressor complex of E2F4', *EMBO Rep*, 10: 1036-42.

Dorsett, M., B. Westlund, and T. Schedl. 2009. 'METT-10, a putative methyltransferase, inhibits germ cell proliferative fate in Caenorhabditis elegans', *Genetics*, 183: 233-47.

Drake, M., T. Furuta, K. M. Suen, G. Gonzalez, B. Liu, A. Kalia, J. E. Ladbury, A. Z. Fire, J. B. Skeath, and S. Arur. 2014. 'A requirement for ERK-dependent Dicer phosphorylation in coordinating oocyte-to-embryo transition in C. elegans', *Dev Cell*, 31: 614-28.

Duret, L., N. Guex, M. C. Peitsch, and A. Bairoch. 1998. 'New insulin-like proteins with atypical disulfide bond pattern characterized in Caenorhabditis elegans by comparative sequence analysis and homology modeling', *Genome Res*, 8: 348-53.

Eckmann, C. R., S. L. Crittenden, N. Suh, and J. Kimble. 2004. 'GLD-3 and control of the mitosis/meiosis decision in the germline of Caenorhabditis elegans', *Genetics*, 168: 147-60.

Edgar, L. G., and J. D. McGhee. 1988. 'DNA synthesis and the control of embryonic gene expression in C. elegans', *Cell*, 53: 589-99.

Evans, M. J., and M. H. Kaufman. 1981. 'Establishment in culture of pluripotential cells from mouse embryos', *Nature*, 292: 154-6.

Evans, T. C., S. L. Crittenden, V. Kodoyianni, and J. Kimble. 1994. 'Translational control of maternal glp-1 mRNA establishes an asymmetry in the C. elegans embryo', *Cell*, 77: 183-94.

Evans, T., E. T. Rosenthal, J. Youngblom, D. Distel, and T. Hunt. 1983. 'Cyclin: a protein specified by maternal mRNA in sea urchin eggs that is destroyed at each cleavage division', *Cell*, 33: 389-96.

Fairman, M. P., and B. Stillman. 1988. 'Cellular factors required for multiple stages of SV40 DNA replication in vitro', *EMBO J*, 7: 1211-8.

Falck, J., N. Mailand, R. G. Syljuasen, J. Bartek, and J. Lukas. 2001. 'The ATM-Chk2-Cdc25A checkpoint pathway guards against radioresistant DNA synthesis', *Nature*, 410: 842-7.

Fay, D. S., and M. Han. 2000. 'Mutations in cye-1, a Caenorhabditis elegans cyclin E homolog, reveal coordination between cell-cycle control and vulval development', *Development*, 127: 4049-60.

Feng, Z., W. Hu, E. de Stanchina, A. K. Teresky, S. Jin, S. Lowe, and A. J. Levine. 2007. 'The regulation of AMPK beta1, TSC2, and PTEN expression by p53: stress, cell and tissue specificity, and the role of these gene products in modulating the IGF-1-AKT-mTOR pathways', *Cancer Res*, 67: 3043-53.

Ferraro, F., C. L. Celso, and D. Scadden. 2010. 'Adult stem cels and their niches', *Adv Exp Med Biol*, 695: 155-68.

Fingar, D. C., C. J. Richardson, A. R. Tee, L. Cheatham, C. Tsou, and J. Blenis. 2004. 'mTOR controls cell cycle progression through its cell growth effectors S6K1 and 4E-BP1/eukaryotic translation initiation factor 4E', *Mol Cell Biol*, 24: 200-16.

Fisher, R. P., and D. O. Morgan. 1994. 'A Novel Cyclin Associates with Mo15/Cdk7 to Form the Cdk-Activating Kinase', *Cell*, 78: 713-24.

Fox, P. M., and T. Schedl. 2015. 'Analysis of Germline Stem Cell Differentiation Following Loss of GLP-1 Notch Activity in Caenorhabditis elegans', *Genetics*, 201: 167-84.

Fox, P. M., V. E. Vought, M. Hanazawa, M. H. Lee, E. M. Maine, and T. Schedl. 2011. 'Cyclin E and CDK-2 regulate proliferative cell fate and cell cycle progression in the C. elegans germline', *Development*, 138: 2223-34.

Franckhauser, C., D. Mamaeva, L. Heron-Milhavet, A. Fernandez, and N. J. Lamb. 2010. 'Distinct pools of cdc25C are phosphorylated on specific TP sites and differentially localized in human mitotic cells', *PLoS One*, 5: e11798.

Franke, T. F., S. I. Yang, T. O. Chan, K. Datta, A. Kazlauskas, D. K. Morrison, D. R. Kaplan, and P. N. Tsichlis. 1995. 'The protein kinase encoded by the Akt proto-oncogene is a target of the PDGF-activated phosphatidylinositol 3-kinase', *Cell*, 81: 727-36.

Fukumoto, H., T. Kayano, J. B. Buse, Y. Edwards, P. F. Pilch, G. I. Bell, and S. Seino. 1989. 'Cloning and characterization of the major insulin-responsive glucose transporter expressed in human skeletal muscle and other insulin-responsive tissues', *J Biol Chem*, 264: 7776-9.

Fukuyama, M., A. E. Rougvie, and J. H. Rothman. 2006. 'C. elegans DAF-18/PTEN mediates nutrient-dependent arrest of cell cycle and growth in the germline', *Curr Biol*, 16: 773-9.

Fung, T. K., H. T. Ma, and R. Y. Poon. 2007. 'Specialized roles of the two mitotic cyclins in somatic cells: cyclin A as an activator of M phase-promoting factor', *Mol Biol Cell*, 18: 1861-73.

Furuta, T., H. J. Joo, K. A. Trimmer, S. Y. Chen, and S. Arur. 2018. 'GSK-3 promotes S-phase entry and progression in C. elegans germline stem cells to maintain tissue output', *Development*, 145.

Gangloff, Y. G., M. Mueller, S. G. Dann, P. Svoboda, M. Sticker, J. F. Spetz, S. H. Um, E. J. Brown, S. Cereghini, G. Thomas, and S. C. Kozma. 2004. 'Disruption of the mouse mTOR gene leads to early postimplantation lethality and prohibits embryonic stem cell development', *Mol Cell Biol*, 24: 9508-16.

Gao, Z., Z. Qiu, M. Lu, J. Shu, and D. Tang. 2017. 'Hybridization chain reaction-based colorimetric aptasensor of adenosine 5'-triphosphate on unmodified gold nanoparticles and two label-free hairpin probes', *Biosens Bioelectron*, 89: 1006-12.

Garcia-Muse, T., and S. J. Boulton. 2005. 'Distinct modes of ATR activation after replication stress and DNA double-strand breaks in Caenorhabditis elegans', *EMBO J*, 24: 4345-55.

Gardner, R. L. 1983. 'Origin and differentiation of extraembryonic tissues in the mouse', *Int Rev Exp Pathol*, 24: 63-133.

Gardner, R. L., and M. H. Johnson. 1973. 'Investigation of early mammalian development using interspecific chimaeras between rat and mouse', *Nat New Biol*, 246: 86-9.

Gardner, R. L., and J. Rossant. 1979. 'Investigation of the fate of 4-5 day post-coitum mouse inner cell mass cells by blastocyst injection', *J Embryol Exp Morphol*, 52: 141-52.

Gartner, A., S. Milstein, S. Ahmed, J. Hodgkin, and M. O. Hengartner. 2000. 'A conserved checkpoint pathway mediates DNA damage--induced apoptosis and cell cycle arrest in C. elegans', *Mol Cell*, 5: 435-43.

Gerhold, A. R., J. Ryan, J. N. Vallee-Trudeau, J. F. Dorn, J. C. Labbe, and P. S. Maddox. 2015. 'Investigating the regulation of stem and progenitor cell mitotic progression by in situ imaging', *Curr Biol*, 25: 1123-34.

Girard, F., U. Strausfeld, A. Fernandez, and N. J. Lamb. 1991. 'Cyclin A is required for the onset of DNA replication in mammalian fibroblasts', *Cell*, 67: 1169-79.

Gleason, J. E., E. A. Szyleyko, and D. M. Eisenmann. 2006. 'Multiple redundant Wnt signaling components function in two processes during C. elegans vulval development', *Dev Biol*, 298: 442-57.

Golden, J. W., and D. L. Riddle. 1984. 'The Caenorhabditis elegans dauer larva: developmental effects of pheromone, food, and temperature', *Dev Biol*, 102: 368-78.

Goss, A. M., Y. Tian, T. Tsukiyama, E. D. Cohen, D. Zhou, M. M. Lu, T. P. Yamaguchi, and E. E. Morrisey. 2009. 'Wnt2/2b and beta-catenin signaling are necessary and sufficient to specify lung progenitors in the foregut', *Dev Cell*, 17: 290-8.

Goto, H., T. Natsume, M. T. Kanemaki, A. Kaito, S. Wang, E. C. Gabazza, M. Inagaki, and A. Mizoguchi. 2019. 'Chk1-mediated Cdc25A degradation as a critical mechanism for normal cell cycle progression', *J Cell Sci*, 132.

Gould, K. L., S. Moreno, D. J. Owen, S. Sazer, and P. Nurse. 1991. 'Phosphorylation at Thr167 is required for Schizosaccharomyces pombe p34cdc2 function', *EMBO J*, 10: 3297-309.

Graham, C. F. 1966a. 'The effect of cell size and DNA content on the cellular regulation of DNA synthesis in haploid and diploid embryos', *Exp Cell Res*, 43: 13-9.

———. 1966b. 'The regulation of DNA synthesis and mitosis in multinucleate frog eggs', *J Cell Sci*, 1: 363-74.

Gu, Y., J. Rosenblatt, and D. O. Morgan. 1992. 'Cell cycle regulation of CDK2 activity by phosphorylation of Thr160 and Tyr15', *EMBO J*, 11: 3995-4005.

Guan, K. L., C. W. Jenkins, Y. Li, M. A. Nichols, X. Wu, C. L. O'Keefe, A. G. Matera, and Y. Xiong. 1994. 'Growth suppression by p18, a p16INK4/MTS1- and p14INK4B/MTS2-related CDK6 inhibitor, correlates with wild-type pRb function', *Genes Dev*, 8: 2939-52.

Guedes, S., and J. R. Priess. 1997. 'The C. elegans MEX-1 protein is present in germline blastomeres and is a P granule component', *Development*, 124: 731-9.

Guertin, D. A., D. M. Stevens, C. C. Thoreen, A. A. Burds, N. Y. Kalaany, J. Moffat, M. Brown, K. J. Fitzgerald, and D. M. Sabatini. 2006. 'Ablation in mice of the mTORC components raptor, rictor, or mLST8 reveals that mTORC2 is required for signaling to Akt-FOXO and PKCalpha, but not S6K1', *Dev Cell*, 11: 859-71.

Gwinn, D. M., D. B. Shackelford, D. F. Egan, M. M. Mihaylova, A. Mery, D. S. Vasquez, B. E. Turk, and R. J. Shaw. 2008. 'AMPK phosphorylation of raptor mediates a metabolic checkpoint', *Mol Cell*, 30: 214-26.

Hagting, A., M. Jackman, K. Simpson, and J. Pines. 1999. 'Translocation of cyclin B1 to the nucleus at prophase requires a phosphorylation-dependent nuclear import signal', *Curr Biol*, 9: 680-9.

Hamperl, S., M. J. Bocek, J. C. Saldivar, T. Swigut, and K. A. Cimprich. 2017. 'Transcription-Replication Conflict Orientation Modulates R-Loop Levels and Activates Distinct DNA Damage Responses', *Cell*, 170: 774-86 e19.

Hannon, G. J., and D. Beach. 1994. 'p15INK4B is a potential effector of TGF-beta-induced cell cycle arrest', *Nature*, 371: 257-61.

Hansen, D., E. J. Hubbard, and T. Schedl. 2004. 'Multi-pathway control of the proliferation versus meiotic development decision in the Caenorhabditis elegans germline', *Dev Biol*, 268: 342-57.

Hansen, D., L. Wilson-Berry, T. Dang, and T. Schedl. 2004. 'Control of the proliferation versus meiotic development decision in the C. elegans germline through regulation of GLD-1 protein accumulation', *Development*, 131: 93-104.

Harper, J. W., G. R. Adami, N. Wei, K. Keyomarsi, and S. J. Elledge. 1993. 'The p21 Cdk-interacting protein Cip1 is a potent inhibitor of G1 cyclin-dependent kinases', *Cell*, 75: 805-16.

Harper, J. W., S. J. Elledge, K. Keyomarsi, B. Dynlacht, L. H. Tsai, P. Zhang, S. Dobrowolski, C. Bai, L. Connell-Crowley, E. Swindell, and et al. 1995. 'Inhibition of cyclin-dependent kinases by p21', *Mol Biol Cell*, 6: 387-400.

Haupt, Y., R. Maya, A. Kazaz, and M. Oren. 1997. 'Mdm2 promotes the rapid degradation of p53', *Nature*, 387: 296-9.

Henderson, S. T., D. Gao, E. J. Lambie, and J. Kimble. 1994. 'lag-2 may encode a signaling ligand for the GLP-1 and LIN-12 receptors of C. elegans', *Development*, 120: 2913-24.

Hermeking, H., C. Lengauer, K. Polyak, T. C. He, L. Zhang, S. Thiagalingam, K. W. Kinzler, and B. Vogelstein. 1997. '14-3-3sigma is a p53-regulated inhibitor of G2/M progression', *Mol Cell*, 1: 3-11.

Hima Bindu, A., and B. Srilatha. 2011. 'Potency of Various Types of Stem Cells and their Transplantation', *Journal of Stem Cell Research & Therapy*, 1: 6.

Hirai, H., M. F. Roussel, J. Y. Kato, R. A. Ashmun, and C. J. Sherr. 1995. 'Novel INK4 proteins, p19 and p18, are specific inhibitors of the cyclin D-dependent kinases CDK4 and CDK6', *Mol Cell Biol*, 15: 2672-81.

Hirao, A., Y. Y. Kong, S. Matsuoka, A. Wakeham, J. Ruland, H. Yoshida, D. Liu, S. J. Elledge, and T. W. Mak. 2000. 'DNA damage-induced activation of p53 by the checkpoint kinase Chk2', *Science*, 287: 1824-7.

Hixson, D. C., J. M. Yep, J. R. Glenney, Jr., T. Hayes, and E. F. Walborg, Jr. 1981. 'Evaluation of periodate/lysine/paraformaldehyde fixation as a method for cross-linking plasma membrane glycoproteins', *J Histochem Cytochem*, 29: 561-6.

Hosoyama, T., K. Nishijo, S. I. Prajapati, G. Li, and C. Keller. 2011. 'Rb1 gene inactivation expands satellite cell and postnatal myoblast pools', *J Biol Chem*, 286: 19556-64.

Hsu, H. J., L. LaFever, and D. Drummond-Barbosa. 2008. 'Diet controls normal and tumorous germline stem cells via insulin-dependent and -independent mechanisms in Drosophila', *Dev Biol*, 313: 700-12.

Illmensee, K., and A. P. Mahowald. 1974. 'Transplantation of posterior polar plasm in Drosophila. Induction of germ cells at the anterior pole of the egg', *Proc Natl Acad Sci U S A*, 71: 1016-20.

———. 1976. 'The autonomous function of germ plasm in a somatic region of the Drosophila egg', *Exp Cell Res*, 97: 127-40.

Inoki, K., Y. Li, T. Xu, and K. L. Guan. 2003. 'Rheb GTPase is a direct target of TSC2 GAP activity and regulates mTOR signaling', *Genes Dev*, 17: 1829-34.

Inoki, K., T. Zhu, and K. L. Guan. 2003. 'TSC2 mediates cellular energy response to control cell growth and survival', *Cell*, 115: 577-90.

Jacinto, E., V. Facchinetti, D. Liu, N. Soto, S. Wei, S. Y. Jung, Q. Huang, J. Qin, and B. Su. 2006. 'SIN1/MIP1 maintains rictor-mTOR complex integrity and regulates Akt phosphorylation and substrate specificity', *Cell*, 127: 125-37.

Jan, E., C. K. Motzny, L. E. Graves, and E. B. Goodwin. 1999. 'The STAR protein, GLD-1, is a translational regulator of sexual identity in Caenorhabditis elegans', *EMBO J*, 18: 258-69.

Jia, K., D. Chen, and D. L. Riddle. 2004. 'The TOR pathway interacts with the insulin signaling pathway to regulate C. elegans larval development, metabolism and life span', *Development*, 131: 3897-906.

Jin, P., Y. Gu, and D. O. Morgan. 1996. 'Role of inhibitory CDC2 phosphorylation in radiation-induced G2 arrest in human cells', *J Cell Biol*, 134: 963-70.

Johnson, M. H., and C. A. Ziomek. 1981. 'The foundation of two distinct cell lineages within the mouse morula', *Cell*, 24: 71-80.

Jones, K. T., E. R. Greer, D. Pearce, and K. Ashrafi. 2009. 'Rictor/TORC2 regulates Caenorhabditis elegans fat storage, body size, and development through sgk-1', *PLoS Biol*, 7: e60.

Jope, R. S., and G. V. Johnson. 2004. 'The glamour and gloom of glycogen synthase kinase-3', *Trends Biochem Sci*, 29: 95-102.

Kadyk, L. C., and J. Kimble. 1998. 'Genetic regulation of entry into meiosis in Caenorhabditis elegans', *Development*, 125: 1803-13.

Kalchhauser, I., B. M. Farley, S. Pauli, S. P. Ryder, and R. Ciosk. 2011. 'FBF represses the Cip/Kip cell-cycle inhibitor CKI-2 to promote self-renewal of germline stem cells in C. elegans', *EMBO J*, 30: 3823-9.

Kasuga, M., J. A. Hedo, K. M. Yamada, and C. R. Kahn. 1982. 'The structure of insulin receptor and its subunits. Evidence for multiple nonreduced forms and a 210,000 possible proreceptor', *J Biol Chem*, 257: 10392-9.

Kasuga, M., Y. Zick, D. L. Blith, F. A. Karlsson, H. U. Haring, and C. R. Kahn. 1982. 'Insulin stimulation of phosphorylation of the beta subunit of the insulin receptor. Formation of both phosphoserine and phosphotyrosine', *J Biol Chem*, 257: 9891-4.

Kasuga, M., Y. Zick, D. L. Blithe, M. Crettaz, and C. R. Kahn. 1982. 'Insulin stimulates tyrosine phosphorylation of the insulin receptor in a cell-free system', *Nature*, 298: 667-9.

Kato, J., H. Matsushime, S. W. Hiebert, M. E. Ewen, and C. J. Sherr. 1993. 'Direct binding of cyclin D to the retinoblastoma gene product (pRb) and pRb phosphorylation by the cyclin D-dependent kinase CDK4', *Genes Dev*, 7: 331-42.

Kato, J. Y., M. Matsuoka, D. K. Strom, and C. J. Sherr. 1994. 'Regulation of cyclin D-dependent kinase 4 (cdk4) by cdk4-activating kinase', *Mol Cell Biol*, 14: 2713-21.

Kawano, T., Y. Ito, M. Ishiguro, K. Takuwa, T. Nakajima, and Y. Kimura. 2000. 'Molecular cloning and characterization of a new insulin/IGF-like peptide of the nematode Caenorhabditis elegans', *Biochem Biophys Res Commun*, 273: 431-6.

Kawasome, H., P. Papst, S. Webb, G. M. Keller, G. L. Johnson, E. W. Gelfand, and N. Terada. 1998. 'Targeted disruption of p70(s6k) defines its role in protein synthesis and rapamycin sensitivity', *Proc Natl Acad Sci U S A*, 95: 5033-8.

Kermi, C., E. Lo Furno, and D. Maiorano. 2017. 'Regulation of DNA Replication in Early Embryonic Cleavages', *Genes (Basel)*, 8.

Kimble, J. E., and J. G. White. 1981. 'On the control of germ cell development in Caenorhabditis elegans', *Dev Biol*, 81: 208-19.

Kimura, K. D., H. A. Tissenbaum, Y. Liu, and G. Ruvkun. 1997. 'daf-2, an insulin receptor-like gene that regulates longevity and diapause in Caenorhabditis elegans', *Science*, 277: 942-6.

King, R. W., P. K. Jackson, and M. W. Kirschner. 1994. 'Mitosis in transition', *Cell*, 79: 563-71.

Kiyokawa, H., and D. Ray. 2008. 'In vivo roles of CDC25 phosphatases: biological insight into the anti-cancer therapeutic targets', *Anticancer Agents Med Chem*, 8: 832-6.

Klippel, A., C. Reinhard, W. M. Kavanaugh, G. Apell, M. A. Escobedo, and L. T. Williams. 1996. 'Membrane localization of phosphatidylinositol 3-kinase is sufficient to activate multiple signal-transducing kinase pathways', *Mol Cell Biol*, 16: 4117-27.

Kodoyianni, V., E. M. Maine, and J. Kimble. 1992. 'Molecular basis of loss-of-function mutations in the glp-1 gene of Caenorhabditis elegans', *Mol Biol Cell*, 3: 1199-213.

Korta, D. Z., and E. J. Hubbard. 2010. 'Soma-germline interactions that influence germline proliferation in Caenorhabditis elegans', *Dev Dyn*, 239: 1449-59.

Korta, D. Z., S. Tuck, and E. J. Hubbard. 2012. 'S6K links cell fate, cell cycle and nutrient response in C. elegans germline stem/progenitor cells', *Development*, 139: 859-70.

Kunkel, T. A. 2004. 'DNA replication fidelity', *J Biol Chem*, 279: 16895-8.

Ladha, M. H., K. Y. Lee, T. M. Upton, M. F. Reed, and M. E. Ewen. 1998. 'Regulation of exit from quiescence by p27 and cyclin D1-CDK4', *Mol Cell Biol*, 18: 6605-15.

LaFever, L., A. Feoktistov, H. J. Hsu, and D. Drummond-Barbosa. 2010. 'Specific roles of Target of rapamycin in the control of stem cells and their progeny in the Drosophila ovary', *Development*, 137: 2117-26.

Lambie, E. J., and J. Kimble. 1991. 'Two homologous regulatory genes, lin-12 and glp-1, have overlapping functions', *Development*, 112: 231-40.

Larner, J., C. Villar-Palasi, N. D. Goldberg, J. S. Bishop, F. Huijing, J. I. Wenger, H. Sasko, and N. B. Brown. 1968. 'Hormonal and non-hormonal control of glycogen synthesis-control of transferase phosphatase and transferase I kinase', *Adv Enzyme Regul*, 6: 409-23.

Lawson, K. A., N. R. Dunn, B. A. Roelen, L. M. Zeinstra, A. M. Davis, C. V. Wright, J. P. Korving, and B. L. Hogan. 1999. 'Bmp4 is required for the generation of primordial germ cells in the mouse embryo', *Genes Dev*, 13: 424-36.

Lee, J. Y., A. E. Bielawska, and L. M. Obeid. 2000. 'Regulation of cyclin-dependent kinase 2 activity by ceramide', *Exp Cell Res*, 261: 303-11.

Lee, M. H., I. Reynisdottir, and J. Massague. 1995. 'Cloning of p57KIP2, a cyclin-dependent kinase inhibitor with unique domain structure and tissue distribution', *Genes Dev*, 9: 639-49.

Lee, S. J., A. Gartner, M. Hyun, B. Ahn, and H. S. Koo. 2010. 'The Caenorhabditis elegans Werner syndrome protein functions upstream of ATR and ATM in response to DNA replication inhibition and double-strand DNA breaks', *PLoS Genet*, 6: e1000801.

Levine, A. J. 1997. 'p53, the cellular gatekeeper for growth and division', *Cell*, 88: 323-31.

Li, C., and J. Jin. 2010. 'DNA replication licensing control and rereplication prevention', *Protein Cell*, 1: 227-36.

Li, J., M. Deng, Q. Wei, T. Liu, X. Tong, and X. Ye. 2011. 'Phosphorylation of MCM3 protein by cyclin E/cyclin-dependent kinase 2 (Cdk2) regulates its function in cell cycle', *J Biol Chem*, 286: 39776-85.

Li, W., S. G. Kennedy, and G. Ruvkun. 2003. 'daf-28 encodes a C. elegans insulin superfamily member that is regulated by environmental cues and acts in the DAF-2 signaling pathway', *Genes Dev*, 17: 844-58.

Liu, B., Q. Xue, Y. Tang, J. Cao, F. P. Guengerich, and H. Zhang. 2016. 'Mechanisms of mutagenesis: DNA replication in the presence of DNA damage', *Mutat Res Rev Mutat Res*, 768: 53-67.

Liu, F., J. J. Stanton, Z. Wu, and H. Piwnica-Worms. 1997. 'The human Myt1 kinase preferentially phosphorylates Cdc2 on threonine 14 and localizes to the endoplasmic reticulum and Golgi complex', *Mol Cell Biol*, 17: 571-83.

Liu, P., D. M. Slater, M. Lenburg, K. Nevis, J. G. Cook, and C. Vaziri. 2009. 'Replication licensing promotes cyclin D1 expression and G1 progression in untransformed human cells', *Cell Cycle*, 8: 125-36.

Liu, S., B. Shiotani, M. Lahiri, A. Marechal, A. Tse, C. C. Leung, J. N. Glover, X. H. Yang, and L. Zou. 2011. 'ATR autophosphorylation as a molecular switch for checkpoint activation', *Mol Cell*, 43: 192-202.

Long, X., C. Spycher, Z. S. Han, A. M. Rose, F. Muller, and J. Avruch. 2002. 'TOR deficiency in C. elegans causes developmental arrest and intestinal atrophy by inhibition of mRNA translation', *Curr Biol*, 12: 1448-61.

Lopez-Aviles, S., M. Grande, M. Gonzalez, A. L. Helgesen, V. Alemany, M. Sanchez-Piris, O. Bachs, J. B. Millar, and R. Aligue. 2005. 'Inactivation of the Cdc25 phosphatase by the stress-activated Srk1 kinase in fission yeast', *Mol Cell*, 17: 49-59.

Lopez-Aviles, S., E. Lambea, A. Moldon, M. Grande, A. Fajardo, M. A. Rodriguez-Gabriel, E. Hidalgo, and R. Aligue. 2008. 'Activation of Srk1 by the mitogen-activated protein kinase Sty1/Spc1 precedes its dissociation from the kinase and signals its degradation', *Mol Biol Cell*, 19: 1670-9.

Lopez-Girona, A., B. Furnari, O. Mondesert, and P. Russell. 1999. 'Nuclear localization of Cdc25 is regulated by DNA damage and a 14-3-3 protein', *Nature*, 397: 172-5.

Lopez-Onieva, L., A. Fernandez-Minan, and A. Gonzalez-Reyes. 2008. 'Jak/Stat signalling in niche support cells regulates dpp transcription to control germline stem cell maintenance in the Drosophila ovary', *Development*, 135: 533-40.

Lopez, A. L., 3rd, J. Chen, H. J. Joo, M. Drake, M. Shidate, C. Kseib, and S. Arur. 2013a. 'DAF-2 and ERK couple nutrient availability to meiotic progression during Caenorhabditis elegans oogenesis', *Dev Cell*, 27: 227-40.

———. 2013b. 'DAF-2 and ERK couple nutrient availability to meiotic progression during Caenorhabditis elegans oogenesis', *Dev Cell*, 27: 227-40.

MacNeill, S. A. 2001. 'DNA replication: partners in the Okazaki two-step', *Curr Biol*, 11: R842-4.

Maduro, M. F., M. D. Meneghini, B. Bowerman, G. Broitman-Maduro, and J. H. Rothman. 2001. 'Restriction of mesendoderm to a single blastomere by the combined action of SKN-1 and a GSK-3beta homolog is mediated by MED-1 and -2 in C. elegans', *Mol Cell*, 7: 475-85.

Mailand, N., J. Falck, C. Lukas, R. G. Syljuasen, M. Welcker, J. Bartek, and J. Lukas. 2000. 'Rapid destruction of human Cdc25A in response to DNA damage', *Science*, 288: 1425-9.

Mairet-Coello, G., A. Tury, and E. DiCicco-Bloom. 2009. 'Insulin-like growth factor-1 promotes G(1)/S cell cycle progression through bidirectional regulation of cyclins and cyclin-dependent kinase inhibitors via the phosphatidylinositol 3-kinase/Akt pathway in developing rat cerebral cortex', *J Neurosci*, 29: 775-88.

Marin, V. A., and T. C. Evans. 2003. 'Translational repression of a C. elegans Notch mRNA by the STAR/KH domain protein GLD-1', *Development*, 130: 2623-32.

Martin, G. R. 1981. 'Isolation of a pluripotent cell line from early mouse embryos cultured in medium conditioned by teratocarcinoma stem cells', *Proc Natl Acad Sci U S A*, 78: 7634-8.

Masai, H., S. Matsumoto, Z. You, N. Yoshizawa-Sugata, and M. Oda. 2010. 'Eukaryotic chromosome DNA replication: where, when, and how?', *Annu Rev Biochem*, 79: 89-130.

Matsumoto, A., S. Takeishi, T. Kanie, E. Susaki, I. Onoyama, Y. Tateishi, K. Nakayama, and K. I. Nakayama. 2011. 'p57 is required for quiescence and maintenance of adult hematopoietic stem cells', *Cell Stem Cell*, 9: 262-71.

Matsuoka, S., M. C. Edwards, C. Bai, S. Parker, P. Zhang, A. Baldini, J. W. Harper, and S. J. Elledge. 1995. 'p57KIP2, a structurally distinct member of the p21CIP1 Cdk inhibitor family, is a candidate tumor suppressor gene', *Genes Dev*, 9: 650-62.

Matsushime, H., M. F. Roussel, R. A. Ashmun, and C. J. Sherr. 1991. 'Colony-stimulating factor 1 regulates novel cyclins during the G1 phase of the cell cycle', *Cell*, 65: 701-13.

McGowan, C. H., and P. Russell. 1995. 'Cell cycle regulation of human WEE1', *EMBO J*, 14: 2166-75.

McManus, E. J., K. Sakamoto, L. J. Armit, L. Ronaldson, N. Shpiro, R. Marquez, and D. R. Alessi. 2005. 'Role that phosphorylation of GSK3 plays in insulin and Wnt signalling defined by knockin analysis', *EMBO J*, 24: 1571-83.

Menon, S., C. C. Dibble, G. Talbott, G. Hoxhaj, A. J. Valvezan, H. Takahashi, L. C. Cantley, and B. D. Manning. 2014. 'Spatial control of the TSC complex integrates insulin and nutrient regulation of mTORC1 at the lysosome', *Cell*, 156: 771-85.

Merritt, C., D. Rasoloson, D. Ko, and G. Seydoux. 2008. '3' UTRs are the primary regulators of gene expression in the C. elegans germline', *Curr Biol*, 18: 1476-82.

Michaelson, D., D. Z. Korta, Y. Capua, and E. J. Hubbard. 2010. 'Insulin signaling promotes germline proliferation in C. elegans', *Development*, 137: 671-80.

Molyneaux, K. A., J. Stallock, K. Schaible, and C. Wylie. 2001. 'Time-lapse analysis of living mouse germ cell migration', *Dev Biol*, 240: 488-98.

Morgan, D. O. 1995. 'Principles of Cdk Regulation', *Nature*, 374: 131-34.

Muller, H., M. C. Moroni, E. Vigo, B. O. Petersen, J. Bartek, and K. Helin. 1997. 'Induction of S-phase entry by E2F transcription factors depends on their nuclear localization', *Mol Cell Biol*, 17: 5508-20.

Munoz, M. J., and D. L. Riddle. 2003. 'Positive selection of Caenorhabditis elegans mutants with increased stress resistance and longevity', *Genetics*, 163: 171-80.

Nakashima, A., Y. Maruki, Y. Imamura, C. Kondo, T. Kawamata, I. Kawanishi, H. Takata, A. Matsuura, K. S. Lee, U. Kikkawa, Y. Ohsumi, K. Yonezawa, and Y. Kamada. 2008. 'The yeast Tor signaling pathway is involved in G2/M transition via polo-kinase', *PLoS One*, 3: e2223.

Nevis, K. R., M. Cordeiro-Stone, and J. G. Cook. 2009. 'Origin licensing and p53 status regulate Cdk2 activity during G(1)', *Cell Cycle*, 8: 1952-63.

Nishijima, H., H. Nishitani, N. Saito, and T. Nishimoto. 2003. 'Caffeine mimics adenine and 2'-deoxyadenosine, both of which inhibit the guanine-nucleotide exchange activity of RCC1 and the kinase activity of ATR', *Genes Cells*, 8: 423-35.

Norbury, C., J. Blow, and P. Nurse. 1991. 'Regulatory phosphorylation of the p34cdc2 protein kinase in vertebrates', *EMBO J*, 10: 3321-9.

Ohinata, Y., H. Ohta, M. Shigeta, K. Yamanaka, T. Wakayama, and M. Saitou. 2009. 'A signaling principle for the specification of the germ cell lineage in mice', *Cell*, 137: 571-84.

Ohtsubo, M., A. M. Theodoras, J. Schumacher, J. M. Roberts, and M. Pagano. 1995. 'Human cyclin E, a nuclear protein essential for the G1-to-S phase transition', *Mol Cell Biol*, 15: 2612-24.

Ohtsuka, S., and S. Dalton. 2008. 'Molecular and biological properties of pluripotent embryonic stem cells', *Gene Ther*, 15: 74-81.

Olson, T. S., M. J. Bamberger, and M. D. Lane. 1988. 'Post-translational changes in tertiary and quaternary structure of the insulin proreceptor. Correlation with acquisition of function', *J Biol Chem*, 263: 7342-51.

Pages, V., and R. P. Fuchs. 2003. 'Uncoupling of leading- and lagging-strand DNA replication during lesion bypass in vivo', *Science*, 300: 1300-3.

Paix, A., A. Folkmann, and G. Seydoux. 2017. 'Precision genome editing using CRISPR-Cas9 and linear repair templates in C. elegans', *Methods*, 121-122: 86-93.

Papaioannou, V. E., M. W. McBurney, R. L. Gardner, and M. J. Evans. 1975. 'Fate of teratocarcinoma cells injected into early mouse embryos', *Nature*, 258: 70-73.

Pardee, A. B. 1974. 'A restriction point for control of normal animal cell proliferation', *Proc Natl Acad Sci U S A*, 71: 1286-90.

Parisi, F., S. Riccardo, M. Daniel, M. Saqcena, N. Kundu, A. Pession, D. Grifoni, H. Stocker, E. Tabak, and P. Bellosta. 2011. 'Drosophila insulin and target of rapamycin (TOR) pathways regulate GSK3 beta activity to control Myc stability and determine Myc expression in vivo', *BMC Biol*, 9: 65.

Peng, C. Y., P. R. Graves, R. S. Thoma, Z. Wu, A. S. Shaw, and H. Piwnica-Worms. 1997. 'Mitotic and G2 checkpoint control: regulation of 14-3-3 protein binding by phosphorylation of Cdc25C on serine-216', *Science*, 277: 1501-5.

Pepper, A. S., D. J. Killian, and E. J. Hubbard. 2003. 'Genetic analysis of Caenorhabditis elegans glp-1 mutants suggests receptor interaction or competition', *Genetics*, 163: 115-32.

Pierce, S. B., M. Costa, R. Wisotzkey, S. Devadhar, S. A. Homburger, A. R. Buchman, K. C. Ferguson, J. Heller, D. M. Platt, A. A. Pasquinelli, L. X. Liu, S. K. Doberstein,

and G. Ruvkun. 2001. 'Regulation of DAF-2 receptor signaling by human insulin and ins-1, a member of the unusually large and diverse C. elegans insulin gene family', *Genes Dev*, 15: 672-86.

Pilch, P. F., and M. P. Czech. 1979. 'Interaction of cross-linking agents with the insulin effector system of isolated fat cells. Covalent linkage of 125I-insulin to a plasma membrane receptor protein of 140,000 daltons', *J Biol Chem*, 254: 3375-81.

Pilkinton, M., R. Sandoval, and O. R. Colamonici. 2007. 'Mammalian Mip/LIN-9 interacts with either the p107, p130/E2F4 repressor complex or B-Myb in a cell cycle-phase-dependent context distinct from the Drosophila dREAM complex', *Oncogene*, 26: 7535-43.

Pines, J. 1991. 'Cyclins: wheels within wheels', *Cell Growth Differ*, 2: 305-10.

Pines, J., and T. Hunter. 1994. 'The differential localization of human cyclins A and B is due to a cytoplasmic retention signal in cyclin B', *EMBO J*, 13: 3772-81.

Pinkston-Gosse, J., and C. Kenyon. 2007. 'DAF-16/FOXO targets genes that regulate tumor growth in Caenorhabditis elegans', *Nat Genet*, 39: 1403-9.

Polager, S., Y. Kalma, E. Berkovich, and D. Ginsberg. 2002. 'E2Fs up-regulate expression of genes involved in DNA replication, DNA repair and mitosis', *Oncogene*, 21: 437-46.

Polyak, K., J. Y. Kato, M. J. Solomon, C. J. Sherr, J. Massague, J. M. Roberts, and A. Koff. 1994. 'p27Kip1, a cyclin-Cdk inhibitor, links transforming growth factor-beta and contact inhibition to cell cycle arrest', *Genes Dev*, 8: 9-22.

Polyak, K., M. H. Lee, H. Erdjument-Bromage, A. Koff, J. M. Roberts, P. Tempst, and J. Massague. 1994. 'Cloning of p27Kip1, a cyclin-dependent kinase inhibitor and a potential mediator of extracellular antimitogenic signals', *Cell*, 78: 59-66.

Popov, B., L. S. Chang, and V. Serikov. 2005. 'Cell cycle-related transformation of the E2F4-p130 repressor complex', *Biochem Biophys Res Commun*, 336: 762-9.

Praitis, V. 2006. 'Creation of transgenic lines using microparticle bombardment methods', *Methods Mol Biol*, 351: 93-107.

Qi, W., X. Huang, E. Neumann-Haefelin, E. Schulze, and R. Baumeister. 2012. 'Cell-nonautonomous signaling of FOXO/DAF-16 to the stem cells of Caenorhabditis elegans', *PLoS Genet*, 8: e1002836.

Qi, W., Y. Yan, D. Pfeifer, V. Gromoff E. Donner, Y. Wang, W. Maier, and R. Baumeister. 2017. 'C. elegans DAF-16/FOXO interacts with TGF-ss/BMP signaling to induce germline tumor formation via mTORC1 activation', *PLoS Genet*, 13: e1006801.

Qiao, L., J. L. Lissemore, P. Shu, A. Smardon, M. B. Gelber, and E. M. Maine. 1995. 'Enhancers of glp-1, a gene required for cell-signaling in Caenorhabditis elegans, define a set of genes required for germline development', *Genetics*, 141: 551-69.

Rawlins, E. L., C. P. Clark, Y. Xue, and B. L. Hogan. 2009. 'The Id2+ distal tip lung epithelium contains individual multipotent embryonic progenitor cells', *Development*, 136: 3741-5.

Reddien, P. W., E. C. Andersen, M. C. Huang, and H. R. Horvitz. 2007. 'DPL-1 DP, LIN-35 Rb and EFL-1 E2F act with the MCD-1 zinc-finger protein to promote programmed cell death in Caenorhabditis elegans', *Genetics*, 175: 1719-33.

Rohde, J., J. Heitman, and M. E. Cardenas. 2001. 'The TOR kinases link nutrient sensing to cell growth', *J Biol Chem*, 276: 9583-6.

Rosen, O. M., R. Herrera, Y. Olowe, L. M. Petruzzelli, and M. H. Cobb. 1983. 'Phosphorylation activates the insulin receptor tyrosine protein kinase', *Proc Natl Acad Sci U S A*, 80: 3237-40.

Rosu, S., and O. Cohen-Fix. 2017. 'Live-imaging analysis of germ cell proliferation in the C. elegans adult supports a stochastic model for stem cell proliferation', *Dev Biol*, 423: 93-100.

Rubin, S. M., A. L. Gall, N. Zheng, and N. P. Pavletich. 2005. 'Structure of the Rb C-terminal domain bound to E2F1-DP1: a mechanism for phosphorylation-induced E2F release', *Cell*, 123: 1093-106.

Rumman, M., J. Dhawan, and M. Kassem. 2015. 'Concise Review: Quiescence in Adult Stem Cells: Biological Significance and Relevance to Tissue Regeneration', *Stem Cells*, 33: 2903-12.

Russell, P., and P. Nurse. 1987. 'Negative regulation of mitosis by wee1+, a gene encoding a protein kinase homolog', *Cell*, 49: 559-67.

Ryder, S. P., L. A. Frater, D. L. Abramovitz, E. B. Goodwin, and J. R. Williamson. 2004. 'RNA target specificity of the STAR/GSG domain post-transcriptional regulatory protein GLD-1', *Nat Struct Mol Biol*, 11: 20-8.

Rylatt, D. B., A. Aitken, T. Bilham, G. D. Condon, N. Embi, and P. Cohen. 1980. 'Glycogen synthase from rabbit skeletal muscle. Amino acid sequence at the sites phosphorylated by glycogen synthase kinase-3, and extension of the N-terminal sequence containing the site phosphorylated by phosphorylase kinase', *Eur J Biochem*, 107: 529-37.

Sa, G., M. Hitomi, J. Harwalkar, A. W. Stacey, G. C. Gc, and D. W. Stacey. 2002. 'Ras is active throughout the cell cycle, but is able to induce cyclin D1 only during G2 phase', *Cell Cycle*, 1: 50-8.

Sanchez, Y., C. Wong, R. S. Thoma, R. Richman, Z. Wu, H. Piwnica-Worms, and S. J. Elledge. 1997. 'Conservation of the Chk1 checkpoint pathway in mammals: linkage of DNA damage to Cdk regulation through Cdc25', *Science*, 277: 1497-501.

Sankaran, V. G., S. H. Orkin, and C. R. Walkley. 2008. 'Rb intrinsically promotes erythropoiesis by coupling cell cycle exit with mitochondrial biogenesis', *Genes Dev*, 22: 463-75.

Sarbassov, D. D., D. A. Guertin, S. M. Ali, and D. M. Sabatini. 2005. 'Phosphorylation and regulation of Akt/PKB by the rictor-mTOR complex', *Science*, 307: 1098-101.

Saxton, R. A., and D. M. Sabatini. 2017. 'mTOR Signaling in Growth, Metabolism, and Disease', *Cell*, 168: 960-76.

Schenker, E., and R. A. Kohanski. 1991. 'The native alpha 2 beta 2 tetramer is the only subunit structure of the insulin receptor in intact cells and purified receptor preparations', *Arch Biochem Biophys*, 290: 79-85.

Schlegel, R., and A. B. Pardee. 1986. 'Caffeine-induced uncoupling of mitosis from the completion of DNA replication in mammalian cells', *Science*, 232: 1264-6.

Schlesinger, A., C. A. Shelton, J. N. Maloof, M. Meneghini, and B. Bowerman. 1999. 'Wnt pathway components orient a mitotic spindle in the early Caenorhabditis elegans embryo without requiring gene transcription in the responding cell', *Genes Dev*, 13: 2028-38.

Schubert, C. M., R. Lin, C. J. de Vries, R. H. Plasterk, and J. R. Priess. 2000. 'MEX-5 and MEX-6 function to establish soma/germline asymmetry in early C. elegans embryos', *Mol Cell*, 5: 671-82.

Schultz, E., M. C. Gibson, and T. Champion. 1978. 'Satellite cells are mitotically quiescent in mature mouse muscle: an EM and radioautographic study', *J Exp Zool*, 206: 451-6.

Schumacher, B., K. Hofmann, S. Boulton, and A. Gartner. 2001. 'The C. elegans homolog of the p53 tumor suppressor is required for DNA damage-induced apoptosis', *Curr Biol*, 11: 1722-7.

Seidel, H. S., and J. Kimble. 2015. 'Cell-cycle quiescence maintains Caenorhabditis elegans germline stem cells independent of GLP-1/Notch', *Elife*, 4.

Serrano, M., G. J. Hannon, and D. Beach. 1993. 'A new regulatory motif in cell-cycle control causing specific inhibition of cyclin D/CDK4', *Nature*, 366: 704-7.

Seydoux, G., and A. Fire. 1994. 'Soma-germline asymmetry in the distributions of embryonic RNAs in Caenorhabditis elegans', *Development*, 120: 2823-34.

Shah, S., E. Lubeck, M. Schwarzkopf, T. F. He, A. Greenbaum, C. H. Sohn, A. Lignell, H. M. Choi, V. Gradinaru, N. A. Pierce, and L. Cai. 2016. 'Single-molecule RNA detection at depth by hybridization chain reaction and tissue hydrogel embedding and clearing', *Development*, 143: 2862-7.

Shea, K. L., W. Xiang, V. S. LaPorta, J. D. Licht, C. Keller, M. A. Basson, and A. S. Brack. 2010. 'Sprouty1 regulates reversible quiescence of a self-renewing adult muscle stem cell pool during regeneration', *Cell Stem Cell*, 6: 117-29.

Shen, T., H. Zhou, C. Shang, Y. Luo, Y. Wu, and S. Huang. 2018. 'Ciclopirox activates ATR-Chk1 signaling pathway leading to Cdc25A protein degradation', *Genes Cancer*, 9: 39-52.

Sherr, C. J. 1994. 'G1 phase progression: cycling on cue', *Cell*, 79: 551-5.

Sherr, C. J., and J. M. Roberts. 1999. 'CDK inhibitors: positive and negative regulators of G1-phase progression', *Genes Dev*, 13: 1501-12.

Shia, M. A., and P. F. Pilch. 1983. 'The beta subunit of the insulin receptor is an insulin-activated protein kinase', *Biochemistry*, 22: 717-21.

Shieh, S. Y., J. Ahn, K. Tamai, Y. Taya, and C. Prives. 2000. 'The human homologs of checkpoint kinases Chk1 and Cds1 (Chk2) phosphorylate p53 at multiple DNA damage-inducible sites', *Genes Dev*, 14: 289-300.

Shieh, S. Y., M. Ikeda, Y. Taya, and C. Prives. 1997. 'DNA damage-induced phosphorylation of p53 alleviates inhibition by MDM2', *Cell*, 91: 325-34.

Shiloh, Y. 2003. 'ATM and related protein kinases: safeguarding genome integrity', *Nat Rev Cancer*, 3: 155-68.

Shima, N., A. Alcaraz, I. Liachko, T. R. Buske, C. A. Andrews, R. J. Munroe, S. A. Hartford, B. K. Tye, and J. C. Schimenti. 2007. 'A viable allele of Mcm4 causes chromosome instability and mammary adenocarcinomas in mice', *Nat Genet*, 39: 93-8.

Sigmond, T., J. Barna, M. L. Toth, K. Takacs-Vellai, G. Pasti, A. L. Kovacs, and T. Vellai. 2008. 'Autophagy in Caenorhabditis elegans', *Methods Enzymol*, 451: 521-40.

Smith, E. J., G. Leone, J. DeGregori, L. Jakoi, and J. R. Nevins. 1996. 'The accumulation of an E2F-p130 transcriptional repressor distinguishes a G0 cell state from a G1 cell state', *Mol Cell Biol*, 16: 6965-76.

Smith, P., W. M. Leung-Chiu, R. Montgomery, A. Orsborn, K. Kuznicki, E. Gressman-Coberly, L. Mutapcic, and K. Bennett. 2002. 'The GLH proteins, Caenorhabditis elegans P granule components, associate with CSN-5 and KGB-1, proteins necessary for fertility, and with ZYX-1, a predicted cytoskeletal protein', *Dev Biol*, 251: 333-47.

Snow, M. H. 1977. 'Myogenic cell formation in regenerating rat skeletal muscle injured by mincing. II. An autoradiographic study', *Anat Rec*, 188: 201-17.

So, S., A. J. Davis, and D. J. Chen. 2009. 'Autophosphorylation at serine 1981 stabilizes ATM at DNA damage sites', *J Cell Biol*, 187: 977-90.

Sonneville, R., M. Querenet, A. Craig, A. Gartner, and J. J. Blow. 2012. 'The dynamics of replication licensing in live Caenorhabditis elegans embryos', *J Cell Biol*, 196: 233-46.

Soukas, A. A., E. A. Kane, C. E. Carr, J. A. Melo, and G. Ruvkun. 2009. 'Rictor/TORC2 regulates fat metabolism, feeding, growth, and life span in Caenorhabditis elegans', *Genes Dev*, 23: 496-511.

Spangrude, G. J., S. Heimfeld, and I. L. Weissman. 1988. 'Purification and characterization of mouse hematopoietic stem cells', *Science*, 241: 58-62.

Spencer, S. L., S. D. Cappell, F. C. Tsai, K. W. Overton, C. L. Wang, and T. Meyer. 2013. 'The proliferation-quiescence decision is controlled by a bifurcation in CDK2 activity at mitotic exit', *Cell*, 155: 369-83.

Spradling, A., M. T. Fuller, R. E. Braun, and S. Yoshida. 2011. 'Germline stem cells', *Cold Spring Harb Perspect Biol*, 3: a002642.

Stead, E., J. White, R. Faast, S. Conn, S. Goldstone, J. Rathjen, U. Dhingra, P. Rathjen, D. Walker, and S. Dalton. 2002. 'Pluripotent cell division cycles are driven by ectopic Cdk2, cyclin A/E and E2F activities', *Oncogene*, 21: 8320-33.

Stergiou, L., K. Doukoumetzidis, A. Sendoel, and M. O. Hengartner. 2007. 'The nucleotide excision repair pathway is required for UV-C-induced apoptosis in Caenorhabditis elegans', *Cell Death Differ*, 14: 1129-38.

Stiernagle, T. 2006. 'Maintenance of C. elegans', *WormBook*: 1-11.

Suen, K. M., C. C. Lin, R. George, F. A. Melo, E. R. Biggs, Z. Ahmed, M. N. Drake, S. Arur, S. T. Arold, and J. E. Ladbury. 2013. 'Interaction with Shc prevents aberrant Erk activation in the absence of extracellular stimuli', *Nat Struct Mol Biol*, 20: 620-7.

Suzuki, K., and T. Kono. 1980. 'Evidence that insulin causes translocation of glucose transport activity to the plasma membrane from an intracellular storage site', *Proc Natl Acad Sci U S A*, 77: 2542-5.

Takada, S., and B. J. Cha. 2011. 'In vivo live-analysis of cell cycle checkpoints in Drosophila early embryos', *Methods Mol Biol*, 782: 75-92.

Tam, P. P., and M. H. Snow. 1981. 'Proliferation and migration of primordial germ cells during compensatory growth in mouse embryos', *J Embryol Exp Morphol*, 64: 133-47.

Taniguchi, C. M., B. Emanuelli, and C. R. Kahn. 2006. 'Critical nodes in signalling pathways: insights into insulin action', *Nat Rev Mol Cell Biol*, 7: 85-96.

Tee, A. R., B. D. Manning, P. P. Roux, L. C. Cantley, and J. Blenis. 2003. 'Tuberous sclerosis complex gene products, Tuberin and Hamartin, control mTOR signaling by acting as a GTPase-activating protein complex toward Rheb', *Curr Biol*, 13: 1259-68.

Tenenhaus, C., C. Schubert, and G. Seydoux. 1998. 'Genetic requirements for PIE-1 localization and inhibition of gene expression in the embryonic germ lineage of Caenorhabditis elegans', *Dev Biol*, 200: 212-24.

Thomson, J. A., J. Itskovitz-Eldor, S. S. Shapiro, M. A. Waknitz, J. J. Swiergiel, V. S. Marshall, and J. M. Jones. 1998. 'Embryonic stem cell lines derived from human blastocysts', *Science*, 282: 1145-7.

Tibbetts, R. S., K. M. Brumbaugh, J. M. Williams, J. N. Sarkaria, W. A. Cliby, S. Y. Shieh, Y. Taya, C. Prives, and R. T. Abraham. 1999. 'A role for ATR in the DNA damage-induced phosphorylation of p53', *Genes Dev*, 13: 152-7.

Timofeev, O., O. Cizmecioglu, E. Hu, T. Orlik, and I. Hoffmann. 2009. 'Human Cdc25A phosphatase has a non-redundant function in G2 phase by activating Cyclin A-dependent kinases', *FEBS Lett*, 583: 841-7.

Toyoshima-Morimoto, F., E. Taniguchi, N. Shinya, A. Iwamatsu, and E. Nishida. 2001. 'Polo-like kinase 1 phosphorylates cyclin B1 and targets it to the nucleus during prophase', *Nature*, 410: 215-20.

Toyoshima, H., and T. Hunter. 1994. 'p27, a novel inhibitor of G1 cyclin-Cdk protein kinase activity, is related to p21', *Cell*, 78: 67-74.

Tran, H., A. Brunet, E. C. Griffith, and M. E. Greenberg. 2003. 'The many forks in FOXO's road', *Sci STKE*, 2003: RE5.

Vakifahmetoglu, H., M. Olsson, and B. Zhivotovsky. 2008. 'Death through a tragedy: mitotic catastrophe', *Cell Death Differ*, 15: 1153-62.

Van Obberghen, E., B. Rossi, A. Kowalski, H. Gazzano, and G. Ponzio. 1983. 'Receptor-mediated phosphorylation of the hepatic insulin receptor: evidence that the Mr 95,000 receptor subunit is its own kinase', *Proc Natl Acad Sci U S A*, 80: 945-9.

Van Zant, G. 1984. 'Studies of hematopoietic stem cells spared by 5-fluorouracil', *J Exp Med*, 159: 679-90.

Vanhaesebroeck, B., J. Guillermet-Guibert, M. Graupera, and B. Bilanges. 2010. 'The emerging mechanisms of isoform-specific PI3K signalling', *Nat Rev Mol Cell Biol*, 11: 329-41.

Vermeulen, K., D. R. Van Bockstaele, and Z. N. Berneman. 2003. 'The cell cycle: a review of regulation, deregulation and therapeutic targets in cancer', *Cell Prolif*, 36: 131-49.

Viatour, P., T. C. Somervaille, S. Venkatasubrahmanyam, S. Kogan, M. E. McLaughlin, I. L. Weissman, A. J. Butte, E. Passegue, and J. Sage. 2008. 'Hematopoietic stem cell quiescence is maintained by compound contributions of the retinoblastoma gene family', *Cell Stem Cell*, 3: 416-28.

Walker, D. H., and J. L. Maller. 1991. 'Role for cyclin A in the dependence of mitosis on completion of DNA replication', *Nature*, 354: 314-7.

Wang, L., Z. Li, and Y. Cai. 2008. 'The JAK/STAT pathway positively regulates DPP signaling in the Drosophila germline stem cell niche', *J Cell Biol*, 180: 721-8.

Weintraub, S. J., C. A. Prater, and D. C. Dean. 1992. 'Retinoblastoma protein switches the E2F site from positive to negative element', *Nature*, 358: 259-61.

White, J., and S. Dalton. 2005. 'Cell cycle control of embryonic stem cells', *Stem Cell Rev*, 1: 131-8.

Wobbe, C. R., L. Weissbach, J. A. Borowiec, F. B. Dean, Y. Murakami, P. Bullock, and J. Hurwitz. 1987. 'Replication of simian virus 40 origin-containing DNA in vitro with purified proteins', *Proc Natl Acad Sci U S A*, 84: 1834-8.

Wold, M. S. 1997. 'Replication protein A: a heterotrimeric, single-stranded DNA-binding protein required for eukaryotic DNA metabolism', *Annu Rev Biochem*, 66: 61-92.

Wold, M. S., and T. Kelly. 1988. 'Purification and characterization of replication protein A, a cellular protein required for in vitro replication of simian virus 40 DNA', *Proc Natl Acad Sci U S A*, 85: 2523-7.

Wolf, N., J. Priess, and D. Hirsh. 1983. 'Segregation of germline granules in early embryos of Caenorhabditis elegans: an electron microscopic analysis', *J Embryol Exp Morphol*, 73: 297-306.

Wu, A. M., J. E. Till, L. Siminovitch, and E. A. McCulloch. 1968. 'Cytological evidence for a relationship between normal hemotopoietic colony-forming cells and cells of the lymphoid system', *J Exp Med*, 127: 455-64.

Xiong, Y., G. J. Hannon, H. Zhang, D. Casso, R. Kobayashi, and D. Beach. 1993. 'p21 is a universal inhibitor of cyclin kinases', *Nature*, 366: 701-4.

Xuan, F., and I. M. Hsing. 2014. 'Triggering hairpin-free chain-branching growth of fluorescent DNA dendrimers for nonlinear hybridization chain reaction', *J Am Chem Soc*, 136: 9810-3.

Yang, H., D. G. Rudge, J. D. Koos, B. Vaidialingam, H. J. Yang, and N. P. Pavletich. 2013. 'mTOR kinase structure, mechanism and regulation', *Nature*, 497: 217-23.

Yang, J., E. S. Bardes, J. D. Moore, J. Brennan, M. A. Powers, and S. Kornbluth. 1998. 'Control of cyclin B1 localization through regulated binding of the nuclear export factor CRM1', *Genes Dev*, 12: 2131-43.

Yip, C. C., M. L. Moule, and C. W. Yeung. 1982. 'Subunit structure of insulin receptor of rat adipocytes as demonstrated by photoaffinity labeling', *Biochemistry*, 21: 2940-5.

Zeiser, E., C. Frokjaer-Jensen, E. Jorgensen, and J. Ahringer. 2011. 'MosSCI and gateway compatible plasmid toolkit for constitutive and inducible expression of transgenes in the C. elegans germline', *PLoS One*, 6: e20082.

Zeman, M. K., and K. A. Cimprich. 2014. 'Causes and consequences of replication stress', *Nat Cell Biol*, 16: 2-9.

Zeng, Y., K. C. Forbes, Z. Wu, S. Moreno, H. Piwnica-Worms, and T. Enoch. 1998. 'Replication checkpoint requires phosphorylation of the phosphatase Cdc25 by Cds1 or Chk1', *Nature*, 395: 507-10.

Zou, L., and S. J. Elledge. 2003. 'Sensing DNA damage through ATRIP recognition of RPA-ssDNA complexes', *Science*, 300: 1542-8.

Zou, L., and B. Stillman. 2000. 'Assembly of a complex containing Cdc45p, replication protein A, and Mcm2p at replication origins controlled by S-phase cyclin-dependent kinases and Cdc7p-Dbf4p kinase', *Mol Cell Biol*, 20: 3086-96.

Zou, P., H. Yoshihara, K. Hosokawa, I. Tai, K. Shinmyozu, F. Tsukahara, Y. Maru, K. Nakayama, K. I. Nakayama, and T. Suda. 2011. 'p57(Kip2) and p27(Kip1) cooperate to maintain hematopoietic stem cell quiescence through interactions with Hsc70', *Cell Stem Cell*, 9: 247-61.

VITA

Kenneth Andrew Trimmer was born in Dallas, TX, the son of Mrs. Clara T. Trimmer, and Charles A. Trimmer. He graduated from Sherwood High School in Sandy Spring, Maryland in May 2004. The following August of 2004, he enrolled at the University of Maryland, Baltimore County, receiving his Bachelor of Science in Biochemistry and Molecular Biology in 2008. In August of 2012, he began his doctoral studies at The University of Texas MD Anderson Cancer Center UTHealth Graduate School of Biomedical Sciences, joining the Genes and Development graduate program under the mentorship of Dr. Swathi Arur.